MycoKeys 39: 1–27 (2018)
doi: 10.3897/mycokeys.39.27014
http://mycokeys.pensoft.net

RESEARCH ARTICLE

A peer-reviewed open-access journal
MycoKeys
Launched to accelerate biodiversity research

Ophiostomatoid fungi associated with pines infected by *Bursaphelenchus xylophilus* and *Monochamus alternatus* in China, including three new species

HuiMin Wang[1], YingYing Lun[1,2,3], Quan Lu[1], HuiXiang Liu[2], Cony Decock[4], XingYao Zhang[1]

1 *Key Laboratory of Forest Protection State Forestry Administration, Research Institute of Forest Ecology, Environment and Protection, Chinese Academy of Forestry, Beijing 100091, China* **2** *College of Plant Protection of Shandong Agricultural University, Taian 271018, China* **3** *Longju Ecological Forest Farm, Dongying 257085, China* **4** *Mycothèque de l'Université Catholique de Louvain (MUCL), Earth and Life Institute, Microbiology, B-1348 Louvain-la-Neuve, Belgium*

Corresponding author: *Quan Lu* (luquan@caf.ac.cn); *HuiXiang Liu* (hxliu@sdau.edu.cn)

Academic editor: *M. Stadler* | Received 29 May 2018 | Accepted 13 August 2018 | Published 4 September 2018

Citation: Wang HM, Lun YY, Lu Q, Liu HX, Decock C, Zhang XY (2018) Ophiostomatoid fungi associated with pines infected by *Bursaphelenchus xylophilus* and *Monochamus alternatus* in China, including three new species. MycoKeys 39: 1–27. https://doi.org/10.3897/mycokeys.39.27014

Abstract

The activity of the pine wood nematode *Bursaphelenchus xylophilus* leads to extremely serious economic, ecological and social losses in East Asia. The nematode causes pine wilt disease, which is currently regarded as the most important forest disease in China. The pathogenic nematode feeds on dendrocola fungi to complete its cycle of infection. As the vector of the nematode, the Japanese pine sawyer (*Monochamus alternatus*) also carries dendrocola fungi. Pine woods, infected by *B. xylophilus* and tunnelled by *M. alternatus,* are also inhabited by ophiostomatoid fungi. These fungi are well known for their association with many bark and ambrosia beetles. They can cause sapstain and other serious tree diseases. The aims of our study were to investigate and identify the ophiostomatoid communities associated with the epidemic pine wood nematode and the pine sawyer in *Pinus massoniana* and *P. thunbergii* forests, which are the main hosts of the pine wood nematode in China. Two hundred and forty strains of ophiostomatoid fungi were isolated from nematode and sawyer–infected trees in the coastal Shandong and Zhejiang Provinces, representing newly and historically infected areas, respectively. Six ophiostomatoid species were identified on the basis of morphological, physiological and molecular data. For the latter, DNA sequences of the internal transcribed spacer (ITS1–5.8S–ITS2) region and partial b-tubulin gene were examined. The ophiostomatoid species included one known species, *Ophiostoma ips*, three novel species, viz. *Ophiostoma album* **sp. nov.**,

Ophiostoma massoniana **sp. nov.** and *Sporothrix zhejiangensis* **sp. nov.** and two species whose identities are still uncertain, *Ophiostoma* cf. *deltoideosporum* and *Graphilbum* cf. *rectangulosporium*, due to the paucity of the materials obtained. The ophiostomatoid community was dominated by *O. ips*. This study revealed that a relatively high species diversity of ophiostomatoid fungi are associated with pine infected by *B. xylophilus* and *M. alternatus* in China.

Keywords
Ophiostoma, taxonomy, *Sporothrix*, *Ophiostoma minus* complex, *Ophiostoma ips* complex

Introduction

The pathogenic pine wood nematode (PWN) *Bursaphelenchus xylophilus* (Steiner & Buhrer) Nickle (Aphelenchida, Parasitaphelenchidae), presumably native to North America (Steiner and Buhrer 1934, Robbins 1982, Ryss et al. 2005, Zhao et al. 2014), is a mild threat to pine trees in its native area. Nevertheless, this species and the concomitant systematic wilt symptom are responsible for pine tree deaths affecting many trees in eastern Asia, notably in Japan and China (Evans et al. 1996, Mota and Vieira 2008, Mamiya and Shoji 2009, Jung 2010, Futai 2013). Since the first report in China, in Nanjing City in 1982, the disease has spread through more than 300 counties in the provinces of Jiangsu, Zhejiang, Shandong and others, which are currently listed as PWN epidemic areas (State Forestry Administration of the People's Republic of China 2018). The wilt disease has caused enormous losses not only to the economy and ecology, but also to society, becoming one of the most serious ecological devastation events in Chinese forests.

Bursaphelenchus xylophilus infects many species of coniferous trees, mainly from the genus *Pinus* (Yan et al. 2003). *Pinus armandii*, *P. kesiya* var. *langbianensis*, *P. koraiensis*, *P. massoniana*, *P. tabuliformis*, *P. taiwanensis*, *P. thunbergii* and *P. yunnanensis* are naturally infected by PWN in China (Zhao and Sun 2017). During the infection cycle, the nematode needs vector beetles for dispersal and inoculation into new hosts. The Japanese pine sawyer, *Monochamus alternatus* Hope (Coleoptera, Cerambycidae), is considered to be the primary PWN vector indigenous to Asia. At the initial stage of infection, PWN feeds on epithelial cells of the host pine (Mota and Vieira 2008, Zhao et al. 2008, Futai 2013). Upon tree death, it feeds on the dendrocola fungi to maintain its population and propagate (Suh et al. 2013, Zhao et al. 2013, 2014).

The ophiostomatoid fungi are one of the most common fungal groups inhabiting wood infected by *B. xylophilus*. Further, many ophiostomatoid reproduction structures are detected in the tunnels of *M. alternatus*, suggesting a relationship between the fungi and the occurrence and development of the disease. For instance, *O. ips* has been found in the PWN vector beetles in North America, China and Korea (Wingfield 1987, Suh et al. 2013, Zhao et al. 2014). There is some evidence that the fungi adhere to the body surface of adult *M. alternatus* and thus are transmitted to the twigs of healthy trees (Suh et al. 2013).

The association of PWN with ophiostomatoid fungi and bacteria likely contributes to the nematode's pathogenicity (Zhao et al. 2013, Zhao and Sun 2017). *Ophiostoma*

minus and *Sporothrix* sp. can stimulate the reproduction of PWN and, consequently, the numbers of PWN carried by the emerging beetles (Maehara and Futai 1997, Zhao et al. 2013, Zhao and Sun 2017). Moreover, the fragrant diacetone alcohol released from wood infected by *Sporothrix* sp. 1 can induce *B. xylophilus* to produce greater number of offspring and promotes beetle growth and survival (Zhao et al. 2013).

Thus far, the association with PWN and *Monochamus* spp. has been documented for only five species of ophiostomatoid fungi worldwide (Wingfield 1987, Maehara and Futai 1997, Hyun et al. 2007, Suh et al. 2013, Zhao et al. 2013, Zhao and Sun 2017). Determination of the identities of these species is mainly based on morphology and sequence comparisons of a single DNA locus. Given the diversity of ophiostomatoid fungi associated with other beetles, the serious impact of the nematode and sawyers on wood and the potential importance of these fungi in the disease infection cycle, studies of the diversity and occurrence of the ophiostomatoid fungi involved in the pine wilt disease should be intensified. Such studies will enable understanding of the interaction between the disease system and the fungi, ultimately helping to redress the current situation of the ceaseless outbreaks and rapid expansion of the disease.

The aims of the current study were to investigate and identify the ophiostomatoid mycobiota associated with the nematode and sawyer in the epidemic forests of Shandong and Zhejiang Provinces in eastern China to facilitate the understanding of pine wilt disease infection and prevalence mechanisms. The two coastal provinces, Shandong and Zhejiang, represent new and historic epidemic areas, with *P. thunbergii* and *P. massoniana* as hosts, respectively.

Materials and methods

Collection of samples and fungus isolations

Fungi were isolated from 98 samples of *M. alternatus* galleries or pupal chambers in *P. massoniana* and *P. thunbergii* in the Zhejiang and Shandong Provinces (Table 1), in November 2012. All host trees used for sample collection in this study were exhibiting weak or dying symptoms, blue stain and 4–5 instar larvae residing inside after dissecting the stems. The nematodes were also isolated from these galleries and pupal chambers by Behrman funnel. The fungi were isolated on the surface of 2% (w/v) water agar (20 g agar powder in 1000 ml of deionised water) in 9 cm wide Petri dishes and incubated at 25 °C (Seifert et al. 1993, Zhao et al. 2013, Chang et al. 2017). Subsequently, all strains were purified by hyphal tip isolation, using the procedure described by Jacobs and Wingfield (2001) and routinely grown on 2% (w/v) malt extract agar (MEA; 20 g malt extract powder and 20 g agar powder in 1000 ml of deionised water). Representative cultures were deposited in the China Forestry Culture Collection Center (CFCC), culture collection of the Chinese Academy of Forestry (CXY) and part of the Belgian Coordinated Collections of Microorganisms (MUCL), culture collection at Université Catholique de Louvain, Belgium.

Culture and morphological studies

The ophiostomatoid fungal strains were incubated on 2% MEA and 2% potato dextrose agar (PDA; 200 g potato and 20 g dextrose, 20 g agar powder in 1000 ml of deionised water: the dextrose was obtained from American Amresco) in the dark at 25 °C in an incubator. Fungal growth on MEA plates was monitored daily. Hyphal tips of emerging colonies were transferred to fresh MEA plates to purify the fungi. Slides were made to observe the sexual/asexual state structures; these were mounted in lactic acid cotton blue on glass slides and examined under a BX51 OLYMPUS microscope. Fifty measurements were made of each microscopic taxonomically informative structure. The measurements are presented in the form: (minimum–) mean minus standard deviation–mean plus standard deviation (–maximum).

A 5-mm mycelium disc was cut from an actively growing fungal colony using a sterile cork borer and placed at the centre of MEA plates, with the aerial mycelium side in contact with the medium. Three replicate plates were prepared for each strain and were incubated at temperatures ranging from 5–40 °C at five-degree intervals. The colony diameters on each Petri dish were determined along two perpendicular axes every day until the entire dish was covered. The colour descriptions were provided according to Rayner (1970).

DNA extraction, PCR and sequencing reactions

DNA was extracted from freshly collected mycelia grown in liquid malt medium (20g malt extract in 1000 ml of deionised water) at 25 °C in the dark for 7 d using an Invisorb Spin Plant mini kit (Invitek, Berlin, Germany), following the manufacturer's instructions. The internal transcribed spacer (ITS) regions and partial β–tubulin (*tub2*) genes were amplified using primer pairs ITS1/ITS4 (White et al. 1990) and Bt2a/Bt2b (Glass and Donaldson 1995), respectively.

PCR reactions were performed in 25 ml volumes (2.5 mM $MgCl_2$, 1X PCR buffer, 0.2 mM dNTP, 0.2 mM of each primer and 2.5 U of Taq polymerase). The conditions for ITS and *tub2* PCR amplifications were as described earlier (White et al. 1990, Glass and Donaldson 1995). PCR products were purified using an MSB Spin PCRapace kit (250) (Invitek), following the manufacturer's instructions.

Sequencing reactions were performed using CEQ DTCS Quick Start KitH (Beckman Coulter, American), following the manufacturer's instructions, with the same PCR primers as above. Nucleotide sequences were determined using a CEQ 2000 XL capillary automated sequencer (Beckman Coulter).

Phylogenetic analyses

Contigs were subjected to BLAST searches of the NCBI GenBank database (https://www.ncbi.nlm.nih.gov/); published sequences of closely related species were retrieved.

Alignments of the related genes (most up-to-date sequence regions deposited in the GenBank) were conducted online using MAFFT v 7.0 (https://mafft.cbrc.jp/alignment/server/index.html) (Katoh and Standley 2013) and the E-INS-i strategy. Subsequently, the datasets were checked manually by using MEGA v 5.2 (Tamura et al. 2011). Gaps were treated as a fifth base. Phylogenetic analyses were performed using maximum parsimony (MP), as implemented in PAUP* v 4.0b10 (Swofford 2003); Bayesian Inference (BI), as implemented in MrBayes v 3.1.2 (Huelsenbeck and Ronquist 2001); and Maximum Likelihood (ML), using PhyML v 3.0 (Guidon and Gascuel 2003).

The most parsimonious trees generated by MP analyses were identified by heuristic searches with a random addition sequence (1000); max trees were set to 200 and further evaluated by bootstrap analysis, retaining clades compatible with the 50% majority rule in the bootstrap consensus tree. The analysis was based on tree bisection reconnection branch swapping (TBR). The tree length (TL), consistency index (CI), retention index (RI), homoplasy index (HI) and rescaled consistency index (RC) were recorded for each dataset after tree generation.

The general-time-reversible (GTR) model for ML analyses was selected using the Akaike Information Criterion (AIC) in ModelTest v 3.7 (Posada and Crandall 1998). ML runs performed using the CIPRES cluster at the San Diego Supercomputing Center (USA). Node support was estimated from 1000 bootstrap replicates.

For BI analyses, the most appropriate substitution models were also selected using the general-time-reversible model (GRT) with AIC in ModelTest v 3.7. BI was carried out with MrBayes using the Markov Chain Monte Carlo (MCMC) approach with 5,000,000 generations, to estimate posterior probabilities.

Results

Fungal isolation and sequence comparison

In total, 240 strains belonging to Ophiostomatales were obtained from PWN-infected galleries and pupal chambers of *M. alternatus*. The strains were sorted into six morphological groups (groups A–F in Table 1), tentatively identified as *Sporothrix*, *Ophiostoma* and *Graphilbum*. After preliminary ITS sequence comparisons of all these strains, 11 strains were clearly disparate to any known species and the remaining 229 strains possessed > 99% similarity with type strain of *O. ips* (GenBank no. AY546704).

Phylogenetic analyses

ITS and *tub2* sequences were generated for 16 strains and deposited in GenBank (Table 1). The ITS alignment matrix contained 110 sequences (Tables 1 and 2) and 651 characters, including gaps, following the preliminary determination of strain

Table 1. Strains of ophiostomatoid fungi isolated from pines infested by Monochamus alternatus and pine wood nematode in the current study.

Group	Species	Strain No.	Host	Origin (Latitude, Longitude)	Genbank No.		Collector
					ITS	β-tubulin	
A	*Sporothrix zhejiangensis* sp. nov.	MUCL 55181 (CFCC52167, CXY1612)	*Pinus massoniana*	Yuyao, Zhejiang (29°58'10.2"N, 121°05'57.1"E)	KY094069	MH397728	Q. Lu, YY Lun
		MUCL 55182 (CFCC52164, CXY1613)	*P. massoniana*	Yuyao, Zhejiang (29°58'10.2"N, 121°05'57.1"E)	KY094070	MH397729	
		MUCL 55183 (CFCC52165, CXY1614)	*P. massoniana*	Yuyao, Zhejiang (29°58'10.2"N, 121°05'57.1"E)	KY094071	MH397730	
		MUCL 55184 (CFCC52166, CXY1615)	*P. massoniana*	Yuyao, Zhejiang (29°58'10.2"N, 121°05'57.1"E)	KY094072	MH397731	
B	*Ophiostoma album* sp. nov.	MUCL 55189 (CFCC52168, CXY1622)	*P. massoniana*	Yuyao, Zhejiang (29°58'10.2"N, 121°05'57.1"E)	KY094073	MH360979	
		MUCL 55190 (CFCC52169, CXY1642)	*P. massoniana*	Yuyao, Zhejiang (29°58'10.2"N, 121°05'57.1"E)	KY094074	MH360980	
		CFCC52170 (CXY1643)	*P. massoniana*	Yuyao, Zhejiang (29°58'10.2"N, 121°05'57.1"E)	KY094075	MH360981	
C	*Ophiostoma ips*	CXY1628	*P. thunbergii*	Changdao, Shandong (37°59'13.5"N, 120°42'18.1"E)	KY593324	MH324804	
		CXY1631	*P. thunbergii*	Zhoushan, Zhejiang (29°52'51.33"N, 122°24'14.13"E)	MH324811	MH324805	
		CXY1635	*P. massoniana*	Yuyao, Zhejiang (29°58'10.2"N, 121°05'57.1"E)	MH324812	MH324808	
		CXY1638	*P. thunbergii*	Fuyang, Zhejiang (30°05'15.1"N, 119°58'55.1"E)	MH324813	MH324809	
		CXY1639	*P. massoniana*	Weihai, Shandong (37°23'23.6"N, 122°32'33.1"E)	MH324814	MH324810	
D	*Ophiostoma massoniana* sp. nov.	MUCL 55179 (CFCC51648, CXY1610)	*P. massoniana*	Fuyang, Zhejiang (30°05'15.1"N, 119°58'55.1"E)	KY094067	MH370810	
		MUCL 55180 (CFCC51649, CXY1611)	*P. massoniana*	Yuyao, Zhejiang (29°59'36.87"N, 121°09'09.90"E)	KY094068	MH370811	
E	*Graphilbum* cf. *rectangulosporium*	CXY1623	*P. massoniana*	Yuyao, Zhejiang (29°59'36.87"N, 121°09'09.90"E)	MH324816	–	
F	*Ophiostoma* cf. *deltoideosporum*	MUCL 55191 (CXY1640)	*P. thunbergii*	Weihai, Shandong (37°23'23.6"N, 122°32'33.1"E)	MH324815	–	

MUCL: part of the Belgian Coordinated Collections of Microorganisms; CFCC: China Forestry Culture Collection Center; Beijing, China; CXY (Culture Xingyao): culture collection of the Research Institute of Forest Ecology, Environment, and Protection, Chinese Academy of Forestry.
Sequences missing data are indicated by [–].

affinities using the BLAST search engine (GenBank). Due to the presence or absence in intron in the *tub2* sequence in the *Sporothrix* and *Ophiostoma* lineage species (Zipfel et al. 2006, de Beer et al. 2016), three separate datasets were built for the *tub2* sequences. These were *Sporothrix*, *Ophiostoma minus* complex and *Ophiostoma tenellum* complex datasets (Linnakoski et al. 2010, de Beer et al. 2013, 2016). The

Table 2. The information of references sequences used for phylogenetic analyses in this study.

Species	Strain No.	Host/insect	Country	Genbank No.		Reference
				ITS	β-tubulin	
Sporothrix abietina	CBS125.89	*Abies vejari*	Mexico	AF484453	KX590755	de Beer et al. 2003
S. aurorae	CMW19362	*Pinus eliottii*	South Africa	DQ396796	DQ396800	Francois et al. 2006
S. bragantina	CBS 474.91	Soil	Brazil	FN546965	FN547387	Madrid et al. 2010
	CBS 430.92	Soil	Brazil	FN546964	FN547386	Madrid et al. 2010
S. brasiliensis	Ss383	*Felis catus*	Brazil	KP890194	FN547387	Araujo et al. 2015
S. brunneoviolacea	CBS 124562	Soil	Spain	FN546959	FN547385	Madrid et al. 2010
	CBS 124564	Soil	Spain	FN546958	FN547384	Madrid et al. 2010
S. dentifunda	CMW13016	Quercus wood	Hungary	AY495434	AY495445	Aghayeva et al. 2005
	CMW13017	Quercus wood	Poland	AY495435	AY495446	Aghayeva et al. 2005
S. epigloea	CBS 573.63	*Tremella fusiformis*	Argentina	KX590817	KX590760	de Beer et al. 2016
S. eucalyptigena	CPC 24638	*Eucalyptus marginata*	Western Australia	KR476721	N/A	Crous et al. 2015
S. gemella	CMW23057	*Protea caffra*	South Africa	DQ821560	DQ821554	Roets et al. 2008
S. inflata	CMW12529	Soil	Canada	AY495428	AY495438	Aghayeva et al. 2005
	CMW12527	wheat-field soil	Germany	AY495426	AY495437	Aghayeva et al. 2005
S. nebularis	CMW27319	*Orthotomicus erosus*	Spain	DQ674375	N/A	Romón et al. 1900
	CMW27900	*O. erosus*	Spain	DQ674376	N/A	Romón et al. 1900
S. pallida	CBS131.56	*Stemonitis fusca*	Japan	EF127880	EF139110	de Meyer et al. 2008
	CBS150.87	*S. fusca*	Japan	EF127879	EF139109	de Meyer et al. 2008
S. palmiculminata	CMW23049	*Protea repens*	South Africa	DQ316191	DQ821543	Francois et al. 2006
S. phasma	CMW20676	*P. laurifolia*	South Africa	DQ316219	DQ821541	Francois et al. 2006
S. proteara	CMW1103	*P. caffra*	South Africa	DQ316203	DQ316165	Francois et al. 2006
S. schenckii	MITS2474	N/A	Mexico	KP132783	N/A	Irinyi et al. 2015
	CBS 938.72	Human	Franch	KP017094	N/A	Irinyi et al. 2015
S. fusiforis	CMW9968	*Populus nigra*	Azerbaijan	AY280481	AY280461	Aghayeva et al. 2004
S. lunata	CMW10563	*Carpinus betulus*	Austria	AY280485	AY280466	Zhou et al. 2006
S. narcissi	CBS138.50	N/A	Canada	AY194510	KX590765	Jacobs et al. 2003
S. splendens	CMW872	*Protea repens*	South Africa	DQ316215	DQ316177	Francois et al. 2006
S. stenoceras	CMW2524	*Acacia mearnsii*	South Africa	AF484459	AY280473	de Beer et al. 2003
	CBS237.32	pine pulp	Norway	AF484462	N/A	de Beer et al. 2003
S. thermara	CMW38930	*Euphorbia ingens*	South Africa	KR051115	KR051103	Ja et al. 2016
	CMW38929	*E. ingens*	South Africa	KR051114	KR051102	Ja et al. 2016
S. stylites	CMW14543	Pine utility poles	Australia	EF127883	EF139096	de Meyer et al. 2008
Ophiostoma adjuncti	CMW135	*Pinus ponderosa*	USA	AY546696	N/A	Zhou et al. 2004
O. allantosporum	CBS185.86	*P. pinaster*	Europe	AY934506	N/A	Villarreal et al. 2005
O. angusticollis	Zoq16	N/A	N/A	EU109671	N/A	de Beer et al. 2016
	CBS186.86	*Pinus banksiana*	USA	AY924383	KX590757	Villarreal et al. 2005
O. bicolor	CBS492.77	*Picea glauca*/*Ips* sp.	USA	DQ268604	DQ268635	Massoumi et al. 2007
O. candidum	CMW26484	*Eucalyptus cloeziana*	South Africa	HM051409	HM041874	Nkuekam et al. 2012
	CMW26483	*E. cloeziana*	South Africa	HM051408	HM041873	Nkuekam et al. 2012
O. catonianum	C1084	*Pyrus*	Italy	AF198243	N/A	Gorton et al. 2004
O. coronatum	CBS 497.77	*Pinus pinaster*	Iberian Peninsula	AY924385	KX590758	Villarreal et al. 2005
O. cupulatum	C1194	*Pseudotsuga*	USA	AF198230	N/A	Uzunovic et al. 2000
O. deltoideosporum	WIN(M)41	N/A	N/A	EU879121	N/A	Mullineux and Hausner 2009

Species	Strain No.	Host/insect	Country	Genbank No.		Reference
				ITS	β-tubulin	
O. fasciatum	UM56	*Pseudotsuga menziesii*	Canada Canada	EU913720	EU913759	Plattner et al. 2009
O. floccosum	C01-021	Girdled *Picea rubens*	Canada	AY194504	N/A	Jacobs et al. 2003
	C1086	Soil	Sweden	AF198231	N/A	Gorton et al. 2004
O. fumeum	CMW26813	*Eucalyptus cloeziana*	South Africa	HM051412	HM041878	Nkuekam et al. 2012
	CMW26818	*E. cloeziana*	South Africa	HM051415	HM041877	Nkuekam et al. 2012
O. fuscum	CMW23196	*Picea abies*	Finland	HM031504	HM031563	Linnakoski et al. 2010
O. himai ulmi	C1183	*Ulmus*	India	AF198233	N/A	Harrington et al. 2001
	C1306	*Ulmus*	India	AF198234	N/A	Harrington et al. 2001
O. ips	CMW7075	N/A	USA	AY546704	N/A	Zhou et al. 2004
	CMW22843	*Orthotomicus erosus*	N/A	DQ539549	N/A	Romón et al. 2007
O. japonicum	YCC099	N/A	N/A	GU134169	N/A	Yamaoka et al. 2009
O. kryptum	DAOM 229701	*Picea abies*/ *Tetropium* sp.	Austria	AY304436	AY305685	Jacobs and Kirisits 2013
	DAOM 229702	*Larix decidua*/ *T. gabrieli*	Austria	AY304434	AY305686	Jacobs and Kirisits 2013
	K6/3/2	*Picea abies*/ *Tetropium* sp.	Austria	AY304428	AY305687	Jacobs and Kirisits 2013
O. minus	PIR 18S	N/A	N/A	AY934509	N/A	Villarreal et al. 2005
	CMW22802	*Dryocoetes autographus*	N/A	DQ539507	N/A	Romón et al. 2005
	RJ-T144	*Tetropium* sp.	Poland	AM943886	N/A	Jankowiak and KolařÍk 2010
	CMW28117	*Picea abies*/ *Tomicus minor*	Russia	HM031497	HM031535	Linnakoski et al. 2010
	AU58.4	*Lodgepole pine*	Canada	AF234834	N/A	Gorton et al. 2004
	DAOM 212686	N/A	Canada	AY304438	AY305690	Jacobs and Kirisits 2013
O. micans	CMW:38903	*Picea crassifolia*	China	KU184432	KU184303	Yin et al. 2016
O. montium	CMW13221	*Pinus ponderosa*/ *Dendroctonus ponderosae*	USA	AY546711	N/A	Zhou et al. 2004
	CMW13222	*P. contorta*/ *D. ponderosae*	Canada	AY546712	N/A	Zhou et al. 2004
O. nigrocarpum	CMW 560	*Abies* sp.	USA	AY280489	AY280479	Aghayeva et al. 2004
	CMW651	*Pseudotsuga menziesii*	USA	AY280490	AY280480	Aghayeva et al. 2004
O. nitidum	CMW:38907	*Picea crassifolia*	China	KU184437	KU184308	Yin et al. 2016
O. novo ulmi	C1185	*Ulmus*	Russia	AF198235	N/A	Harrington et al. 2001
	C510	*Ulmus*	USA	AF198236	N/A	Harrington et al. 2001
O. olgensis	CXY1404	*Larix gmelinii*/ *Ips subelongatus*	China	KU551299	KU882938	Wang et al. 2016
	CXY1405	*L. gmelinii*/ *I. subelongatus*	China	KU551300	KU882939	Wang et al. 2016
	CXY1410	*L. gmelinii*/ *I. subelongatus*	China	KU551303	KU882942	Wang et al. 2016
O. pallidulum	CMW23279	*Pinus sylvestris*/ *Hylastes brunneus*	Finland	HM031509	N/A	Linnakoski et al. 2010
	CMW23278	*P. sylvestris*/ *H. brunneus*	Finland	HM031510	HM031566	Linnakoski et al. 2010

Species	Strain No.	Host/insect	Country	Genbank No.		Reference
				ITS	β-tubulin	
O. piceae	C1087	N/A	Germany	AF198226	N/A	Uzunovic et al. 2000
	C1246	*Pseudotsuga*	USA	AF198227	N/A	Uzunovic et al. 2000
O. pseudotsugae	92-634/302/6	*Pinus menziesii*/ *Dendroctonus frontalis*	Canada	AY542502	AY548744	Gorton et al. 2004
	D48/3	N/A	Canada	AY542501	AY542511	Gorton et al. 2004
O. proteasedis	CMW*28601*	*Protea caffra*	Zambia	EU660449	EU660464	Roets et al. 2009
O. pulvinisporum	CMW9022	*Pinus pseudostrobus*/ *Dendroctonus mexicanus*	Mexico	AY546714	DQ296100	Zhou et al. 2004
O. qinghaiense	CMW:38902	*Picea crassifolia*	China	KU184445	KU184316	Yin et al. 2016
O. querci	C970	*Quercus*	United Kingdom	AF198239	N/A	Gorton et al. 2004
	C969	*Quercus*	United Kingdom	AF198238	N/A	Gorton et al. 2004
	C1085	*Fagus*	Germany	AF198237	N/A	Gorton et al. 2004
O. rostrocoronatum	CBS434.77	Woodpulp	USA	AY194509	KX590771	Jacobs et al. 2003
O. saponiodorum	CMW29497	*Picea abies*/*Ips typographus*	Finland	HM031507	HM031571	Linnakoski et al. 2010
	CMW28135	*P. abies*	Russia	HM031508	N/A	Linnakoski et al. 2010
O. sejunctum	Ophi 1B	N/A	N/A	AY934520	N/A	Villarreal et al. 2005
	Ophi 1A	N/A	N/A	AY934519	N/A	Villarreal et al. 2005
O. setosum	AU160-38	*Pseutotsugae menziesii*	North America	AF128929	N/A	Uzunovic et al. 2000
	CMW12378	*Tsuga* sp.	China	FJ430485	FJ430515	Grobbelaar et al. 2009
O. tenellum	CBS189.86	*Pinus banksiana*	USA	AY934523	KX590772	Villarreal et al. 2005
O. tetropii	C00-027a	*Tetropium fuscum*	Canada	AY194482	NA	Jacobs et al. 2003
	C00-003	*T. fuscum*	Canada	AY194485	AY305701	Jacobs et al. 2003
O. ulmi	C1182	*Ulmus*	Netherlands	AF198232	N/A	Harrington et al. 2001
Graphilbum crescericum	CMW 22829	*Hylastes ater*	Spain	DQ539535	N/A	Romón et al. 2007
Gra. fragrans	C1224	*Pinus sylvestris*	Sweden	AF198248	N/A	Harrington et al. 2001
Gra. microcarpum	YCC612	Japanese larch logs	Japan	GU134170	N/A	Yamaoka et al. 2009
Gra. rectangulosporium	MAFF 238951	N/A	Japan	AB242825	N/A	Ohtaka et al. 2006
Raffaelea canadensis	CBS 168.66	N/A	N/A	GQ225699	N/A	Kyunghee et al. 2009
Leptographium lundbergii	DAOM 64746	N/A	N/A	EU879151	AY534943	Mullineux and Hausner 2009
L. truncatum	WIN(M)1435	*Pinus taeda*	South Africa	AY935626	N/A	Hausner et al. 2005

ITS = internal transcribed spacer regions 1 and 2 of the nuclear ribosomal DNA operon, including the 5.8S region; *tub*2 = beta-tubulin;

N/A= represents information that are not available.

CMW = Culture Collection of the Forestry and Agricultural Biotechnology Institute; CBS = The culture collection of Westerdijk Fungal Biodiversity Institute, Utrecht, the Netherlands; MAFF = Ministry of Agriculture, Forestry, and Fisheries, Genetic Resource Centre, Culture Collection of National Institute of Agrobiological Resources, Japan; CXY (Culture Xingyao): Culture collection of the Research Institute of Forest Ecology, Environment and Protection, Chinese Academy of Forestry.

Sporothrix dataset contained 8 species, 17 sequences and 403 characters, including gaps. The *O. minus* dataset contained 5 species, 17 sequences and 447 characters, including gaps. The *O. tenellum* dataset contained 8 species, 14 sequences and 280 characters, including gaps.

For each phylogenetic tree, MP, ML and BI analyses yielded trees with very similar topologies. Phylograms, generated by the MP analysis, are presented for all the datasets, with nodal support obtained from ML indicated at the nodes (Figure 1). In addition, posterior probabilities (above 90%), obtained from BI, are indicated by bold lines at the relevant branching points. Analyses of the ITS1–5.8S–ITS2 region revealed that the analysed strains formed six distinct clades (Figure 1).

According to the ITS sequence analysis, strains of the morphological group A nested in the *Sporothrix* lineage, as defined by de Beer et al. (2016). They form a well-supported independent clade, closely related to *S. nebularis*, *S. epigloea* and *S. eucalyptigena*. Strains exhibiting morphotypes B, C and D formed three clades in the *Ophiostoma s. str* lineage (de Beer and Wingfield 2013). Group B strains nested in the *O. minus* complex, with *O. olgensis* forming a well-supported clade, which closely related to *O. kryptum* (Linnakoski et al. 2010, de Beer and Wingfield 2013, Wang et al. 2016). Group C strains nested within the well-supported *O. ips* clade. Group D strains nested within the *Ophiostoma* lineage and closely related to *O. saponiodorum* and *O. pallidulum*. Finally, strains exhibiting morphotypes E and F nested in the *Graphilbum* and *Raffaelea s. l.* lineages, respectively (de Beer and Wingfield 2013) (TL=821, CI=0.5445, RI=0.8046, HI=0.4555, RC=0.4381 in the MP phylogenetic tree).

Phylogenetic inferences based on *tub2* sequences revealed that clade A, B and D strains formed three well-supported independent clades within the *Sporothrix* and *Ophiostoma* lineages, respectively. Clade C strains nested within the well-supported *O. ips* clade (Suppl. material 1).

Considering morphological differences, strains in groups A, B and D represent three undescribed species of *Sporothrix* or *Ophiostoma*. We concluded that group C strains belong to *O. ips*; group E and F strains clustered together with the well-supported *Graphilbum rectangulosporium* and *O. deltoideosporum* clades, respectively. However, because of a limited number of strains, further analysis of this potential species will need to be postponed until a sufficient amount of material obtained.

Taxonomy

Based on the phylogenetic signals of the ITS and *tub2* and morphological characteristics, all strains analysed in the current study were assigned to six different groups (A–F). They represent one known species, *O. ips* (Rumbold 1931, Upadhyay 1981, Benade et al. 1995, Rane and Tattar 1987, Suh et al. 2013, Zhao et al. 2013) and two uncertain species (*Gra*. cf. *rectangulosporium* and *O*. cf. *deltoideosporum*) and the three species are hereby described as new species.

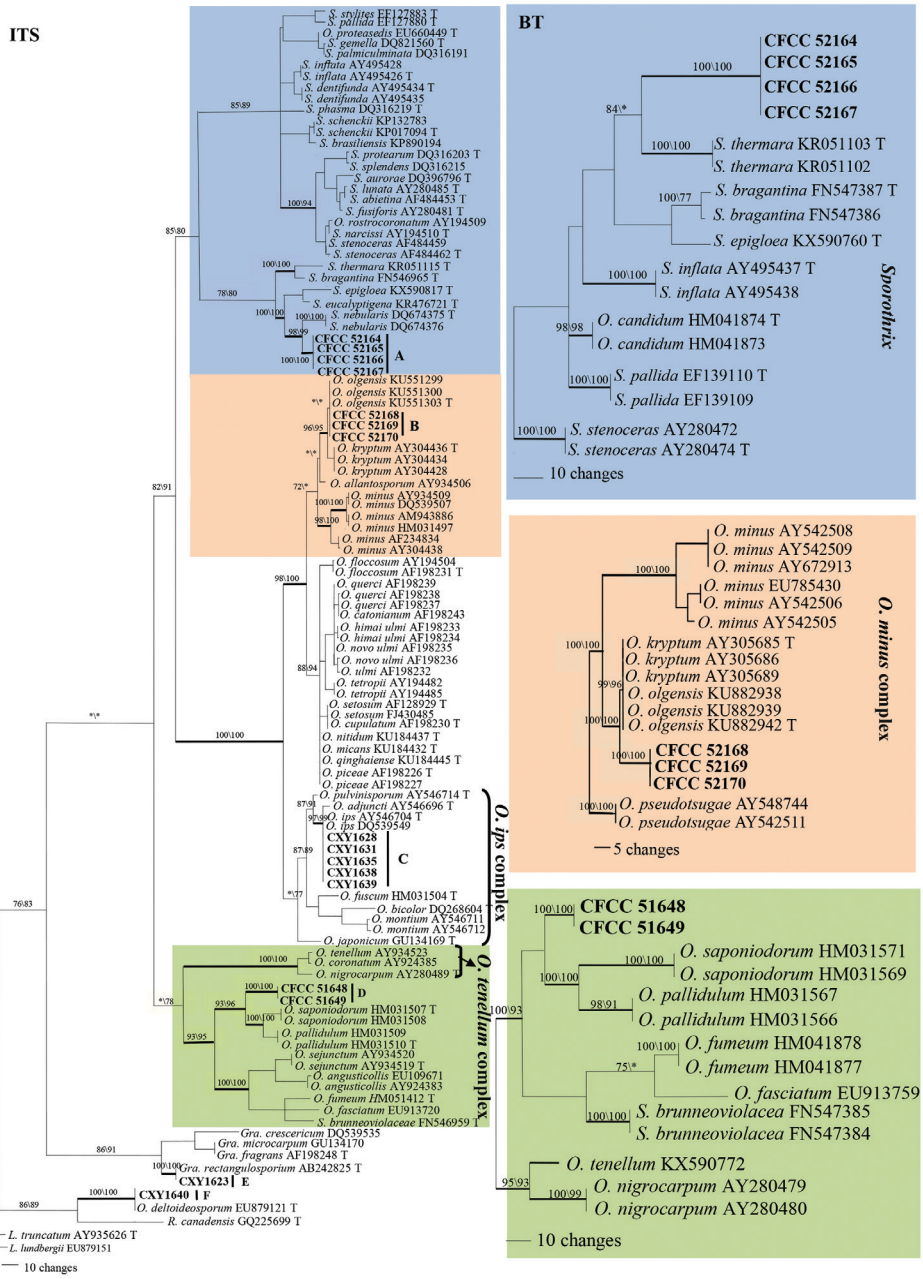

Figure 1. Phylograms of fungal associates of pine infected by PWN and *Monochamus alternatus* in China. The phylograms were generated after MP analysis of the ITS1–5.8S–ITS2 rDNA and partial *tub2* sequences. Novel sequences obtained in the current study are indicated in bold type. MP bootstrap values (10,000 replicates) and ML bootstrap support values (1000 replicates) (normal type) above 70% are indicated at the nodes. Values below 70% are indicated by asterisk (*). Posterior probabilities (above 90%) obtained from BI are indicated by bold lines at the relevant branching points. Scale bar, total nucleotide differences between taxa; ML, maximum likelihood; MP, maximum parsimony; BI, Bayesian inference.

Sporothrix zhejiangensis **Wang & Lu, sp. nov.**
MycoBank: MB825556
Figure 2

Etymology. The epithet reflects Zhejiang Province in China where the species was first collected.

Type. CHINA, Zhejiang, Yuyao City, from *Monochamus alternatus* gallery in *Pinus massoniana* infested by numerous PWN, November 2012, collected by Q Lu and YY Lun, culture ex-holotype MUCL 55183 = CFCC52165 = CXY1614.

Description. Sexual morph perithecial: Perithecia occasional on 2% MEA, emerging from the superficial mycelium or partly iμmersed, with a globose base, (75–)80–108(–120) μm in diameter, with some basal hyphal ornamentation, black; extending progressively into a straight, brown to black neck, (127–)156–550(–631) μm long, (26–)32–58.5(–65) μm wide at the base, (7–)7.5–10.7(–12) μm wide at the apex; ending in a crown of hyaline, (6–)9–19.5(–24) μm long ostiolar hyphae; ascospores reniform in side view, without sheath, aseptate, hyaline, (2–)2.2–3.4(–4) × (0.6–)0.74–2(–2.5) μm.

Asexual morph: pesotum-like and sporothrix-like.

Pesotum-like: Conidiophores macronematous, synnematous, abundant in 2% MEA. Synnemata occurring singly, enlarging towards both the apex and the base, dark brown at base, becoming paler toward the apex, (100–)120–260(–290) μm long including the conidiogenous apparatus, (56–)63–145(–158) μm wide at base, rhizoids present; conidiogenous cells (7–)9.5–29(–45.5) × 1–2(–1.7) μm; conidia hyaline, aseptate, single-celled, smooth, cylindrical or obovoid, (2–)2.5–4.8(–6) × (0.5–)0.8–2.1(–2.6) μm.

Sporothrix-like: Conidiophores micronematous, single on aerial mycelia, unbranched, (4.5–)9.6–31.5(–51.5) × (1.0–)1.5–2(–2.4) μm; conidia hyaline, smooth, aseptate, ellipsoid to ovoid, (2.5–)3–4.8(–5) × (0.7–)1–2.1(–2.5) μm.

Culture characteristics. Colonies on 2% MEA medium are white, with colony edge thinning radially. Hyphae are superficial on agar. Diameter reaches 50 μm in the dark after 8 d at 25 °C, able to grow at 5 °C and 40 °C, with the optimal growth temperature of 30 °C. Growth characteristics on PDA medium are similar.

Habitat and distribution. Galleries of *Monochamus alternatus* in *Pinus massoniana* infested by PWN; known hitherto from Zhejiang Province, China.

Additional specimens examined. CHINA, Zhejiang, Yuyao City, from *Monochamus alternatus* galleries in *Pinus massoniana* infested by PWN, November 2012, collected by Q Lu and YY Lun, MUCL 55181 = CFCC 52167 = CXY1612, MUCL 55182 = CFCC 52164 = CXY1613, MUCL 55184 = CFCC 52166 = CXY1615.

Note. *Sporothrix zhejiangensis* is characterised by a sexual and two asexual forms (pesotum-like and sporothrix-like). It is phylogenetically related to *S. nebulare*, *S. eucalyptigena* and *S. epigloea* (Figure 1). *Sporothrix zhejiangensis* differs from *S. nebulare* in both ascomatal and conidial features. The perithecial neck of *S. nebulare* is shorter than that of *S. zhejiangensis*, respectively (140–)169–293(–365) μm and (127–)156–550(–631) μm.

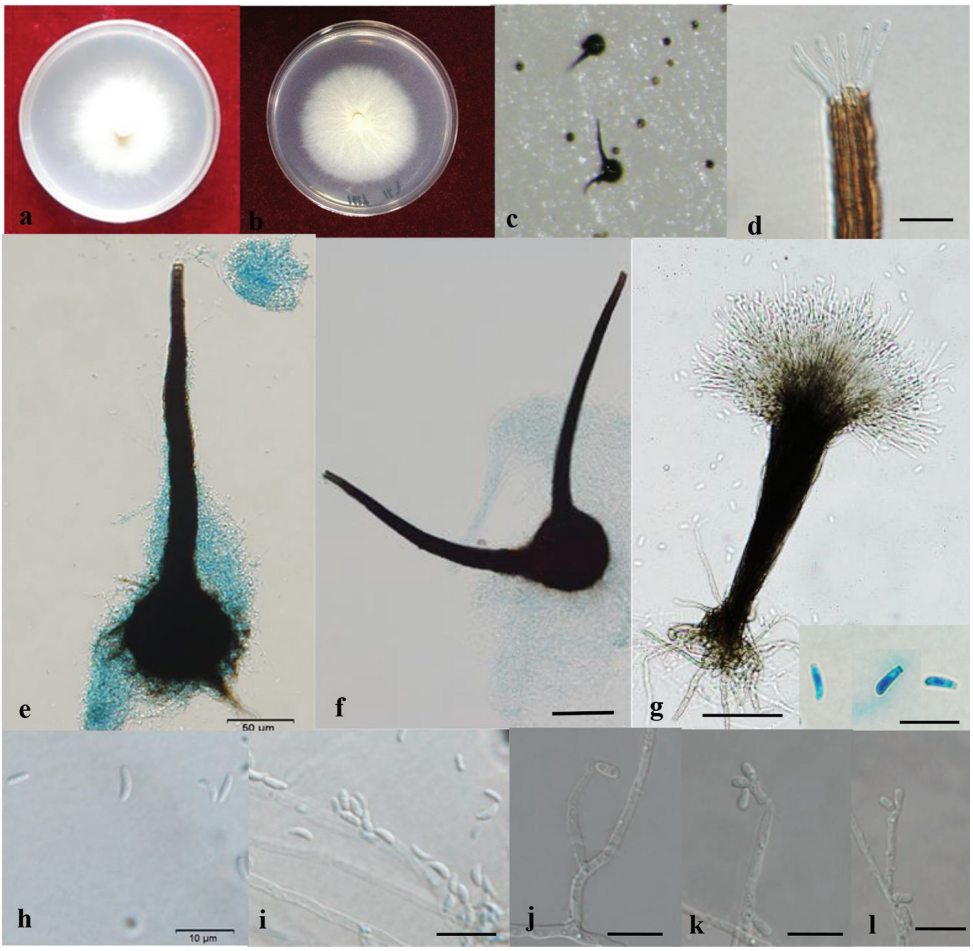

Figure 2. Light micrographs of *Sporothrix zhejiangensis*. **a–c** Growth on 2% MEA and 2% PDA, 2 weeks after inoculation **d** Occasionally observed ostiolar hyphae (scale bar, 20 µm) **e–f** Perithecium (scale bar, 20 µm) **g** Pesotum-like anamorph, rhizoid, conidiophores, conidiogenous apparatus (scale bar, 20 µm), and conidia (bottom right corner) (scale bar, 10 µm) **h, i** Reniform ascospores without sheaths (scale bar, 10 µm) **j–l** Sporothrix-like anamorph, conidiophores, and conidia (scale bar, 10 µm).

The conidia of *S. nebulare* also are smaller than those of *S. zhejiangensis*, mostly respectively 2.9–3.7 × 1.1–1.3 µm and 3–4.8 × 1–2.1 µm (Romón et al. 1900).

Sporothrix eucalyptigena and *S. epigloea* produce perithecia and ascospores similar to those of *S. zhejiangensis* (Crous et al. 2015, Upadhyay 1981). However, *S. eucalyptigena* has a slightly wider neck than *S. zhejiangensis* (20–35 *vs*. 9–19.5 µm) and longer ostiolar hyphae. Furthermore, *S. eucalyptigena* and *S. epigloea* only produce a sporothrix-like asexual state and their conidia differ from those of *S. zhejiangensis* either in size or in shape. *Sporothrix eucalyptigena* has drop-shaped (lacrymoid) conidia, differing from the ellipsoid to ovoid conidia in *S. zhejiangensis*. Conidia of *S. epigloea*

are larger than those of *S. zhejiangensis* (2.5–9 × 1–3.5 *vs*. 3–4.8 × 1–2.1 µm) (Crous et al. 2015). Another conspicuous difference between *S. zhejiangensis* and *S. eucalyptigena* is the growth rate; the former grows much faster than the latter (50 µm in 8 d *vs*. 50 µm in 30 d at 25 °C) (Upadhyay 1981).

Sporothrix zhejiangensis is also closely related to *S. bragantina* and *S. thermara* (Figure 1) (Pfenning and Oberwinkler 1993, de Beer et al. 2016). These three species display the same optimal growth temperature (30 °C) and a similar conidial shape (ellipsoid to obovoid) of their sporothrix-like morph. However, the perithecial base of *S. bragantina* is larger than that of *S. zhejiangensis* [globose base: 130–220 µm *vs*. (75–)80–108(–120) µm and the neck also is longer, 700–1200 µm *vs*. (127–)156–550(–631) µm]. The sporothrix-like conidia of *S. bragantina* also are larger than those of *S. zhejiangensis* (4–6 × 2–2.5 µm *vs*. 3–4.8 × 1–2.1 µm). *Sporothrix thermara*, hitherto, has no known sexual state. It only known by sporothrix-like state; conidia of *S. thermara* are larger than those of *S. zhejiangensis* (4–6 × 2–3 µm *vs*. 3–4.8 × 1–2.1 µm).

Ophiostoma album **Wang & Lu, sp. nov.**
MycoBank: MB825557
Figure 3

Etymology. The epithet reflects the white colour of the colonies.

Type. CHINA, Zhejiang, Yuyao City, from *Monochamus alternatus* gallery of *Pinus massoniana* infested by numerous PWN, November 2012, collected by Q Lu and YY Lun, culture ex-holotype MUCL 55189 = CFCC 52168 = CXY1622.

Description. Sexual form: Unknown. Asexual form: Hyalorhinocladiella-like. Conidiogenous cells micronematous, (4.2–)9.5–16.5(–20.5) × (0.5–)1–2(–2.5) µm; conidia hyaline, single-celled, aseptate, clavate or fusiform obovoid with pointed bases and (occasionally) rounded apices, slightly curved at the base (4–)4.2–14.5(–18) × (0.5–)1–2(–2.3) µm.

Culture characteristics. Colonies on 2% MEA white, with the mycelium edge thinning radially; Hyphae are superficial on agar, sporulation weak. Colonies slowly growing, reaching 18.5 µm in diameter at 8 d at 25 °C, able to grow at 40 °C but not at 5 °C, with the optimal growth temperature of 35 °C. Growth characteristics on PDA culture medium are similar but the growth rate is slower than on MEA.

Habitat and distribution. Galleries of *Monochamus alternatus* in *Pinus massoniana*, infested by PWN, in Zhejiang Province, China.

Additional specimens examined. CHINA, Zhejiang, Yuyao City, from *Monochamus alternatus* galleries of *Pinus massoniana* infested by numerous PWN, November 2012, collected by Q Lu and YY Lun, MUCL 55190 = CFCC 52169 = CXY1642, CXY1643 = CFCC 52170.

Note. *Ophiostoma album* only known in its asexual hyalorhinocladiella-like form. According to both ITS and *tub2* based phylogenetic analysis, it is closely related to *O. kryptum* and *O. olgensis* in the *O. minus* complex (Figure 1). *Ophiostoma album* is

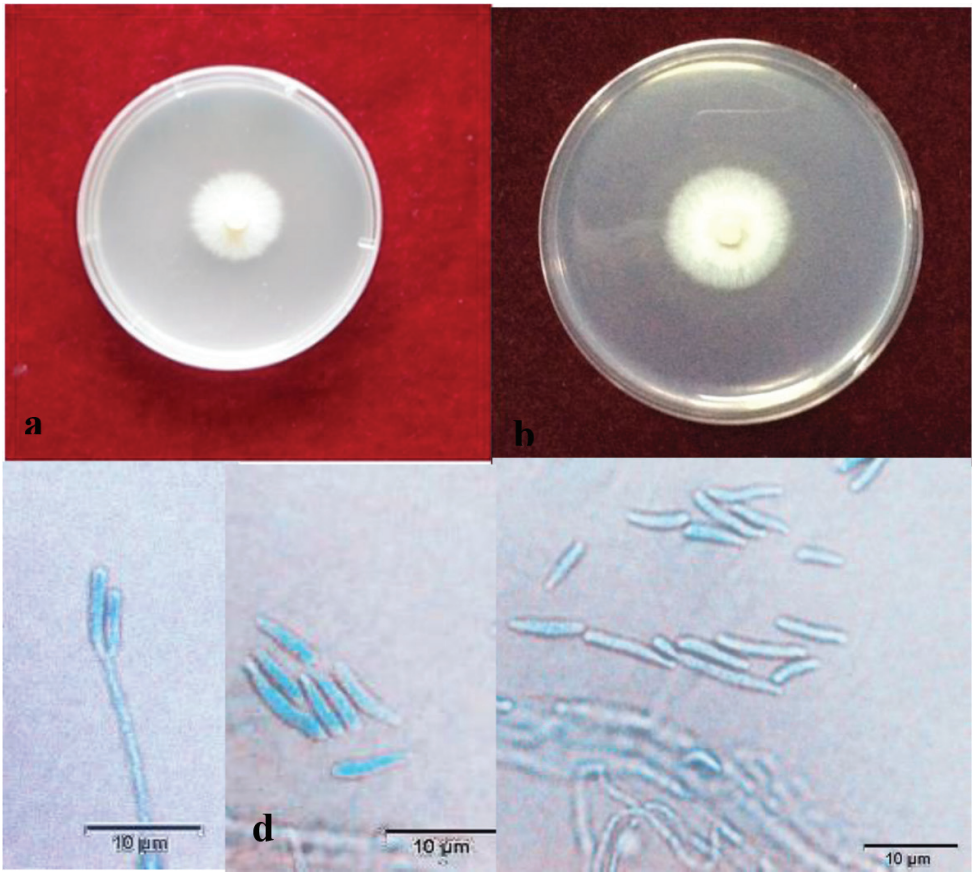

Figure 3. Light micrographs of *Ophiostoma album*. **a, b** Growth on 2% MEA and 2% PDA, 2 weeks after inoculation **c–e** Hyalorhinocladiella-like anamorph, conidiophores, and conidia (scale bar, 10 mm).

easily distinguished from *O. olgensis* and *O. kryptum* based on their reproduction structure. *Ophiostoma album* only produces a hyalorhinocladiella-like asexual form *in vitro*, whereas the two other species produce both a sexual and asexual forms *in vitro* (Jacobs and Kirisits 2003, Wang et al. 2016). The conidial size and shape of the three species are obviously different. *Ophiostoma album* produces clavate or fusiform to obovoid and sometimes, slightly curved conidia; these are obovoid with pointed bases in both *O. olgensis* and *O. kryptum*. Furthermore, the conidia of *O. album* are much larger, 4.2–14.5 × 1.0–1.9 µm *vs*. 1.5–7 × 1.5–5 µm in the two other species.

Ophiostoma massoniana **Wang & Lu, sp. nov.**
MycoBank: MB825558
Figure 4

Etymology. The epithet reflects the host tree, *Pinus massoniana*.

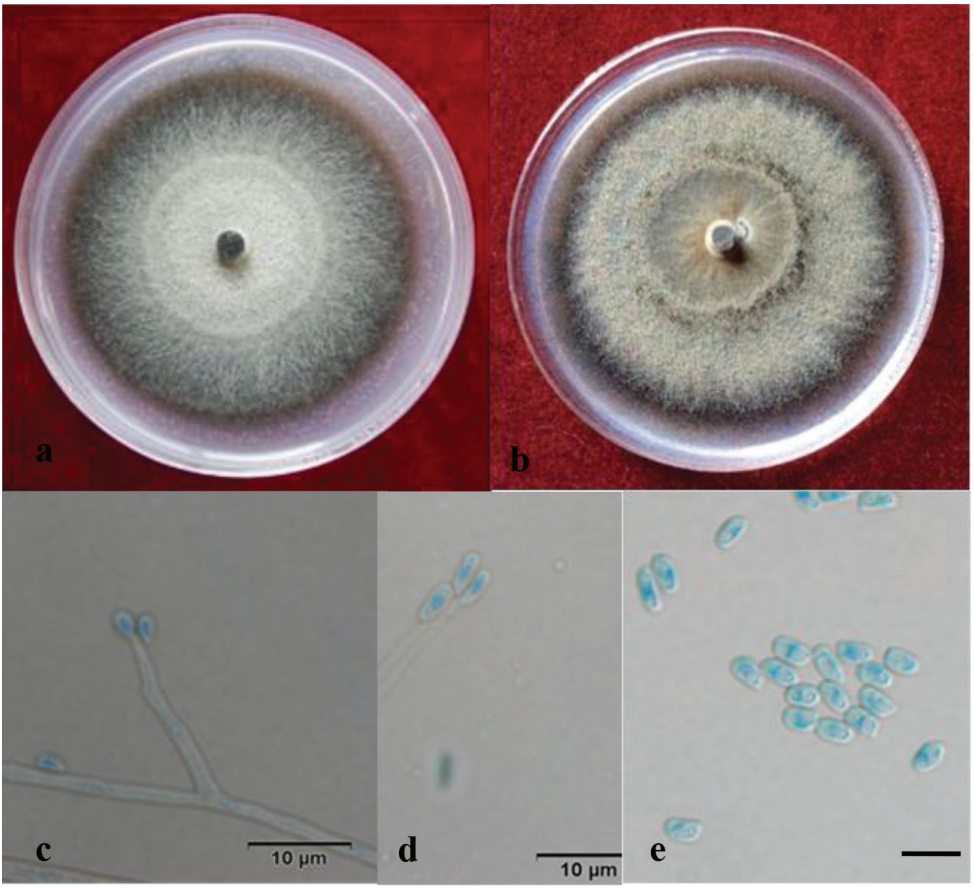

Figure 4. Light micrographs of *Ophiostoma massoniana*. **a, b** Growth on 2% MEA and 2% PDA, 2 weeks after inoculation **c–e** Hyalorhinocladiella-like anamorph, conidiophores, conidia (scale bar, 10 µm).

Type. CHINA, Zhejiang Province, Fuyang City, from *Monochamus alternatus* gallery in *Pinus massoniana* infested by numerous PWN, November 2012, collected by Q Lu and YY Lun, culture ex-holotype, MUCL 55179 = CFCC 51648 = CXY1610.

Description. Sexual form: Unknown. Asexual form: Hyalorhinocladiella-like. Conidiophores abundant, single, borne on aerial hyphae, (3.3–)10.5–27.5(–42.5) × (0.7–)1.3–2.0(–2.7) µm; conidia hyaline, single-celled, aseptate, obovoid or globose with pointed bases and rounded apices, (2–)2.2–3.9(–5) × (0.5–)0.7–1.7(–2) µm.

Culture characteristics. Colonies on 2% MEA brown, the marginal hyphae sparse and radiating; some white mycelium produced early during growth that becomes black after 3–5 d. Colonies slowly growing, reaching 37.5 µm in diameter over 8 d at 25 °C, able to grow at 5 °C and 40 °C, with an optimal growth temperature of 30 °C; sporulation weak. On PDA culture medium, the colonies are dark brown; the mycelium is white, long and dense, with a daily growth of 4 µm at 25 °C.

Habitat and distribution. Galleries of *Monochamus alternatus* in *Pinus massoniana* infested by PWN, in Zhejiang Province, China.

Additional specimens examined. CHINA, Zhejiang Province, Yuyao City, from *Monochamus alternatus* galleries in *Pinus massoniana* infested by numerous PWN, November 2012, collected by Q Lu and YY Lun, MUCL 55180 = CFCC 51649 = CXY1611.

Note. *Ophiostoma massoniana*, only known by its asexual, hyalorhinocladiella-like state, does not cluster in any of the 10 species complexes defined by de Beer and Wingfield (2013) in *Ophiostoma* s. l. According to the ITS and *tub2* phylogenetic analysis, the species is related to *O. saponiodorum* and *O. pallidulum* (Figure 1). *Ophiostoma pallidulum* also only produces asexual hyalorhinocladiella-like morphs *in vitro*, whereas *O. saponiodorum* produces a sexual and two asexual morphs (pesotum-like and hyalorhinocladiella-like). In addition, *O. massoniana* differs from *O. saponiodorum* in producing smaller conidia [(2–)2.2–3.9(–5) × (0.5–)0.7–1.7(–2) µm vs. (3–)4–6(–7) × 1–1.5(–2) µm] (Linnakoski et al. 2010). Further, the colour of *O. massoniana* colonies is different from that of the other two species. Namely, *O. massoniana* forms brown to dark brown colonies, while the other two species form pale colonies (Linnakoski et al. 2010).

Discussion

In the current study, six ophiostomatoid species were found associated with pines infected by *M. alternatus* and PWN in the eastern provinces of Shandong and Zhejiang in China: *O. ips*, the newly described *S. zhejiangensis*, *O. album*, *O. massoniana* and two species whose identities are uncertain; *O*. cf. *deltoideosporum* and *Gra*. cf. *rectangulosporium*. *Ophiostoma ips* was the most frequently isolated species, accounting for over 90% of all Ophiostomatales strains.

Ophiostoma ips was originally reported in association with bark beetles infecting pines in south-eastern North America (Rumbold 1931). It has been since reported in Central and South America (Mexico and Chile), Europe (Austria and Sweden), Asia (China, Japan and Korea), Africa (South Africa) and Australasia (New Zealand) (Rumbold 1931, Benade et al. 1995, Rane and Tattar 1987, Zhou et al. 2002; Lu et al. 2009, Suh et al. 2013, Zhao et al. 2013; 2014). Furthermore, *O. ips* is a ubiquitous sapstain fungus associated with PWN and *Monochamus* spp. (Zhao et al. 2014).

In China, *O. ips* was reportedly associated with *P. massoniana* infected by PWN (Zhao 1992, Zhao et al. 2006, 3013) and with *P. tabuliformis* infected by *Dendroctonus valens* (Lu et al. 2009), two invasive pests of the local conifer ecosystems. Zhao et al. (2013) reported *O. ips* an isolation frequency of 37% in three ophiostomatoid fungal communities associated with PWN, much lower than that reported in the current study.

Ophiostoma ips appears to have travelled long-distances in wood materials presumably originating from North America (Zhou et al. 2007). The cited study did not consider any Asian population, however. Nevertheless, the high population density of *O. ips* in China suggests either indigenous origin or effective adaption after the inva-

sion to local pine forests, with a long evolution history. To verify this hypothesis, it will be necessary to analyse the dispersal routes of PWN populations in different areas globally and of the fungus–including Asian populations.

Members of *Sporothrix* are reportedly associated with a wide range of habitats (De Hoog 1974, Kwon-Chung and Bennet 1992, Roets et al. 2006, Zhou et al. 2006, Madrid et al. 2009), e.g. wood (Aghayeva et al. 2004), human (de Beer et al. 2016) and the soil (De Meyer et al. 2008). The genus is characterised by reniform ascospores without a mucilaginous sheath and sporothrix- and pesotum-like asexual states (Linnakoski et al. 2010, de Beer et al. 2013). Genetically, the species of the *Sporothrix* lineages lack the intron 4 but have intron 5 in the BT gene (Zipfel et al. 2006).

Sporothrix zhejiangensis forms an independent lineage according to both ITS and *tub2* based on phylogenetic inferences. It is closely related to *S. nebulare*, *S. eucalyptigena*, *S. epigloea*, *S. bragantina* and *S. thermara* (Madrid et al. 2010, Romón et al. 1900, Crous et al. 2015, de Beer et al. 2016, Van der Linde et al. 2016) (Figure 1). *Sporothrix nebulare* was first described after isolation from *Hylastes attenuatus* infesting *P. radiata* in Spain (Romón et al. 1900). *Sporothrix eucalyptigena* was recently isolated from *Eucalyptus marginata* (Myrtaceae) in Western Australia (Crous et al. 2015). *Sporothrix epigloea* was isolated from *Tremella fuciformis* in Argentina (Upadhyay 1981). *S. bragantina* was isolated from the rhizosphere soil in Brazil (Pfenning and Oberwinkler 1993) and *S. thermara* from *Cyrtogenius africus* galleries in diseased *Euphorbia ingens* trees in South Africa (Van der Linde et al. 2016). Hence, *S. zhejiangensis* and these five species differ with respect to their (known) hosts and geographic distributions.

Although *S. zhejiangensis* is unrelated to *S. fusiforis*, *S. lunata* and *S. stenoceras* (Figure 1), these strains exhibit a similar sexual state (Hsiau 1996, Yamaoka et al. 2000, Aghayeva et al. 2004, Zhou et al. 2004). For instance, they all develop one to two perithecial necks emerging from the globular base; occasionally, abnormal specimens of *O. stenoceras* develop up to five necks *in vitro* (Yamaoka et al. 2000).

In the current study, *S. zhejiangensis* was notably different from *Sporothrix* sp. 1 and *Sporothrix* sp. 2 (Zhao et al. 2013) with regard to colony characteristics (*S. zhejiangensis* has a white and radially thinning edge; *Sporothrix* sp. 1: dark, superficial mycelium; *Sporothrix* sp. 2: white, radially dense mycelium). Consequently, the role of *S. zhejiangensis* in PWN needs further research and analysis, ruling out the possibility that the species had been already discovered and its ecological role partially studied.

According to ITS phylogeny analysis, *Ophiostoma album* is related to *O. olgensis* (Wang et al. 2016) in a single but weakly supported clade (Figure 1). This clade nests within the *O. minus* complex, in which it is closely related to *O. kryptum* (Jacobs and Kirisits 2003). The *tub2* dataset confirmed that *O. album* and *O. olgensis* formed two clades.

The *O. minus* complex currently includes *O. minus*, *O. pseudotsugae*, *O. allantosporum*, *O. kryptum* and *O. olgensis* (Jacobs and Kirisits 2003, Gorton et al. 2004, de Beer and Wingfield 2013, Wang et al. 2016). The *tub2* gene of the *O. minus* complex members includes intron 4 but lacks intron 5 (Gorton et al. 2004). *Ophiostoma album* is phylogenetically closely related to *O. olgensis* and *O. kryptum*. Both *O. olgensis* and *O. kryptum* inhabit *Larix* spp. (Jacobs and Kirisits 2003; Wang et al. 2016), whereas

O. album inhabits *P. massoniana*. Both *O. olgensis* and *O. album* occur in China, whereas *O. kryptum* is found in central Europe. Moreover, the three species are associated with different vectors (Jacobs and Kirisits 2003, Wang et al. 2016).

According to both ITS and *tub2* phylogenetic trees, *O. massoniana* forms a separated well-supported clade (Figure 1). It groups with *O. pallidulum* and *O. saponiodorum* (Figure 1), which has been isolated from *Pinus sylvestris* in Finland and *Picea abies* in Russia in association with various bark beetles (Linnakoski et al. 2010). The three species produce a hyalorhinocladiella-like asexual form (Linnakoski et al. 2010; de Beer et al. 2013) and their *tub2* genes lack intron 4 but contain intron 5 (Zipfel et al. 2006).

Conclusions

In the current study, a relatively large number of ophiostomatoid fungal species associated with *B. xylophilus* and *M. alternatus* in Shandong and Zhejiang Provinces in China was identified. Three novel species, *O. album*, *O. massoniana* and *S. zhejiangensis* were discovered and described. Fourteen additional provinces in China are currently also listed as PWN epidemic areas (State Forestry Administration of the People's Republic of China 2018). Hence, additional ophiostomatoid fungi associated with *B. xylophilus* and *M. alternatus* should be discovered and described. Future in-depth studies of the biodiversity, biogeography and ecology of fungi associated with pine wilt disease will contribute to the understanding of disease mechanisms and provide information on effective management methods to alleviate the subsequent plant losses.

Acknowledgments

This work was supported by the National Key R&D Programme of China (2017YFD0600103) and the National Natural Science Foundation of China (Project No.: 31770682). Cony Decock gratefully acknowledges the financial support received from the Belgian State (Belgian Federal Science Policy through the BCCMTM research programme). We are grateful to Professor Yuichi Yamaoka and Hugo Madrid for their invaluable suggestions to improve the manuscript.

References

Aghayeva DN, Wingfield MJ, Kirisits T, Wingfield BD (2005) *Ophiostoma dentifundum* sp. nov. from oak in europe, characterized using molecular phylogenetic data and morphology. Mycological Research 109(Pt 10): 1127. https://doi.org/10.3767/003158509X468038

Aghayeva DN, Wingfield MJ, de Beer ZW, Kirisits T (2004) Two new *Ophiostoma* species with *Sporothrix* anamorphs from Austria and Azerbaijan. Mycologia 96(4): 866–878. https://doi.org/10.2307/3762119

Araujo ML, Rodrigues AM, Fernandes GF, Camargo ZP, Hoog GS (2015) Human *Sporotrichosis* beyond the epidemic front reveals classical transmission types in espírito santo, brazil. Mycoses 58(8): 485. https://doi.org/10.1111/myc.12346

Benade E, Wingfield MJ, Van Wyk PS (1995) Conidium development in the *Hyalorhinocladiella* anamorph of *Ophiostoma ips*. Mycologia 87(3): 298–303. https://doi.org/10.2307/3760826

Chang R, Duong TA, Taerum SJ, Wingfield MJ, Zhou X, De Z B (2017) Ophiostomatoid fungi associated with conifer-infesting beetles and their phoretic mites in yunnan, China. Mycokeys 28(28): 19–64. https://doi.org/10.3897/mycokeys.28.21758

Crous PW, Wingfield MJ, Guarro J, Hernández-Restrepo M, Sutton DA, Acharya K, Barber PA, Boekhout T, Dimitrov RA, Dueñas M, Dutta AK, Gené J, Gouliamova DE, Groenewald M, Lombard L, Morozova OV, Sarkar J, Smith MT, Stchigel AM, Wiederhold NP, Alexandrova AV, Antelmi I, Armengol J, Barnes I, Cano-Lira JF, Castañeda Ruiz RF, Contu M, Courtecuisse PR, da Silveira AL, Decock CA, de Goes A, Edathodu J, Ercole E, Firmino AC, Fourie A, Fournier J, Furtado EL, Geering AD, Gershenzon J, Giraldo A, Gramaje D, Hammerbacher A, He XL, Haryadi D, Khemmuk W, Kovalenko AE, Krawczynski R, Laich F, Lechat C, Lopes UP, Madrid H, Malysheva EF, Marín-Felix Y, Martín MP, Mostert L, Nigro F, Pereira OL, Picillo B, Pinho DB, Popov ES, Rodas Peláez CA, Rooney-Latham S, Sandoval-Denis M, Shivas RG, Silva V, Stoilova-Disheva MM, Telleria MT, Ullah C, Unsicker SB, van der Merwe NA, Vizzini A, Wagner HG, Wong PT, Wood AR, Groenewald JZ (2015) Fungal Planet description sheets: 320–370. Persoonia 34: 167–266. https://doi.org/10.3767/003158515X688433

de Beer ZW, Wingfield MJ (2013) Emerging lineages in the Ophiostomatales. In: Seifert KA, de Beer ZW, Wingfield MJ (Eds) The Ophiostomatoid Fungi: Expanding Frontiers. CBS-KNAW Fungal Biodiversity Centre, Utrecht, The Netherlands, 21–46.

de Beer ZW, Duong TA, Wingfield MJ (2016) The divorce of *Sporothrix* and *Ophiostoma*: solution to a problematic relationship. Studies in Mycology 83: 165–191. https://doi.org/10.1016/j.simyco.2016.07.001

de Beer ZW, Seifert KA, Wingfield MJ (2013) The ophiostomatoid fungi: Their dual position in the sordariomycetes. In: Seifert KA, de Beer ZW, Wingfield MJ (Eds) The Ophiostomatoid Fungi: Expanding Frontiers. CBS-KNAW Fungal Biodiversity Centre, Utrecht, The Netherlands, 1–19.

de Hoog GS (1974) The genera *Blastobotrys*, *Sporothrix*, *Calcarisporium* and *Calcarisporiella* gen. nov. Studies in Mycology 7: 1–84.

de Meyer EM, de Beer ZW, Summerbell RC, Moharram AM, de Hoog GS, Vismer HF, Wingfield MJ (2008) Taxonomy and phylogeny of new wood- and soil-inhabiting species in the *Ophiostoma stenoceras-Sporothrix schenckii* complex. Mycologia 100(4): 647–661. https://doi.org/10.3852/07-157R

Evans H, McNamara DG, Braasch H, Chadoeuf J, Magnusson C (1996) Pest Risk Analysis (PRA) for the territories of the European Union (as PRA Area) on *Bursaphelenchus xylophilus* and its vectors in the genus *Monochamus*. European and Mediterranean Plant Protection Organization Bulletin 26(2): 199–249. https://doi.org/10.1111/j.1365-2338.1996.tb00594.x

Francois R, Wilhelm DBZ, Dreyer LL, Renate Z, Crous P, Wingfield MJ (2006) Multi-gene phylogeny for *Ophiostoma* spp. reveals two new species from *Protea* infructescences. Studies in Mycology 55(1): 199–212.

Futai K (2013) Pine wood nematode, *Bursaphelenchus xylophilus*. Annual Review of Phytopathology 51: 61–83. https://doi.org/10.1146/annurev-phyto-081211-172910

Glass NL, Donaldson GC (1995) Development of primer sets designed for use with the PCR to amplify conserved genes from filamentous ascomycetes. Applied and Environmental Microbiology 61(4): 1323–1330.

Gorton C, Kim SH, Henricot B, Webber J, Breuil C (2004) Phylogenetic analysis of the bluestain fungus *Ophiostoma minus* based on partial ITS rDNA and β-tubulin gene sequences. Mycological Research 108: 759–765. https://doi.org/10.1017/S0953756204000012

Grobbelaar JW, Aghayeva DN, Beer ZWD, Bloomer P, Wingfield MJ, Wingfield BD (2009) Delimitation of *Ophiostoma quercus*, and its synonyms using multiple gene phylogenies. Mycological Progress 8(3): 221–236. https://doi.org/10.1007/s11557-009-0594-4

Guidon S, Gascuel O (2003) A simple, fast, and accurate algorithm to estimate large phylogenies by maximum likelihood. Syst Biol 52: 696–704. https://doi.org/10.1080/10635150390235520

Harrington TC, Mcnew D, Steimel J, Hofstra D, Farrell R (2001) Phylogeny and taxonomy of the *Ophiostoma piceae* complex and the dutch elm disease fungi. Mycologia 93(1): 111–136. https://doi.org/10.2307/3761610

Hsiau PTW (1996) The taxonomy and phylogeny of the mycangial fungi from *Dendroctonus brevicomis* and *D. frontalis* (Coleoptera: Scolytidae). PhD Thesis, Iowa State University, Ames, Iowa.

Hausner G, Iranpour M, Kim JJ, Breuil C, Davis CN, Gibb EA, Loewen PC, Hopkin AA (2005) Fungi vectored by the introduced bark beetle *Tomicus piniperda* in Ontario, Canada, and comments on the taxonomy of *Leptographium lundbergii*, *Leptographium terebrantis*, *Leptographium truncatum*, and *Leptographium wingfieldii*. Canadian Journal of Botany 83(10): 1222–1237. https://doi.org/10.1139/b05-095

Hyun MW, Kim JH, Suh DY, Lee SK, Kim SH (2007) Fungi isolated from pine wood nematode, its vector Japanese pine sawyer, and the nematode-infected Japanese black pine wood in Korea. Mycobiology 35(3): 159–161. https://doi.org/10.4489/MYCO.2007.35.3.159

Irinyi L, Serena C, Garcia-Hermoso D, Arabatzis M, Desnos-Ollivier M, Vu D, Cardinal G, Arthur I, Normand AC, Giraldo A, da Cunha KC, Sandoval-Denis M, Hendrickx M, Nishikaku AS, de Azevedo Melo AS, Merseguel KB, Khan A, Parente Rocha JA, Sampaio P, da Silva Briones MR, Carmona e Ferreira R, de Medeiros Muniz M, Castanon-Olivares LR, Estrada-Barcenas D, Cassagne C, Mary C, Duan SY, Kong F, Sun AY, Zeng X, Zhao Z, Gantois N, Botterel F, Robbertse B, Schoch C, Gams W, Ellis D, Halliday C, Chen S, Sorrell TC, Piarroux R, Colombo AL, Pais C, de Hoog S, Zancope-Oliveira RM, Taylor ML, Toriello C, de Almeida Soares CM, Delhaes L, Stubbe D, Dromer F, Ranque S, Guarro J, Cano-Lira JF, Robert V, Velegraki A, Meyer W (2015) International society of human and animal mycology (isham)-its reference DNA barcoding database-the quality controlled standard tool for routine identification of human and animal pathogenic fungi. Medical Mycology 53(4): 313. https://doi.org/10.1093/mmy/myv008

Ja VDL, Six DL, De Beer WZ, Wingfield MJ, Roux J (2016) Novel ophiostomatalean fungi from galleries of *Cyrtogenius Africus* (scolytinae) infesting dying *Euphorbia Ingens*. Antonie Van Leeuwenhoek 109(4): 589–601. https://doi.org/10.1007/s10482-016-0661-1

Jacobs K, Kirisits T (2003) *Ophiostoma kryptum* sp. nov. from *Larix decidua* and *Picea abies* in Europe, similar to *O. minus*. Mycological Research 107(10): 1231–1242. https://doi.org/10.1017/S0953756203008402

Jacobs K, Seifert KA, Harrison KJ, Kirisits T (2003) Identity and phylogenetic relationships of ophiostomatoid fungi associated with invasive and native *Tetropium* species (coleoptera: cerambycidae) in Atlantic Canada. Canadian Journal of Botany 81(4): 316–329. https://doi.org/10.1139/b03-025

Jacobs K, Wingfield MJ (2001) *Leptographium* Species: tree pathogens, insect associates and agents of blue-stain. American Phytopathological Society Press, St Paul, MN.

Jankowiak R, KolařÍk M (2010) Diversity and pathogenicity of ophiostomatoid fungi associated with *Tetropium* species (coleoptera: cerambycidae) colonizing *Picea abies* in Poland. Folia Microbiologica 55(2): 145–154. Https://doi.org/10.1007/s12223-010-0022-9

Jung J, Han H, Ryu SH, Kim W (2010) Microsatellite variation in the pinewood nematode, *Bursaphelenchus xylophilus* (Steiner and Buhrer) Nickle in South Korea. Genes & Genomics 32(2): 151–158. https://doi.org/10.1007/s13258-009-0842-7

Katoh K, Standley DM (2013) MAFFT multiple sequence alignment software version 7: improvements in performance and usability. Molecular biology and evolution 30(4): 772–780. https://doi.org/10.1093/molbev/mst010t

Kwon-Chung KJ, Bennett JE (1992) Medical mycology. Lea & Febiger, Philadelphia, 866 pp. https://doi.org/10.1590/S0036-46651992000600018

Kyunghee K, Youngjoon C, Sangtae S, Hyeondong S (2009) *Raffaelea quercus-mongolicae* sp. nov. associated with *Platypus koryoensis* on oak in Korea. Mycotaxon 110(8): 189–197.

Linnakoski R, de Beer ZW, Ahtiainen J, Sidorov E, Niemelä P, Pappinen A, Wingfield MJ (2010) *Ophiostoma* spp. associated with pine-and spruce-infesting bark beetles in Finland and Russia. Persoonia: Molecular Phylogeny and Evolution of Fungi 25: 72. https://doi.org/10.3767/003158510X550845

Lu M, Zhou XD, de Beer ZW, Wingfield MJ, Sun JH (2009) Ophiostomatoid fungi associated with the invasive pine-infesting bark beetle, *Dendroctonus valens*, in China. Fungal Divers 38: 133–45.

Madrid H, Cano J, Gene J, Bonifaz A, Toriello C, Guarro J (2009) *Sporothrix globosa*, a pathogenic fungus with widespread geographical distribution. Rev Iberoam Micol 26: 218–222. https://doi.org/10.1016/j.riam.2009.02.005

Madrid H, Gene J, Cano J, Silvera C, Guarro J (2010) *Sporothrix brunneoviolacea* and *Sporothrix dimorphospora*, two new members of the *Ophiostoma stenoceras-Sporothrix schenckii* complex. Mycologia 102(5): 1193–1203. https://doi.org/10.3852/09-320

Maehara N, Futai K (1997) Effect of fungal interactions on the numbers of the pinewood nematode, *Bursaphelenchus xylophilus* (Nematoda: Aphelenchoididae), carried by the Japanese pine sawyer, *Monochamus alternatus* (Coleoptera: Cerambycidae). Fundamental and applied Nematology 20(6): 611–618.

Mamiya Y, Shoji T (2009) Pathogenicity of the pinewood nematode, *Bursaphelenchus xylophilus*, to Japanese larch, *Larix kaempferi*, seedlings. J. Nematol 41: 157–162.

Mota M, Vieira P (2008) Pine wilt disease: a worldwide threat to forest ecosystems. M M. Mota. Springer, Dordrecht, 428 pp.

Massoumi AS, Kim JJ, Humble LM, Uzunovic A, Breuil C (2007) Ophiostomatoid fungi associated with the Northern *Spruce engraver*, *Ips perturbatus*, in Western Canada. Antonie Van Leeuwenhoek 91(1): 19–34. https://doi.org/10.1007/s10482-006-9092-8

Mota MM, Vieira P (2008) Pine Wilt Disease: A Worldwide Threat to Forest Ecosystems. Springer, Netherlands. https://doi.org/10.1007/978-1-4020-8455-3

Mullineux T, Hausner G (2009) Evolution of rdna its1 and ITS2 sequences and RNA secondary structures within members of the fungal genera *Grosmannia* and *Leptographium*. Fungal Genetics & Biology Fg & B, 46(11): 855. https://doi.org/10.1016/j.fgb.2009.08.001

Nkuekam GK, Beer ZWD, Wingfield MJ, Roux J (2012) A diverse assemblage of *Ophiostoma*, species, including two new taxa on Eucalypt trees in South Africa. Mycological Progress, 11(2): 515–533. https://doi.org/10.1007/s11557-011-0767-9

Ohtaka N, Masuya H, Yamaoka Y, Kaneko S (2006) Two new *Ophiostoma* species lacking conidial states isolated from bark beetles and bark beetle-infested *Abies* species in Japan. Revue Canadienne De Botanique, 84(84): 282–293. https://doi.org/10.1139/B05-164

Pérez-Vera OA, Cárdenas-Soriano E, Alvarado-Rosales D, Cibrián-Tovar D, Equihua-Martínez A (2011) Histopathology of Hartweg pine (*Pinus hartwegii* lindl.) innoculated with three ophiostomatoid fungi. Revista Chapingo Serie Ciencias Forestales Y Del Ambiente 17(1): 91–102. https://doi.org/10.5154/r.rchscfa.2010.03.006

Pfenning L, Oberwinkler F (1993) *Ophiostoma bragantinum* n. sp., a possible teleomorph of Sporothrix inflata, found in Brazil. Mycotaxon 46: 381–385.

Plattner A, Jaejin K, Reid J, Hausner G, Youngwoon L, Yamaoka Y, Breuil C (2009) Resolving taxonomic and phylogenetic incongruence within species *Ceratocystiopsis minuta*. Mycologia, 101(6): 878. https://doi.org/10.3852/08-132

Posada D, Crandall KA (1998) MODELTEST: testing the model of DNA substitution. Bioinformatics 14: 817–818. https://doi.org/10.1093/bioinformatics/14.9.817

Rane KK, Tattar TA (1987) Pathogenicity of blue-stain fungi associated with *Dendroctonus terebrans*. Plant Dis 71: 8798–8883. https://doi.org/10.1094/PD-71-0879

Rayner RW (1970) A mycological colour chart. Commonwealth Mycological Institute and British Mycological Society.

Robbins K (1982) Distribution of the pinewood nematode in the United States. In: Appleby JE, Malek RB (Eds) Proceedings of the national pine wilt disease workshop. III. Natural History Survey, Champaign, IL, USA, 3–6.

Roets F, Wingfield MJ, Crous PW, Dreyer LL, Savolainen V, Dreyer LL (2009) Fungal radiation in the cape floristic region: an analysis based on *Gondwanamyces* and *Ophiostoma*. Molecular Phylogenetics & Evolution 51(1): 111–119. https://doi.org/10.1016/j.ympev.2008.05.041

Roets F, de Beer ZW, Wingfield MJ, Crous PW, Dreyer LL (2008) *Ophiostoma gemellus* and *Sporothrix variecibatus* from mites infesting Protea infructescences in South Africa. Mycologia 100: 496–510. https://doi.org/10.3852/07-181R

Roets F, de Beer ZW, Dreyer LL, Zipfel R, Crous PW, Wingfield MJ (2006) Multi-gene phylogeny for *Ophiostoma* spp. reveals two new species from Protea infructescences. Stud Mycol 55: 199–212. https://doi.org/10.3114/sim.55.1.199

Romón P, Zhou X, Iturrondobeitia JC, Wingfield MJ, Goldarazena A (2007) *Ophiostoma* species (ascomycetes: ophiostomatales) associated with bark beetles (coleoptera: scolytinae) colonizing *Pinus radiata* in Northern Spain. Canadian Journal of Microbiology 53(6): 756–767. https://doi.org/10.1139/W07-001

Romón P, de Beer ZW, Zhou XD, Duong TA, Wingfield BD, Wingfield MJ (1900) Multigene phylogenies of Ophiostomataceae associated with Monterey pine bark beetles in Spain reveal three new fungal species. Mycologia 106(1): 119–32. https://doi.org/10.3852/13-073

Rumbold CT (1931) Two blue-staining fungi associated with bark beetle infestation of pines. Journal of Agricultural Research 43(10): 847–873.

Ryss A, Vieira P, Mota M, Kulinich O (2005) A synopsis of the genus *Bursaphelenchus Fuchs*, 1937 (Aphelenchida: Parasitaphelenchidae) with keys to species. Nematology 7(3): 393–458. https://doi.org/10.1163/156854105774355581

Seifert KA, Webber JF, Wingfield MJ (1993) Methods for studying species of *Ophiostoma* and *Ceratocystis*. In: Wingfield MJ, Seifert KA, Webber JF, eds. *Ceratocystis* and *Ophiostoma*: taxonomy, ecology and pathogenicity. Minnesota, U.S.A.: The American Phytopathological Society Press, 255–259.

State Forestry Administration of the People's Republic of China (2018) Announcement of State Forestry Administration of the People's Republic of China No. 1, 2018.

Steiner G, Buhrer EM (1934) *Aphelenchoides Xylophilus* N. Sp., a Nematode Associated with Blue-Stain and Other Fungi in Timber. Journal of Agricultural Research 48(10): 949–951.

Suh DY, Hyun MW, Kim JJ, Son SY, Kim SH (2013) *Ophiostoma ips* from Pinewood Nematode Vector, Japanese Pine Sawyer Beetle (*Monochamus alternatus*), in Korea. Mycobiology 41(1): 59–62. http://dx.doi.org/10.5941/MYCO.2013. 41.1.59

Swofford DL (2003) PAUP*: phylogenetic analysis using parsimony, version 4.0 b10.

Tamura K, Peterson D, Peterson N, Stecher G, Nei M, Kumar S (2011) MEGA5: molecular evolutionary genetics analysis using maximum likelihood, evolutionary distance, and maximum parsimony methods. Mol Biol Evol 28: 2731–2739. https://doi.org/10.1093/molbev/msr121

Upadhyay HP (1981) A monograph of *Ceratocystis* and *Ceratocystiopsis*. The University of Georgia Press, Athens, GA, USA, 95 pp.

Uzunovic A, Seifert KA, Kim SH, Breuil C (2000) *Ophiostoma setosum*, a common sapwood staining fungus from western North America, a new species of the *Ophiostoma piceae*, complex. Mycological Research 104(4): 486–494. https://doi.org/10.1017/S0953756299001446

Van der Linde JA, Six DL, de Beer WZ, Wingfield MJ, Roux J (2016) Novel ophiostomatalean fungi from galleries of *Cyrtogenius africus* (Scolytinae) infesting dying *Euphorbia ingens*. Antonie van Leeuwenhoek 109(4): 589–601. https://doi.org/10.1007/s10482-016-0661-1

Villarreal M, Rubio V, Mtde T, Arenal F (2005) A new *Ophiostoma* species isolated from *Pinus pinaster* in the Iberian peninsula. Mycotaxon 92(3): 259–268.

Wang HM, Lu Q, Meng XJ, Liu XW, Decock C, Zhang XY (2016) *Ophiostoma olgensis*, a new species associated with *Larix* spp. and *Ips subelongatus* in northern China. Phytotaxa 282(4): 282–290. https://doi.org/10.11646/phytotaxa.282.4.5

White TJ, Bruns T, Lee SJWT, Taylor JL (1990) Amplification and direct sequencing of fungal ribosomal RNA genes for phylogenetics. PCR protocols: a guide to methods and applications 18(1): 315–322. https://doi.org/10.1016/B978-0-12-372180-8.50042-1

Wingfield MJ (1987) Fungi associated with the pinewood nematode, *Bursaphelenchus xylophilus*, and cerambycid beetles in Wisconsin. Mycologia 79: 325–328. https://doi.org/10.2307/3807667

Yamaoka Y, Chung WH, Masuya H, Hizai M (2009) Constant association of ophiostomatoid fungi with the bark beetle *Ips subelongatus*, invading Japanese larch logs. Mycoscience, 50(3): 165–172. https://doi.org/10.1007/s10267-008-0468-7

Yamaoka Y, Takahashi I, Iguchi K (2000) Virulence of ophiostomatoid fungi associated with the spruce bark beetle *Ips typographus* f. *japonicus* in Yezo spruce. Journal of Forest Research 5(2): 87–94. https://doi.org/10.1007/BF02762525

Yan DH, Lu Q, Zhang XY (2003) Pine Wilt *Bursaphelenchus xylophilus* (Steiner&Buhrer) Nickle. In: Zhang XY, Luo YQ (Eds) Major Forest Diseases and Insect Pests in China. Beijing: China Forestry Publishing House, 1–29.

Yin M, Wingfield MJ, Zhou X, Beer ZWD (2016) Multigene phylogenies and morphological characterization of five new *Ophiostoma* spp. associated with *Spruce*-infesting bark beetles in China. Fungal Biol 120(4): 454-470. https://doi.org/10.1007/s11557-009-0594-4

Zhao L, Sun J (2017) Pinewood Nematode Bursaphelenchus xylophilus (Steiner and Buhrer) Nickle//Biological Invasions and Its Management in China. Springer, Singapore, 3–21. https://doi.org/10.1007/978-981-10-3427-5_1

Zhao L, Mota M, Vieira P, Butcher RA, Sun J (2014) Interspecific communication between pinewood nematode, its insect vector, and associated microbes. Trends in parasitology 30(6): 299–308. https://doi.org/10.1016/j.pt.2014.04.007

Zhao L, Lu M, Niu H, Fang G, Zhang S, Sun J (2013) A native fungal symbiont facilitates the prevalence and development of an invasive pathogen-native vector symbiosis. Ecology 94(12): 2817–2826. https://doi.org/10.1890/12-2229.1

Zhao BG, Futai K, Sutherland JR, Takeuchi Y (2008) Pine Wilt Disease. Springer, Tokyo, 144–161. https://doi.org/10.1007/978-4-431-75655-2

Zhao GH, Chen XY, Wu YZ (2006) Study on the Fungi from the Diseased Pine Wood Nematode. Journal of Nanjing Forestry University (Natural Sciences Edition) 30(2): 79–81.

Zhao GH (1992) Two new species of the genus *Ceratocystis*. Journal of Nanjing Forestry University 16(2): 81–86.

Zhou XD, Burgess T, de Beer ZW, Wingfield BD, Wingfield MJ (2002) Development of polymorphic microsatellite markers for the tree pathogen and sapstain agent, *Ophiostoma ips*. Molecular Ecology Resources 2(3): 309–312. https://doi.org/10.1046/j.1471-8286.2002.00225.x-i2

Zhou X, Burgess TI, de Beer ZW, Lieutier F, Yart A, Klepzig K, Carnegie A, Portales JM, Wingfield BD, Wingfield MJ (2007) High intercontinental migration rates and population admixture in the sapstain fungus *Ophiostoma ips*. Molecular Ecology 16(1): 89–99. https://doi.org/10.1111/j.1365-294X.2006.03127.x

Zhou X, de Beer ZW, Wingfield MJ (2006) DNA sequence comparisons of *Ophiostoma* spp., including *Ophiostoma aurorae* sp. nov., associated with pine bark beetles in South Africa. Stud Mycol 55: 269–277. https://doi.org/10.3114/sim.55.1.269

Zhou X, de Beer Z, Cibrian D, Wingfield BD, Wingfield MJ (2004) Characterisation of *Ophiostoma* species associated with pine bark beetles from Mexico, including *O. pulvin-*

isporum sp. nov. Mycological Research 108(Pt 6): 690–698. https://doi.org/10.1017/S0953756204009918

Zipfel RD, Beer ZW de, Jacobs K, Wingfield BD, Wingfield MJ (2006) Multigene phylogenies define *Ceratocystiopsis* and *Grosmannia* distinct from Ophiostoma. Studies in Mycology 55: 75–97. https://doi.org/10.3114/sim.55.1.75

Supplementary material 1

Figure S1. Phylogram of fungal associates of pine infected by PWN and *Monochamus alternatus* in China

Authors: HuiMin Wang, YingYing Lun, Quan Lu, HuiXiang Liu, Cony Decock, XingYao Zhang

Data type: phylogenetic data

Explanation note: The phylogram was generated after MP analysis of partial *tub2* sequences. *O. ips* sequences obtained in the current study are designated in bold type. MP bootstrap value and BI values are indicated at the branch nodes; values below 70% are indicated by asterisk (*).

Link: https://doi.org/10.3897/mycokeys.39.27014.suppl1

Supplementary material 2

Figure S2. Phylograms of fungal associates of pine infected by PWN and *Monochamus alternatus* in China

Authors: HuiMin Wang, YingYing Lun, Quan Lu, HuiXiang Liu, Cony Decock, XingYao Zhang

Data type: phylogenetic data

Explanation note: The phylograms were generated after MP analysis of the ITS1–5.8S–ITS2 rDNA and partial *tub2* sequences. Novel sequences obtained in the current study are indicated in bold type. MP bootstrap values (10,000 replicates) and ML bootstrap support values (1000 replicates) (normal type) above 70% are indicated at the nodes. Values below 70% are indicated by asterisk (*). Posterior probabilities (above 90%) obtained from BI are indicated by bold lines at the relevant branching points. Scale bar, total nucleotide differences between taxa; ML, maximum likelihood; MP, maximum parsimony; BI, Bayesian inference.

Link: https://doi.org/10.3897/mycokeys.39.27014.suppl2

Supplementary material 3

Figure S3. Three ML phylogenetic threes based on tub2 after excluding introns
Authors: HuiMin Wang, YingYing Lun, Quan Lu, HuiXiang Liu, Cony Decock, XingYao Zhang
Data type: phylogenetic data

Link: https://doi.org/10.3897/mycokeys.39.27014.suppl3

MycoKeys 39: 29–40 (2018)
doi: 10.3897/mycokeys.39.28109
http://mycokeys.pensoft.net

RESEARCH ARTICLE

A peer-reviewed open-access journal
MycoKeys
Launched to accelerate biodiversity research

Great differences in performance and outcome of high-throughput sequencing data analysis platforms for fungal metabarcoding

Sten Anslan[1], R. Henrik Nilsson[2], Christian Wurzbacher[3], Petr Baldrian[4], Leho Tedersoo[5], Mohammad Bahram[6,7,8]

1 *Braunschweig University of Technology, Zoological Institute, Mendelssohnstr. 4, 38106 Braunschweig, Germany* **2** *Gothenburg Global Biodiversity Centre, Department of Biological and Environmental Sciences, University of Gothenburg, Box 461, 405 30 Gothenburg, Sweden* **3** *Technical University of Munich, Am Coulombwall 3, 85748 Garching, Germany* **4** *Institute of Microbiology of the Czech Academy of Sciences, Videnska 1083, 14220 Praha 4, Czech Republic* **5** *Natural History Museum of Tartu University, 14a Ravila, 50411 Tartu, Estonia* **6** *Institute of Ecology and Earth Science, Tartu University, 14a Ravila, 50411 Tartu, Estonia* **7** *Department of Organismal Biology, Evolutionary Biology Centre, Uppsala University, Norbyvägen 18D, Uppsala, Sweden* **8** *Department of Ecology, Swedish University of Agricultural Sciences, Ulls väg 16, 756 51 Uppsala, Sweden*

Corresponding author: *Sten Anslan* (s.anslan@tu-braunschweig.de); *Mohammad Bahram* (bahram@ut.ee)

Academic editor: *T. Lumbsch* | Received 3 July 2018 | Accepted 27 August 2018 | Published 11 September 2018

Citation: Anslan S, Nilsson RH, Wurzbacher C, Baldrian P, Tedersoo L, Bahram M (2018) Great differences in performance and outcome of high-throughput sequencing data analysis platforms for fungal metabarcoding. MycoKeys 39: 29–40. https://doi.org/10.3897/mycokeys.39.28109

Abstract

Along with recent developments in high-throughput sequencing (HTS) technologies and thus fast accumulation of HTS data, there has been a growing need and interest for developing tools for HTS data processing and communication. In particular, a number of bioinformatics tools have been designed for analysing metabarcoding data, each with specific features, assumptions and outputs. To evaluate the potential effect of the application of different bioinformatics workflow on the results, we compared the performance of different analysis platforms on two contrasting high-throughput sequencing data sets. Our analysis revealed that the computation time, quality of error filtering and hence output of specific bioinformatics process largely depends on the platform used. Our results show that none of the bioinformatics workflows appears to perfectly filter out the accumulated errors and generate Operational Taxonomic Units, although PipeCraft, LotuS and PIPITS perform better than QIIME2 and Galaxy for the tested fungal amplicon dataset. We conclude that the output of each platform requires manual validation of the OTUs by examining the taxonomy assignment values.

Keywords

Microbial communities, microbiome, mycobiome, fungal biodiversity, metagenomics, amplicon sequencing

Introduction

Fungi are major ecological and functional players in terrestrial ecosystems. The full diversity of fungi remains largely uncharted due to their largely unculturable nature, the lack of tangible morphological manifestations and shortcomings of the mycological community to sample beyond traditional habitats and substrates (Grossart et al. 2016; Hibbett et al. 2017; Lücking et al. 2018). As a result, identification of fungi has come to rely mainly on direct DNA sequencing of material containing fungal hyphae or spores. In this regard, several DNA barcoding regions have been evaluated and the current consensus is that the nuclear ribosomal internal transcribed spacer (ITS) region is the best region for delimiting fungal taxa at the species level across a variety of fungal groups (Schoch et al. 2012). Recent advances in high-throughput sequencing (HTS) have made it possible to sequence millions of reads and identify thousands of fungal taxa from a single sample. Handling this enormous amount of data is often complicated and requires extensive bioinformatics expertise.

Multiple analysis platforms have been introduced to facilitate the bioinformatics treatment of HTS data. However, most of these software suites were developed for the prokaryotic 16S rRNA gene and may therefore perform poorly with other markers and other organisms, in particular ITS sequences due to their length variation and non-alignability across taxonomic expanses. To accommodate this, several tailored platforms have recently been developed to specifically address fungal ITS datasets (Anslan et al. 2017; Gweon et al. 2015; Hildebrand et al. 2014; Vetrovský et al. 2018). These platforms cover multiple steps of the analysis procedure, including quality control, clustering, taxonomic assignment and generating Operational Taxonomic Unit (OTU) abundance tables. Many of these platforms cover all these analysis steps, whereas others do not.

The application of different bioinformatics workflows may introduce variation in the data quality and output OTU tables (Majaneva et al. 2015; Sinha et al. 2017). However, to date, there are no data on the relative performance of the available tools for fungal HTS data analysis. In this study, we report on the relative performance of the most popular software pipelines on two contrasting HTS datasets.

Methods

Sequence data and general workflow

We compared the performance of bioinformatics analysis platforms on two fungal ITS datasets. Tested datasets included Illumina MiSeq paired-end ITS2 amplicons from arthropod substrates (Anslan et al. 2018) and full ITS circular consensus sequences from Pacific Biosciences (PacBio) Sequel machine, amplified from soil samples. PacBio data set is available through PlutoF database (Abarenkov et al. 2010b), https://plutof.ut.ee/#/datacite/10.15156%2FBIO%2F781236). For bioinformatics analyses, we

used multiple platforms that support all steps in the analysis of HTS-based metabarcoding datasets: QIIME2 (v2018.2; Caporaso et al. 2010), LotuS (v1.59; Hildebrand et al. 2014), Galaxy (v.2.1.1; Afgan et al. 2016), PipeCraft (v1.0; Anslan et al. 2017) and PIPITS (v2.0; Gweon et al. 2015) (Table 1; Figure 1). Depending on the analysis platform, quality filtering was performed using either VSEARCH (Rognes et al. 2016), trimmomatic (Bolger et al. 2014), DADA2 (Callahan et al. 2016), sdm (Hildebrand et al. 2014) or fastx (http://hannonlab.cshl.edu/fastx_toolkit). Quality filtered sequences were passed through chimeric reads removal algorithms as implemented in USEARCH (Edgar 2013; Edgar et al. 2011) or VSEARCH. Using PipeCraft, LotuS and PIPITS, reads were also subjected to ITS extraction using ITSx (Bengtsson-Palme et al. 2013) to remove conservative flanking genes of the ITS region. OTU formation (clustering) was performed using USEARCH or VSEARCH as outlined below (Platform specific options). For each platform, we relied on *de-novo* single linkage clustering, which is the most popular approach in fungal community studies, knowing that reference-based clustering methods can provide similar results (Cline et al. 2017). Taxonomic affiliations were assigned to OTUs using DP Naive Bayesian rRNA Classifier (RDP classifier v2.11; Wang et al. 2007) with the Warcup Fungal ITS trainset 2 (confidence threshold: 80%; Deshpande et al. 2016) as well as BLAST+ (Camacho et al. 2009) search (e-value = 0.001, word size = 7, reward = 1, penalty = -1, gap open = 1, gap extend = 2) against the UNITE v7.2 reference database (Abarenkov et al. 2010a).

Platform specific options

Using QIIME2, reads were assembled (Illumina data) and quality filtered using DADA2 (Callahan et al. 2016) with default options, except --p-trunc-len = 0, --p-max-ee = 1 and --p-chimera-method = none (with chimera-method = consensus, QIIME2 reported error for our data). Clustering was performed with VSEARCH cluster-features-de-novo (--p-perc-identity 0.97).

In LotuS pipline, data was assembled (Illumina data), quality filtered (minimum length = 170, minAvgQuality = 27, TruncateSequenceLength = 170, maxAccumulatedError = 0.75) and demultiplexed with sdm (pdiffs = 1, bdiffs = 1). Chimera filtering was undertaken using USEARCH *de novo* chimera filtering (abundance annotation = 0.97, abskew = 2) and USEARCH reference-based chimera filtering using UNITE v7.2 as reference database. Flanking genes of the ITS region were discarded using ITSx (v1.0.11; default options). ITS reads were clustered to OTUs with USEARCH/UPARSE algorithm (-id = 3, -minsize = 2).

Using web-based Galaxy pipeline, Illumina data were assembled with Fastq joiner (Galaxy Version 2.0.1.1; Blankenberg et al. 2010) with default options. Quality filtering was performed with Trimmomatic (Galaxy Version 0.36.3) − SLIDINGWINDOW; number of bases to average across = 15, average quality required = 30, minimum length of kept reads = 45. Fastq files were converted to FASTA files using FASTQ to FASTA converter (Galaxy Version 1.0.0). Fasta files were demultiplexed

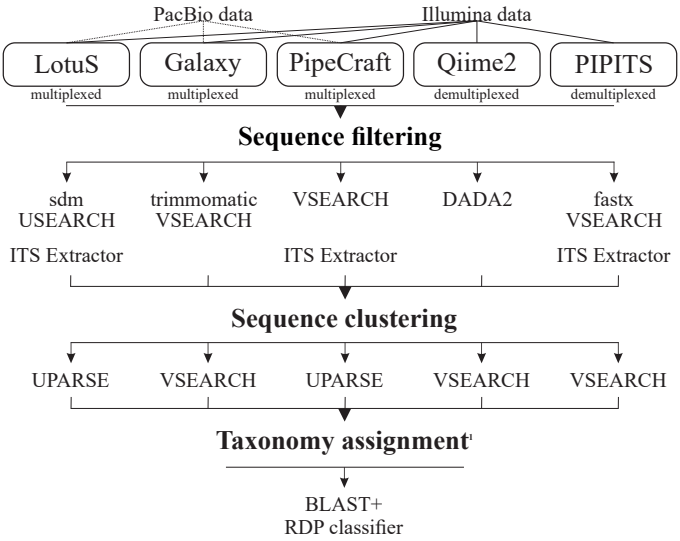

Figure 1. Outline of workflow in different analysis pipelines.

using mothur (Galaxy Version 1.39.5.0; Schloss et al. 2009) − pdiffs = 2, bdiffs = 1. As sequences were of mixed orientation in the files (5'-3' and 3'-5'), the demultiplexing step was repeated for reverse orientated sequences (reads were reversed using mothur reverse.seqs). Chimera filtering was undertaken using VSEARCH chimera detection (Galaxy Version 1.9.7.0) with default settings (abundance annotation = 97% similarity threshold) and using the UNITE v7.2 database as reference. Clustering was performed using VSEARCH (--cluster-fast, --id 0.97, --iddef 1).

In PipeCraft, platform reads were assembled (Illumina data) and quality filtered using VSEARCH (minimum overlap = 15, minimum length = 100, E max = 1, max ambiguous = 0, allowstagger = T). Demultiplexing was undertaken using mothur (pdiffs = 2, bdiffs = 1). In this step, sequences are also re-orientated into the 5'-3' orientation based on primers (2 mismatches allowed).

Chimeric sequences were removed using VSEARCH *de novo* (abundance annotation = 0.97, abskew = 2) and reference-based (UNITE v7.2 as reference) chimera filtering algorithms. In the chimera filtering step, the PipeCraft supported option for "primer artefact" removal was also used (sequences where primer strings were found in the middle of the sequence were removed). ITS reads were extracted using ITSx (default options). Clustering was performed using USEARCH/UPARSE algorithm (id = 3, minsize = 2).

Using PIPITS, sequences were assembled with VSEARCH and quality-filtering was undertaken with fastx through the PIPITS command pispino_createreadpairslist. The ITSx was executed through the PIPITS command pipits_funits. Chimera filtering and clustering were undertaken using VSEARCH through the PIPITS command pipits_process.

Table 1. Used software, sequence and OTU counts (values in bold) by **a**) Illumina and **b**) PacBio analysis platforms. The number of sequences denotes raw input reads and remaining reads after each analysis step. Singleton OTUs were excluded from the OTU counts.

a)	**LotuS**	**Qiime2**	**PipeCraft**	**Galaxy**	**PIPITS**
Raw reads	7,981,812a	7,335,838b	7,981,812a	7,981,812a	7 335 838b
Assembly	FLASH/ NA	DADA2/ NA	VSEARCH/ 7,511,274	FASTQ joiner/ 7,911,554	VSEARCH/ 7,198,094
Quality filtering	sdm/NA	DADA2/ 5,428,563	VSEARCH/ 7,511,274	trimmomatic/ 7,879,960	fastqx/ 7,142,354
Demultiplexing	sdm/ 6,727,631	NP	mothur/ 6,558,772	mothur/ 1,643,879	NP
Chimera filtering	USEARCH/ 6,486,802	NP	VSEARCH/ 6,300,085	VSEARCH/ 1,621,330	VSEARCH/ NA
ITS extractor	5,919,084	NP	6,262,000	NP	6,401,097
Clustering (OTUs)	UPARSE/ 8,659	VSEARCH/ 7,477	UPARSE/ 7,598	VSEARCH/ 23,167	VSEARCH/ 7,887
b)	**LotusS**	**PipeCraft**	**Galaxy**		
CCSc reads	720,222a	720,222a	720,222a		
Quality filtering	sdm/ NA	VSEARCH/ 462,010	trimmomatic/ 672,292		
Demultiplexing	sdm/ 258,085	mothur/ 380,722	mothur/ 457,173		
Chimera filtering	USEARCH/ 255,746	VSEARCH/ 341,154	VSEARCH/ 405,025		
ITS extraction	192,485	338,150	NP		
Clustering (OTUs)	UPARSE/ 942	UPARSE/ 4,176	VSEARCH/ 8,338		

[a]multiplexed input data; [b]demultiplexed input data; [c]circular consensus sequences; NA: indicate not available; NP: not performed.

Additional filtering

The additional manual OTU table filtering was based on the BLAST similarity scores when run against UNITE (v7.2) reference database. Any OTUs that had no BLAST hit or that were not classified to the kingdom Fungi were discarded from the OTU table. The remaining OTUs were filtered based on BLAST e-value and query coverage. OTUs with higher e-value than $1e^{-25}$ and query coverage less than 70% were excluded from the dataset (as putative artefacts or non-fungal OTUs). Additionally, OTUs with low numbers of sequences per sample were removed (less than 10 sequences per sample; Brown et al. (2015)). Finally, the LULU (Frøslev et al. 2017) algorithm was applied (minimum_ratio_type = "min", minimum_match = 97) to merge consistently co-occurring 'daughter' OTUs.

Data pooling

To detect the effect of analysis platform choice on the OTU composition, we pooled sequences originating from different platforms and applied the common clustering

method to generate a single OTU table. For Illumina data, filtered reads from PipeCraft, LotuS and PIPITS were pooled and clustered using CD-HIT (Fu et al. 2012) at 97% sequence similarity (Table 1). The pooled PacBio dataset included filtered sequences from LotuS, PipeCraft and Galaxy platform, clustering was performed using UPARSE algorithm with 97% sequence similarity threshold (Table 1).

Statistical analysis

We used PERMANOVA analysis (Anderson and Walsh 2013; Type III SS, 4,999 permutations) on Bray-Curtis distances of Hellinger-transformed OTU matrices, using PRIMER6 (Clarke and Gorley 2006). Outliers were screened and removed using analysis of non-metric multidimensional scaling (NMDS). The numbers of sequences per sample were included in the analysis as covariates. Rarefaction curves were generated based on OTU abundance matrices for each dataset using the RTK package (Saary et al. 2017) of R (R-Core-Team 2015).

Results and discussion

Properties of bioinformatics analysis platforms

All tested bioinformatics platforms offer straightforward installation. While Galaxy provides a freely available online platform, the benefits of PipeCraft and QIIME2 include easy-to-use graphical user interfaces and multiple options for data analysis. These platforms bundle many tools for diverse tasks. LotuS and PIPITS represent command-line based platforms. PIPITS offers a limited number of tools, but data analysis is easily performed with a straightforward pipeline. LotuS has been developed to minimise computational time and memory requirements. Specifically, for accuracy of ITS-based analyses of fungi and other eukaryotes, PipeCraft, LotuS and PIPITS implement the ITSx tool (Bengtsson-Palme et al. 2013), which removes the fragments of conservative flanking genes for precise clustering purposes. There is no such option in QIIME2 and Galaxy.

Bioinformatics platforms differ by specific requirements to the input data, with the options being a raw multiplexed file (a single file containing all sequences from one run) and multiple demultiplexed files (reads split into separate files based on indexes). PipeCraft and Galaxy use raw multiplexed data, whereas QIIME2 and PIPITS require demultiplexed files. Only LotuS allows both, multiplexed and demultiplexed files as input. As the raw data files are multiplexed by default, QIIME2 and PIPITS platforms required additional steps of analyses outside these tools to meet the input requirements. Using a Python script, we demultiplexed the raw Illumina data, allowing 2 and 1 mismatches to primer and index strings, respectively. However, PacBio data analysis was dropped for QIIME2 and PIPITS as the present versions of these platforms are limited to analysis of short read (Illumina) data.

Performance of bioinformatics platforms on sequence data

For both the Illumina and PacBio datasets, the final OTU richness (singleton OTUs excluded) differed considerably amongst the tested workflows (Table 1). We found that pipelines, which produced roughly comparable numbers of total OTUs (QIIME2, PipeCraft, PIPITS and LotuS for Illumina data), still exhibited large variations in OTU richness per sample (Figures 2 and 3). By performing joint *de-novo* clustering for filtered sequences from different pipelines (total number of OTUs = 16333), we observed a weak but significant effect of pipeline choice on overall OTU composition for the Illumina data set (PERMANOVA: pseudo-$F_{2,868} = 5.88$, $R^2_{adj} = 0.012$, $P < 0.001$). For the PacBio dataset (total number of OTUs = 4448), differences amongst platforms were slightly stronger (pseudo-$F_{2,512} = 9.174$; $R^2_{adj} = 0.033$, $P < 0.001$).

Taxonomic annotation tools differed in the ability to classify OTUs. In general, BLAST searches revealed many cases of high-quality matches to non-fungal organisms (in some cases for hundreds of OTUs), while RDP when combined with the Warcup Fungal ITS trainset optimistically classified all OTUs to Fungi (100% confidence). Numerous papers have evaluated the performance of different methods on the accuracy of taxonomic assignment and performance inevitably hinges on the completeness of the reference database used (e.g. Gdanetz et al. 2017; Richardson et al. 2017). In spite of its relatively rapid performance, the RDP Fungal ITS trainset does not include any non-fungal data, which explains its shortcomings in detecting non-fungal OTUs. However, the confidence score of an RDP classifier did not exceed 64% for non-fungal OTUs, mostly overestimating the group of unclassified fungi.

We also observed that the quality-filtered datasets included up to ~10% of obvious erroneous/chimeric OTUs that produced matches with low query coverage and confidence scores. A long tail of satellite OTUs, assigned to a single species hypothesis with 99–100% BLAST identity and RDP classifier confidence level, were also common – especially in the results where a relatively high number of OTUs was observed (Galaxy platform). After filtering the spurious OTUs manually (see Methods), we found that richness estimates per sample became more homogeneous across pipelines (Illumina data: Figure 3). When OTU table filtering was applied to jointly clustered reads from different pipelines, the significant effect of pipeline choice on the community composition diminished (Illumina data: pseudo-$F_{2,837} = 0.955$, $R^2_{adj} = 0.007$, $P = 0.779$).

In conclusion, our results indicate that bioinformatics analysis pipelines greatly differ in their relative performance on ITS datasets targeting fungi, although roughly similar quality-orientated settings were implemented. Overall, our recommended Illumina data workflow would be PipeCraft, PIPITS or LotuS, which provide a good balance between speed, mycological accuracy (including support for ITS Extractor) and technical quality. For PacBio, the tools implemented in PipeCraft were most suitable for the long-read analysis. Conversely, the widely used platform in prokaryote 16S-based studies, our options chosen in Galaxy, performed relatively poorly on the ITS data. While QIIME2 implements an accurate quality filtering algorithm of DADA2, the lack of ITS region extraction lowers the accuracy for mycological studies. Of clas-

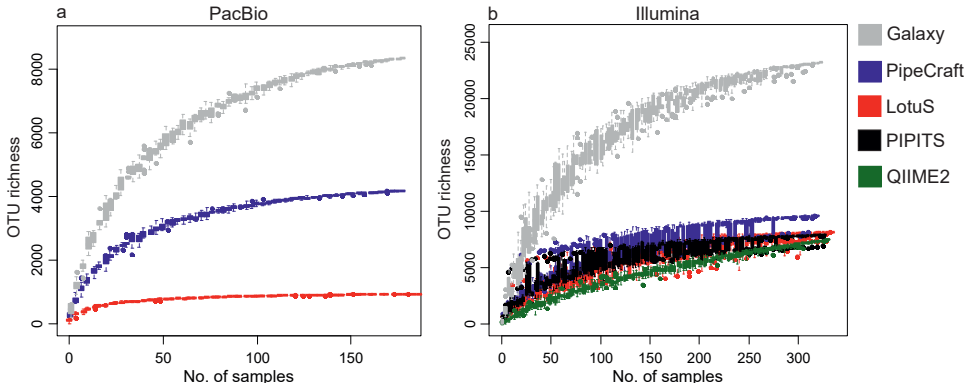

Figure 2. OTU accumulation curves of the evaluated pipelines for a) PacBio and b) Illumina datasets.

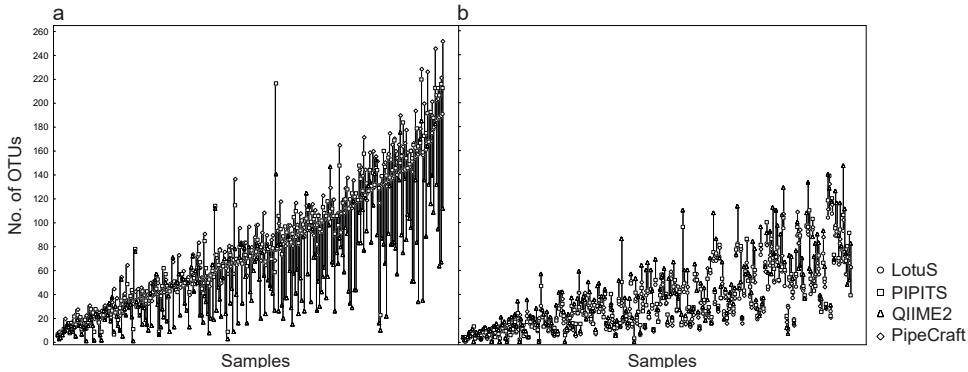

Figure 3. Number of OTUs per sample for Illumina data recorded from a) pipeline-generated OTU tables (median differences = 38 OTUs) and from b) filtered OTU tables (median differences = 12 OTUs). The Galaxy workflow was excluded here.

sification tools, BLAST searches against the UNITE database provided more accurate results on the kingdom and phylum levels compared with the RDP and Warcup ITS trainset combined. We emphasise that none of the tested bioinformatics workflows is able to fully filter out the errors that accumulated during sample preparation and sequencing, even when using the most elaborate error-filtering options. Therefore, manual curation of OTU tables continues to be an important step in obtaining robust datasets, although semi-automatic tools to assist evaluation are becoming available (Frøslev et al. 2017). It is also important to rely on high-coverage reference databases to be able to recognise non-target organisms and metagenomic reads.

Acknowledgments

We thank Falk Hildebrand for advice on bioinformatics analysis. This study was supported by the Estonian Research Council (grant no. PUT1317).

References

Abarenkov K, Nilsson RH, Larsson K-H, Alexander IJ, Eberhardt U, Erland S, Hoiland K, Kjoller R, Larsson E, Pennanen T, Sen R, Taylor AFS, Tedersoo L, Ursing BM, Vralstad T, Liimatainen K, Peintner U, Kõljalg U (2010a) The UNITE database for molecular identification of fungi – recent updates and future perspectives. New Phytologist 186: 281–285. https://doi.org/10.1111/j.1469-8137.2009.03160.x

Abarenkov K, Tedersoo L, Nilsson RH, Vellak K, Saar I, Veldre V, Parmasto E, Prous M, Aan A, Ots M, Kurina O, Ostonen I, Jogeva J, Halapuu S, Poldmaa K, Toots M, Truu J, Larsson K-H, Koljalg U (2010b) PlutoF-a Web Based Workbench for Ecological and Taxonomic Research, with an Online Implementation for Fungal ITS Sequences. Evolutionary Bioinformatics 6: 189–196. https://doi.org/10.4137/ebo.s6271

Afgan E, Baker D, Van den Beek M, Blankenberg D, Bouvier D, Čech M, Chilton J, Clements D, Coraor N, Eberhard C (2016) The Galaxy platform for accessible, reproducible and collaborative biomedical analyses: 2016 update. Nucleic Acids Research 44: 3–10. https://doi.org/10.1093/nar/gkw343

Anderson MJ, Walsh DCI (2013) PERMANOVA, ANOSIM, and the Mantel test in the face of heterogeneous dispersions: What null hypothesis are you testing? Ecological Monographs 83: 557–574. https://doi.org/10.1890/12-2010.1

Anslan S, Bahram M, Hiiesalu I, Tedersoo L (2017) PipeCraft: flexible open-source toolkit for bioinformatics analysis of custom high-throughput amplicon sequencing data. Molecular Ecology Resources 17: e234–e240. https://doi.org/10.1111/1755-0998.12692

Anslan S, Bahram M, Tedersoo L (2018) Seasonal and annual variation in fungal communities associated with epigeic springtails (Collembola spp.) in boreal forests. Soil Biology and Biochemistry 116: 245–252. doi:https://doi.org/10.1016/j.soilbio.2017.10.021

Bengtsson-Palme J, Ryberg M, Hartmann M, Branco S, Wang Z, Godhe A, De Wit P, Sanchez-Garcia M, Ebersberger I, de Sousa F, Amend AS, Jumpponen A, Unterseher M, Kristiansson E, Abarenkov K, Bertrand YJK, Sanli K, Eriksson KM, Vik U, Veldre V, Nilsson RH (2013) Improved software detection and extraction of ITS1 and ITS2 from ribosomal ITS sequences of fungi and other eukaryotes for analysis of environmental sequencing data. Methods in Ecology and Evolution 4: 914–919. https://doi.org/10.1111/2041-210x.12073

Blankenberg D, Gordon A, Von Kuster G, Coraor N, Taylor J, Nekrutenko A, Team G (2010) Manipulation of FASTQ data with Galaxy. Bioinformatics 26: 1783–1785. https://doi.org/10.1093/bioinformatics/btq281

Bolger AM, Lohse M, Usadel B (2014) Trimmomatic: a flexible trimmer for Illumina sequence data. Bioinformatics 30: 2114–2120. https://doi.org/10.1093/bioinformatics/btu170

Brown SP, Veach AM, Rigdon-Huss AR, Grond K, Lickteig SK, Lothamer K, Oliver AK, Jumpponen A (2015) Scraping the bottom of the barrel: are rare high throughput sequences artifacts? Fungal Ecology 13: 221–225. http://dx.doi.org/10.1016/j.funeco.2014.08.006

Callahan BJ, McMurdie PJ, Rosen MJ, Han AW, Johnson AJA, Holmes SP (2016) DADA2: high-resolution sample inference from Illumina amplicon data. Nature Methods 13: 581. https://doi.org/10.1038/nmeth.3869

Camacho C, Coulouris G, Avagyan V, Ma N, Papadopoulos J, Bealer K, Madden TL (2009) BLAST+: architecture and applications. BMC Bioinformatics 10: 421. https://doi.org/10.1186/1471-2105-10-421

Caporaso JG, Kuczynski J, Stombaugh J, Bittinger K, Bushman FD, Costello EK, Fierer N, Peña AG, Goodrich JK, Gordon JI (2010) QIIME allows analysis of high-throughput community sequencing data. Nature Methods 7: 335–336. https://doi.org/10.1038/nmeth.f.303

Clarke K, Gorley R (2006) PRIMER V6: User Manual / Tutorial. Primer-E Ltd, Plymouth, 192 pp.

Cline LC, Song Z, Al-Ghalith GA, Knights D, Kennedy PG (2017) Moving beyond de novo clustering in fungal community ecology. New Phytol. 216(3): 629–634. https://doi.org/10.1111/nph.14752

Deshpande V, Wang Q, Greenfield P, Charleston M, Porras-Alfaro A, Kuske CR, Cole JR, Midgley DJ, Tran-Dinh N (2016) Fungal identification using a Bayesian classifier and the Warcup training set of internal transcribed spacer sequences. Mycologia 108: 1–5. https://doi.org/10.3852/14-293

Edgar RC (2013) UPARSE: highly accurate OTU sequences from microbial amplicon reads. Nature Methods 10. https://doi.org/10.1038/nmeth.2604

Edgar RC, Haas BJ, Clemente JC, Quince C, Knight R (2011) UCHIME improves sensitivity and speed of chimera detection. Bioinformatics 27: 2194–2200. https://doi.org/10.1093/bioinformatics/btr381

Frøslev TG, Kjøller R, Bruun HH, Ejrnæs R, Brunbjerg AK, Pietroni C, Hansen AJ (2017) Algorithm for post-clustering curation of DNA amplicon data yields reliable biodiversity estimates. Nature communications 8: 1188. https://doi.org/10.1038/s41467-017-01312-x

Fu L, Niu B, Zhu Z, Wu S, Li W (2012) CD-HIT: accelerated for clustering the next-generation sequencing data. Bioinformatics 28: 3150–3152. https://doi.org/10.1093/bioinformatics/bts565

Grossart H-P, Wurzbacher C, James TY, Kagami M (2016) Discovery of dark matter fungi in aquatic ecosystems demands a reappraisal of the phylogeny and ecology of zoosporic fungi. Fungal Ecology 19: 28–38. doi:https://doi.org/10.1016/j.funeco.2015.06.004

Gweon HS, Oliver A, Taylor J, Booth T, Gibbs M, Read DS, Griffiths RI, Schonrogge K (2015) PIPITS: an automated pipeline for analyses of fungal internal transcribed spacer sequences from the Illumina sequencing platform. Methods in Ecology and Evolution 6: 973–980. https://doi.org/10.1111/2041-210x.12399

Hibbett D, Abarenkov K, Koljalg U, Opik M, Chai B, Cole JR, Wang Q, Crous PW, Robert VARG, Helgason T, Herr J, Kirk P, Lueschow S, O'Donnell K, Nilsson H, Oono R, Schoch CL, Smyth C, Walker D, Porras-Alfaro A, Taylor JW, Geiser DM (2017) Sequence-based classification and identification of Fungi. Mycologia 108: 1049–1068

Hildebrand F, Tadeo R, Voigt AY, Bork P, Raes J (2014) LotuS: an efficient and user-friendly OTU processing pipeline. Microbiome 2: 30. https://doi.org/10.1186/2049-2618-2-30

Lücking R, Kirk PM, Hawksworth DL (2018) Sequence-based nomenclature: a reply to Thines et al. and Zamora et al. and provisions for an amended proposal. IMA fungus 9: 185–198. https://doi.org/10.5598/imafungus.2018.09.01.12

Majaneva M, Hyytiäinen K, Varvio SL, Nagai S, Blomster J (2015) Bioinformatic amplicon read processing strategies strongly affect eukaryotic diversity and the taxonomic composition of communities. PLoS ONE 10: e0130035. https://doi.org/10.1371/journal.pone.0130035

R-Core-Team (2015) R: A language and environment for statistical computing. R Foundation for Statistical Computing, Vienna.

Rognes T, Flouri T, Nichols B, Quince C, Mahé F (2016) VSEARCH: a versatile open source tool for metagenomics. PeerJ 4: e2584. https://doi.org/10.7717/peerj.2584

Saary P, Forslund K, Bork P, Hildebrand F (2017) RTK: efficient rarefaction analysis of large datasets. Bioinformatics 33: 2594–2595. https://doi.org/10.1093/bioinformatics/btx206

Schloss PD, Westcott SL, Ryabin T, Hall JR, Hartmann M, Hollister EB, Lesniewski RA, Oakley BB, Parks DH, Robinson CJ, Sahl JW, Stres B, Thallinger GG, Van Horn DJ, Weber CF (2009) Introducing mothur: Open-Source, Platform-Independent, Community-Supported Software for Describing and Comparing Microbial Communities. Applied and Environmental Microbiology 75: 7537–7541. https://doi.org/10.1128/aem.01541-09

Schoch CL, Seifert KA, Huhndorf S, Robert V, Spouge JL, Levesque CA, Chen W, Bolchacova E, Voigt K, Crous PW, Miller AN, Wingfield MJ, Aime MC, An KD, Bai FY, Barreto RW, Begerow D, Bergeron MJ, Blackwell M, Boekhout T, Bogale M, Boonyuen N, Burgaz AR, Buyck B, Cai L, Cai Q, Cardinali G, Chaverri P, Coppins BJ, Crespo A, Cubas P P, Cummings C, Damm U, de Beer ZW, de Hoog GS, Del-Prado R, Dentinger B, Dieguez-Uribeondo J, Divakar PK, Douglas B, Duenas M, Duong TA, Eberhardt U, Edwards JE, Elshahed MS, Fliegerova K, Furtado M, Garcia MA, Ge ZW, Griffith GW, Griffiths K, Groenewald JZ, Groenewald M, Grube M, Gryzenhout M, Guo LD, Hagen F, Hambleton S, Hamelin RC, Hansen K, Harrold P, Heller G, Herrera G, Hirayama K, Hirooka Y, Ho HM, Hoffmann K, Hofstetter V, Hognabba F, Hollingsworth PM, Hong SB, Hosaka K, Houbraken J, Hughes K, Huhtinen S, Hyde KD, James T, Johnson EM, Johnson JE, Johnston PR, Jones EB, Kelly LJ, Kirk PM, Knapp DG, Koljalg U, Kovacs GM, Kurtzman CP, Landvik S, Leavitt SD, Liggenstoffer AS, Liimatainen K, Lombard L, Luangsa-Ard JJ, Lumbsch HT, Maganti H, Maharachchikumbura SS, Martin MP, May TW, McTaggart AR, Methven AS, Meyer W, Moncalvo JM, Mongkolsamrit S, Nagy LG, Nilsson RH, Niskanen T, Nyilasi I, Okada G, Okane I, Olariaga I, Otte J, Papp T, Park D, Petkovits T, Pino-Bodas R, Quaedvlieg W, Raja HA, Redecker D, Rintoul T, Ruibal C, Sarmiento-Ramirez JM, Schmitt I, Schussler A, Shearer C, Sotome K, Stefani FO, Stenroos S, Stielow B, Stockinger H, Suetrong S, Suh SO, Sung GH, Suzuki M, Tanaka K, Tedersoo L, Telleria MT, Tretter E, Untereiner WA, Urbina H, Vagvolgyi C, Vialle A, Vu TD, Walther G, Wang QM, Wang Y, Weir BS, Weiss M, White MM, Xu J, Yahr R, Yang ZL, Yurkov A, Zamora JC, Zhang N, Zhuang WY, Schindel D, Fungal Barcoding C (2012) Nuclear ribosomal internal transcribed spacer (ITS) region as a universal DNA barcode marker for Fungi. Proceedings of the National Academy of Sciences of the United States of America 109: 6241–6246. https://doi.org/10.1073/pnas.1117018109

Sinha R, Abu-Ali G, Vogtmann E, Fodor AA, Ren B, Amir A, Schwager E, Crabtree J, Ma S, Abnet CC (2017) Assessment of variation in microbial community amplicon sequencing by the Microbiome Quality Control (MBQC) project consortium. Nature Biotechnology volume 35, pages 1077–1086. https://doi.org/10.1038/nbt.3981

Wang Q, Garrity GM, Tiedje JM, Cole JR (2007) Naive Bayesian classifier for rapid assignment of rRNA sequences into the new bacterial taxonomy. Applied and Environmental Microbiology 73. https://doi.org/10.1128/aem.00062-07

Vetrovský T, Baldrian P, Morais D, Berger B (2018) SEED 2: a user-friendly platform for amplicon high-throughput sequencing data analyses. Bioinformatics 1: 3. https://doi.org/10.1093/bioinformatics/bty071

MycoKeys 39: 41–61 (2018)
doi: 10.3897/mycokeys.39.26743
http://mycokeys.pensoft.net

RESEARCH ARTICLE

A peer-reviewed open-access journal
MycoKeys
Launched to accelerate biodiversity research

The genus *Coprinellus* (Basidiomycota; Agaricales) in Pakistan with the description of four new species

Shah Hussain[1], Muhammad Usman[2], Najam-ul-Sehar Afshan[3], Habib Ahmad[4], Junaid Khan[1], Abdul Nasir Khalid[2]

1 *Centre for Plant Sciences and Biodiversity, University of Swat, Swat, Pakistan* **2** *Department of Botany, University of the Punjab, Lahore 54590, Pakistan* **3** *Centre for Undergraduate Studies, University of the Punjab, Lahore 54590, Pakistan* **4** *Islamia College Peshawar, Pakistan*

Corresponding author: *Shah Hussain* (shahpk85@gmail.com)

Academic editor: *Bryn Dentinger* | Received 17 May 2018 | Accepted 28 August 2018 | Published 11 September 2018

Citation: Hussain S, Usman M, Afshan N-ul-S, Ahmad H, Khan J, Khalid AN (2018) The genus *Coprinellus* (Basidiomycota; Agaricales) in Pakistan with the description of four new species. MycoKeys 39: 41–61. https://doi.org/10.3897/mycokeys.39.26743

Abstract

Mushrooms with a thin-fleshed pileus that becomes plicate on opening, deliquescent lamellae and dark brown to blackish basidiospores are commonly called coprinoid mushrooms. The genus *Coprinellus* is one of the important lineages of coprinoid mushroom in the family Psathyrellaceae. Species-level taxonomy in *Coprinellus* is based mainly on the presence or absence and the structure of veil and cystidia on the pileus, of cystidia on the lamellae and on basidiospore morphology. In this study, four new species of *Coprinellus* (*Co. campanulatus*, *Co. disseminatus-similis*, *Co. pakistanicus* and *Co. tenuis*) are described from Pakistan. Species descriptions are based on morphological and molecular data. Phylogenetic analyses based on nuc rDNA ITS region show that the new species *Co. campanulatus* and *Co. disseminatus-similis* are clustered in a clade including members of section *Micacei*; *Co. tenuis* falls in a clade with members of section *Domestici*; and *Co. pakistanicus* recovered in a separate clade adjacent to other recently described clades of genus *Coprinellus*. Morpho-anatomical descriptions of the new species and comparison with closely allied taxa are provided. With this study, the number of known species of *Coprinellus* in Pakistan has reached eight.

Keywords

Coprinellus section *Domestici*, *Coprinellus* sect. *Micacei*, coprinoid fungi, taxonomy

Introduction

Coprinoid fungi form an important group of macrofungi and are striking in the field because of their deliquescent lamellae. Coprinoid mushrooms have generally a thin-fleshed pileus that becomes plicate on opening with deliquescent lamellae and dark brown to blackish basidiospores with germ-pore (Schafer 2010). The evolutionary lineages of coprinoid taxa are set amongst those that are not, or not fully coprinoid. Fully coprinoid genera include: *Coprinus* Pers. in Agaricaceae; *Coprinellus* P. Karst., *Coprinopsis* P. Karst. and *Parasola* Redhead, Vilgalys & Hopple in Psathyrellaceae. Certain species of *Leucocoprinus* Pat. (*L. birnbaumii*, *L. brebissonii*, *L. fragilissimus*) in Agaricaceae have a coprinoid combination of characters (Nagy 2011). Within the Bolbitiaceae, coprinoid taxa include: species of *Conocybe* Fayod belonging to section *Candidae* Watling, few *Bolbitius* Fr. species (*B. coprophilus*, *B. elegans*, *B. lacteus*, *B. reticulatus*, *B. subvolvatus*, *B. titubans*) and two species of *Galerella* Earle (*G. floriformis*, *G. nigeriensis*). Nevertheless, taken together, at least eight independent lineages with coprinoid fruiting bodies have hitherto been identified in the Psathyrellaceae (3), Bolbitiaceae (3) and Agaricaceae (2) (Matheny et al. 2006, Nagy 2011, Nagy et al. 2011, Tóth et al. 2013).

The genus *Coprinellus*, with approximately 80 described species, represents an independent lineage in Psathyrellaceae (Redhead et al. 2001, Walther et al. 2005, Vašutová et al. 2008, Padamsee et al. 2008, Nagy et al. 2011, 2012, 2013, Örstadius et al. 2015). These mushrooms are common saprotrophs of, for example, wood chip, leaf-litter and herbivore dung (Schafer 2010). Species of this genus are divided into three sections on the basis of veil anatomy and the presence or absence of cap pileocystidia. Section *Domestici* (Singer) D.J. Schaf. has a veil on the pileus in the form of floccose scales, consisting of chains of fusiform or subglobose cells, often with encrusted walls. In *Micacei* (Fr.) D.J. Schaf., veil remnants are present in the form of scattered, granulose flocks, often disappearing and consisting of globose cells arising from a matrix of narrow branched hyphae. In *Setulosi* (J.Lange) D.J. Schaf., the veil may be present or absent, but the pileus and stipe are covered with thin-walled pileocystidia and caulocystidia, respectively (Schafer 2010). However, Nagy et al. (2012) showed that these sections were not entirely consistent with the molecular phylogeny, in particular because clades corresponding to sections *Micacei* and *Domestici* each included some setulose species.

Previously, only 18 species of coprinoid mushrooms have been reported from Pakistan (Ahmad 1980, Hussain et al. 2016, 2017, 2018). These include two species of *Coprinus* (*C. comatus* (O.F. Müll.) Pers., *C. hookeri* Berk.); four of *Coprinellus* (*Co. disseminatus* (Pers.) J.E. Lange, *Co. marculentus* (Britzelm.) Redhead, Vilgalys & Moncalvo, *Co. micaceus* (Bull.) Vilgalys, Hopple & Jacq. Johnson, *Co. radians* (Desm.) Vilgalys, Hopple & Jacq. Johnson); five of *Coprinopsis* (*Cop. atramentaria* (Bull.) Redhead, Vilgalys & Moncalvo, *Cop. jonesii* (Peck) Redhead, Vilgalys & Moncalvo, *Cop. lagopus* (Fr.) Redhead, Vilgalys & Moncalvo, *Cop. macropus* (Berk. & Broome) Redhead, Vilgalys & Moncalvo, *Cop. patouillardii* (Quél.) G. Moreno); and seven of *Parasola* (*P. auricoma* (Pat.) Redhead, Vilgalys & Hopple, *P. glabra* Hussain, Afshan, Ahmad

& Khalid, *P. lilatincta* (Bender & Uljé) Redhead, Vilgalys & Hopple, *P. malakandensis* Hussain, Afshan & Ahmad, *P. plicatilis* (Curtis) Redhead, Vilgalys & Hopple, *P. pseudolactea* Sadiqullah, Hussain & Khalid, *P. setulosa* (Berk. & Broome) Redhead, Vilgalys & Hopple).

During explorations of basidiomycetous fungi in Pakistan in 2014–2017, some interesting collections of *Coprinellus* were encountered. Upon further examination, it was discovered that these collections represent four new species. The current report provides species descriptions based on morphological characters and molecular phylogenetic analyses of nuc rDNA internal transcribed spacers (ITS1-5.8S-ITS2 = ITS). With this study, the number of known species in *Coprinellus* in Pakistan increases to eight.

Materials and methods

Sampling and morphology

Samples were collected in August–September 2014–2017, in the Malakand district of Khyber Pakhtunkhwa and Pabbi district of Punjab, Pakistan. Specimens were photographed, tagged and morphological features including size, shape and colour of basidiomata were noted. For colour designations, the Munsell (1975) colour system was followed. For anatomical study, slides were prepared in 5% aqueous KOH (w/v). Anatomical features, including size and shape of basidiospores, basidia, cheilocystidia, pileipellis and position of germ-pore in basidiospores, were studied using a light microscope (MX4300H, Meiji Techo Co., Ltd., Japan). Data of morpho-anatomical features were recorded from at least 20 measurements. In case of basidiospores, at least 50 spores were measured in face view and side view at a magnification of 1000× and measurements were rounded to the nearest 0.5 µm. Basidiospore measurements are presented as: length range × breadth range × width range. Q values were calculated as: Q_1 = length divided by breadth; Q_2 = length divided by width (Nagy et al. 2010). Specimens studied during this work are deposited in the Herbarium of University of the Punjab, Lahore (LAH) and the Herbarium of University of Swat, Swat, Pakistan (SWAT).

DNA extraction, PCR amplification and sequencing

For DNA extraction, we used the DNeasy Plant Mini Kit (Qiagen, Redwood City, California, USA). We amplified nuc rDNA internal transcribed spacer region (ITS) using the primer combination ITS1F/ITS4 (White et al. 1990). The polymerase chain reaction (PCR) was performed in a 25 µl reaction volume: containing 2.5 µl 10× Econo Taq Buffer (Lucigen, Middleton, Wisconsin, USA), 0.5 µl dNTPs, 1.25 µl of each primer (10 µM/µl), 0.125 µl of Econo Taq® DNA Polymerase (Lucigen), 14.375 µl H_2O and 5 µl DNA template. PCR amplification were performed with 4 min initial denaturation at 95°C, followed by 34 cycles of 50 s at 94°C, 40 s at 54°C, 50 s at 72°C

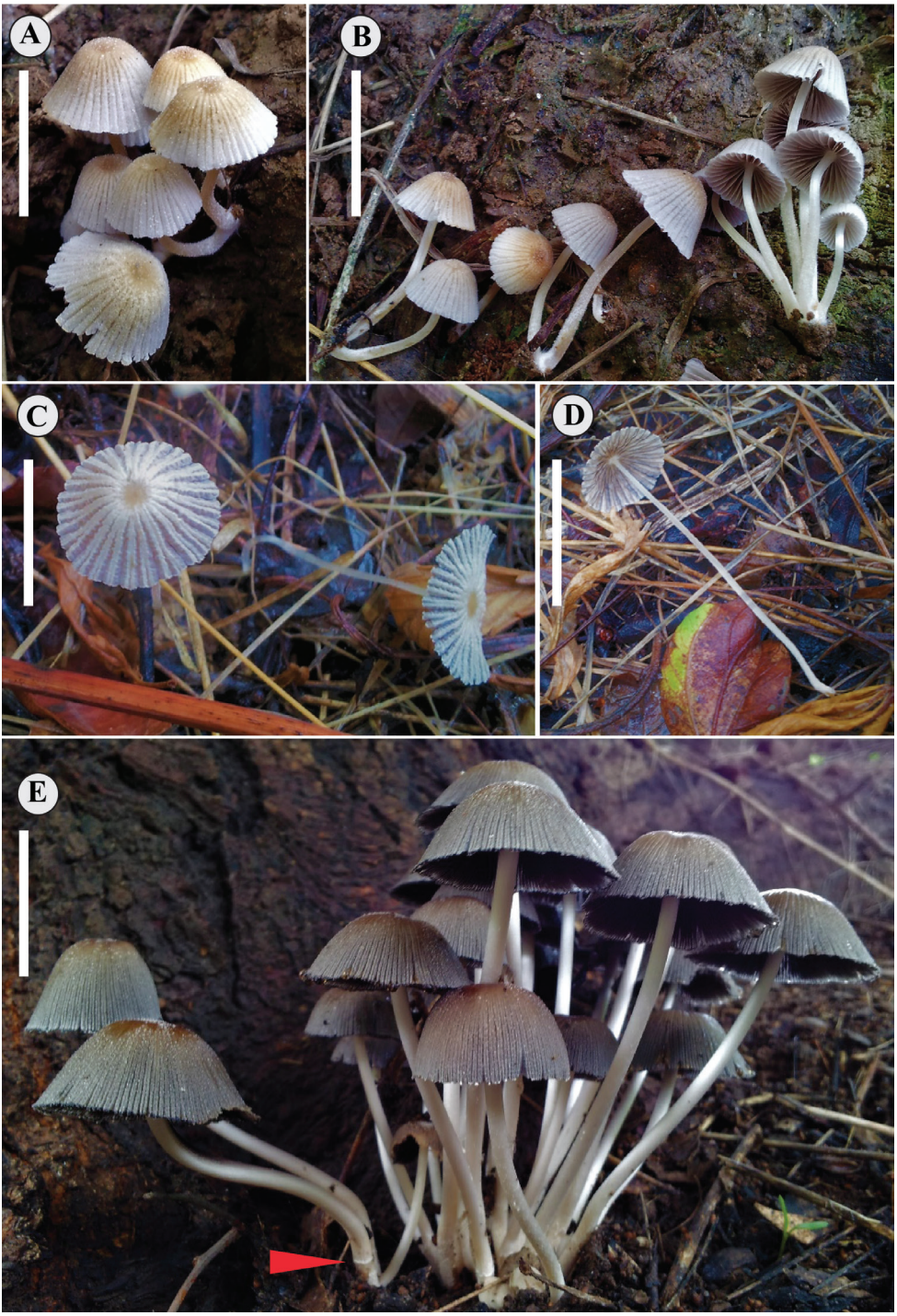

Figure 1. Basidiomata of species of *Coprinellus*. **A–B** *Coprinellus disseminates-similis* (holotype SHCr3W) **C–D** *Coprinellus tenuis* (holotype SHP10) **E** *Coprinellus campanulatus* (holotype SH144). The arrow shows remnants of membranous annulus. Scale bars: 20 mm.

Figure 2. Basidiomata of *Coprinellus pakistanicus* Holotype (MU37). Scale bar: 20 mm.

and a final extension of 7 min at 72°C followed the last cycle. The PCR products were purified using a QIAquick PCR purification kit (Qiagen Inc., Valencia, California, USA). Sequencing was performed using a Bigdye terminator cycle sequencing kit (Applied Biosystems, Foster City, California, USA). Sequencing reactions were purified using Pellet Paint (Novagen, Madison, Wisconsin, USA) and were run on an Applied Biosystems 377 XL automated DNA sequencer. Sequence chromatograms were compiled with Sequencher 4.1 software (GeneCodes Corporation, Ann Arbor, Michigan, USA). Sequences generated for this study are deposited in GenBank (MH366735–MH366737, MH753663–MH753670).

Alignment and phylogenetic analyses

Consensus sequences were generated from both forward and reverse primer reads in BioEdit sequence alignment editor version 7.2.5 (Hall 1999) and then homology searches were performed at the National Center for Biotechnology Information (NCBI) Web site using BLAST. These BLAST results, along with the sequences recently employed in the phylogeny of *Coprinellus* (Nagy et al. 2012), were used in the phylogenetic analyses. DNA sequences were aligned in Clustal X 2.1 (Larkin et al. 2007). *Psathyrella candolleana* (Fr.) Maire was used as outgroup. Sequence alignment was deposited in TreeBase (http://purl.org/phylo/treebase/phylows/study/TB2:S23199).

Phylogenetic inference was conducted using Bayesian and Maximum Likelihood (ML) methods. For Bayesian inference, we used BEAST 1.6.2 (Drummond and Rambaut 2007) with a Markov chain Monte Carlo (MCMC) coalescent approach. For tree prior, a Yule-type speciation model (Gernhard 2008) was used in all simulations

and the starting tree was randomly generated. Four independent runs were undertaken. Chain length was 20 million generations, with a sampling frequency of 1000. Tracer 1.6 (Rambaut et al. 2014) was used to check the effective sample size (ESS) and burn-in values were adjusted to achieve an overall ESS of ≥200. A Maximum Clade Credibility Tree (MCCT) with 20% burn-in was generated using TreeAnnotator 1.6.2 (Drummond and Rambaut 2007). Maximum Likelihood analyses were run in RAXML-VI-HPC (Stamatakis 2006) under the GTRCAT model. Branch support was calculated by 1000 bootstrap replicates. Nodes were considered strongly supported when the maximum likelihood bootstrap (MLB) values were ≥ 70% and Bayesian posterior probability (BPP) values were ≥ 0.95.

Results

Phylogenetic analyses

The ITS dataset comprises 97 sequences and the resulting alignment was 708 bp in length. Phylogenetic trees reconstructed using both Bayesian and ML methods were mostly congruent with each other. Taxa of *Coprinellus* were recovered in seven clades (Figure 3). Clades I–IV consisted of species of section *Setulosi*, three corresponding to clades described in Nagy et al. (2012). Clade I, corresponding to core *Setulosi* clade, was recovered with strong statistical support (BPP/ML 1/98). Clade II corresponded to *Sabulicola* clade with a single species *Co. sabulicola* L. Nagy, Házi, Papp & Vágvölgyi with strong statistical support (1/100). Clade III was the new species *Coprinellus pakistanicus*, forming an independent lineage (1/100). Clade IV corresponded to *Eurysporoid* clade with strong support (1/100). Clade V consisted of species of the *Micacei* clade of Nagy et al. (2012), including *Co. disseminatus* (morphologically placed in section *Setulosi*) along with species of morphological section *Micacei* and recovered with strong statistical support (1/99). The two new species *Coprinellus campanulatus* and *Co. disseminatus-similis* fall in this clade. *Coprinellus campanulatus* formed a sister clade (weak statistical support) with *Co. micaceus* (Bull.) Vilgalys, Hopple & Jacq. Johnson and *Co. truncorum* (Scop.) Redhead, Vilgalys & Moncalvo and would be placed in morphological section *Micacei*. *Coprinellus disseminatus-similis* (1/100) formed a sister clade with *Co. disseminatus* (Pers.) J.E. Lange, adding a further setulose species to this group. Clades VI and VII collectively consisted of species of the *Domestici* clade of Nagy et al. (2012), including species that would be placed morphologically in section *Setulosi*. The fourth new species, *Co. tenuis*, formed a sister clade (1/100) with *Co. curtus* (Kalchbr.) Vilgalys, Hopple & Jacq. Johnson.

Figure 3. Phylogenetic inference of *Coprinellus* species inferred from 97 ITS sequences, with species names following GenBank accessions, specimen voucher numbers and country. Values above branch node represent Bayesian posterior probabilities (BPP) and maximum likelihood bootstrap (MLP), the new species are represented with bold fonts and T represents the holotype collection.

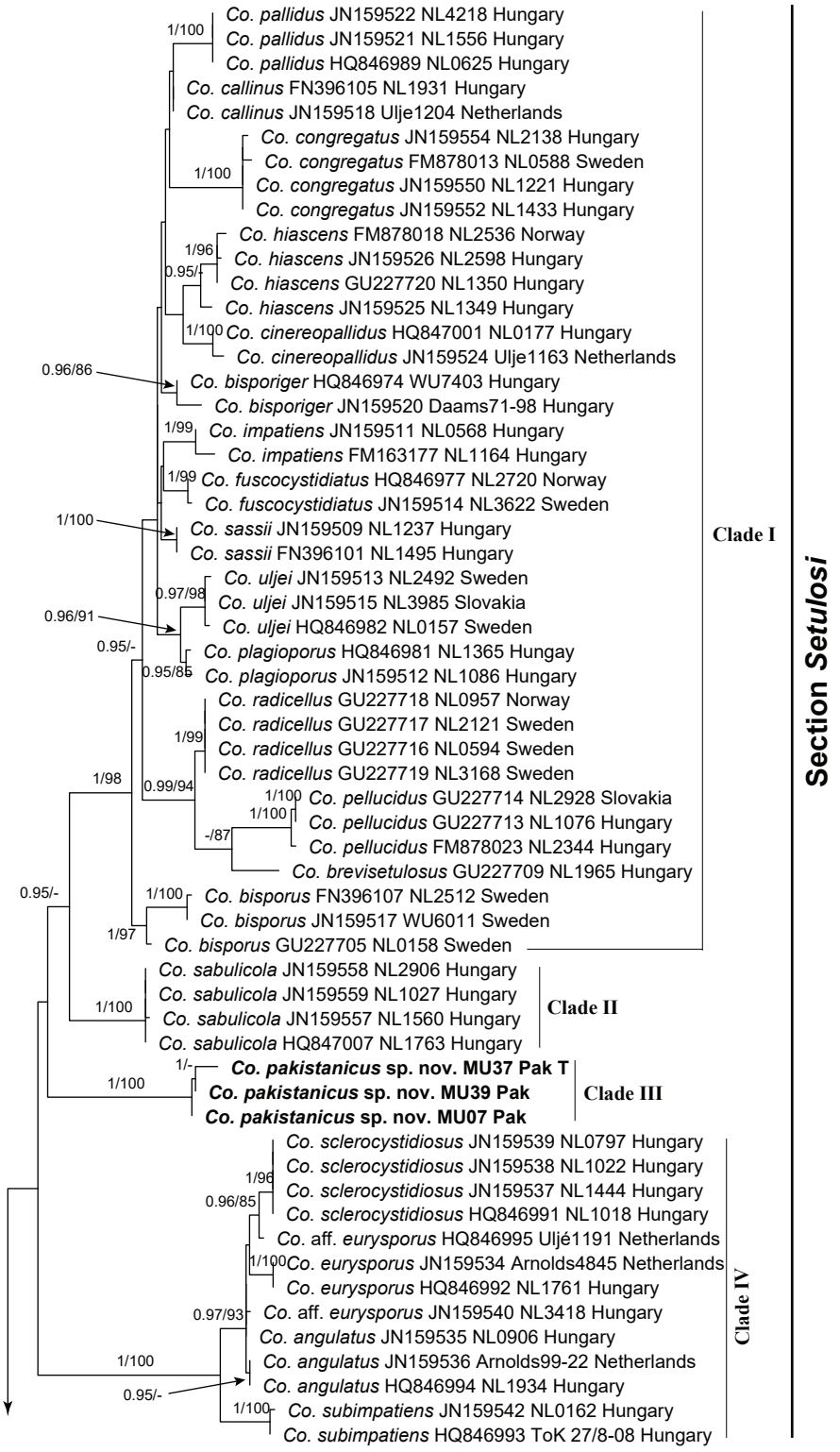
Co. pallidus JN159522 NL4218 Hungary
Co. pallidus JN159521 NL1556 Hungary
Co. pallidus HQ846989 NL0625 Hungary
Co. callinus FN396105 NL1931 Hungary
Co. callinus JN159518 Ulje1204 Netherlands
Co. congregatus JN159554 NL2138 Hungary
Co. congregatus FM878013 NL0588 Sweden
Co. congregatus JN159550 NL1221 Hungary
Co. congregatus JN159552 NL1433 Hungary
Co. hiascens FM878018 NL2536 Norway
Co. hiascens JN159526 NL2598 Hungary
Co. hiascens GU227720 NL1350 Hungary
Co. hiascens JN159525 NL1349 Hungary
Co. cinereopallidus HQ847001 NL0177 Hungary
Co. cinereopallidus JN159524 Ulje1163 Netherlands
Co. bisporiger HQ846974 WU7403 Hungary
Co. bisporiger JN159520 Daams71-98 Hungary
Co. impatiens JN159511 NL0568 Hungary
Co. impatiens FM163177 NL1164 Hungary
Co. fuscocystidiatus HQ846977 NL2720 Norway
Co. fuscocystidiatus JN159514 NL3622 Sweden
Co. sassii JN159509 NL1237 Hungary
Co. sassii FN396101 NL1495 Hungary
Co. uljei JN159513 NL2492 Sweden
Co. uljei JN159515 NL3985 Slovakia
Co. uljei HQ846982 NL0157 Sweden
Co. plagioporus HQ846981 NL1365 Hungay
Co. plagioporus JN159512 NL1086 Hungary
Co. radicellus GU227718 NL0957 Norway
Co. radicellus GU227717 NL2121 Sweden
Co. radicellus GU227716 NL0594 Sweden
Co. radicellus GU227719 NL3168 Sweden
Co. pellucidus GU227714 NL2928 Slovakia
Co. pellucidus GU227713 NL1076 Hungary
Co. pellucidus FM878023 NL2344 Hungary
Co. brevisetulosus GU227709 NL1965 Hungary
Co. bisporus FN396107 NL2512 Sweden
Co. bisporus JN159517 WU6011 Sweden
Co. bisporus GU227705 NL0158 Sweden
Co. sabulicola JN159558 NL2906 Hungary
Co. sabulicola JN159559 NL1027 Hungary
Co. sabulicola JN159557 NL1560 Hungary
Co. sabulicola HQ847007 NL1763 Hungary
Co. pakistanicus sp. nov. MU37 Pak T
Co. pakistanicus sp. nov. MU39 Pak
Co. pakistanicus sp. nov. MU07 Pak
Co. sclerocystidiosus JN159539 NL0797 Hungary
Co. sclerocystidiosus JN159538 NL1022 Hungary
Co. sclerocystidiosus JN159537 NL1444 Hungary
Co. sclerocystidiosus HQ846991 NL1018 Hungary
Co. aff. eurysporus HQ846995 Uljé1191 Netherlands
Co. eurysporus JN159534 Arnolds4845 Netherlands
Co. eurysporus HQ846992 NL1761 Hungary
Co. aff. eurysporus JN159540 NL3418 Hungary
Co. angulatus JN159535 NL0906 Hungary
Co. angulatus JN159536 Arnolds99-22 Netherlands
Co. angulatus HQ846994 NL1934 Hungary
Co. subimpatiens JN159542 NL0162 Hungary
Co. subimpatiens HQ846993 ToK 27/8-08 Hungary
Clade I
Clade II
Clade III
Clade IV
Section Setulosi
1/100
1/100
1/96
0.95/-
1/100
0.96/86
1/99
1/99
1/100
0.97/98
0.96/91
0.95/-
0.95/85
1/99
1/98
0.99/94
1/100
1/100
-/87
0.95/-
1/100
1/97
1/100
1/-
1/100
1/96
0.96/85
1/100
0.97/93
1/100
0.95/-
1/100

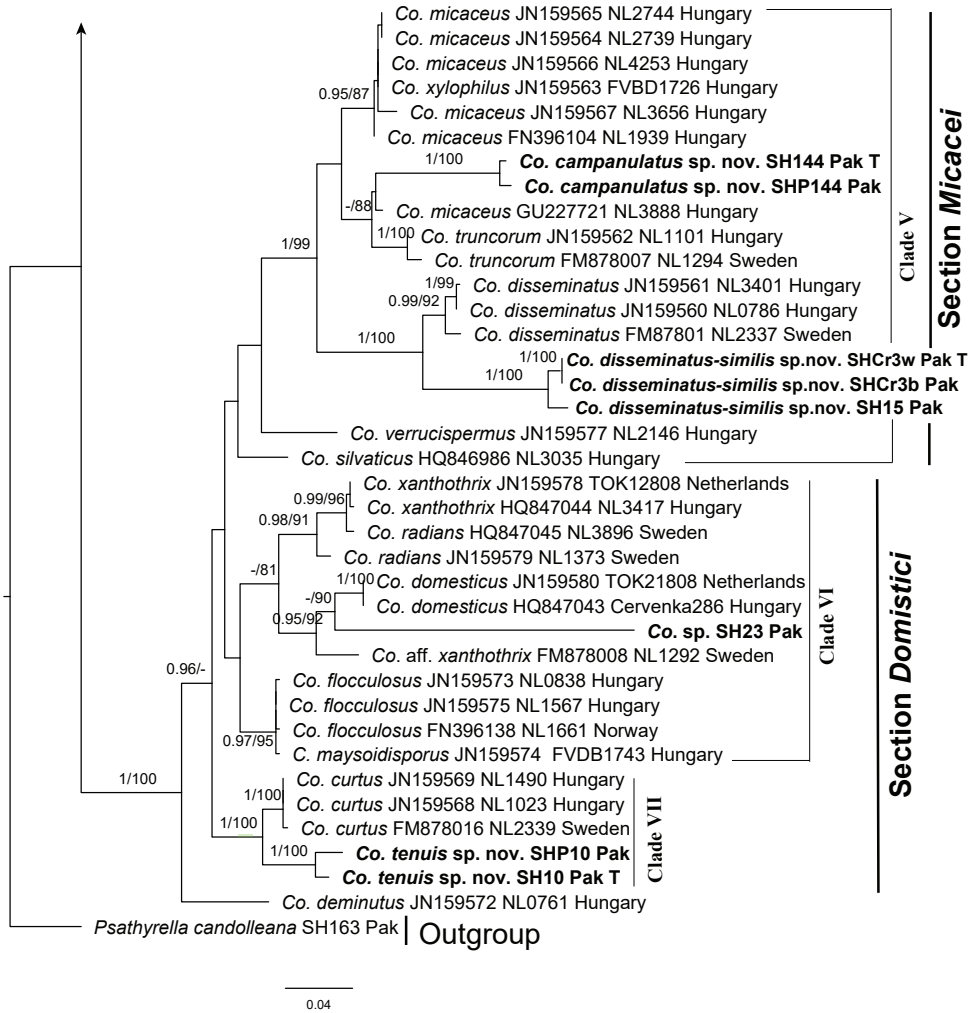

Figure 3. Continued.

Taxonomy

Coprinellus campanulatus Hussain & Ahmad, sp. nov.

MycoBank: MB825477
Figures 1E and 4

Diagnosis. The diagnostic features of *Coprinellus campanulatus* are: campanulate pileus with greyish-olive tinge, surface with glistening clusters of micaceous veil at maturity, dark yellowish-brown centre, basidiospores 8.0–10.5 × 5.5–6.5 × 4.5–5.5 µm, spores mitriform in face view and cylindrical to amygdaliform in side view.

Type. PAKISTAN: **Khyber Pakhtunkhwa**, Qaldara, Dargai, Malakand, 480 m alt., gregarious on wood chip, 14 Aug 2014, *S. Hussain*, SH144 (LAH-SH-144, holotype); GenBank accession ITS: MH753667.

Etymology. The epithet "*campanulatus*" (Latin) refers to the campanulate shape of the pileus of this species.

Macroscopic characters. Pileus at young stage 3–8 × 3–7 mm, ovoid to parabolic, light orange-yellow (7.5YR 9/8) to pale orange-yellow (7.5YR 9/4), surface pruinose; at mature stage 25–40 × 10–15 mm, pulvinate to campanulate, light greyish-olive (10Y 5/2) to greyish-olive (5Y 3/2), centre slightly campanulate, strong yellowish-brown (10YR 4/8) to dark yellowish-brown (10YR 1/2); surface finely furfuraceous to granulose, with clusters of micaceous-glistening veil, bright white, plicate from near centre to margin; context membranous to submembranous. Lamellae adnexed, narrow, with fimbriate edge, crowded with 1–4 series of lamellulae, pale orange-yellow (7.5YR 9/4) at young stage, dark yellowish-brown at maturity (10YR 2/2). Stipe 70–100 × 3–7 mm, equal, white, surface smooth, context hollow. Annulus absent with a membranous layer at the base. Odour pungent. Not tasted.

Microscopic characters. Basidiospores (7.0–)8.0–10.5(–11.5) × (5.0–)5.5–6.5(–7.0) × (4.0–)4.5–5.5(–6.0) µm, on average 9.4 × 5.7 × 5.1 µm, Q_1 = 1.6, Q_2 = 1.8, av. Q = 1.7; in face view mitrifrom, triangular to ellipsoid; in side view cylindrical, amygdaliform to ellipsoid; dark brown to blackish in KOH, smooth, thick-walled, with truncate base, apiculus visible, germ-pore 1.5–2.5 µm wide, central, prominent, pale to hyaline. Basidia 19–29 × 7–10 µm, cylindrical, clavate to subclavate, hyaline, 4-spored. Cheilocystidia 36–47 × 35–45 µm, globose to subglobose, hyaline, abundant. Pleurocystidia absent. Pileipellis an epithelium of loosely arranged globose to subglobose or ellipsoid, hyaline to light olive, thin-walled elements, 30–80 × 25–60 µm. Veil composed of globose to subglobose cells, 50–90 µm diam., slightly thick-walled, yellowish-brown in KOH. Caulocystidia absent. Clamp connections rarely present.

Habitat and distribution. Gregarious on woody litter under *Morus alba*, so far only known from lowland northern Pakistan.

Additional specimens examined. PAKISTAN: Khyber Pakhtunkhwa, Malakand, Qaldara, on woody pasture, 14 August 2014, *S. Hussain*, SH144 (SWAT SHP144).

Comments. The main distinguishing features of *Coprinellus campanulatus* are: campanulate pileus with greyish-olive tinge, dark yellowish-brown centre, veil on pileus in the form of micaceous-glistening clusters which are composed of globose to subglobose cells and basidiospores 8.0–10.5 × 5.5–6.5 × 4.5–5.5 µm, spores mitriform in face view and cylindrical to amygdaliform in side view. Based on veil anatomy, *Co. campanulatus* belongs in sect. *Micacei*. *Coprinellus micaceus* and *Co. truncorum* are most closely related to *Co. campanulatus* amongst the species sampled for our phylogenetic analyses. The new species *Co. campanulatus* with pulvinate to campanulate pileus can be differentiated from *Co. micaceus* and *Co. truncorum*, which have broadly convex pilei. At maturity, the pileus is light brown in *Co. micaceus* and *Co. truncorum* when compared to *Co. campanulatus* with greyish-olive pileus. On basis of spore morphology, *Co. campanulatus* can be differentiated from *Co. micaceus*. Basidiospores in

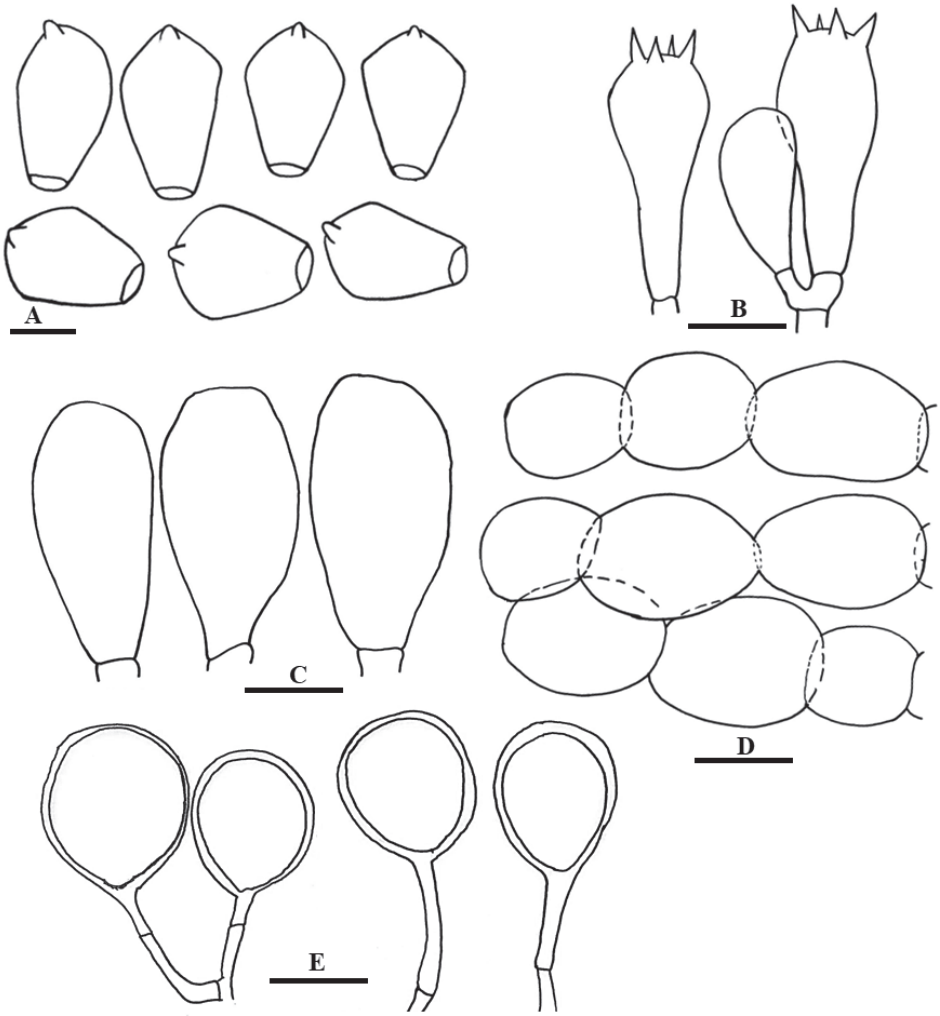

Figure 4. Line drawing of anatomical characters of *Coprinellus campanulatus* **A** Basidiospores **B** Basidia **C** Cheilocystidia **D** Pileipellis **E** Veil elements. Scale bars: 10 µm (**A**), 20 µm (**B–E**).

Co. micaceus are slightly smaller (6.5–10.0 × 4.5–7 µm), lacrimiform to submitriform or mitriform in face view, conical towards base (Keirle et al. 2004, Uljé 2005). In *Co. micaceus*, voluminous, broadly clavate, (sub)globose to ellipsoid pleurocystidia up to 150 × 70 µm are present, in *Co. campanulatus* pleurocystidia are absent. Also, in *C. micaceus*, caulocystidia are abundant, in *Co. campanulatus* absent. Spores of *Co. truncorum* are 8.5–9.0 × 5.5–6 µm, ellipsoid in all views, not distinctly lentiform, with very broad central to slightly eccentric germ pore, broadly rounded apex, not truncate, smooth, dark grey to grey brown or black (Keirle et al. 2004, Uljé 2005).

Coprinellus disseminatus-similis **Hussain, sp. nov.**
MycoBank: MB825478
Figures 1A–B and 5

Diagnosis. The most important features of *Co. disseminatus-similis* are: pileus parabolic to campanulate, greyish-brown, with umbonate centre; surface pruinose to pulverulent, with sparse micaceous-glistening veil, bright white, deeply plicate from centre to margin; basidiospores 8.0–9.0 × 5.0–5.5 × 4.5–5.5 µm, in face view ellipsoid to cylindrical or obovoid, in side view ellipsoid to amygdaliform, smooth, thick-walled, with truncate base, germ-pore central, 0.5–1.0 µm wide.

Type. PAKISTAN: Khyber Pakhtunkhwa, Malakand, Sarogai, 450 m alt., gregarious on wood chips, 23 Sept 2014, *S. Hussain*, SHCr3w (SWAT-SHCr3w, holotype); GenBank accession ITS: MH753670.

Etymology. "*Similis*" (Latin) meaning like, referring to the similarity of the new species to *Coprinellus disseminatus*.

Macroscopic characters. Pileus at young stage cylindrical and closed, 3–5 × 3–7 mm, whitish to light greyish (2.5Y 7/4), surface pruinose, slightly plicate toward margin; at mature stage 15–20 × 20 mm, parabolic to campanulate to umbonate, light greyish-brown (7.5YR 6/2) to greyish-yellowish-brown (7.5YR 6/2); with umbonate centre, in old specimens centre papillate, centre moderate orange (2.5YR 6/8) to brownish-orange (2.5YR 5/8); surface pruinose to pulverulent, with sparse micaceous-glistening veil, bright white, deeply plicate from centre to margin; context membranous. Lamellae sinuate to uncinate, distant with 0–2 lamellulae, initially white, fading with age and dark greyish-brown at maturity. Stipe 20–40 × 1 mm, equal, central, white, surface pruinose to pulverulent with sparse micaceous-glistening veil, context hollow, annulus absent. Odour pungent, not tasted.

Microscopic characters. Basidiospores (7.5–)8.0–9.0(–9.5) × (4.5–)5.0–5.5(–6.0) × (4.0–)4.5–5.5(–6.0) µm, on average 8.5 × 5.2 × 4.9 µm, Q_1 = 1.53–1.7, Q_2 = 1.7–1.9, av. Q = 1.6; in face view, ellipsoid to cylindrical or obovoid, in side view, ellipsoid to amygdaliform, dark brown to blackish in KOH, smooth, thick-walled, with truncate base, germ-pore central, 0.5–1.0 µm wide. Basidia 26–30 × 7–10 µm, clavate to cylindrical, 2 to 4–spored, hyaline. Cheilocystidia 70–165 × 11–15 µm, cylindrical, narrowly clavate to narrowly utriform, some with subcapitate apex, abundant, smooth, hyaline. Pleurocystidia absent. Pileipellis a loosely arranged euhymeniderm with narrowly utriform to utriform pileocystidia, 118–165 × 23–28 µm, light-brownish to hyaline, smooth. Veil elements 20–40 µm, globose to subglobose, greyish-brown, smooth. Clamp connection not observed.

Habitat and distribution. Gregarious on leaf litter under *Populus alba* and *Morus alba*, so far only known from lowland northern Pakistan.

Additional specimens examined. PAKISTAN. Khyber Pakhtunkhwa: Malakand, Sarogai, on leaf litter under *Populus alba* and *Morus alba*, 22 Sept 2014, *S. Hussain*, SH-Cr3-b (SWAT SH-Cr3-b).

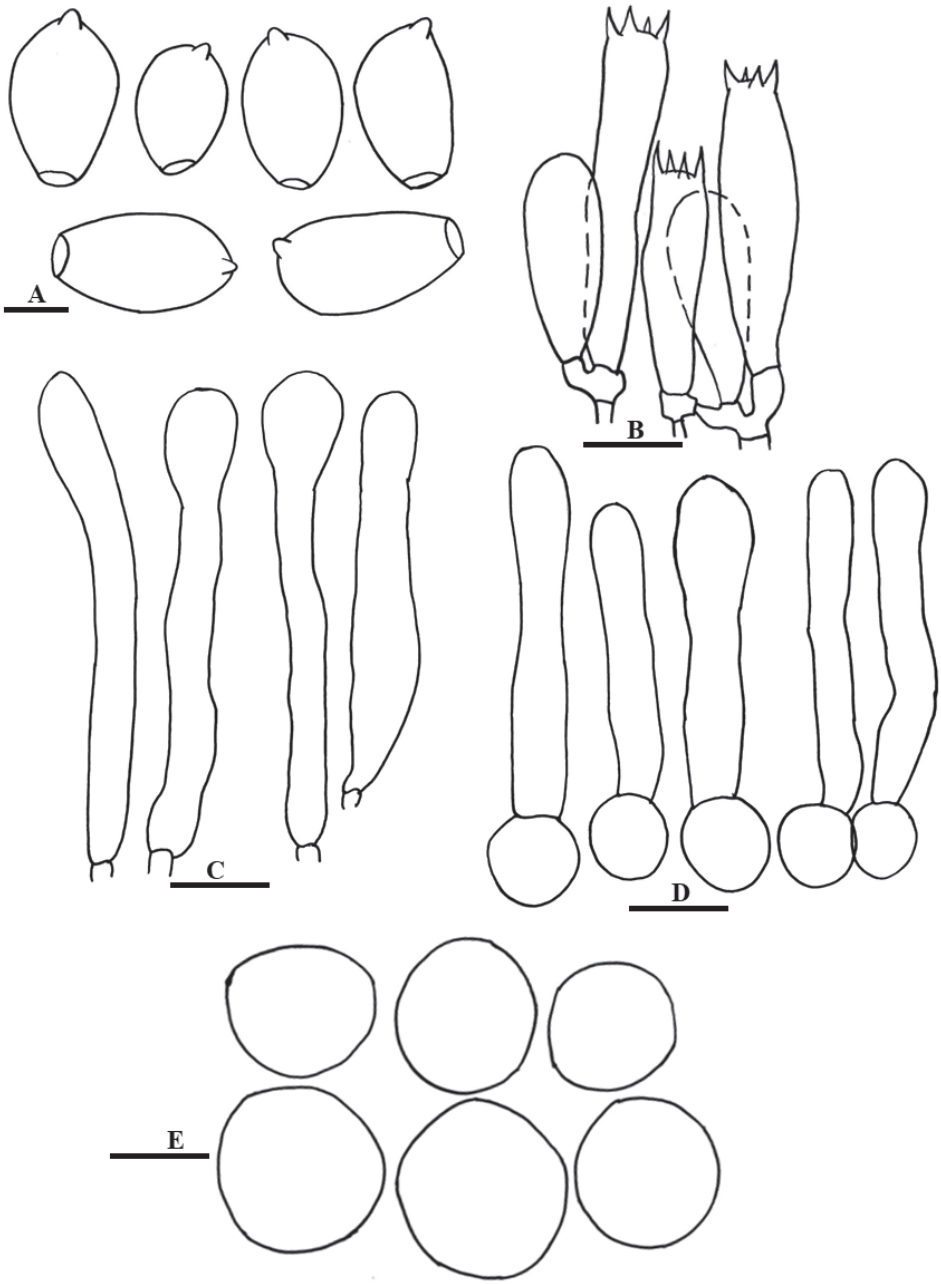

Figure 5. Line drawing of anatomical characters of *Coprinellus disseminatus-similis* **A** Basidiospores **B** Basidia **C** Cheilocystidia **D** Pileipellis with pileocystidia **E** Veil elements. Scale bars: 10 μm (**A**), 20 μm (**B–E**).

Comments. The new species would be placed in sect. *Setulosi* because of its pileocystidia. However, as with *Co. disseminatus*, which it resembles and is close to in the molecular phylogram, *Co. disseminatus-similis* falls in a clade along with members of

section *Micacei* that lack such pileocystidia, underlining the need to update the formal description of the sections. Both these species share basidiospore morphology. However, they differ on the basis of: (i) pileus shape and colour, (ii) cheilocystidia and (iii) pileocystidia and veil anatomy. In *Co. disseminatus*, initially the pileus is (sub)globose or ovoid, then hemispherical or obtusely conical to convex, rarely flat, the fruit bodies often form in very large groups and are initially very pale, almost white, darkening as the spores mature; cheilocystidia are absent along most of the gill edge; pileocystidia are lageniform with cylindrical neck and rounded, rarely subcapitate, apex and large 50–200 × 15–24 µm; and veil elements are globose to subglobose, generally with golden brown incrustations (Uljé and Bas 1991, Uljé 2005). In *Co. disseminatus-similis*, at young stage, the pileus is cylindrical and closed, parabolic to campanulate to umbonate at mature stage, with papillate centre in some old specimens; cheilocystidia are large (70–165 × 11–15 µm), narrowly clavate to narrowly utriform, some with subcapitate apex; pileocystidia are narrowly utriform to utriform; and veil elements are globose to subglobose and smooth. Using ML and Bayesian analyses, *Coprinellus verrucispermus* (Joss. & Enderle) Redhead, Vilgalys & Moncalvo is another species close to *Co. disseminatus-similis*. Spores in *Co. verrucispermus* are substantially larger (11.0–14.5 × 7.0–9.0 µm), ellipsoid to slightly amygdaliform, chestnut brown, apiculus slight, warty with perisporial sac and central germ pore (Uljé and Bas 1991, Keirle et al. 2004).

Coprinellus pakistanicus **Usman & Khalid, sp. nov.**
MycoBank: MB825483
Figures 2 and 6

Diagnosis. The distinguishing features of *Coprinellus pakistanicus* are: light yellowish-green to greyish-yellow pileus, surface smooth with sub-membranous context, basidiospores 8.5–11.5 × 6.5–8.0 × 5.5–6.5 µm, on average 10 × 7.4 × 6.2 µm, in face view broadly ellipsoid, obovoid to phaseoliform, in side view ovoid, ellipsoid to obovoid, base not truncate, apiculus visible in side view, germ-pore central.

Type. PAKISTAN: Punjab, Pabbi Forest Park, 286 m alt., 11 Aug 2016, *M. Usman* and *Abdul N. Khalid*, MU37 (Holotype LAH35323); GenBank accession ITS: MH366736.

Etymology. The specific epithet "*pakistanicus*" refers to the holotype locality of this species.

Macroscopic characters. Pileus 25–35 mm diam, convex to plan, with depressed centre, light yellow green (2.5GY 8/6) to greyish-greenish-yellow (7.5Y 7/4); surface smooth with sparsely pulverulent to granulose, deeply plicate from centre towards margin; centre depressed to slightly papillate, orange yellow (7.5YR 6/8); context sub-membranous, light greyish (10Y 5/2). Lamellae free, crowded, regular, dark brown to blackish, with 0–2 series of lamellulae. Stipe 27–50 × 1 mm, central, hollow, smooth, white, with slightly bulbous base. Annulus and volva absent. Odour and taste not recorded.

Microscopic characters. Basidiospores (7–)8.5–11.5(–12) × (6.0–)6.5–8.0(–8.5) × (–5.0)5.5–6.5(–7.0) µm, on average 10 × 7.4 × 6.2 µm, Q_1 = 1.4, Q_2 = 1.6, av. Q =

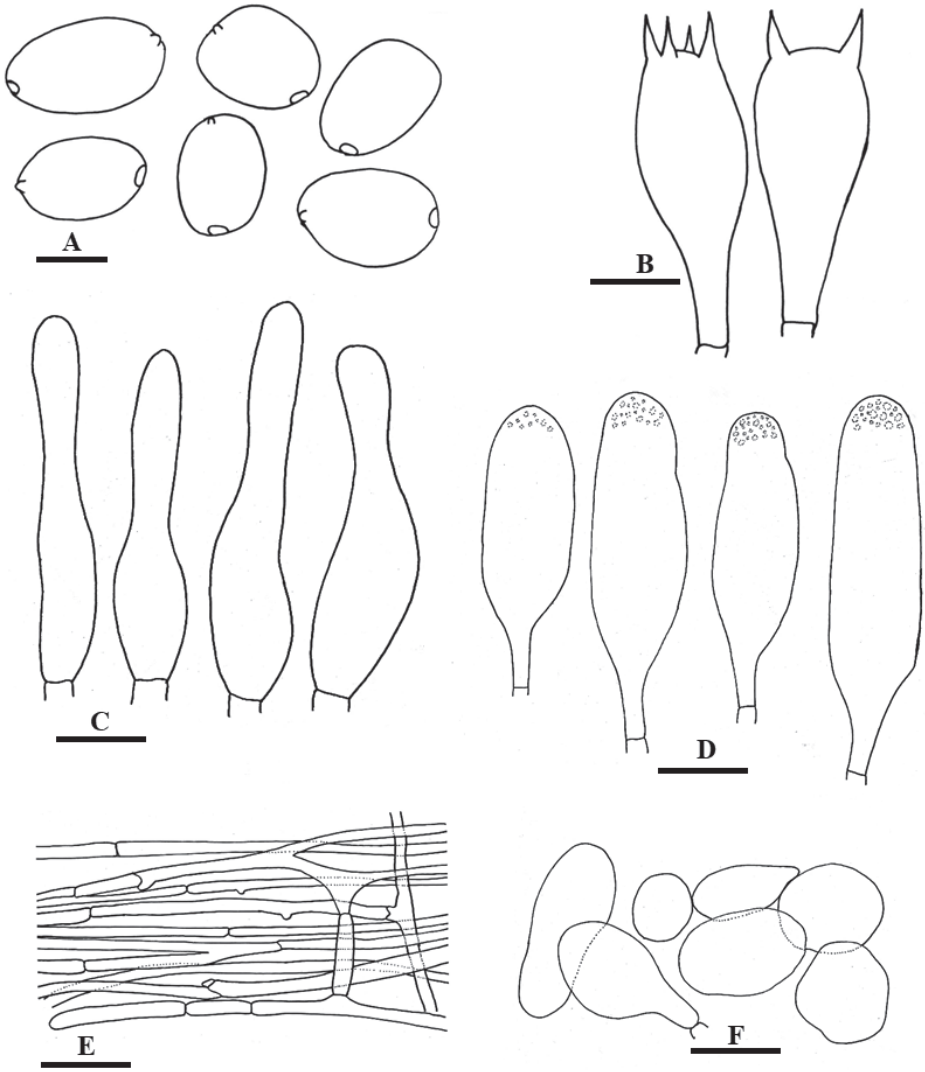

Figure 6. Line drawing of anatomical characters of *Coprinellus pakistanicus* **A** Basidiospores **B** Basidia **C** Pileocystidia **D** Cheilocystidia **E** Pileal hyphae **F** Veil elements. Scale bars: 10 µm (**A**), 20 µm (**B–F**).

1.3; in face view, broadly ellipsoid, obovoid to phaseoliform, in side view, ovoid, ellipsoid to obovoid, base not truncate, apiculus slightly visible, germ-pore central, smooth, slightly thin-walled, dark brown to blackish in KOH. Basidia 13.5–32 × 8.5–12 µm, clavate to narrowly clavate, hyaline, smooth, 2- to 4-spored, sterigmata up to 4 µm in length. Cheilocystidia 42–75 × 14–25 µm, cylindrical to lageniform, hyaline with crystals usually at the apex of cystidium. Pleurocystidia absent. Pileipellis irregular epithelium, 3.5–7.5 µm diam., pale to hyaline in KOH. Pileocystidia 30–90 × 9–24

µm, lageniform to cylindrical with tapering neck and obtuse apex, pale to hyaline in KOH. Veil rounded to globose cells, 15–25 µm diam., slightly thick-walled, yellowish in KOH. Clamp connection present.

Habitat and distribution. Scattered on moist soil, under trees of *Acacia nilotica* and *A. modesta*, so far only known from lowland northern Pakistan.

Additional specimens examined. PAKISTAN. Punjab: Pabbi Forest Park, 286 m alt., 20 Aug 2016 & 2017, M. Usman, Abdul N. Khalid and A. Hameed, MU07, MU39 (LAH35324 and LAH35325).

Comments. In phylogenetic analyses, *Coprinellus pakistanicus* forms Clade III, adjacent to the *Sabulicola* and *Eurysporoid* clades of Nagy et al. (2012) and morphologically would be placed in sect. *Setulosi*. The new species is compared with the following species of sect. *Setulosi*: *Co. bisporus* (J.E. Lange) Vilgalys, Hopple & Jacq. Johnson, *Co. cinereopallidus* L. Nagy, Házi, Papp & Vágvölgyi, *Co. congregatus* (Bull.) P. Karst., *Co. pellucidus* (P. Karst.) Redhead, Vilgalys & Moncalvo, *Co. radicellus* Házi, L. Nagy, Papp & Vágvölgyi and *Co. sabulicola* L. Nagy, Házi, Papp & Vágvölgyi.

In *Co. bisporus,* the pileus is small, up to 20 mm diam., ochre or pale brown; with dark red-brown basidiospores; cheilocysticdia subglobose, ovoid, ellipsoid to broadly utriform and smaller in size (24–40 × 16–23 µm) when compared to *Co. pakistanicus* (Prydiuk 2010). In *Co. cinereopallidus*, basidiospores are larger 12.1 × 6.5 µm, ellipsoid to subamygdaloid, not lentiform (Nagy et al. 2012). Similarly, *Co. congregatus* with pileus up to 20 mm in diam., cream-coloured, at centre ochre-brown to light brown, cheilocystidia subglobose, ovoid to ellipsoid, sometimes utriform, 22–50 × 15–36 µm in size (Prydiuk 2010). *Coprinellus pellucidus* with substantially small pileus (7 mm diam.), basidiospores 9.25 × 4.75 µm, elongate-ellipsoid to cylindrical-ellipsoid, with subglobose cheilocystidia, 20–25 × 14–22 µm (Prydiuk 2010). Pileus in *Co. radicellus* up to 10 mm diam., cream coloured to dark melleous-brown, expanding to convex applanate with uprolled margin, basidiospores on average 9.48 × 4.91 µm, reddish-brown, ellipsoid to subcylindrical, with globose to subglobose or clavate cheilocystidia, 9–20 × 8–14 µm in size (Házi et al. 2011). *Co. sabuilcola* has concave, warm reddish-brown pileus, basidiospores on average 17.3 × 10.9 µm, cheilocystidia 17–32 × 12.5–27 µm, globose to vesiculose or broadly ellipsoid (Nagy et al. 2012).

***Coprinellus tenuis* Hussain, sp. nov.**
MycoBank: MB825479
Figures 1C–D and 7

Diagnosis. The new species *Coprinellus tenuis* can be recognised by its thin and membranous pileus, surface glabrous and furred, deeply plicate towards margin; lamellae sinuate to uncinate; basidiospores 10.5–14.5 × 8.0–9.5 × 6.5–8.5 µm, in face view, broadly ellipsoid to ovoid, in side view, slightly pyriform to ellipsoid, usually with truncate base, apiculus mostly not visible, with eccentric germ-pore, 1.5–2 µm wide.

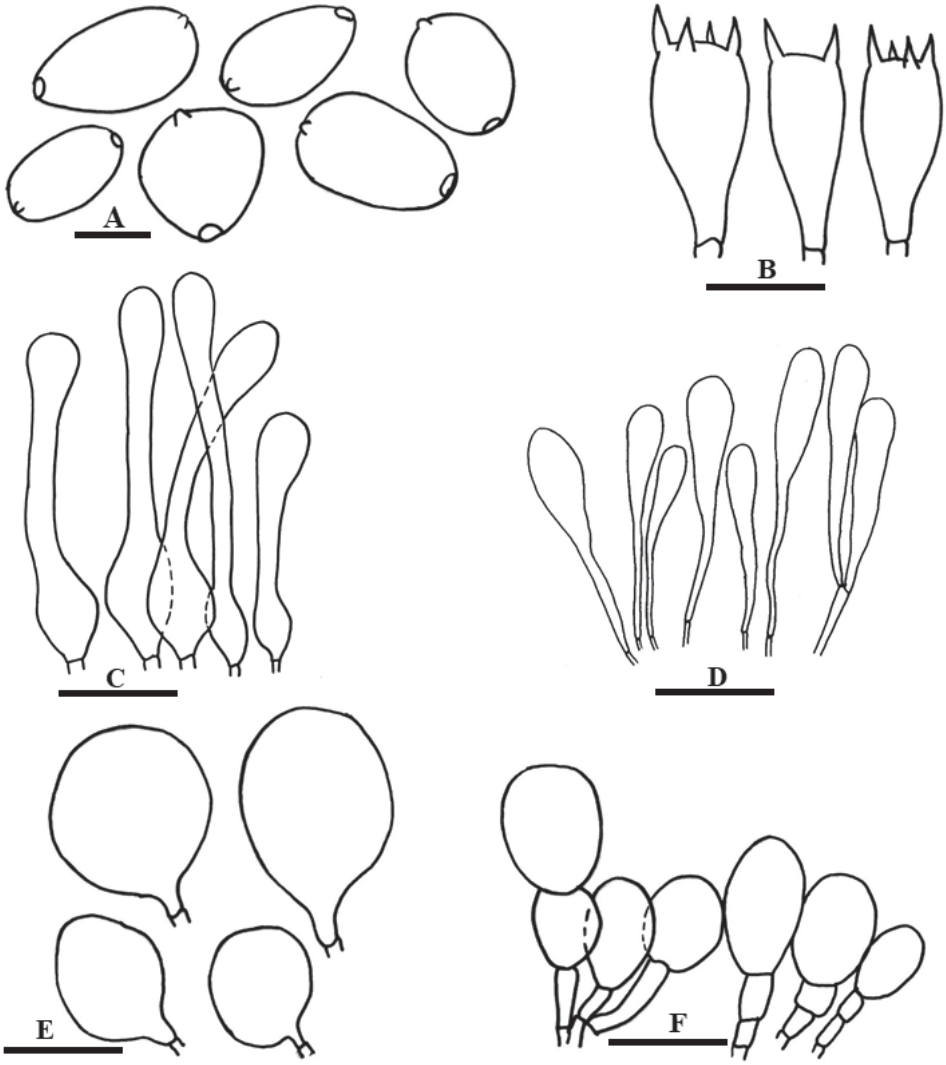

Figure 7. Anatomical features of *Coprinellus tenuis* **A** Basidiospores **B** Basidia **C** Pileocystidia **D** Caulocystidia **E** Cheilocystidia **F** Veil cells. Scale bars: 10 μm (**A**), 20 μm (**B–F**).

Type. PAKISTAN: Khyber Pakhtunkhwa, Malakand, Qaldara, 430 m alt., solitary on leaf litter, 7 July 2014, *S. Hussain*, SHP10 (SWAT-SH-P10, holotype); GenBank accession ITS: MH753663.

Etymology. "*tenuis*" (Latin) meaning thin, referring to the membranous pileus of the new species.

Macroscopic characters. Pileus 15–20 mm diam, pulvinate to convex to plane, light greyish-brown (7.5YR 5/2) to light brown (5YR 6/4); surface glabrous, furred, deeply plicate from centre towards margin; centre truncately conical, moderate red-

dish-orange (10R 5/8) to greyish-reddish-orange (2.5YR 5/6); context membranous. Lamellae sinuate to uncinate, distant, with 0–2 series of lamelullae, light greyish-brown (7.5YR 5/2) to light brown (5YR 6/4), lamellae edge blackish and fimbriate to eroded. Stipe 40–60 × 1 mm, equal, cylindrical, surface scabrous, white, translucent, fragile, context hollow.

Microscopic characters. Basidiospores (9.0–)10.5–14.5(–15.5) × (7.5–)8.0–9.5(–10.5) × (5.0–)6.5–8.5(–9.0) µm, on average 13.1 × 9.0 × 7.8 µm; Q_1 = 1.25–1.49, Q_2 = 1.57–1.63, av. Q = 1.45; in face view, broadly ellipsoid to ovoid, in side view, slightly pyriform to ellipsoid, usually with truncate base, apiculus mostly not visible, germ-pore eccentric, 1.5–2 µm wide, wall 1.5 µm thick, dark brown to almost black. Basidia 22–24 × 9–12 µm, clavate, 2- to 4-spored, hyaline in KOH. Cheilocystidia 22–30 × 19–28 µm, rounded to globose, abundant, hyaline. Pleurocystidia absent. Pileocystidia 78–94 × 10–12 µm, lageniform to cylindrical with rounded apex, elongated rod shape neck with rounded enlarged base, hyaline in KOH. Caulocystidia 50–67 × 9–11 µm, narrowly clavate to clavate, with rounded to obtuse apex, cylindrical base. Veil comprised of rounded to subglobose cells, arranged in short chain, thick-walled with encrusted walls, dark brown, with terminal cell 17–23 × 12–15 µm.

Habitat and distribution. Scattered on leaf litter under *Acacia modesta*, so far only known from lowland northern Pakistan.

Additional specimens examined. PAKISTAN. Khyber Pakhtunkhwa: Malakand, Qaldara, on leaf litter under *Acacia modesta*, 10 July 2014, *S. Hussain*, SH10 (SWAT SH-10).

Comments. *Coprinellus tenuis* with thin membranous pileus, shows similarities with *Co. curtus*. Both these species can be differentiated on (i) pileus morphology (ii) basidiospore shape and (iii) habitat. Pileus is deeply plicate in both these species, in *Co. tenuis* pileus is glabrous and furred; however, there is no furcation in the pileus of *Co. curtus*. Spores in *Co. curtus* are substantially smaller (8.0–10.0 × 5.5–7.0 µm), ellipsoid to ovoid in face view, narrowly ellipsoid or phaseoliform in side view, apiculus often not visible, with a distinct central to slightly eccentric germ-pore, not truncate. Basidiospores in *Co. tenuis* are larger (10.5–14.5 × 8.0–9.5 × 6.5–8.5 µm), in face view broadly ellipsoid to ovoid, in side view slightly pyriform to ellipsoid, usually with truncate base, apiculus mostly not visible, with eccentric germ-pore of 1.5–2 µm diam. *Coprinellus curtus* has a substrate preference and is most commonly collected from herbivores' dung as opposed to *Co. tenuis* basidioma on leaf litter (Uljé and Bas 1991).

Discussion

The genus *Coprinellus* is one of the most species-rich genera in Psathyrellaceae, with approximately 80 described species (Kirk et al. 2008, Nagy et al. 2012, Gomes and Wartchow 2014). Species of *Coprinellus* have been classified in three sections, reflecting earlier sub-sections of *Coprinus* sensu lato, primarily based on veil anatomy and the presence or absence of cap pileocystidia (Schafer 2010). The most recent phylogenetic

study of this genus by Nagy et al. (2012), does not provide evidence for the monophyly of morphologically based sections of previous classifications (Orton and Watling 1979, Uljé 2005, Schafer 2010).

In the phylogeny we present here, based on ITS sequences, the genus is recovered in seven clades (Figure 3). In morphology-based taxonomy, species in section *Setulosi* have setules on their pilei and the majority of such species recovered as a non-monophyletic lineage consisting of four clades in this study. Clade I, corresponding to core *Setulosi* clade in the Nagy et al. (2012) phylogeny, is a large group of species with the characteristic setules on the pileus. Clade II corresponds to *Sabulicola* clade with a single species *Co. sabulicola* L. Nagy, Házi, Papp & Vágvölgyi. This species bears some unique features compared with other *Coprinellus* species; amongst these are relatively large basidiospores (15–22 × 10–13 µm), lack of a pedicel on the cystidia, habitat in dry, sandy sites and short, capitate pileocystidia with incrusted base (Nagy et al. 2012). Clade III represents the new species *Coprinellus pakistanicus*. This species has ellipsoid to phaseoliform basidiospores, cylindrical to lageniform cheilocystidia, pileocystidia lageniform to cylindrical with tapering neck and obtuse apex, veil with rounded to globose cells, slightly thick-walled, clamp connections present amongst most tissues. Clade IV, corresponding to the *Eurysporoid* clade (fig. 1 of Nagy et al. 2012), was inferred with strong statistical support (1/100) and consisted of some well-studied species, forming a basal group in this phylogeny. Amongst the species, there are *Coprinellus eurysporus* (M. Lange & A.H. Sm.) Redhead, Vilgalys & Moncalvo, *Co. sclerocystidiosus* (M. Lange & A.H. Sm.) Vilgalys, Hopple & Jacq. Johnson, *Co. subimpatiens* (M. Lange & A.H. Sm.) Redhead, Vilgalys & Moncalvo.

Clade V includes species of sect. *Micacei*, along with *Co. disseminatus* and our new species *Co. disseminatus-similis*, reflecting the *Micacei* clade of Nagy et al. 2012. It also includes *Co. verrucispermus* and *Co. deliquescens* (=*Co. silvaticus*), which were placed in the *Domestici* clade in that study, although data would allow a plausible phylogenetic position for those two species in the *Micacei* clade (Nagy et al. 2012, p.256). Taxa in section *Micacei* have a veil in the form of glistening mica-like granules, consisting of thin-walled globose cells in a matrix of narrow branched hyphae. The granules can be easily washed off by rain drops, causing difficulties in differentiation (Schafer 2010). Rich veil coverage on the pileus was suggested as a character linking the non-setulose and setulose species in both the *Domestici* and *Micacei* clades, the key feature for the *Micacei* clade being mitriform shaped basidiospores (Nagy et al. 2012).

Clade VI and VII, if taken together, would collectively correspond to the *Domestici* clade, inferred as a non-monophyletic group in *Coprinellus*. Species in clade VI have a veil consisting of floccose scales, made up of generally thick-walled, yellow-brown chains of inflated, ellipsoid or globose cells (thin-walled and hyaline in *Co. flocculosus*) and correspond to section *Domestici*. "*Coprinus maysodisporus*" in Nagy et al. 2012 ("*Coprinus maysoidisporus*" in GenBank) appears to refer to collection FVDB1743 and appears to relate to a collection of a provisionally named species "*Coprinus maydisiformis*", close to *Co. xanthothrix*, from Washington State, USA in 1972 (Van de Bogart 1975). Clade VII is entirely comprised of species containing thick-walled, encrusted veil cells as well as pileal setules with capitate or swollen apex

(*Coprinellus curtus*, *Co. tenuis*). These differences between the clades found in our study and those in Nagy 2012 might therefore provide DNA phylogenic support for the morphologically defined section *Domestici*, but still leave the remaining sections in need of updating, clade VII being a separate *Curtus* clade.

In the present study, we demonstrated that low-altitude mountains and grasslands of Pakistan are rich in species of *Coprienllus*. The climatic conditions of these areas of the country are favourable for growth of coprinoid mushrooms. With the description of these four new species, the number of know species of *Coprinellus* from Pakistan increases to eight.

Acknowledgments

We greatly thank Dr Mykola Prydiuk (M.G. Kholodny Institute of Botany, Ukraine) for review of the manuscript. S.H. thanks all members of Farlow Herbarium (Harvard University) for facilitating his stay during this study. The authors also thank Derek J. Schafer (UK) for the critical review of the manuscript. Financial support for this study was provided by the Higher Education Commission of Pakistan under the International Research Support Initiative Program (IRSIP).

References

Ahmad S (1980) A contribution to the Agaricales of Pakistan. Bulletin of Mycology 1: 35–90.

Drummond AJ, Rambaut A (2007) BEAST: Bayesian evolutionary analysis by sampling trees. BMC Evolutionary Biology 7(1): 214. https://doi.org/10.1186/1471-2148-7-214

Gernhard T (2008) The conditioned reconstructed process. Journal of Theoretical Biology 253(4): 769–778. https://doi.org/10.1016/j.jtbi.2008.04.005

Gomes ARP, Wartchow F (2014) *Coprinellus arenicola*, a new species from Paraíba, Brazil. Sydowia 66: 249–256. https://doi.org/10.12905/0380.sydowia66(2)2014-0249

Hall TA (1999) BioEdit: a user-friendly biological sequence alignment editor and analysis program for Windows 95/98/NT. Nucleic Acids Symposium Series No. 41: Oxford University Press, 95–98. https://doi.org/10.1021/bk-1999-0734.ch008

Házi J, Nagy GL, Vágvölgyi C, Papp T (2011) *Coprinellus radicellus*, a new species with northern distribution. Mycological Progress 10: 363–371. https://doi.org/10.1007/s11557-010-0709-y

Hussain S, Afshan NS, Ahmad H (2016) First record of *Parasola lilatincta* from Pakistan. Mycotaxon 131(2): 317–323. https://doi.org/10.5248/131.317

Hussain S, Afshan NS, Ahmad H, Khalid AN, Niazi AR (2017) *Parasola malakandensis* (Psathyrellaceae; Basidiomycota) from Malakand, Pakistan. Mycoscience 58(2): 69–76. https://doi.org/10.1016/j.myc.2016.09.002

Hussain S, Ahmad H, Ullah S, Afshan N, Pfister DH, Sher H, Ali H, Khalid AN (2018) The genus *Parasola* in Pakistan with the description of two new species. MycoKeys 30: 41–60. https://doi.org/10.3897/mycokeys.30.21430

Keirle MR, Hemmes DE, Desjardin DE (2004) Agaricales of the Hawaiian Islands. 8. Agaricaceae: *Coprinus* and *Podaxis*; Psathyrellaceae: *Coprinopsis*, *Coprinellus* and *Parasola*. Fungal Diversity 15(3): 33–124.

Kirk PM, Cannon PF, Minter DW, Stalpers JA (2008) Dictionary of the Fungi (10th edn). CABI, Wallingford.

Larkin MA, Blackshields G, Brown NP, Chenna R, McGettigan PA, McWilliam H, Valentin F, Wallace IM, Wilm A, Lopez R, Thompson JD, Gibson TJ, Higgins DG (2007) ClustalW and ClustalX version 2.0. Bioinformatics 23(21): 2947–2948. https://doi.org/10.1093/bioinformatics/btm404

Matheny PB, Curtis JM, Hofstetter V, Aime MC, Moncalvo JM, Ge ZW, Yang ZL, Slot JC, Ammirati JF, Baroni TJ, Bougher NL (2006) Major clades of Agaricales: a multilocus phylogenetic overview. Mycologia 98(6): 982–995. https://doi.org/10.1080/15572536.2006.11832627

Munsell AH (1975) Munsell soil color charts. Baltimore, Munsell Color Inc., Baltimore.

Nagy GL (2008) Identification key to *Coprinus* species known from Europe. Clusiana 47: 31–44.

Nagy GL, Vágvölgyi C, Papp T (2010) Type studies and nomenclatural revisions in *Parasola* (Psathyrellaceae) and related taxa. Mycotaxon 112: 103–141. https://doi.org/10.5248/112.103

Nagy L (2011) An investigation of the phylogeny and evolutionary processes of deliquescent fruiting bodies in the mushroom family Psathyrellaceae (Agaricales). PhD Thesis, University of Szeged, Hungary.

Nagy LG, Walther G, Hazi J, Vágvölgyi C, Papp T (2011) Understanding the evolutionary processes of fungal fruiting bodies: correlated evolution and divergence times in the Psathyrellaceae. Systematic Biology 60(3): 303–317. https://doi.org/10.1093/sysbio/syr005

Nagy GL, Hazi J, Vágvölgyi C, Papp T (2012) Phylogeny and species delimitation in the genus *Coprinellus* with special emphasis on the haired species. Mycologia 104: 254–275. https://doi.org/10.3852/11-149

Nagy GL, Vágvölgyi C, Papp T (2013) Morphological characterization of clades of the Psathyrellaceae (Agaricales) inferred from a multigene phylogeny. Mycological Progress 12: 505–517. https://doi.org/10.1007/s11557-012-0857-3

Örstadius L, Ryberg M, Larsson E (2015) Molecular phylogenetics and taxonomy in Psathyrellaceae (Agaricales) with focus on psathyrelloid species: introduction of three new genera and 18 new species. Mycological Progress 14(5): 25. https://doi.org/10.1007/s11557-015-1047-x

Orton PD, Watling R (1979) Coprinaceae, Part 1: *Coprinus*. In: Henderson DM, Orton PD, Watling R (Ed.) British fungus flora Agarics and Boleti. Royal Botanic Garden, Edinburgh, 1–149.

Padamsee M, Matheny PB, Dentinger BT, McLaughlin DJ (2008) The mushroom family *Psathyrellaceae*: evidence for large-scale phylogeny of the genus *Psathyrella*. Molecular Phylogenetics and Evolution 46(2): 415–429. https://doi.org/10.1016/j.ympev.2007.11.004

Prydiuk MP (2010) New records of dung-inhabiting *Coprinus* species in Ukraine I. Section *Pseudocoprinus*. Czech Mycology 62: 43–58.

Rambaut A, Suchard MA, Xie D, Drummond AJ (2014) TRACER v 1.6. Computer program and documentation distributed by the authors. http://beast.bio.ed.ac.uk/Tracer [Accessed 18 Oct 2016]

Redhead SA, Vilgalys R, Moncalvo JM, Johnson J, Hopple JS (2001) *Coprinus* Pers.oon and the disposition of *Coprinus* species *sensu lato*. Taxon 50: 203–241. https://doi.org/10.2307/1224525

Schafer DJ (2010) Keys to sections of *Parasola*, *Coprinellus*, *Coprinopsis* and *Coprinus* in Britain. Field Mycology 11(2): 44–51. https://doi.org/10.1016/j.fldmyc.2010.04.006

Stamatakis A (2006) RAxML-VI-HPC: maximum likelihood-based phylogenetic analyses with thousands of taxa and mixed models. Bioinformatics 22(21): 2688–2690. https://doi.org/10.1093/bioinformatics/btl446

Tóth A, Hausknecht A, Krisai-Greilhuber I, Papp T, Vágvölgyi C, Nagy LG (2013) Iteratively refined guide trees help improving alignment and phylogenetic inference in the mushroom family Bolbitiaceae. PLoS One 8(2): e56143. https://doi.org/10.1371/journal.pone.0056143

Uljé CB, Bas C (1991) Studies in *Coprinus* II. Subsection *Setulosi* of section Pseudocoprinus. Persoonia 14(3): 275–339.

Uljé CB (2005) *Coprinus*. In: Noordeloos ME, Kuyper TW, Vellinga EC, eds. Flora Agaricina Neerlandica 6: 22–109.

Van de Bogart F (1975) The genus *Coprinus* in Washington and adjacent Western States. PhD Thesis, University of Washington, USA.

Vašutová M, Antonin V, Urban A (2008) Phylogenetic studies in *Psathyrella* focusing on section *Pennatae* and *Spadiceae* – new evidence for the paraphyly of the genus. Mycological Research 112(10): 1153–1164. https://doi.org/10.1016/j.mycres.2008.04.005

Walther G, Garnica S, Weiss M (2005). The systematic relevance of conidiogenesis modes in the gilled Agaricales. Mycological Research 109(5): 525–544. https://doi.org/10.1017/S0953756205002868

White TJ, Bruns T, Lee S, Taylor J (1990) Amplification and direct sequencing of fungal ribosomal RNA genes for phylogenetics. In: Innis MA, Gelfand DH, Sninsky JJ, White TJ, (Eds) PCR Protocols: A Guide to Methods and Applications. Academic Press, San Diego, 315–322. https://doi.org/10.1016/B978-0-12-372180-8.50042-1

MycoKeys 39: 63–73 (2018)
doi: 10.3897/mycokeys.39.27378
http://mycokeys.pensoft.net

RESEARCH ARTICLE

A peer-reviewed open-access journal
MycoKeys
Launched to accelerate biodiversity research

Puccinia modiolae in North America: distribution and natural host range

M. Catherine Aime[1], Mehrdad Abbasi[1],

1 *Purdue University, Department of Botany and Plant Pathology, West Lafayette, Indiana, USA*

Corresponding author: *M. Catherine Aime* (maime@purdue.edu)

Academic editor: *Marco Thines* | Received 11 June 2018 | Accepted 17 August 2018 | Published 11 September 2018

Citation: Aime MC, Abbasi M (2018) *Puccinia modiolae* in North America: distribution and natural host range. MycoKeys 39: 63–73. https://doi.org/10.3897/mycokeys.39.27378

Abstract

Puccinia modiolae, a rust fungus pathogen of Carolina bristlemallow, *Modiola caroliniana* (Malvaceae), is newly reported from North America, appears to be well established along the Gulf coast and is likely to have been introduced from South America. Its taxonomy, distribution and natural host range are discussed and a lectotype designated for this species. *Malva sylvestris* and *Alcea rosea* are reported as new hosts for the rust. Additional new records for Malvaceae rusts are made for *P. modiolae* on *Alcea rosea* from Brazil, *P. heterospora* on *Herissantia crispa* in Florida and *P. heterogenea* on *Malva* sp. in Peru. Finally, an identification key for the microcyclic *Puccinia* species on members of Malvaceae in North America is provided.

Keywords

Neomycetes, Phytopathogens, Pucciniales, Uredinales

Introduction

Neomycetes are alien fungi entering a new area (country or continent), typically as a result of non-intentional human activity, that become established in the new region (Kreisel and Scholler 1994, Negrean and Anastasiu 2006). The most common origin for alien species of rust fungi in the USA appears to be South and Central America. In many cases, the pathogens are introduced concurrently with their host species, e.g. on crop plants, ornamentals or weeds.

Puccinia modiolae P. Syd. & Syd. (Pucciniaceae, Pucciniales) is a microcyclic rust fungus that was originally reported on *Modiola prostrata* A.St.-Hil. (=*M. caroliniana*

(L.) G. Don; Malvaceae) from South America on the basis of specimens from Argentina and Uruguay (Sydow and Sydow 1904). *Modiola caroliniana* is the only species in the genus *Modiola*, grows in disturbed vegetation and at forest margins and flowers in all seasons (Kearney 1951, Fryxell 1988). *Modiola caroliniana* is believed to be native to northern Argentina and the Paraná basin of South America and probably came to the USA from southern South America in wool or cotton (Hanes 2015). Today, it is widely distributed as a weed in warmer parts of the world and is naturalised from the southern United States to northern Argentina including the West Indies. Despite the wide distribution of *M. caroliniana*, its parasitic rust, *P. modiolae*, has only been reported from Argentina and Uruguay (Lindquist 1982).

In this study, we examine numerous fresh collections and herbarium materials and conduct phylogenetic analyses of the 28S rDNA locus to provide the first reports of *P. modiolae* from North America, discuss its host range and distribution and establish a lectotype for this taxon. A key to the microcyclic *Puccinia* species on Malvaceae in North America is provided.

Methods

Materials studied here were obtained from the Arthur Fungarium (PUR), the U.S. National Fungus Collections (BPI) and from fresh collections (listed in specimens examined below). Voucher specimens for new material are deposited in PUR. Rust spores and cross sections were routinely mounted in lactic acid in glycerol. Light microscopic analyses were performed using a Nikon Eclipse 80i microscope. Photomicrographs were obtained with a DS-Fi1 Nikon camera. In all studied specimens, thirty spores were randomly selected and measured.

DNA was extracted and the 5' end of the nuclear 28S rDNA, amplified with rust-specific primers and sequenced following previous published protocols (Aime 2006, Aime et al. 2018). Sequences were edited using Sequencher 5.2.3 (Gene Codes Corp., Ann Arbor, MI) and aligned using the MUSCLE algorithm in Geneious 9.1.5 (Biomatters Ltd., Newark, NJ). Additional sequences of *Puccinia* species on Malvaceae were included for context from the studies of Aime (2006), Demers et al. (2015) and McTaggart et al. (2016). Phylogenies were reconstructed using maximum likelihood in RaxML v.2.2.3 via the CIPRES portal (Miller et al. 2010). Trees were visualised in FigTree v1.4.2 (http://tree.bio.ed.ac.uk/software/figtree/) and edited in Inkscape v2 (Free Software Foundation Inc., Boston, MA). Newly generated sequences are deposited in GenBank, accessions MH742974–MH743006.

Results

Study of recently collected materials of malvaceous plants from Texas, Louisiana and Indiana revealed the widespread presence of *Puccinia modiolae* along the Gulf coast on

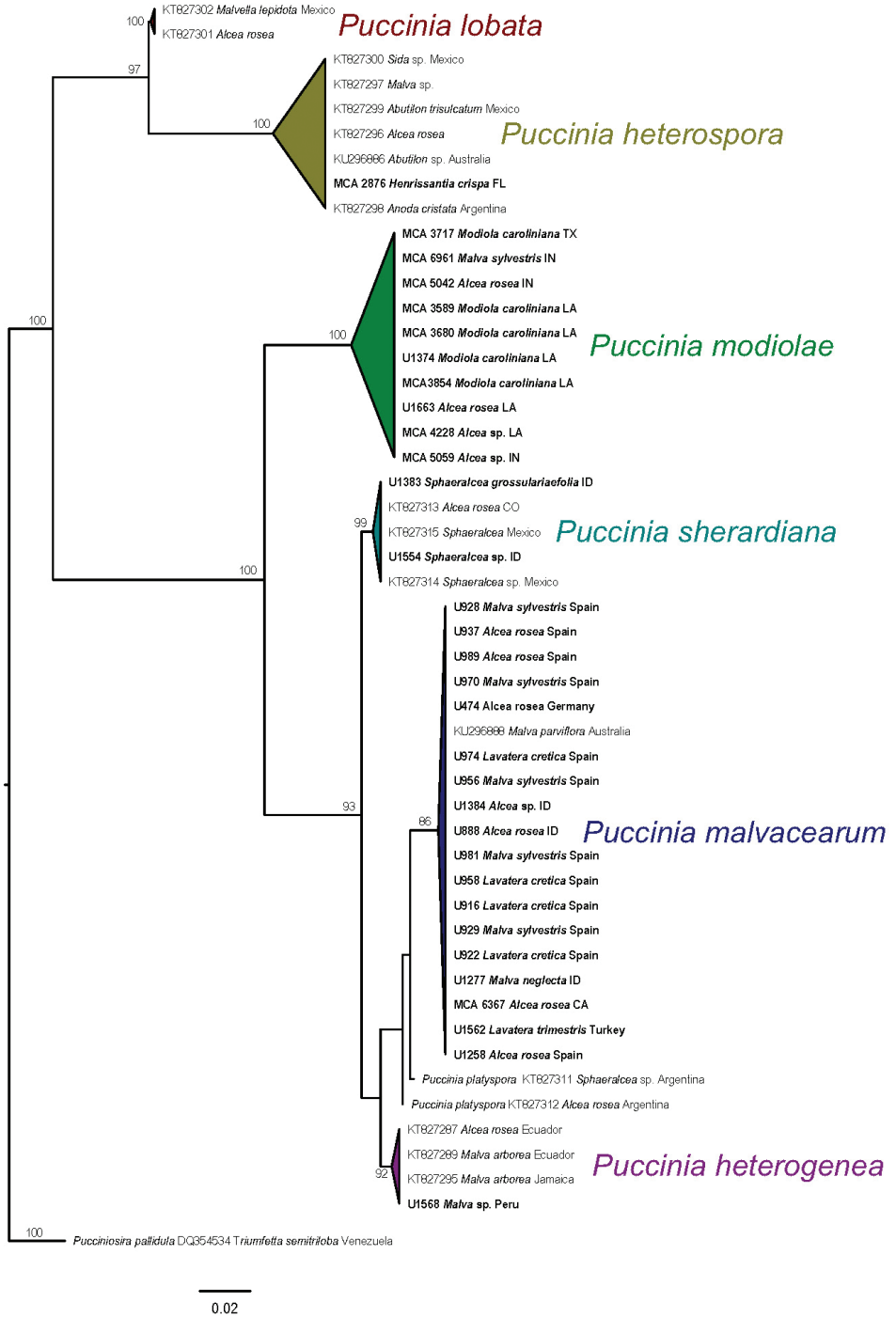

Figure 1. Maximum likelihood tree, based on 28S sequences, of *Puccinia* species on Malvaceae. Sequences newly generated for this study indicated in bold type. Numbers at nodes represent bootstrap support values. *Pucciniosira pallidula* was used as outgroup for rooting purposes.

Figure 2. *Puccinia modiolae*. **A** on *Modiola caroliniana*, LA (MCA 3671) **B** on *Alcea rosea*, IN (MCA 5059).

Modiola caroliniana and occurring as far north as Indiana on new hosts *Alcea rosea* L. and *Malva sylvestris* L. Examination of herbarium material also reveals *P. modiolae* as far south as Brazil on *A. rosea* (PUR N15322). Additional new records for Malvaceae rusts are made for *P. heterospora* on *Herissantia crispa* in Florida and *P. heterogenea* on *Malva* sp. in Peru. In total, we generated 28S rDNA sequences for 32 collections of *Puccinia* species on Malvaceae, including ten collections of *P. modiolae* for phylogenetic analyses (Fig. 1); all sequences of *P. modiolae* shared 100% identity across the locus.

Taxonomy

Puccinia modiolae **P. Syd. & Syd., Monogr. Uredin. (Lipsiae) 1(3): 478 (1903) [1904]**

P. malvacearum var. *modiolae* Pennington, Anales de la Sociedad Cientifica Argentina 55: 34 (1903). Figures 2–4. Syn.

Type: Lectotype: on *Modiola caroliniana* (as *M. prostrata*), Argentina, 1880–1881, C. Spegazzini, Decades Mycologiae Argentinae No. 10, PUR N6057, named as *P. malvacearum* (designated here). Isolectotype: BPI 086498.

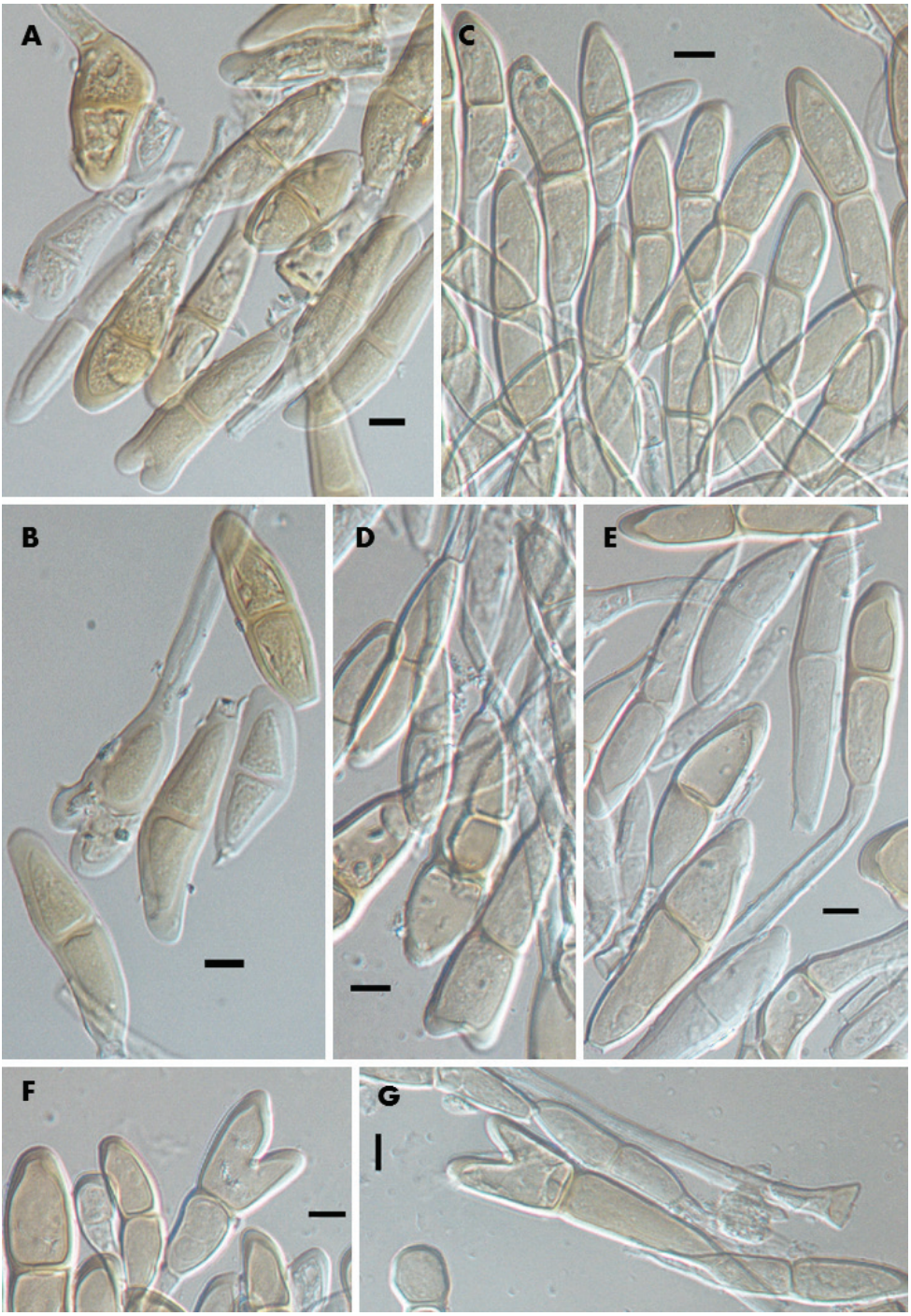

Figure 3. Teliospores of *Puccinia modiolae*: **A–B** on *Modiola caroliniana* (Lectotype PUR N6057) **C** on *M. caroliniana* (PUR N12041) **D** on *M. caroliniana* (PUR N12040) **E** on *M. caroliniana* (PUR N12550); **F** on *M. caroliniana* (PUR N12552) **G** on *Alcea rosea* (PUR N12039). Scale bars: 10 µm.

Description. Spermogonia usually epiphyllous, located on the opposite side of the telia in small groups, globose, 140–150 µm in diameter, yellowish-brown, with abundant and outward growing periphyses (Fig. 4). Telia mostly hypophyllous, occasionally on upper side of leaves and on petioles, round, compact, mostly in aggregated groups up to 3 mm in diameter, reddish-brown (Fig. 2). Teliospores diverse, with many anomalies because of the concretion of spores, mostly narrowly fusoid or linear, 31–81(–95) × 10.5–20 (–25) µm, attenuated above and below or notched at apex, not or hardly constricted at septum, wall smooth, hyaline to yellowish, 1.5–3 µm at sides, 3–8 µm at apex, pedicel hyaline, thick walled, persistent up to µm 150 µm (Fig. 3). One-celled and three-celled spores were rarely seen.

Specimens examined. ***Puccinia modiolae*** – ARGENTINA: on *Modiola caroliniana* (as *M. prostrata*), C. Spegazzini, Decades Mycologiae Argentinae No. 10, 1880–1881 (Lectotype, PUR N6057, as *P. malvacearum*; Isolectotype, BPI 086498, as *P. malvacearum*). USA: Indiana, Tippecanoe Co., Lafayette, *Alcea rosea* L., M.C. Aime, MCA5059, 2012 Nov 05 (PUR N12038; GenBank accession #MH742985); *A. rosea*, M.C. Aime, MCA5042, 2012 Oct 01 (PUR N12039; GenBank accession #MH742978); West Lafayette, Purdue University Campus, *Malva sylvestris* L., Amnat Eamvijarn, MCA6961, 2016 Sept 16 (PUR N15171; GenBank accession #MH742977); Louisiana, East Baton Rouge Parish, Baton Rouge, Louisiana State University campus, *M. caroliniana* (L.) G. Don, Amnat Eamvijarn, U1374, July 2008 (PUR N12550; GenBank accession #MH742981); *M. caroliniana*, M.C. Aime, MCA3680, 2009 Mar 26 (PUR N12040; GenBank accession #MH742980); *M. caroliniana*, Don Ferrin, MCA3565, 2008 Mar 14 (PUR N12547, GenBank accession #MH742975); LSU Campus parking lot, *M. caroliniana*, Don Ferrin, MCA3589, 2008 May 14 (PUR N12552; GenBank accession #MH742979); Baton Rouge, private house, Malvaceae sp., Chris Clark, MCA4228, 2011 May 09 (PUR N22678; GenBank accession #MH742984); Bossier Parish, Red River Research Station, *M. caroliniana*, M.C. Aime, MCA4719, 2012 Apr 19 (PUR N12551); Evangeline Parish, Mamou, Main Street, Malvaceae sp., M.C. Aime, MCA3523, 2008 Feb 05 (PUR N22676); Tangipahoa Parish, 10 mi East of Independence, *M. caroliniana*, Charles Rush, MCA3854, 2009 Oct 22 (PUR N12549; GenBank accession #MH742982); St. James Parish, Convent, on the River Road in lawn next to Manresa House of Retreats, *M. caroliniana*, M.C. Aime & Tom Bruns, MCA3671, 2009 Jan 22 (PUR N12546); Orleans Parish, New Orleans, private residence, Malvaceae sp., Beth Kennedy, U1663, 2017 Mar 03 (PUR N22654; GenBank accession #MH742983); *Modiola* sp., M.C. Aime, MCA3568, 2008 Mar 23 (PUR N16658); Texas, Harris Co., Shell Station on Rt. 146, Seabrook Waterfront District, *M. caroliniana*, M.C. Aime, MCA3717, 2009 May 04 (PUR N12041; GenBank accession #MH742976). BRAZIL: Sao Paulo, *Alcea rosea*, M. Figueiredo, J. Hennen s.n., 1999 Jan 12 (PUR N15322).

Puccinia heterogenea – PERU: Cajamarca Provence, Shudall, *Malva* sp., Jorge Diaz Valderrama, U1568, 2014 Dec 30 (PUR N12885; GenBank accession #MH743006).

Puccinia heterospora – USA: Florida, Monroe Co., Marathon, *Herissantia crispa* (L.) Briz., M.C. Aime, MCA2876, 2004 Dec 31 (PUR N22677; GenBank accession #MH742974).

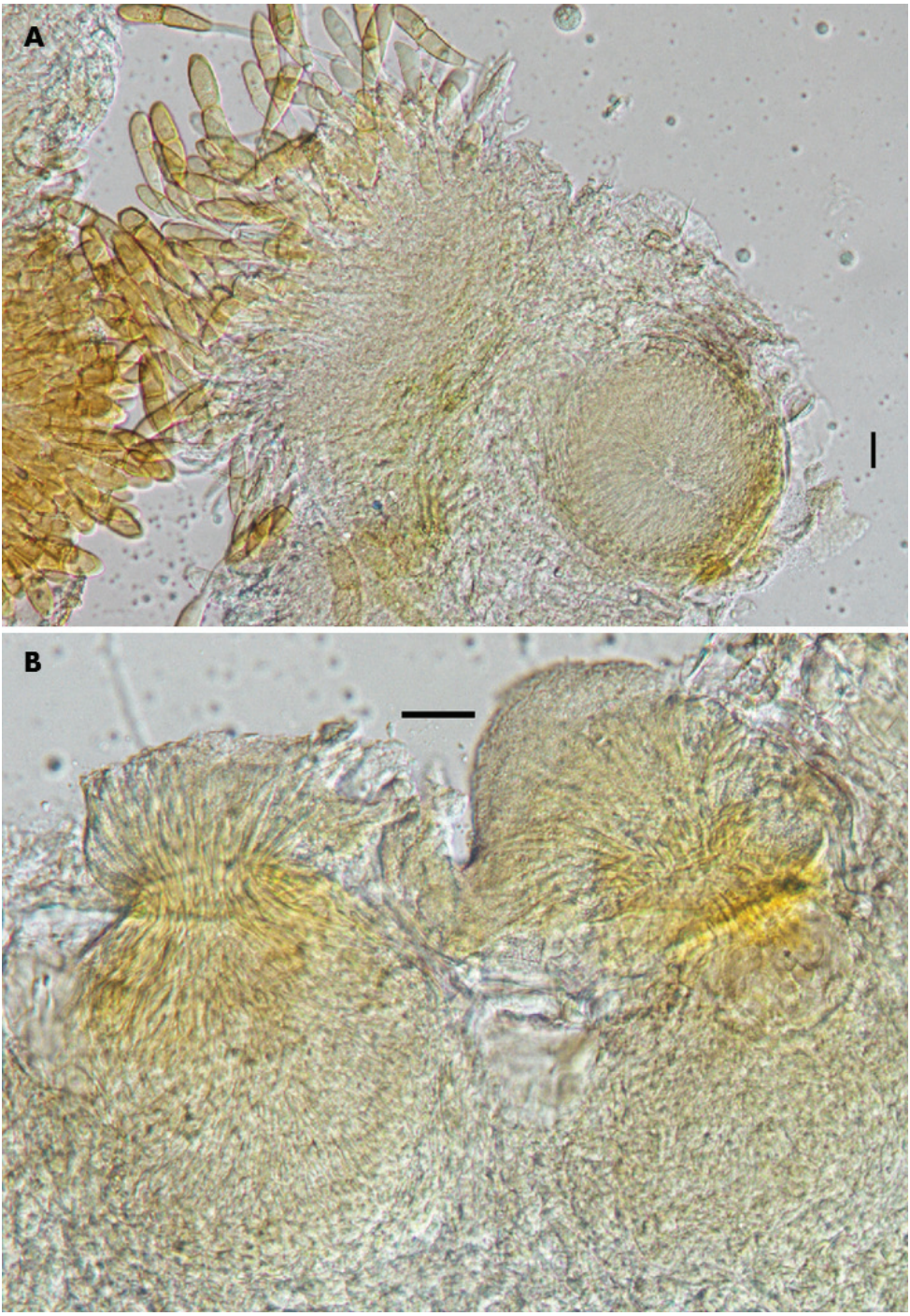

Figure 4. *Puccinia modiolae* on *Modiola caroliniana* (PUR N12551) **A** Spermogonium in connection with telium **B** Spermogonia with mass of spermatia on top. Scale bars: 25 μm.

Puccinia malvacearum–USA: California, Alameda Co., Berkeley, *Alcea rosea*, M.C. Aime, MCA6367, 2016 Aug 05 (PUR N15060; GenBank accession #MH743003); Idaho, Gem Co., *Alcea rosea*, Krishna Mohan, U888, 2006 May 26 (BPI 878033; GenBank accession #MH742996); Canyon Co., Parma, *Alcea* sp., Ram Sampangi, U1384, April 2009 (PUR N16292; GenBank accession #MH742995); *Malva neglecta*, Krishna Mohan, U1277, 2007 (PUR N16174; GenBank accession #MH743002); TURKEY: Bingöl Province, *Lavatera trimestris*, Lütfi Behçet, U1562, Jun 21 2014 (PUR N11582; GenBank accession #MH743004); SPAIN: Córdoba Province, near Montilla, *Malva sylvestris*, Walter J. Kaiser, U928, 2006 May 19 (BPI 878041; GenBank accession #MH742988); *M. sylvestris*, Walter J. Kaiser, U981, 2006 May 19 (BPI 878046; GenBank accession #MH742997); edge of wheat field, *M. sylvestris*, Walter J. Kaiser, U929, 2006 May 21 (BPI 878042; GenBank accession #MH743000); Cabra, edge of olive grove at Centro de Investigacion y Foirmacion Agraria, *M. sylvestris*, Walter J. Kaiser, U970, 2006 May 15 (BPI 878044; GenBank accession #MH742991); *M. sylvestris*, Walter J. Kaiser, U956, 2006 May 15 (BPI 878043; GenBank accession #MH742994); near Carcabury, *Alcea* sp., Walter J. Kaiser, U1258, April 2007 (PUR N16156; GenBank accession #MH743005); Córdoba, Colegio Mayor Universitario, Nuestra Senora de la Asuncion, Avenida Menendez Pidal, *Lavatera cretica*, Walter J. Kaiser, U958, 2006 May 09 (BPI 878038; GenBank accession #MH742998); *L. cretica*, Walter J. Kaiser, U916, 2006 May 09 (BPI 878035; GenBank accession #MH742999); Malaga Province, outskirts of El Burgo, *Alcea rosea*, U937, 2006 May 27 (BPI 875152; GenBank accession #MH742989); *A. rosea*, Walter J. Kaiser, U989, 2006 May 27 (BPI 878034; GenBank accession #MH742990); Jaén Province, Baéza, *L. cretica*, Walter J. Kaiser, U974, 2006 May 19 (BPI 878040; GenBank accession #MH742993); *L. cretica*, Walter J. Kaiser, U922, 2006 May 19 (BPI 878036; GenBank accession #MH743001); GERMANY, Thuringia, Weimar, *A. rosea*, G.R.W. Arnold, U474, 2004 Jun 22 (BPI 878032; GenBank accession #MH742992).

Puccinia malvastri–Arizona, Cochise, Cottonwood Canyon, Peloncillo Mountains, *Sphaeralcea* sp., George Cummins 61265, 1961 Sep 27 (topotype, PUR 59015).

Puccinia sherardiana sensu Arthur (1922)–USA: Idaho, Canyon Co., Parma, *Sphaeralcea grossulariifolia* (Hook. & Arn.) Rydb., Ram Sampangi, U1383, April 2009 (PUR N12548; GenBank accession #MH742986); *S. grossulariifolia*, Krishna Mohan, U1554, 2009 Aug 18 (PUR N11663; GenBank accession #MH742987).

Puccinia sphaeralceae–New Mexico, Mesilla Park, *Sphaeralcea angustifolia*, T. Cockerell 3478, 1896 Aug 01 (isotype, PUR 39636).

Discussion

Phytoparasitic neomycetes have the potential to cause great losses across the world via infestation of crops, ornamental plants and native flora (Scholler and Aime 2006). Introduction of alien phytoparasitic fungi also has ecological consequences which have

been little investigated (Scholler 1999). There is no updated list of neomycetes in the United States. However, alien rust fungi have had conspicuous economic and ecological consequences in North America. Here we report another introduced rust fungus, *P. modiolae*, as a new neomycete in the USA.

Pennington (1903) was the first to realise the difference between rust populations on *Modiola* compared to those on other members of the Malvaceae. He named the *Puccinia* species on *Modiola* as *P. malvacearum* var. *modiolae*, based on material collected from Río Paraná, Argentina. Sydow and Sydow (1904) described the rust population on *Modiola* as a separate species based on different material (syntype) collected from Argentina and Uruguay, but designated no holotype for the species. They later considered *P. malvacearum* var. *modiolae* as a synonym of *P. modiolae* in the appendix of their book (appendix to the first volume of Monographia Uredinearum, p. 892). Our phylogenetic analyses show *P. modiolae* and *P. malvacearum* are distinct species (Fig. 1); designation of a lectotype and isolectotype are made herein to stabilise the taxonomy for this species.

Puccinia modiolae is a native rust fungus of South America and was most likely introduced in the USA by accompanying its host plant *Modiola*. The rust species is quite common on *Modiola caroliniana* in Louisiana and was also found in Texas, making the Gulf coast a likely site for the original introduction of the rust species in North America. We are unable to pinpoint when *P. modiolae* was introduced into the USA. However, we were unable to locate any historical North American herbarium material of *P. modiolae* in BPI or PUR, nor were we able to find records of any rust species on *Modiola* in the USA, Canada or Mexico in all available literature, making it likely that *P. modiolae* became established in the southern USA probably no earlier than the second half of the 20th century. Before the present study, *P. modiolae* was only known from Argentina and Uruguay. In Argentina, *Althaea officinalis* L., *Lavatera arborea* L. and *Malva parviflora* L., in addition to *M. caroliniana,* have been reported as the natural host range of the rust species; only *M. caroliniana* is a reported host in Uruguay (Lindquist 1982). We have identified *Alcea rosea* and *Malva sylvestris* as new hosts for this rust species, ranging from southern Brazil to the upper Midwest USA.

The presence or absence of spermogonia is one of the morphological features for distinguishing microcyclic rust fungi on Malvaceae members (Lindquist 1982). Our study revealed that this feature is stable and meaningful for separating *Puccinia* spp. on Malvaceae. All studied specimens of *P. modiolae* in this research produced spermogonia in close connection to telia (Fig. 4). Eight microcyclic *Puccinia* species have been reported on Malvaceae in North America thus far.

Identification key to the microcyclic species of *Puccinia* on Malvaceae in North America

1 spermogonia absent **2**
– spermogonia present **6**
2 one-celled teliospores predominating ..... ***P. heterospora***
– one-celled teliospores rare or absent **3**

3 telia usually dark brown ..... ***P. lobata***
– telia usually light brown **4**
4 teliospore length mostly > 40 µm ..... ***P. malvacearum***
– teliospore length mostly < 40 µm **5**
5 teliospore wall 2–3 µm thick at sides, much thicker above ..... ***P. anodae***
– teliospore wall 1–2 µm thick at sides, scarcely thicker above ..... ***P. exilis***
6 teliospores with many anomalies because of the concretion of spores, making them appear notched at apex ..... ***P. modiolae***
– teliospores without spore anomalies ..... (***P. sherardiana*** **s. lat.**) 7
7 teliospore length mostly > 50 µm, oblong-ellipsoid ..... ***P. sphaeralceae****
– teliospore length mostly < 50 µm, broadly ellipsoid ..... ***P. malvastri****

Acknowledgements

MCA gratefully acknowledges funding from the National Science Foundation (CSBR program: DEB-1458290; TCN program: DEB-1502887) for the Purdue University herbaria, without which this work would not have been possible. This work was also supported by the USDA National Institute of Food and Agriculture Hatch project 1010662.

References

Abbasi M (2013) New reports of rust fungi for mycobiota of Iran. Iranian J. Plant Path. 49(3): 351–356.

Aime MC (2006) Toward resolving family-level relationships in rust fungi (Uredinales). Mycoscience 47: 112–122. https://doi.org/10.1007/S10267-006-0281-0

Aime MC, Bell C, Wilson AW (2018) Deconstructing the evolutionary complexity between rust fungi (Pucciniales) and their plant hosts. Studies in Mycology 89: 143–152. https://doi.org/10.1016/j.simyco.2018.02.002

Arthur JC (1922) Uredinales – Aecidiaceae. North American Flora 7(8): 543.

Demers JE, Romberg MK, Castlebury LA (2015) Microcyclic rusts of hollyhock (*Alcea rosea*). IMA Fungus 6: 477–482. https://doi.org/10.5598/imafungus.2015.06.02.11

* Arthur (1922) considered *Puccinia malvastri* and *P. sphaeralceae* as synonyms of *P. sherardiana* Körn. However, *P. sherardiana* is an old world species reported originally from Armenia on *Malvella sherardiana* Jaub. & Spach. There are a few reports of this species in the old world from Central Asia (Ulyanishchen 1978) and Iran (Abbasi 2013). Determining whether *P. malvastri* and *P. sphaeralceae* are synonyms of *P. sherardiana* needs additional study including study of type materials and molecular analysis of old world material. However, study of the isotype of *P. sphaeralceae* (PUR 39636) and topotype of *P. malvastri* (PUR 59015) showed that these two species can be distinguished by distinct differences in size of teliospores (see the key), thus we retain them as separate species pending additional studies.

Fryxell PA (1988) Malvaceae of Mexico. Systematic Botany Monographs. 25: 1–522. https://doi.org/10.2307/25027717

Hanes MM (2015) Malvaceae. In: Flora of North America Editorial Committee (Eds) Flora of North America North of Mexico (6 vol.). New York and Oxford, 187–375.

Kearney TH (1951) The American genera of Malvaceae. The American Midland Naturalist 46(1): 93–131. https://doi.org/10.2307/2421950

Kreisel H, Scholler M (1994) Chronology of phytoparasitic fungi introduced to Germany and adjacent countries. Botanica Acta 107: 387–392. https://doi.org/10.1111/j.1438-8677.1994.tb00812.x

Lindquist JC (1982) Royas de la Republica Argentina y Zonas Limitrofes. Inst. Nacional de Tecnologia Agropecuaria., 574 p.

McTaggart AR, Shivas RG, Doungsa-ard C, Weese TL, Beasley DR, Hall BH, Metcalf DA, Geering ADW (2016) Identification of rust fungi (Pucciniales) on species of *Allium* in Australia. Australasian Plant Pathology 45: 581–592. https://doi.org/10.1007/s13313-016-0445-0

Miller MA, Pfeiffer W, Schwartz T (2010) "Creating the CIPRES Science Gateway for inference of large phylogenetic trees" in Proceedings of the Gateway Computing Environments Workshop (GCE), 14 Nov. 2010, New Orleans, LA: 1–8. https://doi.org/10.1109/GCE.2010.5676129

Negrean G, Anastasiu P (2006) Invasive and potentially invasive parasite neomycetes from Romania. Plant, fungal and habitat diversity investigation and conservation. Proceedings of IV BBS, Sofia.

Pennington MS (1903) Uredineas del delta del Rio Parana. Anales de la Sociedad Cientifica Argentina 55: 31–40.

Scholler M (1999) Obligate phytoparasitic neomycetes in Germany: Diversity, distribution, introduction patterns and consequences. Texte 18: 64–75.

Scholler M, Aime MC (2006) On some rust fungi (Uredinales) collected in an *Acacia koa-Metrosideros polymorpha* woodland, Mauna Loa Road, Big Island, Hawaii. Mycoscience 47: 159–165. https://doi.org/10.1007/S10267-006-0286-8

Sydow P, Sydow H (1904) Monographia Uredinearum. Vol. I, Genus Puccinia. Leipzig, Gebr. Bornträger, 972 pp.

Ulyanishchev VI (1978) Opredelitel rzhavchinnykh gribov SSSR II. Nauk, Leningerad, 382 pp.

MycoKeys 39: 75–96 (2018)
doi: 10.3897/mycokeys.39.28010
http://mycokeys.pensoft.net

RESEARCH ARTICLE

A peer-reviewed open-access journal
MycoKeys
Launched to accelerate biodiversity research

Hydnophanerochaete and *Odontoefibula*, two new genera of phanerochaetoid fungi (Polyporales, Basidiomycota) from East Asia

Che-Chih Chen[1], Sheng-Hua Wu[1,2], Chi-Yu Chen[1]

1 *Department of Plant Pathology, National Chung Hsing University, Taichung 40227, Taiwan* **2** *Department of Biology, National Museum of Natural Science, Taichung 40419, Taiwan*

Corresponding author: *Sheng-Hua Wu* (shwu@mail.nmns.edu.tw)

Academic editor: *Alfredo Vizzini* | Received 27 June 2018 | Accepted 4 September 2018 | Published 17 September 2018

Citation: Chen C-C, Wu S-H, Chen C-Y (2018) *Hydnophanerochaete* and *Odontoefibula*, two new genera of phanerochaetoid fungi (Polyporales, Basidiomycota) from East Asia. MycoKeys 39: 75–96. https://doi.org/10.3897/mycokeys.39.28010

Abstract

Two new genera with phylogenetic affinities to *Phanerochaete* s.l. are presented, namely *Hydnophanerochaete* and *Odontoefibula*. The generic type of *Hydnophanerochaete* is *Phanerochaete odontoidea*. *Odontoefibula* is established based on a new species: *O. orientalis* (generic type). Both genera have effused basidiocarps with odontioid hymenial surface, simple-septate generative hyphae, cystidia lacking, clavate basidia and ellipsoid basidiospores that are smooth, thin-walled, inamyloid, non-dextrinoid and acyanophilous. *Hydnophanerochaete* is additionally characterised by a compact texture in the subiculum with thick-walled generative hyphae and quasi-binding hyphae. *Odontoefibula* has a dense texture of subiculum with thin- to slightly thick-walled hyphae and further a dark reddish reaction of basidiocarps when treated with KOH. Multi-marker phylogenetic analyses based on sequences, inferred from the ITS+nuc 28S+*rpb1*+*rpb2*+*tef1* dataset, indicate that *Hydnophanerochaete* and *Odontoefibula* are placed in the Meruliaceae and *Donkia* clades of Phanerochaetaceae, respectively. *Phanerochaete subodontoidea* is a synonym of *P. odontoidea*, according to morphological and molecular evidence.

Keywords

Meruliaceae, multi-marker phylogeny, new species, Phanerochaetaceae, phlebioid clade

Introduction

The genus *Phanerochaete* P. Karst., typified by *P. alnea* (Fr.) P. Karst., belongs to Polyporales Gäum of the Basidiomycota R.T. Moore and is one of the largest genera of corticoid fungi, including over 150 names according to Index Fungorum (http://www.indexfungorum.org/). Basidiocarps are typically membranaceous, effused, with various hymenial surfaces (i.e. smooth, tuberculate, odontioid, hydnoid, merulioid or poroid). Microscopically, *Phanerochaete* has a monomitic hyphal system, ordinarily simple-septate generative hyphae (rare clamp connections can be found in the subiculum), ellipsoid to cylindrical thin-walled basidiospores and clavate basidia. *Phanerochaete* is widespread and grows on diverse woody substrates (i.e. twigs and branches or trunks of angiosperms or gymnosperms), causing a white rot. *Phanerochaete* s.l. has attracted increasing study interest due to its abundant taxonomic diversity and potential applications in the field of biodegradation and bioconversion (Sánchez 2009).

Phanerochaete was traditionally treated as a genus in the broad sense (Eriksson et al. 1978; Burdsall 1985; Wu 1990). In recent years, *Phanerochaete* has been shown to be a polyphyletic group with members distributed throughout the phlebioid clade of Polyporales (De Koker et al. 2003; Wu et al. 2010; Floudas and Hibbett 2015; Miettinen et al. 2016), which was recently recognised as three families: Phanerochaetaceae Jülich, Irpicaceae Spirin & Zmitr and Meruliaceae Rea (Justo et al. 2017). Based on the combined morphological and molecular approaches, many studies have been conducted to revise the generic concept of *Phanerochaete* s.l. Some segregated genera have been recovered or proposed, e.g. *Efibula* Sheng H. Wu, *Hydnophlebia* Parmasto, *Phaeophlebiopsis* Floudas & Hibbett, *Phlebiopsis* Jülich, *Rhizochaete* Gresl., Nakasone & Rajchenb. and *Scopuloides* (Massee) Höhn. & Litsch. (Wu 1990; Greslebin et al. 2004; Wu et al. 2010; Floudas and Hibbett 2015).

Phanerochaete odontoidea Sheng H. Wu and *P. subodontoidea* Sheng H. Wu were described from Taiwan (Wu 2000). Both species have ceraceous basidiocarps with odontioid to hydnoid hymenial surface, compact subiculum, but no cystidia. These species have been shown to be phylogenetically far from the core *Phanerochaete* clade (Wu et al. 2010; Ghobad-Nejhad et al. 2015; Wu et al. 2018) and were placed by Justo et al. (2017) in Meruliaceae. In this study, we evaluate the generic placement of *P. odontoidea* and *P. subodontoidea,* as well as morphologically similar species. To accommodate our target taxa, we found it necessary to introduce two new genera placed within Meruliaceae and Phanerochaetaceae, respectively.

When *Phanerochaete odontoidea* and *P. subodontoidea* were described, they were separated by basidiospore width (Wu 2000). After 2000, we have accumulated more collections identified as *P. odontoidea* and *P. subodontoidea* from China, Japan, Taiwan and Vietnam. To better reflect their morphological variations, this study provides updated morphological and molecular evidence for revising their species concepts.

Table 1. Species and sequences used in the phylogenetic analyses. Newly generated sequences are set in bold.

Taxon	Strain/Specimen	ITS	nuc 28S	*rpb1*	*rpb2*	*tef1*
Antrodia serialis	KHL 12010 (GB)	JX109844	JX109844	–	JX109870	JX109898
Aurantiporus croceus	Miettinen-16483	KY948745	KY948901	KY948927	–	–
Bjerkandera adusta	HHB-12826-Sp	KP134983	KP135198	KP134784	KP134913	KT305938
Bjerkandera aff. *centroamericana*	L-13104-sp	KY948791	KY948855	KY948936	–	–
Byssomerulius corium	FP-102382	KP135007	KP135230	KP134802	KP134921	–
Candelabrochaete africana	FP-102987-Sp	KP135294	KP135199	KP134872	KP134975	–
Ceraceomyces serpens	HHB-15692-Sp	KP135031	KP135200	KP134785	KP134914	–
Ceriporia alachuana	FP-103881-Sp	KP135341	KP135201	KP134845	KP134896	–
Ceriporia reticulata	KHL 11981 (GB)	–	–	–	–	JX109899
Ceriporia reticulata	RLG-11354-Sp	KP135041	KP135204	KP134794	KP134922	–
Ceriporiopsis aneirina	HHB-15629-Sp	KP135023	KP135207	KP134795	–	–
Ceriporiopsis carnegieae	RLG-7277-T	KY948792	KY948854	KY948935	–	–
Ceriporiopsis fimbriata	Dai 11672	KJ698633	KJ698637	–	–	–
Ceriporiopsis gilvescens	L-3519-sp	KY948761	–	KY948919	–	–
Ceriporiopsis gilvescens	Niemela-5516	–	HQ659222	–	–	–
Ceriporiopsis guidella	HUBO 7659	FJ496687	FJ496722	–	–	–
Ceriporiopsis kunmingensis	C.L. Zhao 152	KX081072	KX081074	–	–	–
Ceriporiopsis lagerheimii	58240	KX008365	KX081077	–	–	–
Ceriporiopsis pseudoplacenta	Miettinen 18997 (H)	KY948744	KY948902	KY948926	–	–
Cerrena unicolor	FD-299	KP135304	KP135209	KP134874	KP134968	–
Climacodon sanguineus	BR5020180728797	KX810931	KX810932	–	–	KX810934
Climacodon septentrionalis	AFTOL-767	AY854082	AY684165	AY864872	AY780941	AY885151
Crustodontia chrysocreas I	HHB-6333-Sp	KP135358	KP135263	KP134861	KP134908	–
Crustodontia chrysocreas II	FBCC307	LN611114	LN611114	–	–	–
Daedalea quercina	FP-56429	KY948809	KY948883	KY948989	–	–
Datronia mollis	RLG6304sp	JN165002	JN164791	JN164818	JN164872	JN164901
Donkia pulcherrima I	GC 1707-11	**LC378994**	**LC379152**	**LC379157**	**LC387351**	**LC387371**
Donkia pulcherrima II	AH39127	–	–	–	KX810937	–
Donkia pulcherrima II	Gothenburg-2022	KX752591	KX752591	–	–	–
Efibula americana	FP-102165	KP135016	KP135256	KP134808	KP134916	–
Emmia lacerata	FP-55521-T	KP135024	KP135202	KP134805	KP134915	–
Fomitopsis pinicola	AFTOL-770	AY854083	AY684164	AY864874	AY786056	AY885152
Gelatoporia subvermispora	FD-354	KP135312	KP135212	KP134879	–	–
Geliporus exilisporus I	GC 1702-15	**LC378995**	**LC379153**	**LC379158**	**LC387352**	**LC387372**
Geliporus exilisporus II	Dai 2172	KU598211	KU598216	–	–	–
Gloeoporus pannocinctus	L-15726-Sp	KP135060	KP135214	KP134867	KP134973	–
Grammothelopsis puiggarii	RP 134	KP859299	KP859308	–	–	–
Hapalopilus nidulans	FD-512	KP135419	–	KP134809	–	–

Taxon	Strain/Specimen	ITS	nuc 28S	*rpb1*	*rpb2*	*tef1*
Hapalopilus nidulans	Josef Vlasak JV0206/2 (JV)	–	KX752623	–	–	–
Hapalopilus ochraceolateritius	Miettinen-16992.1	KY948741	KY948891	KY948965	–	–
Heterobasidion annosum	AFTOL-ID 470	DQ206988	–	DQ667160	–	DQ028584
Heterobasidion annosum	DAOM-73191	–	AF287866	–	AY544206	–
Hydnophanerochaete odontoidea	Chen 1376	**LC363485**	–	–		
Hydnophanerochaete odontoidea	GC 1308-45	**LC363486**	**LC363492**	**LC363497**	**LC387353**	**LC387373**
Hydnophanerochaete odontoidea	GC 1607-20	**LC378996**	–	–	–	–
Hydnophanerochaete odontoidea	GC 1710-59	**LC378997**	–	–	–	–
Hydnophanerochaete odontoidea	WEI 15-309	**LC378998**	–	–	–	–
Hydnophanerochaete odontoidea	WEI 15-348	**LC378999**	–	–	–	–
Hydnophanerochaete odontoidea	Wu 0106-35	**LC379000**	**LC379154**	LC379159	**LC387354**	**LC387374**
Hydnophanerochaete odontoidea (*Phanerochaete subodontoidea*)	Wu 911206-38	**LC379001**	–	–	–	–
Hydnophanerochaete odontoidea	Wu 9310-29	**LC379002**	–	–	–	–
Hydnophanerochaete odontoidea	Wu 9310-8	MF399408	GQ470653	LC314328	**LC387355**	**LC387375**
Hydnophanerochaete odontoidea (*Phanerochaete subodontoidea*)	CWN00776	**LC363487**	GQ470663	**LC363498**	**LC387356**	**LC387376**
Hydnophlebia chrysorhiza	FD-282	KP135338	KP135217	KP134848	KP134897	–
Hydnophlebia omnivora I	KKN-112-Sp	KP135334	KP135216	KP134846	–	–
Hydnophlebia omnivora II	ME-497	KP135332	KP135218	KP134847	–	–
Hydnopolyporus fimbriatus	Meijer3729 (O)	JN649346	JN649346	–	JX109875	JX109904
Hyphoderma mutatum	HHB-15479-Sp	KP135296	KP135221	KP134870	KP134967	–
Hyphoderma setigerum	CHWC 1209-9	–	–	–	**LC387357**	LC270919
Hyphoderma setigerum	FD-312	KP135297	KP135222	KP134871	–	–
Hyphodermella corrugata	MA-Fungi 24238	FN600378	JN939586	–	–	–
Hyphodermella poroides	Dai 10848	KX008368	KX011853	–	–	–
Hyphodermella rosae	FP-150552	KP134978	KP135223	KP134823	KP134939	–
Irpex lacteus	DO 421/951208 (O)	–	–	–	JX109882	JX109911
Irpex lacteus	FD-9	KP135026	KP135224	KP134806	–	–
Leptoporus mollis	TJV–93–174T	KY948795	EU402510	KY948957	–	–
Lilaceophlebia livida I	FBCC937	LN611122	LN611122	–	–	–
Lilaceophlebia livida II	FP-135046-sp	KY948758	KY948850	KY948917	–	–

Taxon	Strain/Specimen	ITS	nuc 28S	*rpb1*	*rpb2*	*tef1*
Lopharia cinerascens	FP-105043-sp	JN165019	JN164813	JN164840	JN164874	–
Luteoporia albomarginata	GC 1702-1	**LC379003**	**LC379155**	**LC379160**	**LC387358**	**LC387377**
Meruliopsis taxicola	SK 0075 (GB)	JX109847	JX109847	–	JX109873	JX109901
Merulius tremellosus	ES2008-2 (GB)	JX109859	–	–	–	JX109916
Merulius tremellosus	FD-323	–	KP135231	KP134856	KP134900	–
Mycoacia fuscoatra	HHB-10782-Sp	KP135365	KP135265	KP134857	KP134910	–
Mycoacia fuscoatra	KHL 13275 (GB)	–	–	–	–	JX109908
Mycoacia nothofagi	HHB-4273-Sp	KP135369	KP135266	KP134858	KP134911	–
Obba rivulosa	FP-135416-Sp	KP135309	KP135208	KP134878	KP134962	–
Odontoefibula orientalis	GC 1604-130	**LC363489**	**LC363494**	**LC363500**	**LC387359**	**LC387378**
Odontoefibula orientalis	GC 1703-76	**LC379004**	**LC379156**	**LC379161**	**LC387360**	**LC387379**
Odontoefibula orientalis	Wu 0805-59	**LC363488**	**LC363493**	**LC363499**	**LC387361**	**LC387380**
Odontoefibula orientalis	Wu 0910-57	**LC363490**	**LC363495**	**LC363501**	**LC387362**	**LC387381**
Odoria alborubescens	BP106943	MG097864	MG097867	MG213724	MG213723	–
Oxychaete cervinogilvus	Schigel-5216	KX752596	KX752596	KX752626	–	–
Phaeophlebiopsis caribbeana	HHB-6990	KP135415	KP135243	KP134810	KP134931	–
Phaeophlebiopsis peniophoroides	FP-150577	KP135417	KP135273	KP134813	KP134933	–
Phanerina mellea	WEI 17-224	**LC387333**	**LC387340**	**LC387345**	**LC387363**	**LC387382**
Phanerochaete arizonica	RLG-10248-Sp	KP135170	KP135239	KP134830	KP134949	–
Phanerochaete chrysosporium	HHB-6251-Sp	KP135094	KP135246	KP134842	KP134954	–
Phanerochaete ericina	HHB-2288	KP135167	KP135247	KP134834	KP134950	–
Phanerochaete exilis	HHB-6988	KP135001	KP135236	KP134799	KP134918	–
Phanerochaete laevis	HHB-15519-Sp	KP135149	KP135249	KP134836	KP134952	–
Phanerochaete livescens	Wu 0711-81	**LC387334**	MF110289	**LC387346**	**LC387364**	LC270920
Phanerochaete magnoliae	HHB-9829-Sp	KP135089	KP135237	KP134838	KP134955	–
Phanerochaete pseudosanguinea	FD-244	KP135098	KP135251	KP134827	KP134942	–
Phanerochaete rhodella	FD-18	KP135187	KP135258	KP134832	KP134948	–
Phanerochaete sp.	HHB-11463	KP134994	KP135235	KP134797	KP134892	–
Phanerochaete taiwaniana	Wu 0112-13	MF399412	GQ470665	LC314332	**LC387365**	**LC387383**
Phebia acerina	FD-301	KP135378	KP135260	KP134862	–	–
Phlebia acanthocystis I	GC 1703-30	**LC387338**	**LC387343**	–	**LC387366**	**LC387384**
Phlebia acanthocystis II	FP150571	KY948767	KY948844	KY948914	–	–
Phlebia albida	GB-1833	KY948748	KY948889	KY948960	–	–
Phlebia brevispora	FBCC1463	LN611135	LN611135	–	–	–
Phlebia centrifuga	HHB-9239-Sp	KP135380	KP135262	KP134844	KP134974	–
Phlebia coccineofulva	HHB-11466-sp	KY948766	KY948851	KY948915	–	–
Phlebia deflectens	FCUG 1568	AF141619	AF141619	–	–	–
Phlebia firma	Edman K268	EU118654	EU118654	–	–	JX109890
Phlebia floridensis	HHB-9905-Sp	KP135383	KP135264	KP134863	KP134899	–
Phlebia hydnoidea	HHB-1993-sp	KY948778	KY948853	KY948921	–	–
Phlebia lilascens	FCUG 1801	AF141621	AF141621	–	–	–

Taxon	Strain/Specimen	ITS	nuc 28S	*rpb1*	*rpb2*	*tef1*
Phlebia ochraceofulva	FBCC295	LN611116	LN611116	–	–	–
Phlebia radiata	AFTOL-484	AY854087	AF287885	AY864881	AY218502	AY885156
Phlebia setulosa	HHB-6891-Sp	KP135382	KP135267	KP134864	KP134901	–
Phlebia sp.	FD-427	KP135342	–	KP134849	–	–
Phlebia sp.	GC 1703-31	**LC387339**	**LC387344**	**LC387347**	**LC387367**	**LC387385**
Phlebia sp.	GC 1708-118	**LC387337**	**LC387342**	**LC387349**	**LC387368**	**LC387386**
Phlebia sp.	GC 1710-83	**LC387336**	**LC387341**	**LC387350**	**LC387369**	**LC387387**
Phlebia sp.	HHB-17984	KP135359	KP135261	KP134860	KP134907	–
Phlebia sp.	HHB-18295	KP135405	KP135269	KP134814	KP134938	–
Phlebia subochracea I	HHB-8715-sp	KY948770	KY948846	KY948913	–	–
Phlebia subochracea II	HHB-8494-sp	KY948768	KY948845	KY948912	–	–
Phlebia subserialis	FCUG 1434	AF141631	AF141631	–	–	–
Phlebia uda	FP-101544-Sp	KP135361	KP135232	KP134859	KP134909	–
Phlebia unica	KHL 11786 (GB)	EU118657	EU118657	–	JX109861	JX109889
Phlebiopsis crassa	KKN-86-Sp	KP135394	KP135215	KP134820	KP134928	–
Phlebiopsis gigantea	FP-70857-Sp	KP135390	KP135272	KP134821	KP134930	–
Phlebiopsis ravenelii	FP-110129-Sp	KP135362	KP135274	KP134850	KP134898	–
Phlebiporia bubalina	Dai 13168	KC782526	KC782528	–	–	–
Pirex concentricus	OSC-41587	KP134984	KP135275	KP134843	KP134940	–
Rhizochaete filamentosa	HHB-3169-Sp	KP135410	KP135278	KP134818	KP134935	–
Rhizochaete radicata	FD-123	KP135407	KP135279	KP134816	KP134937	–
Rhizochaete rubescens	Wu 0910-45	**LC387335**	MF110294	**LC387348**	**LC387370**	LC270925
Riopa metamorphosa	Viacheslav Spirin 2395 (H)	KX752601	KX752601	KX752628	–	–
Sarcodontia crocea	OMC-1488	KY948798	KY948903	KY948928	–	–
Scopuloides rimosa I	HHB-7042-Sp	KP135350	KP135282	KP134853	KP134903	–
Scopuloides rimosa II	RLG-5104	KP135351	KP135283	KP134852	KP134904	–
Skeletocutis nivea	ES2008-1 (GB)	JX109858	JX109858	–	JX109886	JX109915
Steccherinum ochraceum	KHL 11902 (GB)	JQ031130	JQ031130	–	JX109865	JX109893
Stereum hirsutum	AFTOL-ID 492	AY854063	–	AY864885	AY218520	AY885159
Stereum hirsutum	FPL-8805	–	AF393078	–	–	–
Terana caerulea	FP-104073	KP134980	KP135276	KP134865	KP134960	–
Trametes versicolor	FP-135156-sp	JN164919	JN164809	JN164825	JN164850	DQ028603
Trametopsis cervina	TJV–93–216T	JN165020	JN164796	JN164839	JN164877	JN164882
Tyromyces chioneus	FD-4	KP135311	KP135291	KP134891	KP134977	–

Materials and methods

Morphological studies

The specimens used for illustrations and descriptions are deposited at the herbarium of National Museum of Natural Science of ROC (TNM, acronym according to Index Herbariorum; http://sweetgum.nybg.org/science/ih/). Free-hand thin sections of basidiocarps were mounted in three mounting media for microscopic studies: 5% (w/v) KOH with 1% (w/v) phloxine was used for observation and measurements; Melzer's reagent (IKI) was utilised to check amyloidity and dextrinoidity; and Cotton Blue (CB, Fluka 61335) was employed to determine cyanophily. Sections were studied with a Leica DM2500 (Leica, Wetzlar) microscope. Drawings were done with the aid of a

drawing tube. We followed the method for measurements of microscopic characters by Wu (1990). The abbreviations below were used when presenting statistical measurements of basidiospores: L = mean basidiospore length, W = mean basidiospore width, Q = variation in L/W ratio, n = number of measured spores. The terminology of microscopic characters follows Wu (1990).

DNA extraction and sequencing

Dried specimens or mycelia grown on MEA were used for isolating genomic DNA. The material was first fragmented into a fine powder with the aid of liquid nitrogen and a TissueLyser II (Qiagen, Hilden, Germany). DNA was obtained using the Plant Genomic DNA Extraction Miniprep System (Viogene-Biotek Corp., New Taipei, Taiwan) based on the manufacturer's instructions. Five genetic markers were amplified in this study: nuc rDNA ITS1-5.8S-ITS2 (ITS) using primer pair ITS1/ITS4 (White et al. 1990); D1-D2 domains of nuc 28S rDNA (nuc 28S) using primer pair LR0R/LR5 (http://www2.clarku.edu/faculty/dhibbett/Protocols_Folder/Primers/Primers.pdf); RNA polymerase II largest subunit (*rpb1*) using primer pair RPB1-Af/RPB1-Cr (Stiller and Hall 1997; Matheny et al. 2002) or alternative primers RPB1- 2f, RPB1-2.1f, RPB1-2.2f and RPB1-2.1r (Frøslev et al. 2005); RNA polymerase II second largest subunit (*rpb2*) using primer pair RPB2-f5F/RPB2-b7.1R (Liu et al. 1999; Matheny 2005); and translation elongation factor 1-α (*tef1*) using primer pair EF1-983F/EF1-2212R (Rehner and Buckley 2005). The PCR protocols for ITS and nuc 28S gene regions were as follows: initial denaturation at 95 °C for 5 min, followed by 40 cycles at 94 °C for 45 s, 53 °C for ITS and 50 °C for nuc 28S for 45 s and 72 °C for 45 s and a final extension of 72 °C for 10 min. The PCR protocols for *rpb1*, *rpb2* and *tef1* include initial denaturation at 94 °C for 2 min, followed by 35 cycles at 94 °C for 40 s, 60 °C for 40 s and 72 °C for 2 min and a final extension of 72 °C for 10 min. PCR products were purified and sequenced by the MB Mission Biotech Company (Taipei, Taiwan). Newly obtained sequences for each of the five markers were assembled and manually adjusted using BioEdit (Hall 1999) and then submitted to the DNA Data Bank of Japan (DDBJ) (http://www.ddbj.nig.ac.jp/; Table 1). We have verified the accuracy and identity of consensus sequences by comparing with sequences in GenBank (https://www.ncbi.nlm.nih.gov/genbank/).

Phylogenetic analyses

Two datasets were compiled for phylogenetic analyses: the ITS+nuc 28S+*rpb1*+*rpb2*+*tef1* dataset was analysed to confirm the generic placement of target species within the phlebioid clade of Polyporales. The ITS dataset was used to get better resolutions on species level within the *Hydnophanerochaete* clade of Meruliaceae. The selection of strains and species for the 5-marker dataset was based on Binder et al. (2013), Flou-

das and Hibbett (2015), Kuuskeri et al. (2015), Justo et al. (2017), Miettinen et al. (2016), Moreno et al. (2017), Papp and Dima (2017), Yuan et al. (2017) and Zhao et al. (2017). Alignment was done with MAFFT v. 7 using two strategies: Q-INS-I for ITS and FFT-NS-I for nuc 28S, *rpb1*, *rpb2* and *tef1* (Katoh and Standley 2013). The resulting alignments were manually adjusted in Mega 7 (Kumar et al. 2016). *Heterobasidion annosum* (Fr.) Bref. and *Stereum hirsutum* (Willd.) Pers., belonging to Russulales Kreisel ex P.M. Kirk, P.F. Cannon & J.C. David, were chosen as the outgroup in the 5-marker dataset. *Phlebia coccineofulva* Schwein., belonging to Meruliaceae, was assigned as the outgroup in the ITS dataset. Optimised datasets were deposited at TreeBASE (submission ID 22932).

The Bayesian Inference (BI) method was carried out for both datasets using MrBayes v. 3.2.6 (Ronquist et al. 2012). The Maximum Likelihood (ML) method was carried out for the 5-marker dataset using RAxML BlackBox (Stamatakis 2014). For the BI analyses, jModeltest 2.1.10 (Darriba et al. 2012) was first used to estimate separate models for each of the markers in both datasets, based on Akaike information criterion (AIC). The Markov chain Monte Carlo (MCMC) search was run for ten million generations, with four chains and trees sampled every 100 generations. The first twenty-five percent of trees were discarded as burn-in while the remaining trees were used to construct the fifty percent majority-rule consensus phylogram with posterior probabilities (PP). For the ML analysis, the best-scoring tree with proportional values of bootstrap (BS) was computed under a GTRGAMMA model with one thousand bootstrap replicates, followed by a thorough ML search. Gaps were treated as missing data. Branches were regarded as having statistical support if values of PP and/or BS were equal to or over 0.9 and 70%, respectively. Both BI and ML analyses were performed at the CIPRES Science Gateway (Miller et al. 2010; http://www.phylo.org/). Phylograms were visualised and edited in TreeGraph 2 (Stöver and Müller 2010) and Adobe Illustrator (Adobe Systems, Inc).

Phylogeny results

The final ITS+nuc 28S+*rpb1*+*rpb2*+*tef1* dataset consisted of 126 sequences and 7253 characters (of which 43.7% were parsimony-informative) including gaps and the ITS dataset comprised 12 sequences and 887 characters (of which 7.7% were parsimony-informative) including gaps. In the BI analyses, since the GTR+G+I model was selected as the best model of nucleotide substitution for each of the five markers in the 5-marker dataset, it was used for the entire alignment with five partitions. The HKY+I+G model was selected as the best model of nucleotide substitution for the ITS dataset. The fifty percent majority-rule consensus phylogram with PP support values was reconstructed after the average standard deviation of split frequencies fell below 0.001. The best-scoring ML tree with BS support values was built. Phylogenetic trees of the 5-marker dataset, inferred from BI and ML algorithms, shared similar topologies and thus only the ML tree was shown (Fig. 1).

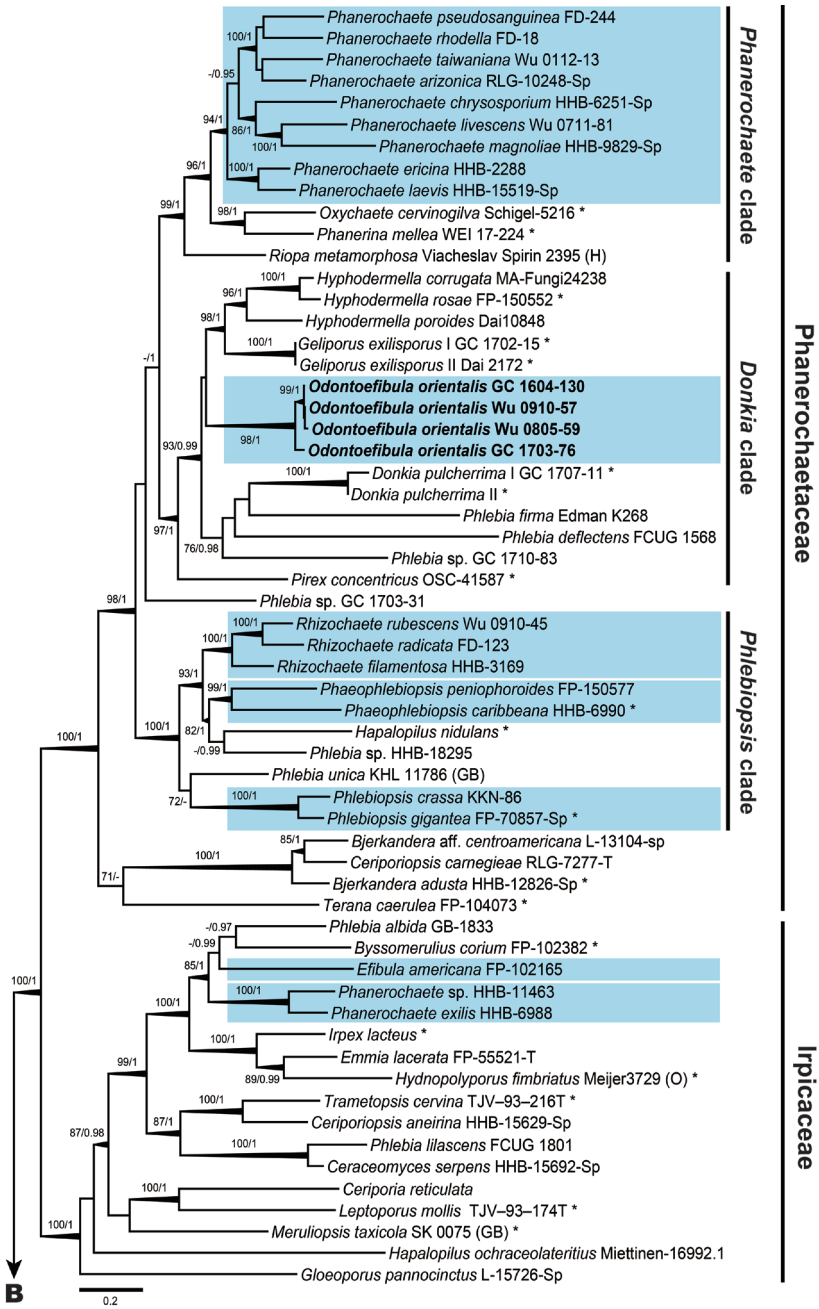

Figure 1. Phylogenetic tree inferred from Maximum Likelihood analysis of the combined ITS, nuc 28S, *rpb1*, *rpb2* and *tef1* sequences of taxa in Polyporales. Nodes are labelled with Maximum Likelihood bootstrap proportional values (BS) ≥ 70% and Bayesian Posterior Probabilities (PP) ≥ 0.9. Thickened branches obtained supports by both BS ≥ 80% and PP ≥ 0.95. The taxa studied in this study are shown in bold. The pale blue boxes indicate lineages of phanerochaetoid fungi within the phlebioid clade. Asterisks (*) represent for strains of generic type species. Scale bars = substitutions per site.

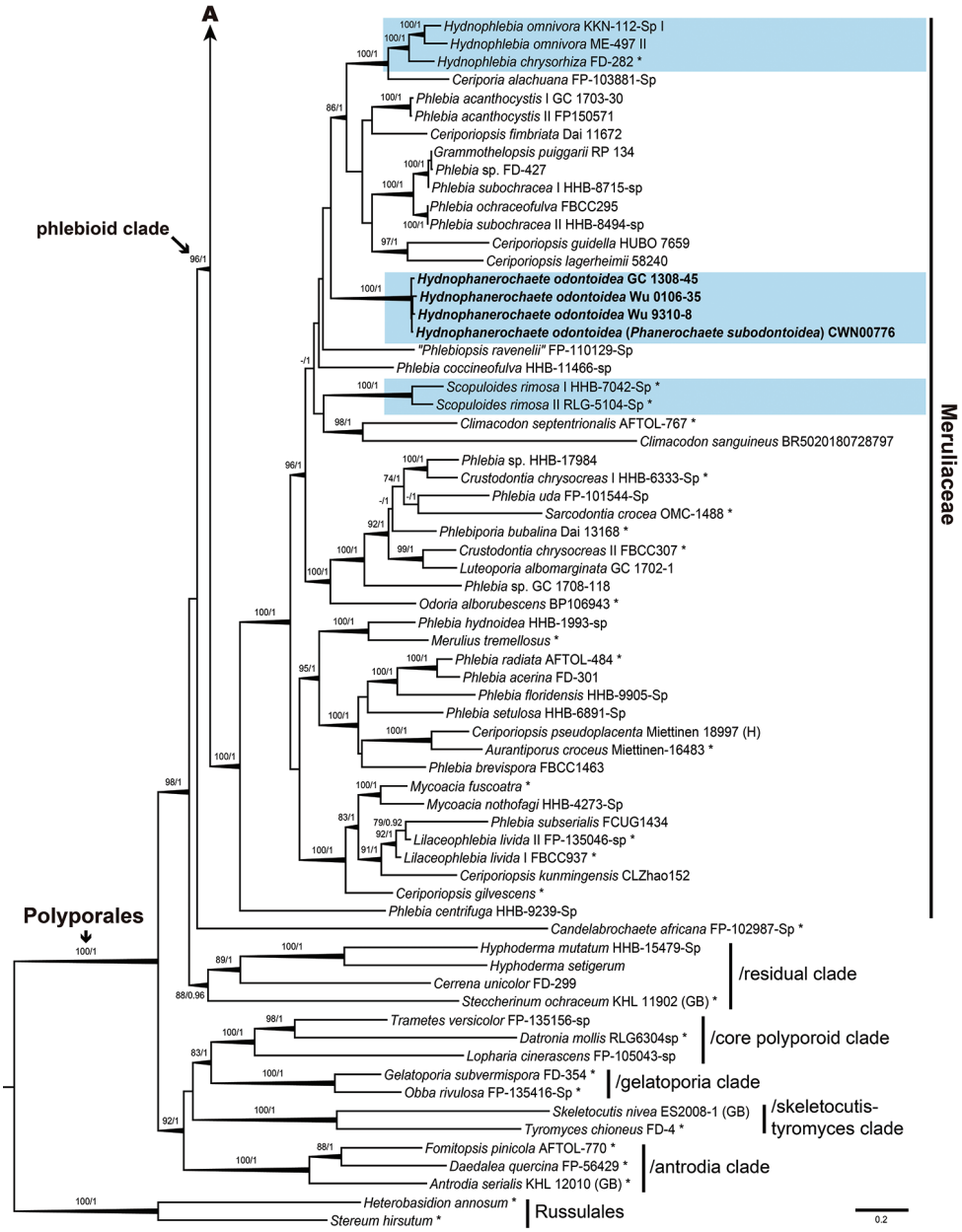

Figure 1. Continued.

In the 5-marker analyses (Fig. 1), six main clades with high statistic supports (BS = 96–100%, PP = 1) could be recognised in the ingroup: the antrodia clade, the core polyporoid clade, the gelatoporia clade, the phlebioid clade, a residual clade and the skeletocutis-tyromyces clade. The phlebioid clade, which is the focus of this study,

included three main subclades recognised as three families (BS = 100%, PP = 1): Irpicaceae, Meruliaceae and Phanerochaetaceae. *Hydnophanerochaete odontoidea* formed a well-supported monophyletic lineage (BS = 100%, PP = 1) within Meruliaceae and was found to be closely related to a lineage consisting of strains of *Ceriporia alachuana* (Murrill) Hallenb, *Ceriporiopsis* spp., *Grammothelopsis puiggarii* (Speg.) Rajchenb. & J.E. Wright, *Hynophlebia* spp. and *Phlebia* spp. (BS = 86%, PP = 1). Sequences of *Odontoefibula orientalis* grouped together and formed a well-supported monophyletic lineage (BS = 98%, PP = 1) within the *Donkia* clade of Phanerochaetaceae (BS = 97%, PP = 1) and were most closely related to a lineage made up of strains of *Geliporus exilisporus* (Y.C. Dai & Niemelä) Yuan Yuan, Jia J. Chen & S.H. He and *Hyphodermella* spp. (BS = 98%, PP = 1).

The tree inferred from the ITS dataset (Fig. 2) showed that sequences of holotype (*CWN00776*) and paratype (*Wu 911206-38*) of *Phanerochaete subodontoidea* were clustered with sequences of *P. odontoidea* within a monophyletic lineage (PP = 1).

Taxonomy

***Hydnophanerochaete* Sheng H. Wu & C.C. Chen, gen. nov.**
MycoBank No: MB824077

Type species. *Hydnophanerochaete odontoidea* (≡ *Phanerochaete odontoidea*).

Etymology. From hydnoid + *Phanerochaete*, referring to the hydnoid hymenial surface and a close affinity to *Phanerochaete*.

Description. Basidiocarps effused, adnate, ceraceous. Hymenial surface at first buff, with age turning ochraceous to pale brown, slightly tuberculate to grandinioid when young, becoming odontioid to hydnoid with age, without colour changes in KOH. Aculei conical to cylindrical, ca. 1–4 per mm, up to 700 µm long.

Hyphal system essentially monomitic; generative hyphae simple-septate. Subiculum fairly uniform, composed of a basal layer, with compact texture; generative hyphae somewhat horizontal, colourless, thick-walled; quasi-binding hyphae present near substratum, colourless. Hymenial layer thickening. Trama of aculei of compact texture; generative hyphae somewhat vertical, colourless, thick-walled. Cystidia lacking, but projecting hyphal ends in the hymenium may be present. Basidia clavate, 4-sterigmate. Basidiospores ellipsoid to cylindrical, smooth, thin-walled, inamyloid, non-dextrinoid, acyanophilous.

Remarks. *Hydnophanerochaete* is morphologically similar to the genus *Hydnophlebia* (Telleria et al. 2017). Both genera have resupinate basidiocarps with odontioid to hydnoid hymenial surface, a monomitic hyphal system, ordinarily simple-septate hyphae and similar basidiospore shape. However, we note three distinguishing differences. First, *Hydnophlebia* has membranaceous basidiocarps usually with rhizomorphic margin, while *Hydnophanerochaete* has ceraceous basidiocarps with fairly determinate margin. Second, occasional single or multiple clamp connections are present in sub-

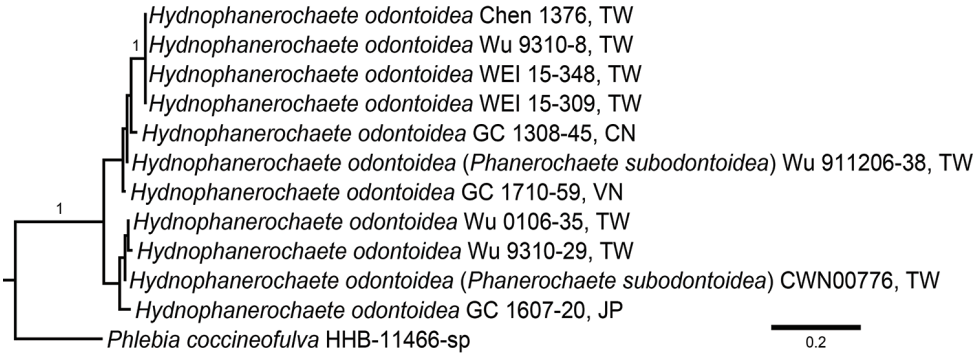

Figure 2. The majority-rule consensus phylograms of the Bayesian Inference analysis of the ITS sequences of *Hydnophanerochaete odontoidea*. Nodes are labelled with Bayesian Posterior Probabilities ≥ 0.9. Scale bars = substitutions per site.

icular or aculei hyphae of *Hydnophlebia*, whereas they are lacking in hyphae of *Hydnophanerochaete*. Third, *Hydnophlebia* occasionally bears tubular to ventricose leptocystidia, which are lacking in *Hydnophanerochaete*.

Little morphological differences exist between *Hydnophanerochaete* and *Odontoefibula*: both genera have monomitic hyphal system with simple-septate hyphae and are lacking cystidia. However, *Hydnophanerochaete* is distinguished from *Odontoefibula* by its basidiocarps without colour change in KOH; additionally, its subiculum is compact, not dense.

Phanerodontia Hjortstam & Ryvarden, a recently proposed genus typified by *P. dentata* Hjortstam & Ryvarden (Hjortstam and Ryvarden 2010), is also morphologically similar to *Hydnophanerochaete*. However, the latter has a compact subiculum and quasi-binding hyphae near the substratum. *Phanerodontia* accommodates four species [*P. chrysosporium* (Burds.) Hjortstam & Ryvarden, *P. dentata*, *P. irpicoides* (Hjortstam) Hjortstam & Ryvarden and *P. magnoliae* (Berk. & M.A. Curtis) Hjortstam & Ryvarden], all of them possessing long leptocystidia (Hjortstam and Ryvarden 2010), whereas this structure is lacking in *Hydnophanerochaete*. Moreover, phylogenetically, strains of two species (*P. chrysosporium* and *P. magnoliae*) were recovered in Phanerochaetaceae which is only distantly related to *Hydnophanerochaete* (Fig. 1). However, the generic type has not been sequenced so far.

Hydnophanerochaete odontoidea **(Sheng H. Wu) Sheng H. Wu & C.C. Chen, comb. nov.**
MycoBank No: MB824078
Figs. 3a and 4

Basionym. *Phanerochaete odontoidea* Sheng H. Wu, Botanical Bulletin of the Academia Sinica 41: 169, 2000.

Synonym. *Phanerochaete subodontoidea* Sheng H. Wu, Botanical Bulletin of the Academia Sinica 41: 172, 2000.

Holotype. TAIWAN. Ilan: Fushan Botanical Garden, 24°46'N, 121°35'E, 600 m alt., on fallen branch of angiosperm, leg. S.H. Wu et al., 7 Aug 1991, *Wu 910807-11* (TNM F14816).

Description. Basidiocarps annual, effused, adnate, ceraceous, somewhat brittle, 50–200 µm thick in section (aculei excluded). Hymenial surface initially buff, with age turning ochraceous to pale brown, no colour changes in KOH, tuberculate to grandinioid when young, becoming odontioid to hydnoid with age, extensively cracked; margin paler to whitish, fairly determinate. Aculei conical to cylindrical, usually separate, with obtuse to acute apex, 1–4 per mm, up to 100–700 × 100–250 µm.

Hyphal system basically monomitic, some specimens with quasi-binding hyphae near substratum; generative hyphae simple-septate. Subiculum fairly uniform, composed of a basal layer of compact texture; generative hyphae mainly horizontal, colourless, 4–6 µm diam., with 0.8–1 µm thick walls; quasi-binding hyphae sometimes present near substratum, colourless, 1–3 µm diam. Hymenial layer thickening, with compact texture, generative hyphae somewhat vertical, colourless, 3–6 µm diam., slightly thick-walled. Trama of aculei of compact texture; generative hyphae mainly vertical, other features similar to those in subiculum; crystal masses present near apex. Cystidia lacking, but projecting hyphal ends in the hymenium may be present. Basidia clavate, 14–18 × 4.5–5.5 µm, 4-sterigmate. Basidiospores narrowly ellipsoid to cylindrical, adaxially slightly concave, smooth, thin-walled, homogeneous, inamyloid, non-dextrinoid, acyanophilous, 6–8.1 × 2.5–3.3 µm (Table 2). See also Wu (2000) for descriptions and illustrations.

Habitat. On fallen branches of angiosperms or gymnosperms.

Distribution. Hitherto known from subtropical to temperate regions of China (Yunnan), Japan, Taiwan and Vietnam.

Additional specimens examined. CHINA. Yunnan: Diqing Tibetan Autonomous Prefecture, Deqin County, Xiayubeng Village, Shenhu Trail, 3500 m alt., on fallen branch of gymnosperm, leg. C.C. Chen, 14 Aug 2013, *GC 1308-45* (TNM F27660). JAPAN. Honshu: Nagano Prefecture, Nagano City, Myoko-Togakushi Renzan National Park, 36°45'35"N, 138°04'20"E, 1235 m alt., on branch of *Quercus* sp., leg. C.C. Chen & C. L. Chen, 29 July 2016, *GC 1607-20* (TNM F30785). TAIWAN. Chiayi: Yushan National Park, Nanhsi Forest Road, 23°28'N, 120°54'E, 1850 m alt., on fallen branch of angiosperm, leg. S.H. Wu & S.Z. Chen, 13 Oct 1993, *Wu 9310-8* (paratype of *P. odontoidea*, TNM F14824); *Wu 9310-29* (TNM F14826); 1800 m alt., on fallen branch of angiosperm, leg. S.H. Wu & S.Z. Chen, 13 Jun 1996, *Wu 9606-55* (TNM F5085). Ilan: Fushan Botanical Garden, 24°46'N, 121°35'E, 650 m alt., on fallen branch of angiosperm, leg. S.H. Wu et al., 28 Jun 2002, *Wu 0106-35* (TNM F13460). Nantou: Tungpu Township, Leleku, 1450 m alt., on fallen rotten wood, leg. W.N. Chou, 13 Apr 1994, *CWN 00776* (holotype of *P. subodontoidea*, TNM F14836). Kaohsiung: Maolin District, Tona Nursery, 22°54'N, 120°44'E, 850 m alt., on fallen branch of angiosperm, leg. S.Z. Chen, 31 Mar 2005, *Chen 1376* (TNM F18764).

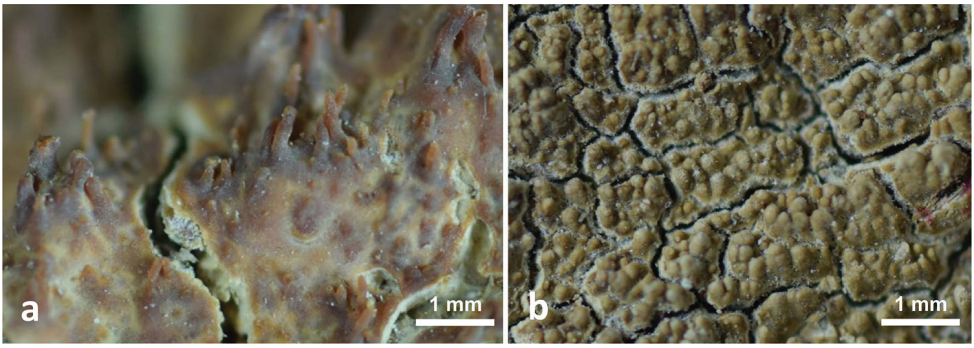

Figure 3. Basidiocarp surfaces **a** *Hydnophanerochaete odontoidea* (holotype of *Phanerochaete subodontoidea*, *CWN 00776*) **b** *Odontoefibula orientalis* (holotype, *Wu 0910-57*). Scale bar: 1 mm.

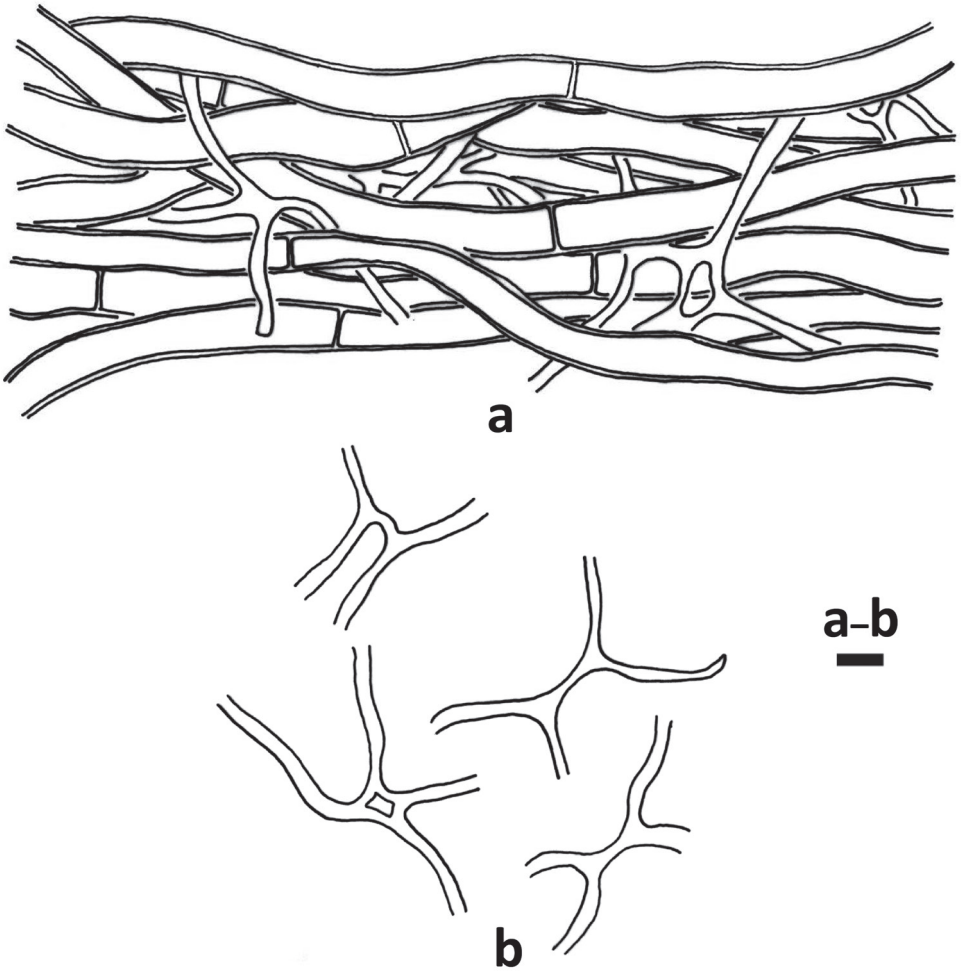

Figure 4. *Hydnophanerochaete odontoidea* (holotype of *Phanerochaete subodontoidea*, *CWN 00776*) **a** Part of the vertical section of subiculum near substratum **b** Quasi-binding hyphae. Scale bar: 5 μm (**a–b**).

New Taipei: Chinshan District, Yangmingshan National Park, Yulu Historical Trail, 25°10'N, 121°35'E, 516 m alt., on fallen branch of angiosperm, leg. C.C. Chen, C.L. Wei, W.C. Chen & S. Li, 26 Aug 2015, *WEI 15-309* (TNM F29370); *WEI 15-348* (TNM F29384). Taichung: Chiapaotai, 850 m alt., on fallen branch of angiosperm, leg. S.H. Wu, 6 Dec 1991, *Wu 911206-38* (paratype of *P. subodontoidea*, TNM F14818). VIETNAM. Lam Dong: Bi Doup Nui Ba National Park, 12°10'45"N, 108°40'48"E, 1447 m alt., on fallen branch of angiosperm, leg. C.C. Chen, 15 Oct 2017, *GC 1710-59* (TNM F31365).

Remarks. *Phanerochaete subodontoidea* morphologically resembles *Phanerochaete odontoidea*, whereas they were distinguished merely based on the width of basidiospores [*P. odontoidea*: 2.6–3 µm vs. *P. subodontoidea*: 3–3.7 µm, Wu (2000)]. However, after carefully measuring the basidiospore size of available specimens of these two species, we found basidiospore ranges are highly overlapping (Table 2). Additionally, the ITS sequences of the holotype of *P. subodontoidea* (*CWN 00776*) is almost identical to the ITS sequences of the paratype of *P. odontoidea* (*Wu 9310-8*). We failed to obtain sequences from the holotype of *P. odontoidea* (*Wu 910807-11*), but *Wu 9310-8* was confirmed as conspecific with the holotype by morphological comparison. Thus, based on morphological and molecular evidence (Fig. 2), *P. subodontoidea* is treated as a synonym of *P. odontoidea*. A paratype specimen named *P. odontoidea* (*Wu 9311-46*) probably belongs to the genus *Flavodon* Ryvarden based on preliminary BLAST results of nuc 28S sequences. However, this specimen was not included in this study.

Odontoefibula **C.C. Chen & Sheng H. Wu, gen. nov.**

MycoBank No: MB824075

Type species. *Odontoefibula orientalis*.

Etymology. From *odonto* (= tooth-like) + *efibula* (= without clamp connection), referring to the odontioid hymenial surface and simple-septate hyphae of the genus.

Description. Basidiocarps annual, resupinate, effused, adnate, membranaceous to ceraceous. Hymenial surface at first honey yellow, becoming ochraceous to pale brown with age, turning dark reddish in KOH, initially smooth to slightly tuberculate, becoming grandinioid to odontioid with age. Aculei conical to cylindrical, separate or fused, up to 0.3 mm long.

Hyphal system monomitic; hyphae normally simple-septate. Subiculum uniform, with dense texture; basal hyphae interwoven, somewhat horizontal or with irregular orientation, colourless, thin- to slightly thick-walled; subicular hyphae somewhat vertical, colourless, thin- to slightly thick-walled. Subhymenium not clearly differentiated from subiculum. Central trama of fairly dense texture; hyphae vertical, colourless, thin- to slightly thick-walled. Cystidia lacking, but projecting hyphal ends in the hymenium may be present. Basidia clavate to narrowly clavate, 4-sterigmate. Basidiospores ellipsoid, smooth, thin-walled, inamyloid, non-dextrinoid, acyanophilous.

Table 2. Aculei and basidiospore measurements of basidiocarps.

Species	Specimens	Aculei (per mm)	Range (µm)	L (µm)	W (µm)	Q	n
Hydnophanerochaete odontoidea	Chen 1376	1–3	(6–) 6.3–7.3 (–7.5) ´ (2.5–) 2.8–3.3 (–3.5)	6.8	3	2.2	30
	CWN 00776 ‡, |	1–3	(6–) 6.8–8 (–8.5) ´ (2.5–) 2.7–3.2 (–3.5)	7.4	2.9	2.5	30
	GC 1308-45 |	2–3	(6.5–) 6.7–7.6 (–8) ´ (2.8–) 2.8–3.3 (–3.8)	7.2	3.1	2.3	30
	GC 1607-20	2–3	(7–) 7.4–9 (–10) ´ (2.8–) 2.9–3.5 (–4)	8.2	3.2	2.6	30
	WEI 15-309	2–3	(6–) 6.1–7 (–7.5) ´ (2.5–) 2.7–3 (–3.3)	6.5	2.9	2.3	30
	WEI 15-348	2–3	6–6.9 (–7.5) ´ (2.5–) 2.8–3.3 (–3.5)	6.5	3	2.1	30
	Wu 0106-35 |	2–3	(6–) 6.4–7.8 (–8) ´ (2.5–) 2.8–3.1 (–3.3)	7.1	2.9	2.4	30
	Wu 910807-11 †	3–4	(6–) 6.1–7 (–8) ´ (2.5–) 2.5–2.9 (–3.3)	6.5	2.7	2.5	30
	Wu 911206-38 ‡	2–3	(6–) 6.3–7.7 (–8) ´ (2.8–) 2.9–3.2 (–3.5)	7	3	2.3	30
	Wu 9310-8 †, |	2–4	(6–) 6.5–8 (–8.5) ´ (2.5–) 2.8–3.2 (–3.5)	7.2	3	2.4	30
	Wu 9310-29	2–4	(6–) 6.9–8.1 (–9) ´ (2.5–) 2.7–3.3 (–3.7)	7.4	3	2.5	30
Odontoefibula orientalis	GC 1604-130 |	4–5	(5–) 5.4–6.6 (–7) ´ (2.5–) 2.8–3.3 (–3.6)	6	3.1	1.96	30
	GC 1703-76 |	4–5	(5.5–) 5.8–7.4 (–8) ´ (3–) 3.2–3.9 (–4)	6.6	3.5	1.85	30
	Wu 0805-59 |	3–5	(5–) 5.1–6.2 (–7) ´ (2.5–) 2.9–3.4 (–3.6)	5.6	3.2	1.79	30
	Wu 0807-53	3–6	(5–) 5.4–6.4 (–7) ´ (3–) 3.1–3.7 (–4)	5.9	3.4	1.71	30
	Wu 0910-57 §, |	3–6	(5–) 5.4–6.1 (–6.5) ´ (2.8–) 2.9–3.4 (–3.6)	5.7	3.2	1.81	30

† Holotype and paratype of *Phanerochaete odontoidea*.

‡ Holotype and paratype of *P. subodontoidea*.

§ Holotype of *Odontoefibula orientalis*.

| Used in phylogenetic analyses of the 5-marker dataset.

Remarks. *Phaneroites* Hjortstam & Ryvarden, a monotypic genus introduced to accommodate *P. subquercinus* (Henn.) Hjortstam & Ryvarden, resembles *Odontoefibula* in having odontioid hymenial surface and a monomitic hyphal system with ordinarily simple-septate hyphae. However, *Phaneroites* is distinguished from *Odontoefibula* by having thin-walled subicular hyphae, a few clamped septa on hyphae next to the substratum and subcapitate cystidia (Hjortstam and Ryvarden 2010). Moreover, basidiocarps of *Odontoefibula* turn dark reddish in KOH, while this reaction was not reported from *Phaneroites*.

Odontoefibula orientalis C.C. Chen & Sheng H. Wu, sp. nov.

MycoBank No: 824076
Figs. 3b and 5

Holotype. CHINA. Beijing: Xiangshan Park, 39°59'N, 116°11'E, 70 m alt., on fallen trunk of *Amygdalus davidiana* (Carrière) de Vos ex Henry, leg. S.H. Wu, 14 Oct 2009, *Wu 0910-57* (TNM F23847).

Etymology. From *orientalis* (= Eastern world), where the specimens were collected.

Description. Basidiocarps annual, effused, adnate, membranaceous to subceraceous, somewhat brittle, 200–400 µm thick in section (aculei excluded). The hymenial surface at first honey yellow, darkening to ochraceous to pale brown with age, turning

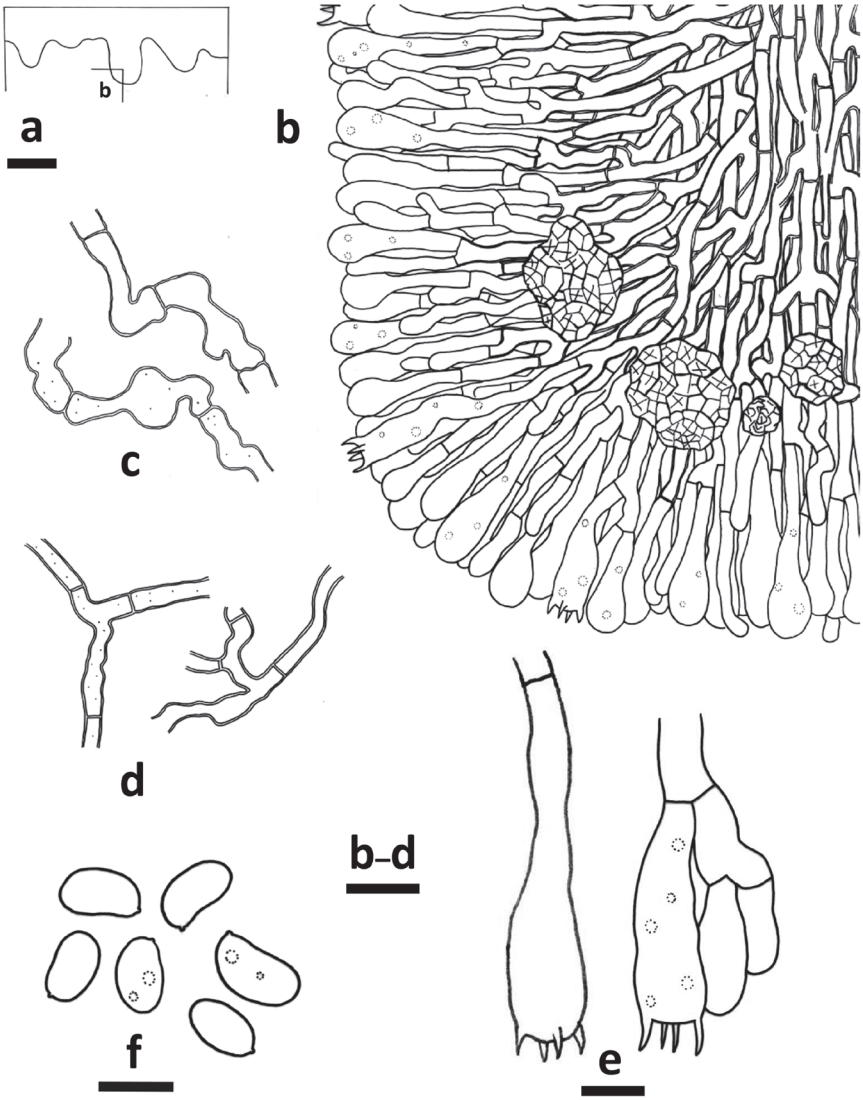

Figure 5. *Odontoefibula orientalis* (holotype, *Wu 0910-57*) **a** Profile of basidiocarp section **b** Part of the vertical section of trama **c** Basal hyphae **d** Subicular hyphae **e** Basidia **f** Basidiospores. Scale bars: 200 µm (**a**); 10 µm (**c–d**); 5 µm (**e–f**).

dark reddish in KOH, slightly tuberculate when young, becoming odontioid with age, extensively cracked; margin paler, thinning out, slightly filamentous. Aculei conical to cylindrical, usually fused at the base, with rounded to obtuse apex, 3–6 per mm, ca. 0.1–0.3 × 0.1–0.2 mm.

Hyphal system monomitic; hyphae simple-septate. Subiculum uniform, with dense texture, 200–300 µm thick; subicular hyphae somewhat vertical, colourless, 2.5–4 µm diam., 0.5–0.8 µm thick walls; hyphae near substratum interwoven, with irregular ori-

entation, tortuous, colourless, irregularly swollen, 4–8 µm diam., 0.5–1 µm thick walls. Subhymenium not clearly differentiated from subiculum, with fairly dense texture, hyphae somewhat vertical, colourless, 3–4 µm diam., thin- to slightly thick-walled. Trama of aculei of dense texture; hyphae mainly vertical, other aspects similar to those in subiculum. Large crystal masses scattered throughout the section. Cystidia lacking, but projecting hyphal ends in the hymenium may be present. Basidia clavate to narrowly clavate, 25–40 × 6–7 µm, 4-sterigmate, often with small oily drops. Basidiospores ellipsoid, adaxially slightly concave, smooth, thin-walled, sometimes with small oily drops, inamyloid, non-dextrinoid, acyanophilous, 5.1–6.6 × 2.8–3.4 µm (Table 2).

Habitat. On fallen trunk of angiosperm (e.g. *Amygdalus*).

Distribution. Hitherto known from China (Beijing), Japan and Taiwan.

Additional specimens examined (paratypes). JAPAN. Honshu: Ibaraki Prefecture, Joso City, Mt. Ju-ichimen-yama, along Kinu-gawa River, on branch of *Prunus* sp., leg. S.H. Wu, 12 July 2008, *Wu 0807-53* (TNM F22091). TAIWAN. Pingtung: Laiyi Township, Pengjishan Trail, 22°30'52"N, 120°38'07"E, 248 m alt., on fallen trunk of angiosperm, leg. C.C. Chen, 25 Mar 2017, *GC 1703-76* (TNM F31460). Taichung: Hoping District, between 27–27.5 km of Dasyueshan Forestry Road, Yuanzueishan Trail, 1800 m alt., on fallen rotten trunk of angiosperm, leg. S.H. Wu, S.Z. Chen & Y.T. Wang, 22 May 2008, *Wu 0805-59* (TNM F22495). Hualien: Sioulin Township, Taroko National Park, Lushui Hiking Trail, 24°10'51"N, 121°30'10"E, 578 m alt., on fallen trunk of angiosperm, leg. C.C. Chen, 24 Apr 2016, *GC 1604-130* (TNM F31364).

Discussion

Our 5-marker phylogenetic analyses (Fig. 1) provided an updated taxonomic framework for evaluating generic placements of the target taxa of the phlebioid clade. The tree topologies are consistent with previous results (Wu et al. 2010; Floudas and Hibbett 2015; Justo et al. 2017; Papp and Dima 2017). Within the phlebioid clade, we recovered two monophyletic lineages of phanerochaetoid fungi (Fig. 1), which supports the status of the two genera erected here: *Hydnophanerochaete*, typified by *P. odontoidea*, is accommodated in Meruliaceae; *Odontoefibula*, typified by *O. orientalis*, is placed in *Donkia* clade of Phanerochaetaceae.

Phylogenetically, *Hydnophanerochaete* and *Odontoefibula* are independent from the nine lineages of phanerochaetoid fungi recognised by Floudas and Hibbett (2015) within the phlebioid clade: *Efibula*, *Hydnophlebia*, *Phaeophlebiopsis*, "*Phanerochaete*" *allantospora* Burds. & Gilb., *Phanerochaete* s.l., *Phanerochaete* s.s., *Phlebiopsis*, *Rhizochaete* and *Scopuloides*. *P. allantospora* was not sampled in this study; it was placed in Irpicaceae, according to the study of Justo et al. (2017). Additionally, "*Phanerochaete*" *ginnsii* Sheng H. Wu represents another lineage of phanerochaetoid fungi that was not analysed in this study, nor in the study of Floudas and Hibbett

(2015). This species was shown to be closely related to *Phlebia centrifuga* P. Karst (Wu et al. 2010).

The 5-marker phylogenetic analyses (Fig. 1) suggest a close relationship amongst *Hydnophanerochaete odontoidea* and the following taxa, which all have a monomitic hyphal system with simple-septate hyphae: *Hydnophlebia*, *Ceriporia alachuana*, *Climacodon septentrionalis* (Fr.) P. Karst. and *Scopuloides rimosa* (Cooke) Jülich. Like *Hydnophanerochaete*, *Hydnophlebia* and *Scopuloides* have an odontioid to hydnoid hymenial surface. However, *Hydnophlebia* differs by its membraneous basidiocarps with rhizomophic margin, occasional clamped subicular hyphae and the presence of tubular to ventricose leptocystidia (Telleria et al. 2017). *Scopuloides* differs by thick-walled encrusted cystidia and rather short, clavate basidia (Wu 1990). *C. alachuana* resembles *H. odontoidea* in lacking cystidia, but has a poroid hymenial surface (Ryvarden and Gilbertson 1993). *C. septentrionalis* has a hydnoid hymenial surface, but is clearly distinguished by its pileate basidiocarps and thick-walled encrusted cystidia (Maas Geesteranus 1971).

Quasi-binding hyphae, one of the diagnostic characters of *H. odontoidea* (Fig. 4), were first introduced by Wu (1990) to refer to narrow and much branched subicular hyphae with thin- to thick walls, found near the substrate. Wu (2000) omitted describing and illustrating the quasi-binding hyphae of *P. odontoidea* and *P. subodontoidea*. Quasi-binding hyphae have been reported from many species of diverse genera: *Amethicium leoninum* (Burds. & Nakasone) Sheng H. Wu, *Crustodontia chrysocreas* (Berk. & M.A. Curtis) Hjortstam & Ryvarden, *Phlebiporia bubalina* Jia J. Chen, B.K. Cui & Y.C. Dai, *Phanerochaete ericina* (Bourdot) J. Erikss. & Ryvarden, *Pseudolagarobasidium calcareum* (Cooke & Massee) Sheng H. Wu and *Radulodon americanus* Ryvarden (Wu 1990; Stalpers 1998; Chen and Cui 2014). In other words, this feature has a polyphyletic origin and does not seem to be very phylogenetically informative.

Within the *Donkia* clade (Fig. 1), systematic positions of two recently proposed taxa, *Geliporus exilisporus* and *Hyphodermella poroides* Y.C. Dai & C.L. Zhao, are confirmed in this study. *Odontoefibula* shares some ubiquitous features with the genera *Donkia*, *Hyphodermella* J. Erikss. & Ryvarden and *Pirex* Hjortstam & Ryvarden, many of which have ochraceous basidiocarps with odontioid to hydnoid hymenial surfaces. However, to better illustrate the correspondence between molecular data and morphology, denser taxon sampling of this clade is necessary in the future.

Acknowledgments

This study was financed by Ministry of Science and Technology of R.O.C (Taiwan) (Grant no 104-2621-B-178-001-MY3). The authors are indebted to Dr. Dimitrios Floudas (Department of Biology, Lund University, Sweden) and reviewers for their valuable comments and suggestions on improving the manuscript. We are also grateful to Ms. Siou-Zhen Chen (TNM) for managing studied specimens and to Shin-Yi Ke (TNM) for the help in DNA sequencing work.

References

Binder M, Justo A, Riley R, Salamov A, Lopez-Giraldez F, Sjökvist E, Copeland A, Foster B, Sun H, Larsson E, Larsson KH, Townsend J, Grigoriev IV, Hibbett DS (2013) Phylogenetic and phylogenomic overview of the Polyporales. Mycologia 105: 1350–1373. https://doi.org/10.3852/13-003

Burdsall HH (1985) A contribution to the taxonomy of the genus *Phanerochaete* (Corticiaceae, Aphyllophorales). Mycologia Memoir 10: 11–65.

Chen JJ, Cui BK (2014) *Phlebiporia bubalina* gen. et. sp. nov. (Meruliaceae, Polyporales) from Southwest China with a preliminary phylogeny based on rDNA sequences. Mycological Progress 13: 563–573. https://doi.org/10.1007/s11557-013-0940-4

Darriba D, Taboada GL, Doallo R, Posada D (2012) jModelTest 2: more models, new heuristics and parallel computing. Nature Methods 9: 772–772. https://doi.org/10.1038/nmeth.2109

De Koker TH, Nakasone KK, Haarhof J, Burdsall HH, Janse BJ (2003) Phylogenetic relationships of the genus *Phanerochaete* inferred from the internal transcribed spacer region. Mycological Research 107: 1032–1040. https://doi.org/10.1017/S095375620300827X

Eriksson J, Hjortstam K, Ryvarden L (1978) The Corticiaceae of North Europe 5. *Mycoaciella-Phanerochaete*. Fungiflora, Oslo.

Eriksson J, Hjortstam K, Ryvarden L (1981) The Corticiaceae of North Europe 6. *Phlebia-Sarcodontia*. Fungiflora, Oslo.

Floudas D, Hibbett DS (2015) Revisiting the taxonomy of *Phanerochaete* (Polyporales, Basidiomycota) using a four gene dataset and extensive ITS sampling. Fungal Biology 119: 679–719. https://doi.org/10.1016/j.funbio.2015.04.003

Frøslev T, Matheny P, Hibbett D (2005) Lower level relationships in the mushroom genus *Cortinarius* (Basidiomycota, Agaricales): a comparison of RPB1, RPB2, and ITS phylogenies. Molecular Phylogenetics and Evolution 37: 602–618. https://doi.org/10.1016/j.ympev.2005.06.016

Ghobad-Nejhad M, Liu SL, Langer E, Dai YC (2015) Molecular and morphological evidence reveal a new non-cystidiate species belonging to the core *Phanerochaete* (Polyporales). Mycological Progress 14: 68. https://doi.org/10.1007/s11557-015-1072-9

Greslebin A, Nakasone KK, Rajchenberg M (2004) *Rhizochaete*, a new genus of phanerochaetoid fungi. Mycologia 96: 260–271. https://doi.org/10.1080/15572536.2005.11832976

Hall TA (1999) BioEdit: a user-friendly biological sequence alignment editor and analysis program for Windows 95/98/NT. Nucleic Acids Symposium Series 41: 95–98.

Hjortstam K, Ryvarden L (2010) *Phanerodontia* and *Phaneroites*, two corticioid taxa (Basidiomycotina) proposed from tropical areas. Synopsis Fungorum 27: 26–33.

Justo A, Miettinen O, Floudas D, Ortiz-Santana B, Sjökvist E, Lindner D, Nakasone KK, Niemelä T, Larsson KH, Ryvarden L (2017) A revised family-level classification of the Polyporales (Basidiomycota). Fungal Biology 121: 798–824. https://doi.org/10.1016/j.funbio.2017.05.010

Katoh K, Standley DM (2013) MAFFT Multiple Sequence Alignment Software Version 7: Improvements in performance and usability. Molecular Biology and Evolution 30: 772–780. https://doi.org/10.1093/molbev/mst010

Kumar S, Stecher G, Tamura K (2016) MEGA7: Molecular Evolutionary Genetics Analysis version 7.0 for bigger datasets. Molecular Biology and Evolution 33: 1870–1874. https://doi.org/10.1093/molbev/msw054

Kuuskeri J, Mäkelä MR, Isotalo J, Oksanen I, Lundell T (2015) Lignocellulose-converting enzyme activity profiles correlate with molecular systematics and phylogeny grouping in the incoherent genus *Phlebia* (Polyporales, Basidiomycota). BMC Microbiology 15: 217. https://doi.org/10.1186/s12866-015-0538-x

Liu YL, Whelen S, Hall BD (1999) Phylogenetic relationships among ascomycetes: evidence from an RNA polymerase II subunit. Molecular Biology and Evolution 16: 1799–1808. https://doi.org/10.1093/oxfordjournals.molbev.a026092

Maas Geesteranus R (1971) Hydnaceous fungi of the eastern old world. Verhandelingen der Koninklijke Nederlandse Akademie van Wetenschappen, Afd. Natuurkunde, Tweede Reeks, deel 60: 1–175.

Matheny PB, Liu YJ, Ammirati JF, Hall BD (2002) Using RPB1 sequences to improve phylogenetic inference among mushrooms (*Inocybe*, Agaricales). American Journal of Botany 89: 688–698. http://dx.doi.org/10.3732/ajb.89.4.688

Matheny PB (2005) Improving phylogenetic inference of mushrooms with RPB1 and RPB2 nucleotide sequences (*Inocybe*; Agaricales). Molecular Phylogenetics and Evolution 35: 1–20. https://doi.org/10.1016/j.ympev.2004.11.014

Miettinen O, Spirin V, Vlasák J, Rivoire B, Stenroos S, Hibbett D (2016) Polypores and genus concepts in Phanerochaetaceae (Polyporales, Basidiomycota). MycoKeys 17: 1–46. https://doi.org/10.3897/mycokeys.17.10153

Miller MA, Pfeiffer W, Schwartz T (2010) Creating the CIPRES Science Gateway for inference of large phylogenetic trees. Proceeding of the Gateway Computing Environments Workshop (GCE), 14 Nov. 2010. New Orleans, LA, 1–8. https://doi.org/10.1109/GCE.2010.5676129

Moreno G, Blanco MN, Platas G, Checa J, Olariaga I (2017) Reappraisal of *Climacodon* (Basidiomycota, Meruliaceae) and reinstatement of *Donkia* (Phanerochaetaceae) using multigene data. Phytotaxa 291: 171–182. https://doi.org/10.11646/phytotaxa.291.3.1

Papp V, Dima B (2017) New systematic position of *Aurantiporus alborubescens* (Meruliaceae, Basidiomycota), a threatened old-growth forest polypore. Mycological Progress 17: 319–332. https://doi.org/10.1007/s11557-017-1356-3

Parmasto E, Hallenberg N (2000) A taxonomic study of phlebioid fungi (Basidiomycota). Nordic Journal of Botany 20: 105–118. https://doi.org/10.1111/j.1756-1051.2000.tb00740.x

Rehner SA, Buckley E (2005) A *Beauveria* phylogeny inferred from nuclear ITS and EF1-α sequences: evidence for cryptic diversification and links to *Cordyceps* teleomorphs. Mycologia 97: 84–98. https://doi.org/10.1080/15572536.2006.11832842

Ronquist F, Teslenko M, Van Der Mark P, Ayres DL, Darling A, Höhna S, Larget B, Liu L, Suchard MA, Huelsenbeck JP (2012) MrBayes 3.2: Efficient Bayesian phylogenetic inference and model choice across a large model space. Systematic Biology 61: 539–542. https://doi.org/10.1093/sysbio/sys029

Ryvarden L, Gilbertson RL (1993) European polypores: Part 1: *Abortiporus—Lindtneria*. Fungiflora, Oslo.

Sánchez C (2009) Lignocellulosic residues: biodegradation and bioconversion by fungi. Biotechnology Advances 27: 185–194. https://doi.org/10.1016/j.biotechadv.2008.11.001

Stalpers JA (1998) On the genera *Sarcodontia*, *Radulodon* and *Pseudolagarobasidium*. Folia Cryptogamica Estonica 33: 133–138.

Stamatakis A (2014) RAxML version 8: a tool for phylogenetic analysis and post-analysis of large phylogenies. Bioinformatics 30: 1312–1313. https://doi.org/10.1093/bioinformatics/btu033

Stiller JW, Hall BD (1997) The origin of red algae: implications for plastid evolution. Proceedings of the National Academy of Sciences 94: 4520–4525.https://doi.org/10.1073/pnas.94.9.4520

Stöver BC, Müller KF (2010) TreeGraph 2: Combining and visualizing evidence from different phylogenetic analyses. BMC Bioinformatics 11: 1–9. https://doi:10.1186/1471-2105-11-7

Telleria MT, Dueñas M, Martín MP (2017) Three new species of *Hydnophlebia* (Polyporales, Basidiomycota) from the Macaronesian Islands. MycoKeys 27: 39–64. https://doi.org/10.3897/mycokeys.27.14866

White TJ, Bruns T, Lee S, Taylor J (1990) Amplification and direct sequencing of fungal ribosomal RNA genes for phylogenetics. In: Innis MA, Gelfand DH, Sninsky JJ, White TJ (Eds) PCR Protocols: A Guide to Methods and Applications. Academic Press, San Diego, 315–322. https://doi.org/10.1016/B978-0-12-372180-8.50042-1

Wu SH (2000) Six new species of *Phanerochaete* from Taiwan. Botanical Bulletin of Academia Sinica 41: 165–174.

Wu SH, Chen YP, Wei CL, Floudas D, Dai YC (2018) Two new species of *Phanerochaete* (Basidiomycota) and redescription of *P. robusta*. Mycological Progress 17: 425–435. https://doi.org/10.1007/s11557-017-1368-z

Wu SH, Nilsson HR, Chen CT, Yu SY, Hallenberg N (2010) The white-rotting genus *Phanerochaete* is polyphyletic and distributed throughout the phleboid clade of the Polyporales (Basidiomycota). Fungal Diversity 42: 107–118. https://doi.org/10.1007/s13225-010-0031-7

Wu SH (1990) The Corticiaceae (Basidiomycetes) subfamilies Phlebioideae, Phanerochaetoideae and Hyphodermoideae in Taiwan. Annales Botanici Fennici 142: 1–123.

Yuan Y, Chen JJ, He SH (2017) *Geliporus exilisporus* gen. et comb. nov., a xanthochroic polypore in Phanerochaetaceae from China. Mycoscience 58: 197–203. https://doi.org/10.1016/j.myc.2017.01.006

Zhao CL, Ren GJ, Wu F (2017) A new species of *Hyphodermella* (Polyporales, Basidiomycota) with a poroid hymenophore. Mycoscience 58: 452–456. https://doi.org/10.1016/j.myc.2017.06.007

MycoKeys 39: 97–149 (2018)
doi: 10.3897/mycokeys.39.26914
http://mycokeys.pensoft.net

RESEARCH ARTICLE

A peer-reviewed open-access journal
MycoKeys
Launched to accelerate biodiversity research

High diversity of *Diaporthe* species associated with dieback diseases in China, with twelve new species described

Qin Yang[1], Xin-Lei Fan[1], Vladimiro Guarnaccia[2,3], Cheng-Ming Tian[1],

1 *The Key Laboratory for Silviculture and Conservation of the Ministry of Education, Beijing Forestry University, Beijing 100083, P.R. China, V. Guarnaccia* **2** *Westerdijk Fungal Biodiversity Institute, Uppsalalaan 8, 3584 CT, Utrecht, The Netherlands* **3** *Department of Plant Pathology, University of Stellenbosch, Matieland 7602, South Africa*

Corresponding author: *Cheng-Ming Tian* (chengmt@bjfu.edu.cn)

Academic editor: *George Mugambi* | Received 24 May 2018 | Accepted 3 September 2018 | Published 17 September 2018

Citation: Yang Q, Fan X-L, Guarnaccia V, Tian C-M (2018) High diversity of *Diaporthe* species associated with dieback diseases in China, with twelve new species described. MycoKeys 39: 97–149. https://doi.org/10.3897/mycokeys.39.26914

Abstract

Diaporthe species have often been reported as important plant pathogens, saprobes and endophytes on a wide range of plant hosts. Although several *Diaporthe* species have been recorded in China, little is known about species able to infect forest trees. Therefore, extensive surveys were recently conducted in Beijing, Heilongjiang, Jiangsu, Jiangxi, Shaanxi and Zhejiang Provinces. The current results emphasised on 15 species from 42 representative isolates involving 16 host genera using comparisons of DNA sequence data for the nuclear ribosomal internal transcribed spacer (ITS), *calmodulin* (*cal*), histone H3 (*his3*), partial translation elongation factor-1α (*tef1*) and β-tubulin (*tub2*) gene regions, as well as their morphological features. Three known species, *D. biguttulata*, *D. eres* and *D. unshiuensis*, were identified. In addition, twelve novel taxa were collected and are described as *D. acerigena*, *D. alangii*, *D. betulina*, *D. caryae*, *D. cercidis*, *D. chensiensis*, *D. cinnamomi*, *D. conica*, *D. fraxinicola*, *D. kadsurae*, *D. padina* and *D. ukurunduensis*. The current study improves the understanding of species causing diebacks on ecological and economic forest trees and provides useful information for the effective disease management of these hosts in China.

Keywords

Dieback, DNA phylogeny, Systematics, Taxonomy

Introduction

The genus *Diaporthe* Nitschke represents a cosmopolitan group of fungi occupying diverse ecological behaviour as plant pathogens, endophytes and saprobes (Muralli et al. 2006, Rossman et al. 2007, Garcia-Reyne et al. 2011, Udayanga et al. 2011, 2012a, b, 2014a, b, 2015, Gomes et al. 2013, Fan et al. 2015, Du et al. 2016, Dissanayake et al. 2017b, Guarnaccia and Crous 2017, Yang et al. 2017a, b, 2018, Guarnaccia et al. 2018, Marin-Felix et al. 2018). *Diaporthe* species are responsible for diseases on a wide range of plant hosts, including agricultural crops, forest trees and ornamentals, some of which are economically important. Several symptoms such as root and fruit rots, dieback, stem cankers, leaf spots, leaf and pod blights and seed decay are caused by *Diaporthe* spp. (Uecker 1988, Rehner and Uecker 1994, Mostert et al. 2001, Santos et al. 2011, Thompson et al. 2011, Udayanga et al. 2011). For example, *D. ampelina*, the causal agent of Phomopsis cane and leaf spot, is known as a severe pathogen of grapevines (Hewitt and Pearson 1988), infecting all green tissues and causing yield reductions of up to 30% in temperate regions (Erincik et al. 2001). *Diaporthe citri* is another well-known pathogen exclusively found on *Citrus* spp. causing melanose, stem-end rot and gummosis in all the citrus production areas except Europe (Mondal et al. 2007, Udayanga et al. 2014a, Guarnaccia and Crous 2017, 2018). Similarly, stem canker, attributed to several *Diaporthe* spp., is one of the most important diseases of sunflower (*Helianthus annuus*) worldwide (Muntañola-Cvetković et al. 1981, Thompson et al. 2011).

Several species of *Diaporthe* include a broad number of endophytes associated with hosts present in temperate and tropical regions (Udayanga et al. 2011). Gomes et al. (2013) considered that *D. endophytica* is a sterile endophyte on *Schinus terebinthifolius* and *Maytenus ilicifolia* based on molecular phylogeny. Huang et al. (2015) distinguished seven undescribed *Diaporthe* species associated with citrus in China. Moreover, some endophytes have been shown to act as opportunistic plant pathogens. For instance, *D. foeniculina* has been found as both endophyte and opportunistic pathogen on various herbaceous weeds, ornamentals and fruit trees (Udayanga et al. 2014a, Guarnaccia et al. 2016).

The genus *Diaporthe* (syn. *Phomopsis*) was established by Nitschke (1870). Species identification criteria in *Diaporthe* were originally based on host association, morphology and culture characteristics (Mostert et al. 2001, Santos and Phillips 2009, Udayanga et al. 2012). As a consequence, a broad increase in the number of proposed *Diaporthe* species occurred. More than 1000 epithets for *Diaporthe* and 950 for *Phomopsis* were listed in Index Fungorum (2018) (http://www.indexfungorum.org/) (accessed 1 March 2018). The abolishment of the dual nomenclature system for pleomorphic fungi raised the question about which generic name to use. Given that both names are well known amongst plant pathologists and have been equally used, Rossman et al. (2015) proposed that the name *Diaporthe* (Nitschke 1870) has priority over *Phomopsis* (Saccardo and Roumeguère 1884) and has been adopted as

the generic name in recent major studies (Gomes et al. 2013, Udayanga et al. 2014a, b, 2015, Fan et al. 2015, Huang et al. 2015, Du et al. 2016, Gao et al. 2017, Yang et al. 2017a, b, c, 2018).

The sexual morph of *Diaporthe* is characterised by immersed ascomata and an erumpent pseudostroma with elongated perithecial necks. Asci are unitunicate, clavate to cylindrical. Ascospores are fusoid, ellipsoid to cylindrical, hyaline, biseriate to uniseriate in the ascus and sometimes with appendages (Udayanga et al. 2011). The asexual morph is characterised by ostiolate conidiomata, with cylindrical phialides producing three types of hyaline, aseptate conidia (Udayanga et al. 2011). Previously, species identification of *Diaporthe* was largely referred to the assumption of host-specificity, leading to the proliferation of names (Gomes et al. 2013). More than one species of *Diaporthe* can colonise a single host, while one species can be associated with different hosts (Santos and Phillips 2009, Diogo et al. 2010, Santos et al. 2011, Gomes et al. 2013). In addition, considerable variability of the phenotype characters is present within a species (Rehner and Uecker 1994, Mostert et al. 2001, Santos et al. 2010, Udayanga et al. 2011, 2012a). Species identification is essential for understanding the epidemiology and plant diseases management and to guide the implementation of phytosanitary measures (Santos and Phillips 2009, Udayanga et al. 2011, Santos et al. 2017). Thus, molecular data are necessary to resolve *Diaporthe* taxonomy and, during the recent years, many species have been described through a polyphasic approach together with morphology (Gomes et al. 2013, Udayanga et al. 2014a, b, 2015, Huang et al. 2015, Gao et al. 2017, Guarnaccia and Crous 2017, Yang et al. 2018). Santos et al. (2017) revealed that the use of a five-loci dataset (ITS-*cal-his3-tef1-tub2*) is the optimal combination for species delimitation, showing the ribosomal ITS locus as the least informative, which is contrary to the result of Santos et al. (2010).

Although the classification of *Diaporthe* has been on-going, species are currently being identified based on a combination of morphological, cultural, phytopathological and phylogenetical analyses (Gomes et al. 2013, Huang et al. 2013, 2015, Udayanga et al. 2014a, b, 2015, Fan et al. 2015, Du et al. 2016, Gao et al. 2016, 2017, Guarnaccia and Crous 2017, Hyde et al. 2017, 2018, Guarnaccia et al. 2018, Jayawardena et al. 2018, Perera et al. 2018a, b, Tibpromma et al. 2018, Wanasinghe et al. 2018). However, fungi isolated from forest trees in China were recorded in old fungal literature without any living culture and molecular data (Teng 1963, Tai 1979, Wei 1979). The current study aimed to investigate the major ecological or economic trees in China by large-scale sampling and to identify isolates via morphology and multi-locus phylogeny based on modern taxonomic concepts. From 2015 to 2017, several surveys were conducted in six Provinces representing 16 host genera. The objectives of the present study were (i) to provide a multi-gene phylogeny for the genus *Diaporthe* based on a large set of freshly collected specimens in China; (ii) to identify *Diaporthe* taxa associated with disease symptoms or non-symptomatic tissues of various host genera distributed over six Provinces in China; (iii) to define the species limits of *D. eres* and closely related species based on multi-gene genealogies.

Table 1. Isolates and GenBank accession numbers used in the phylogenetic analyses of *Diaporthe*.

Species	Isolate	Host	Location	GenBank accession numbers				
				ITS	*cal*	*his3*	*tef1*	*tub2*
D. acaciarum	CBS 138862	*Acacia tortilis*	Tanzania	KP004460	N/A[a]	N/A[a]	N/A[a]	KP004509
D. acaciigena	CBS 129521	*Acacia retinodes*	Australia	KC343005	KC343247	KC343489	KC343731	KC343973
D. acericola	MFLUCC 17-0956	*Acer negundo*	Italy	KY964224	KY964137	N/A[a]	KY964180	KY964074
D. acerigena	**CFCC 52554**	***Acer tataricum***	**China**	**MH121489**	**MH121413**	**MH121449**	**MH121531**	**N/A[a]**
	CFCC 52555	***Acer tataricum***	**China**	**MH121490**	**MH121414**	**MH121450**	**MH121532**	**N/A[a]**
D. acutispora	CGMCC 3.18285	*Coffea* sp.	China	KX986764	KX999274	N/A[a]	KX999155	KX999195
D. alangii	**CFCC 52556**	***Alangium kurzii***	**China**	**MH121491**	**MH121415**	**MH121451**	**MH121533**	**MH121573**
	CFCC 52557	***Alangium kurzii***	**China**	**MH121492**	**MH121416**	**MH121452**	**MH121534**	**MH121574**
	CFCC 52558	***Alangium kurzii***	**China**	**MH121493**	**MH121417**	**MH121453**	**MH121535**	**MH121575**
	CFCC 52559	***Alangium kurzii***	**China**	**MH121494**	**MH121418**	**MH121454**	**MH121536**	**MH121576**
D. alleghaniensis	CBS 495.72	*Betula alleghaniensis*	Canada	KC343007	KC343249	KC343491	KC343733	KC343975
D. alnea	CBS 146.46	*Alnus* sp.	Netherlands	KC343008	KC343250	KC343492	KC343734	KC343976
D. ambigua	CBS 114015	*Pyrus communis*	South Africa	KC343010	KC343252	KC343494	KC343736	KC343978
D. ampelina	STEU2660	*Vitis vinifera*	France	AF230751	AY745026	N/A[a]	AY745056	JX275452
D. amygdali	CBS 126679	*Prunus dulcis*	Portugal	KC343022	KC343264	KC343506	AY343748	KC343990
D. anacardii	CBS 720.97	*Anacardium occidentale*	East Africa	KC343024	KC343266	KC343508	KC343750	KC343992
D. angelicae	CBS 111592	*Heracleum sphondylium*	Austria	KC343027	KC343269	KC343511	KC343753	KC343995
D. apiculatum	CGMCC 3.17533	*Camellia sinensis*	China	KP267896	N/A[a]	N/A[a]	KP267970	KP293476
D. aquatica	IFRDCC 3051	*Aquatic habitat*	China	JQ797437	N/A[a]	N/A[a]	N/A[a]	N/A[a]
D. arctii	CBS 139280	*Arctium lappa*	Austria	KJ590736	KJ612133	KJ659218	KJ590776	KJ610891
D. arecae	CBS 161.64	*Areca catechu*	India	KC343032	KC343274	KC343516	KC343758	KC344000
D. arengae	CBS 114979	*Arenga enngleri*	Hong Kong	KC343034	KC343276	KC343518	KC343760	KC344002
D. aseana	MFLUCC 12-0299a	Unknown dead leaf	Thailand	KT459414	KT459464	N/A[a]	KT459448	KT459432
D. asheicola	CBS 136967	*Vaccinium ashei*	Chile	KJ160562	KJ160542	N/Aa	KJ160594	KJ160518
D. aspalathi	CBS 117169	*Aspalathus linearis*	South Africa	KC343036	KC343278	KC343520	KC343762	KC344004
D. australafricana	CBS 111886	*Vitis vinifera*	Australia	KC343038	KC343280	KC343522	KC343764	KC344006
D. baccae	CBS 136972	*Vaccinium corymbosum*	Italy	KJ160565	N/A[a]	MF418264	KJ160597	N/A[a]

Species	Isolate	Host	Location	GenBank accession numbers				
				ITS	*cal*	*his3*	*tef1*	*tub2*
D. batatas	CBS 122.21	*Ipomoea batatas*	USA	KC343040	KC343282	N/A[a]	KC343766	KC344008
D. beilharziae	BRIP 54792	*Indigofera australis*	Australia	JX862529	N/A[a]	N/A[a]	JX862535	KF170921
D. benedicti	BPI 893190	*Salix* sp.	USA	KM669929	KM669862	N/A[a]	KM669785	N/A[a]
D. betulae	CFCC 50469	*Betula platyphylla*	China	KT732950	KT732997	KT732999	KT733016	KT733020
	CFCC 50470	*Betula platyphylla*	China	KT732951	KT732998	KT733000	KT733017	KT733021
D. betulicola	CFCC 51128	*Betula albo-sinensis*	China	KX024653	KX024659	KX024661	KX024655	KX024657
	CFCC 51129	*Betula albo-sinensis*	China	KX024654	KX024660	KX024662	KX024656	KX024658
D. betulina	**CFCC 52560**	***Betula albo-sinensis***	**China**	**MH121495**	**MH121419**	**MH121455**	**MH121537**	**MH121577**
	CFCC 52561	***Betula costata***	**China**	**MH121496**	**MH121420**	**MH121456**	**MH121538**	**MH121578**
	CFCC 52562	***Betula platyphylla***	**China**	**MH121497**	**MH121421**	**MH121457**	**MH121539**	**MH121579**
D. bicincta	CBS 121004	*Juglans* sp.	USA	KC343134	KC343376	KC343618	KC343860	KC344102
D. biconispora	CGMCC 3.17252	*Citrus grandis*	China	KJ490597	KJ490539	KJ490539	KJ490476	KJ490418
D. biguttulata	CGMCC 3.17248	*Citrus limon*	China	KJ490582	N/A[a]	KJ490524	KJ490461	KJ490403
	CFCC 52584	***Juglans regia***	**China**	**MH121519**	**MH121437**	**MH121477**	**MH121561**	**MH121598**
	CFCC 52585	***Juglans regia***	**China**	**MH121520**	**MH121438**	**MH121478**	**MH121562**	**MH121599**
D. biguttusis	CGMCC 3.17081	*Lithocarpus glabra*	China	KF576282	N/A[a]	N/A[a]	KF576257	KF576306
D. bohemiae	CPC 28222	*Vitis vinifera*	Czech Republic	MG281015	MG281710	MG281361	MG281536	MG281188
D. brasiliensis	CBS 133183	*Aspidosperma tomentosum*	Brazil	KC343042	KC343284	KC343526	KC343768	KC344010
D. caatingaensis	CBS 141542	*Tacinga inamoena*	Brazil	KY085927	N/A[a]	N/A[a]	KY115603	KY115600
D. camptothecicola	CFCC 51632	*Camptotheca acuminata*	China	KY203726	KY228877	KY228881	KY228887	KY228893
D. canthii	CBS 132533	*Canthium inerme*	South Africa	JX069864	KC843174	N/A[a]	KC843120	KC843230
D. caryae	**CFCC 52563**	***Carya illinoensis***	**China**	**MH121498**	**MH121422**	**MH121458**	**MH121540**	**MH121580**
	CFCC 52564	***Carya illinoensis***	**China**	**MH121499**	**MH121423**	**MH121459**	**MH121541**	**MH121581**
D. cassines	CPC 21916	*Cassine peragua*	South Africa	KF777155	N/A[a]	N/A[a]	KF777244	N/A[a]
D. caulivora	CBS 127268	*Glycine max*	Croatia	KC343045	KC343287	N/A[a]	KC343771	KC344013
D. celeris	CPC 28262	*Vitis vinifera*	Czech Republic	MG281017	MG281712	MG281363	MG281538	MG281190
D. celastrina	CBS 139.27	*Celastrus* sp.	USA	KC343047	KC343289	KC343531	KC343773	KC344015
D. cercidis	**CFCC 52565**	***Cercis chinensis***	**China**	**MH121500**	**MH121424**	**MH121460**	**MH121542**	**MH121582**
	CFCC 52566	***Cercis chinensis***	**China**	**MH121501**	**MH121425**	**MH121461**	**MH121543**	**MH121583**

Species	Isolate	Host	Location	GenBank accession numbers				
				ITS	*cal*	*his3*	*tef1*	*tub2*
D. chamaeropis	CBS 454.81	*Chamaerops humilis*	Greece	KC343048	KC343290	KC343532	KC343774	KC344016
D. charlesworthii	BRIP 54884m	*Rapistrum rugostrum*	Australia	KJ197288	N/A[a]	N/A[a]	KJ197250	KJ197268
D. chensiensis	**CFCC 52567**	***Abies chensiensis***	**China**	**MH121502**	**MH121426**	**MH121462**	**MH121544**	**MH121584**
	CFCC 52568	***Abies chensiensis***	**China**	**MH121503**	**MH121427**	**MH121463**	**MH121545**	**MH121585**
D. cichorii	MFLUCC 17-1023	*Cichorium intybus*	Italy	KY964220	KY964133	N/A[a]	KY964176	KY964104
D. cinnamomi	**CFCC 52569**	***Cinnamomum* sp.**	**China**	**MH121504**	N/A[a]	**MH121464**	**MH121546**	**MH121586**
	CFCC 52570	***Cinnamomum* sp.**	**China**	**MH121505**	N/A[a]	**MH121465**	**MH121547**	**MH121587**
D. cissampeli	CBS 141331	*Cissampelos capensis*	South Africa	KX228273	N/A[a]	KX228366	N/A[a]	KX228384
D. citri	AR 3405	*Citrus* sp.	USA	KC843311	KC843157	N/A[a]	KC843071	KC843187
D. citriasiana	CGMCC 3.15224	*Citrus unshiu*	China	JQ954645	KC357491	KJ490515	JQ954663	KC357459
D. citrichinensis	CGMCC 3.15225	*Citrus* sp.	China	JQ954648	KC357494	N/A[a]	JQ954666	N/A[a]
D. collariana	MFLU 17-2770	*Magnolia champaca*	Thailand	MG806115	MG783042	N/A[a]	MG783040	MG783041
D. compacta	CGMCC 3.17536	*Camellia sinensis*	China	KP267854	N/A[a]	KP293508	KP267928	KP293434
D. conica	**CFCC 52571**	***Alangium chinense***	**China**	**MH121506**	**MH121428**	**MH121466**	**MH121548**	**MH121588**
	CFCC 52572	***Alangium chinense***	**China**	**MH121507**	**MH121429**	**MH121467**	**MH121549**	**MH121589**
	CFCC 52573	***Alangium chinense***	**China**	**MH121508**	**MH121430**	**MH121468**	**MH121550**	**MH121590**
	CFCC 52574	***Alangium chinense***	**China**	**MH121509**	**MH121431**	**MH121469**	**MH121551**	**MH121591**
D. convolvuli	CBS 124654	*Convolvulus arvensis*	Turkey	KC343054	KC343296	KC343538	KC343780	KC344022
D. crotalariae	CBS 162.33	*Crotalaria spectabilis*	USA	KC343056	KC343298	KC343540	KC343782	KC344024
D. cucurbitae	CBS 136.25	*Arctium* sp.	Unknown	KC343031	KC343273	KC343515	KC343757	KC343999
D. cuppatea	CBS 117499	*Aspalathus linearis*	South Africa	KC343057	KC343299	KC343541	KC343783	KC344025
D. cynaroidis	CBS 122676	*Protea cynaroides*	South Africa	KC343058	KC343300	KC343542	KC343784	KC344026
D. cytosporella	FAU461	*Citrus limon*	Italy	KC843307	KC843141	N/A[a]	KC843116	KC843221
D. diospyricola	CPC 21169	*Diospyros whyteana*	South Africa	KF777156	N/A[a]	N/A[a]	N/A[a]	N/A[a]
D. discoidispora	ZJUD89	*Citrus unshiu*	China	KJ490624	N/A[a]	KJ490566	KJ490503	KJ490445
D. dorycnii	MFLUCC 17-1015	*Dorycnium hirsutum*	Italy	KY964215	N/A[a]	N/A[a]	KY964171	KY964099
D. elaeagni-glabrae	CGMCC 3.18287	*Elaeagnus glabra*	China	KX986779	KX999281	KX999251	KX999171	KX999212
D. ellipicola	CGMCC 3.17084	*Lithocarpus glabra*	China	KF576270	N/A[a]	N/A[a]	KF576245	KF576291
D. endophytica	CBS 133811	*Schinus terebinthifolius*	Brazil	KC343065	KC343307	KC343549	KC343791	KC343065

Species	Isolate	Host	Location	GenBank accession numbers				
				ITS	*cal*	*his3*	*tef1*	*tub2*
D. eres	AR5193	*Ulmus* sp.	Germany	KJ210529	KJ434999	KJ420850	KJ210550	KJ420799
	CFCC 52575	***Castanea mollissima***	**China**	**MH121510**	**N/A[a]**	**MH121470**	**MH121552**	**MH121592**
	CFCC 52576	***Castanea mollissima***	**China**	**MH121511**	**MH121432**	**MH121471**	**MH121553**	**MH121593**
	CFCC 52577	***Acanthopanax senticosus***	**China**	**MH121512**	**MH121433**	**MH121472**	**MH121554**	**MH121594**
	CFCC 52578	***Sorbus* sp.**	**China**	**MH121513**	**MH121434**	**MH121473**	**MH121555**	**MH121595**
	CFCC 52579	***Juglans regia***	**China**	**MH121514**	**N/A[a]**	**MH121474**	**MH121556**	**N/A[a]**
	CFCC 52580	***Melia azedarace***	**China**	**MH121515**	**N/A[a]**	**MH121475**	**MH121557**	**MH121596**
	CFCC 52581	***Rhododendron simsii***	**China**	**MH121516**	**N/A[a]**	**MH121476**	**MH121558**	**MH121597**
D. eucalyptorum	CBS 132525	*Eucalyptus* sp.	Australia	NR120157	N/Aa	N/Aa	N/Aa	N/Aa
D. foeniculacea	CBS 123208	*Foeniculum vulgare*	Portugal	KC343104	KC343346	KC343588	KC343830	KC344072
D. fraxini-angustifoliae	BRIP 54781	*Fraxinus angustifolia*	Australia	JX862528	N/A[a]	N/A[a]	JX862534	KF170920
D. fraxinicola	**CFCC 52582**	***Fraxinus chinensis***	**China**	**MH121517**	**MH121435**	**N/A[a]**	**MH121559**	**N/A[a]**
	CFCC 52583	***Fraxinus chinensis***	**China**	**MH121518**	**MH121436**	**N/A[a]**	**MH121560**	**N/A[a]**
D. fukushii	MAFF 625034	*Pyrus pyrifolia*	Japan	JQ807469	N/A[a]	N/A[a]	JQ807418	N/A[a]
D. fusicola	CGMCC 3.17087	*Lithocarpus glabra*	China	KF576281	KF576233	N/A[a]	KF576256	KF576305
D. ganjae	CBS 180.91	*Cannabis sativa*	USA	KC343112	KC343354	KC343596	KC343838	KC344080
D. garethjonesii	MFLUCC 12-0542a	*Unknown dead leaf*	Thailand	KT459423	KT459470	N/A[a]	KT459457	KT459441
D. goulteri	BRIP 55657a	*Helianthus annuus*	Australia	KJ197290	N/A[a]	N/A[a]	KJ197252	KJ197270
D. gulyae	BRIP 54025	*Helianthus annuus*	Australia	JF431299	N/A[a]	N/A[a]	KJ197271	JN645803
D. helianthi	CBS 592.81	*Helianthus annuus*	Serbia	KC343115	KC343357	KC343599	KC343841	KC344083
D. helicis	AR5211	*Hedera helix*	France	KJ210538	KJ435043	KJ420875	KJ210559	KJ420828
D. heterophyllae	CBS 143769	*Acacia heterohpylla*	France	MG600222	MG600218	MG600220	MG600224	MG600226
D. hickoriae	CBS 145.26	*Carya glabra*	USA	KC343118	KC343360	KC343602	KC343844	KC344086
D. hispaniae	CPC 30321	*Vitis vinifera*	Spain	MG281123	MG281820	MG281471	MG281644	MG281296
D. hongkongensis	CBS 115448	*Dichroa febrífuga*	China	KC343119	KC343361	KC343603	KC343845	KC344087
D. incompleta	CGMCC 3.18288	*Camellia sinensis*	China	KX986794	KX999289	KX999265	KX999186	KX999226
D. inconspicua	CBS 133813	*Maytenus ilicifolia*	Brazil	KC343123	KC343365	KC343607	KC343849	KC344091

Species	Isolate	Host	Location	GenBank accession numbers				
				ITS	*cal*	*his3*	*tef1*	*tub2*
D. infecunda	CBS 133812	*Schinus terebinthifolius*	Brazil	KC343126	KC343368	KC343610	KC343852	KC344094
D. isoberliniae	CPC 22549	*Isoberlinia angolensis*	Zambia	KJ869133	N/A[a]	N/A[a]	N/A[a]	KJ869245
D. juglandicola	CFCC 51134	*Juglans mandshurica*	China	KU985101	KX024616	KX024622	KX024628	KX024634
	CFCC 51135	*Juglans mandshurica*	China	KU985102	KX024617	KX024623	KX024629	KX024635
D. kadsurae	**CFCC 52586**	***Kadsura longipedunculata***	**China**	**MH121521**	**MH121439**	**MH121479**	**MH121563**	**MH121600**
	CFCC 52587	***Kadsura longipedunculata***	**China**	**MH121522**	**MH121440**	**MH121480**	**MH121564**	**MH121601**
	CFCC 52588	***Acer* sp.**	**China**	**MH121523**	**MH121441**	**MH121481**	**MH121565**	**MH121602**
	CFCC 52589	***Acer* sp.**	**China**	**MH121524**	**MH121442**	**MH121482**	**MH121566**	**MH121603**
D. kochmanii	BRIP 54033	*Helianthus annuus*	Australia	JF431295	N/A[a]	N/A[a]	JN645809	N/A[a]
D. kongii	BRIP 54031	*Portulaca grandiflora*	Australia	JF431301	N/A[a]	N/A[a]	JN645797	KJ197272
D. litchicola	BRIP 54900	*Litchi chinensis*	Australia	JX862533	N/A[a]	N/A[a]	JX862539	KF170925
D. lithocarpus	CGMCC 3.15175	*Lithocarpus glabra*	China	KC153104	KF576235	N/A[a]	KC153095	KF576311
D. longicicola	CGMCC 3.17089	*Lithocarpus glabra*	China	KF576267	N/A[a]	N/A[a]	KF576242	KF576291
D. longicolla	ATCC 60325	*Glycine max*	USA	KJ590728	N/A[a]	KJ659188	KJ590767	KJ610883
D. longispora	CBS 194.36	*Ribes* sp.	Canada	KC343135	KC343377	KC343619	KC343861	KC344103
D. lonicerae	MFLUCC 17-0963	*Lonicera* sp.	Italy	KY964190	KY964116	N/A[a]	KY964146	KY964073
D. lusitanicae	CBS 123212	*Foeniculum vulgare*	Portugal	KC343136	KC343378	KC343620	KC343862	KC344104
D. macinthoshii	BRIP 55064a	*Rapistrum rugostrum*	Australia	KJ197289	N/A[a]	N/A[a]	KJ197251	KJ197269
D. mahothocarpus	CGMCC 3.15181	*Lithocarpus glabra*	China	KC153096	N/A[a]	N/A[a]	KC153087	KF576312
D. malorum	CAA734	*Malus domestica*	Portugal	KY435638	KY435658	KY435648	KY435627	KY435668
D. maritima	DAOMC 250563	*Picea rubens*	Canada	N/A[a]	N/A[a]	N/A[a]	N/A[a]	KU574616
D. masirevicii	BRIP 57892a	*Helianthus annuus*	Australia	KJ197277	N/A[a]	N/A[a]	KJ197239	KJ197257
D. mayteni	CBS 133185	*Maytenus ilicifolia*	Brazil	KC343139	KC343381	KC343623	KC343865	KC344107
D. maytenicola	CPC 21896*	*Maytenus acuminata*	South Africa	KF777157	N/A[a]	N/A[a]	N/A[a]	KF777250
D. melonis	CBS 507.78	*Cucumis melo*	USA	KC343142	KC343384	KC343626	KC343868	KC344110
D. middletonii	BRIP 54884e	*Rapistrum rugostrum*	Australia	KJ197286	N/A[a]	N/A[a]	KJ197248	KJ197266
D. miriciae	BRIP 54736j	*Helianthus annuus*	Australia	KJ197282	N/A[a]	N/A[a]	KJ197244	KJ197262
D. momicola	MFLUCC 16-0113	*Prunus persica*	China	KU557563	KU557611	N/A[a]	KU557631	KU55758
D. multigutullata	ZJUD98	*Citrus grandis*	China	KJ490633	N/A[a]	KJ490575	KJ490512	KJ490454

Species	Isolate	Host	Location	GenBank accession numbers				
				ITS	*cal*	*his3*	*tef1*	*tub2*
D. musigena	CBS 129519	*Musa* sp.	Australia	KC343143	KC343385	KC343627	KC343869	KC344111
D. neilliae	CBS 144.27	*Spiraea* sp.	USA	KC343144	KC343386	KC343628	KC343870	KC344112
D. neoarctii	CBS 109490	*Ambrosia trifida*	USA	KC343145	KC343387	KC343629	KC343871	KC344113
D. neoraonikayaporum	MFLUCC 14-1136	*Tectona grandis*	Thailand	KU712449	KU749356	N/A[a]	KU749369	KU743988
D. nobilis	CBS 113470	*Castanea sativa*	Korea	KC343146	KC343388	KC343630	KC343872	KC344114
D. nothofagi	BRIP 54801	*Nothofagus cunninghamii*	Australia	JX862530	N/A[a]	N/A[a]	JX862536	KF170922
D. novem	CBS 127270	*Glycine max*	Croatia	KC343155	KC343397	KC343640	KC343881	KC344123
D. ocoteae	CBS 141330	*Ocotea obtusata*	France	KX228293	N/A[a]	N/A[a]	N/A[a]	KX228388
D. oraccinii	CGMCC 3.17531	*Camellia sinensis*	China	KP267863	N/A[a]	KP293517	KP267937	KP293443
D. ovalispora	ICMP20659	*Citrus limon*	China	KJ490628	N/A[a]	KJ490570	KJ490507	KJ490449
D. ovoicicola	CGMCC 3.17093	*Citrus* sp.	China	KF576265	KF576223	N/A[a]	KF576240	KF576289
D. oxe	CBS 133186	*Maytenus ilicifolia*	Brazil	KC343164	KC343406	KC343648	KC343890	KC344132
D. padina	**CFCC 52590**	***Padus racemosa***	**China**	**MH121525**	**MH121443**	**MH121483**	**MH121567**	**MH121604**
	CFCC 52591	***Padus racemosa***	**China**	**MH121526**	**MH121444**	**MH121484**	**MH121568**	**MH121605**
D. pandanicola	MFLU 18-0006	*Pandanus* sp.	Thailand	MG646974	N/A[a]	N/A[a]	N/A[a]	MG646930
D. paranensis	CBS 133184	*Maytenus ilicifolia*	Brazil	KC343171	KC343413	KC343655	KC343897	KC344139
D. parapterocarpi	CPC 22729	*Pterocarpus brenanii*	Zambia	KJ869138	N/A[a]	N/A[a]	N/A[a]	KJ869248
D. pascoei	BRIP 54847	*Persea americana*	Australia	JX862532	N/A[a]	N/A[a]	JX862538	KF170924
D. passiflorae	CBS 132527	*Passiflora edulis*	South America	JX069860	N/A[a]	KY435654	N/A[a]	N/A[a]
D. passifloricola	CBS 141329	*Passiflora foetida*	Malaysia	KX228292	N/A[a]	KX228367	N/A[a]	KX228387
D. penetriteum	CGMCC 3.17532	*Camellia sinensis*	China	KP714505	N/A[a]	KP714493	KP714517	KP714529
D. perjuncta	CBS 109745	*Ulmus glabra*	Austria	KC343172	KC343414	KC343656	KC343898	KC344140
D. perseae	CBS 151.73	*Persea gratissima*	Netherlands	KC343173	KC343415	KC343657	KC343899	KC344141
D. pescicola	MFLUCC 16-0105	*Prunus persica*	China	KU557555	KU557603	N/A[a]	KU557623	KU557579
D. phaseolorum	AR4203	*Phaseolus vulgaris*	USA	KJ590738	N/A[a]	KJ659220	N/A[a]	KP004507
D. podocarpi-macrophylli	CGMCC 3.18281	*Podocarpus macrophyllus*	China	KX986774	KX999278	KX999246	KX999167	KX999207
D. pseudomangiferae	CBS 101339	*Mangifera indica*	Dominican Republic	KC343181	KC343423	KC343665	KC343907	KC344149

Species	Isolate	Host	Location	GenBank accession numbers				
				ITS	*cal*	*his3*	*tef1*	*tub2*
D. pseudophoenicicola	CBS 462.69	*Phoenix dactylifera*	Spain	KC343184	KC343426	KC343668	KC343910	KC344152
D. pseudotsugae	MFLU 15-3228	*Pseudotsuga menziesii*	Italy	KY964225	KY964138	N/A[a]	KY964181	KY964108
D. psoraleae	CBS 136412	*Psoralea pinnata*	South Africa	KF777158	N/A[a]	N/A[a]	KF777245	KF777251
D. psoraleae-pinnatae	CBS 136413	*Psoralea pinnata*	South Africa	KF777159	N/A[a]	N/A[a]	N/A[a]	KF777252
D. pterocarpi	MFLUCC 10-0571	*Pterocarpus indicus*	Thailand	JQ619899	JX197451	N/A[a]	JX275416	JX275460
D. pterocarpicola	MFLUCC 10-0580a	*Pterocarpus indicus*	Thailand	JQ619887	JX197433	N/A[a]	JX275403	JX275441
D. pulla	CBS 338.89	*Hedera helix*	Yugoslavia	KC343152	KC343394	KC343636	KC343878	KC344120
D. pyracanthae	CAA483	*Pyracantha coccinea*	Portugal	KY435635	KY435656	KY435645	KY435625	KY435666
D. racemosae	CBS 143770	*Euclea racemosa*	South Africa	MG600223	MG600219	MG600221	MG600225	MG600227
D. raonikayaporum	CBS 133182	*Spondias mombin*	Brazil	KC343188	KC343430	KC343672	KC343914	KC344156
D. ravennica	MFLUCC 15-0479	*Tamarix* sp.	Italy	KU900335	N/A[a]	N/A[a]	KX365197	KX432254
D. rhusicola	CBS 129528	*Rhus pendulina*	South Africa	JF951146	KC843124	N/A[a]	KC843100	KC843205
D. rosae	MFLU 17-1550	*Rosa* sp.	Thailand	MG828894	N/A[a]	N/A[a]	N/A[a]	MG843878
D. rosicola	MFLU 17-0646	*Rosa* sp.	UK	MG828895	N/A[a]	N/A[a]	MG829270	MG843877
D. rostrata	CFCC 50062	*Juglans mandshurica*	China	KP208847	KP208849	KP208851	KP208853	KP208855
	CFCC 50063	*Juglans mandshurica*	China	KP208848	KP208850	KP208852	KP208854	KP208856
D. rudis	AR3422	*Laburnum anagyroides*	Austria	KC843331	KC843146	N/A[a]	KC843090	KC843177
D. saccarata	CBS 116311	*Protea repens*	South Africa	KC343190	KC343432	KC343674	KC343916	KC344158
D. sackstonii	BRIP 54669b	*Helianthus annuus*	Australia	KJ197287	N/A[a]	N/A[a]	KJ197249	KJ197267
D. salicicola	BRIP 54825	*Salix purpurea*	Australia	JX862531	N/A[a]	N/A[a]	JX862537	JX862531
D. sambucusii	CFCC 51986	*Sambucus williamsii*	China	KY852495	KY852499	KY852503	KY852507	KY852511
	CFCC 51987	*Sambucus williamsii*	China	KY852496	KY852500	KY852504	KY852508	KY852512
D. schini	CBS 133181	*Schinus terebinthifolius*	Brazil	KC343191	KC343433	KC343675	KC343917	KC344159
D. schisandrae	CFCC 51988	*Schisandra chinensis*	China	KY852497	KY852501	KY852505	KY852509	KY852513
	CFCC 51989	*Schisandra chinensis*	China	KY852498	KY852502	KY852506	KY852510	KY852514
D. schoeni	MFLU 15-1279	*Schoenus nigricans*	Italy	KY964226	KY964139	N/A[a]	KY964182	KY964109
D. sclerotioides	CBS 296.67	*Cucumis sativus*	Netherlands	KC343193	KC343435	KC343677	KC343919	KC344161

Species	Isolate	Host	Location	GenBank accession numbers				
				ITS	*cal*	*his3*	*tef1*	*tub2*
D. sennae	CFCC 51636	*Senna bicapsularis*	China	KY203724	KY228875	N/A[a]	KY228885	KY228891
	CFCC 51637	*Senna bicapsularis*	China	KY203725	KY228876	N/Aa	KY228886	KY228892
D. sennicola	CFCC 51634	*Senna bicapsularis*	China	KY203722	KY228873	KY228879	KY228883	KY228889
	CFCC 51635	*Senna bicapsularis*	China	KY203723	KY228874	KY228880	KY228884	KY228890
D. serafiniae	BRIP 55665a	*Helianthus annuus*	Australia	KJ197274	N/A[a]	N/A[a]	KJ197236	KJ197254
D. siamensis	MFLUCC 10-573a	*Dasymaschalon* sp.	Thailand	JQ619879	N/A[a]	N/A[a]	JX275393	JX275429
D. sojae	FAU635	*Glycine max*	USA	KJ590719	KJ612116	KJ659208	KJ590762	KJ610875
D. spartinicola	CBS 140003	*Spartium junceum*	Spain	KR611879	N/A[a]	KR857696	N/A[a]	KR857695
D. sterilis	CBS 136969	*Vaccinium corymbosum*	Italy	KJ160579	KJ160548	MF418350	KJ160611	KJ160528
D. stictica	CBS 370.54	*Buxus sampervirens*	Italy	KC343212	KC343454	KC343696	KC343938	KC344180
D. subclavata	ICMP20663	*Citrus unshiu*	China	KJ490587	N/A[a]	KJ490529	KJ490466	KJ490408
D. subcylindrospora	MFLU 17-1195	*Salix* sp.	China	MG746629	N/A[a]	N/A[a]	MG746630	MG746631
D. subellipicola	MFLU 17-1197	on dead wood	China	MG746632	N/A[a]	N/A[a]	MG746633	MG746634
D. subordinaria	CBS 464.90	*Plantago lanceolata*	New Zealand	KC343214	KC343456	KC343698	KC343940	KC344182
D. taoicola	MFLUCC 16-0117	*Prunus persica*	China	KU557567	N/Aa	N/A[a]	KU557635	KU557591
D. tectonae	MFLUCC 12-0777	*Tectona grandis*	China	KU712430	KU749345	N/A[a]	KU749359	KU743977
D. tectonendophytica	MFLUCC 13-0471	*Tectona grandis*	China	KU712439	KU749354	N/A[a]	KU749367	KU749354
D. tectonigena	MFLUCC 12-0767	*Tectona grandis*	China	KU712429	KU749358	N/A[a]	KU749371	KU743976
D. terebinthifolii	CBS 133180	*Schinus terebinthifolius*	Brazil	KC343216	KC343458	KC343700	KC343942	KC344184
D. thunbergii	MFLUCC 10-576a	*Thunbergia laurifolia*	Thailand	JQ619893	JX197440	N/A[a]	JX275409	JX275449
D. thunbergiicola	MFLUCC 12-0033	*Thunbergia laurifolia*	Thailand	KP715097	N/A[a]	N/A[a]	KP715098	N/A[a]
D. tibetensis	CFCC 51999	*Juglandis regia*	China	MF279843	MF279888	MF279828	MF279858	MF279873
	CFCC 52000	*Juglandis regia*	China	MF279844	MF279889	MF279829	MF279859	MF279874
D. torilicola	MFLUCC 17-1051	*Torilis arvensis*	Italy	KY964212	KY964127	N/A[a]	KY964168	KY964096
D. toxica	CBS 534.93	*Lupinus angustifolius*	Australia	KC343220	KC343462	C343704	KC343946	KC344188
D. tulliensis	BRIP 62248a	*Theobroma cacao* fruit	Australia	KR936130	N/A[a]	N/A[a]	KR936133	KR936132
D. ueckerae	FAU656	*Cucumis melo*	USA	KJ590726	KJ612122	KJ659215	KJ590747	KJ610881
D. ukurunduensis	**CFCC 52592**	***Acer ukurunduense***	**China**	**MH121527**	**MH121445**	**MH121485**	**MH121569**	N/A[a]
	CFCC 52593	***Acer ukurunduense***	**China**	**MH121528**	**MH121446**	**MH121486**	**MH121570**	N/A[a]

Species	Isolate	Host	Location	GenBank accession numbers				
				ITS	*cal*	*his3*	*tef1*	*tub2*
D. undulata	CGMCC 3.18293	Leaf of unknown host	China-Laos border	KX986798	N/A[a]	KX999269	KX999190	KX999230
D. unshiuensis	CGMCC 3.17569	*Citrus unshiu*	China	KJ490587	N/A[a]	KJ490529	KJ490408	KJ490466
	CFCC 52594	***Carya illinoensis***	**China**	**MH121529**	**MH121447**	**MH121487**	**MH121571**	**MH121606**
	CFCC 52595	***Carya illinoensis***	**China**	**MH121530**	**MH121448**	**MH121488**	**MH121572**	**MH121607**
D. vaccinii	CBS 160.32	*Oxycoccus macrocarpos*	USA	KC343228	KC343470	KC343712	KC343954	KC344196
D. vangueriae	CPC 22703	*Vangueria infausta*	Zambia	KJ869137	N/A[a]	N/A[a]	N/A[a]	KJ869247
D. vawdreyi	BRIP 57887a	*Psidium guajava*	Australia	KR936126	N/A[a]	N/A[a]	KR936129	KR936128
D. velutina	CGMCC 3.18286	*Neolitsea* sp.	China	KX986790	N/A[a]	KX999261	KX999182	KX999223
D. virgiliae	CMW40748	*Virgilia oroboides*	South Africa	KP247566	N/A[a]	N/A[a]	N/A[a]	KP247575
D. xishuangbanica	CGMCC 3.18282	*Camellia sinensis*	China	KX986783	N/A[a]	KX999255	KX999175	KX999216
D. yunnanensis	CGMCC 3.18289	*Coffea* sp.	China	KX986796	KX999290	KX999267	KX999188	KX999228
Diaporthella corylina	CBS 121124	*Corylus* sp.	China	KC343004	KC343246	KC343488	KC343730	KC343972

Newly sequenced material is indicated in bold type.

Table 2. Genes used in this study with PCR primers, process and references.

Gene	PCR primers (forward/reverse)	PCR: thermal cycles: (Annealing temp. in bold)	References of primers used
ITS	ITS1/ITS4	(95 °C: 30 s, **51 °C**: 30 s, 72 °C: 1 min) × 35 cycles	White et al. 1990
cal	CAL228F/CAL737R	(95 °C: 15 s, **55 °C**: 20 s, 72 °C: 1 min) × 35 cycles	Carbone and Kohn 1999
his3	CYLH4F/H3-1b	(95 °C: 30 s, **58** °C: 30 s, 72 °C: 1 min) × 35 cycles	Glass and Donaldson 1995, Crous et al. 2004a
tef1	EF1-728F/EF1-986R	(9 °C: 15 s, **55 °C**: 20 s, 72 °C: 1 min) × 35 cycles	Carbone and Kohn 1999
tub2	T1(Bt2a)/Bt2b	(95 °C: 30 s, **55** °C: 30 s, 72 °C: 1 min) × 35 cycles	Glass and Donaldson 1995, Glass and Donaldson 1995

Materials and methods

Isolates

From 2015 to 2017, fresh specimens of *Diaporthe* were collected from symptomatic or non-symptomatic twigs or branches from Beijing, Heilongjiang, Jiangsu, Jiangxi, Shaanxi and Zhejiang Provinces in China (Table 1). A total of 105 isolates were obtained by removing a mucoid spore mass from conidiomata and spreading the suspension on the surface of 1.8% potato dextrose agar (PDA) in a Petri dish and incubating at 25 °C for up to 24 h. Single germinating conidia were transferred on to fresh PDA plates. Forty-two representative *Diaporthe* strains were selected based on cultural characteristics on PDA, conidia morphology and ITS sequence data. Specimens were deposited in the Museum of the Beijing Forestry University (BJFC). Axenic cultures are maintained in the China Forestry Culture Collection Centre (CFCC).

Morphological analysis

Agar plugs (6 mm diam.) were taken from the edge of actively growing cultures on PDA and transferred on to the centre of 9 cm diam Petri dishes containing 2% tap water agar supplemented with sterile pine needles (PNA; Smith et al. 1996) and potato dextrose agar (PDA) and incubated at 20–21 °C under a 12 h near-ultraviolet light/12 h dark cycle to induce sporulation as described in recent studies (Gomes et al. 2013, Lombard et al. 2014). Colony characters and pigment production on PNA and PDA were noted after 10 d. Colony colours were rated according to Rayner (1970). Cultures were examined periodically for the development of ascomata and conidiomata. The morphological characteristics were examined by mounting fungal structures in clear lactic acid and 30 measurements at 1000× magnification were determined for each isolate using a Leica compound microscope (DM 2500) with interference contrast (DIC) optics. Descriptions, nomenclature and illustrations of taxonomic novelties are deposited in MycoBank (www.MycoBank.org; Crous et al. 2004b).

DNA extraction, PCR amplification and sequencing

Genomic DNA was extracted from colonies grown on cellophane-covered PDA using a modified CTAB [cetyltrimethylammonium bromide] method (Doyle and Doyle 1990). DNA was estimated by electrophoresis in 1% agarose gel and the quality was measured using the NanoDrop 2000 (Thermo Scientific, Waltham, MA, USA), following the user manual (Desjardins et al. 2009). PCR amplifications were performed in a DNA Engine Peltier Thermal Cycler (PTC-200; Bio-Rad Laboratories, Hercules, CA, USA). The primer sets ITS1/ITS4 (White et al. 1990) were used to amplify the ITS region. The primer pair CAL228F/CAL737R (Carbone and Kohn 1999) were

used to amplify the calmodulin gene (*cal*) and the primer pair CYLH4F (Crous et al. 2004a) and H3-1b (Glass and Donaldson 1995) were used to amplify part of the histone H3 (*his3*) gene. The primer pair EF1-728F/EF1-986R (Carbone and Kohn 1999) were used to amplify a partial fragment of the translation elongation factor 1-α gene (*tef1*). The primer sets T1 (O'Donnell and Cigelnik 1997) and Bt2b (Glass and Donaldson 1995) were used to amplify the beta-tubulin gene (*tub2*); the additional combination of Bt2a/Bt2b (Glass and Donaldson 1995) was used in case of amplification failure of the T1/Bt2b primer pair. Amplifications of different loci were performed under different conditions (Table 2). PCR amplification products were assayed via electrophoresis in 2% agarose gels. DNA sequencing was performed using an ABI PRISM® 3730XL DNA Analyser with a BigDye Terminater Kit v.3.1 (Invitrogen, USA) at the Shanghai Invitrogen Biological Technology Company Limited (Beijing, China).

Phylogenetic analyses

DNA generated sequences were used to obtain consensus sequences using SeqMan v.7.1.0 DNASTAR Lasergene Core Suite software programme (DNASTAR Inc., Madison, WI, USA). Sequences were aligned using MAFFT v.6 (Katoh and Toh 2010) and edited manually using MEGA6 (Tamura et al. 2013). Two different datasets were employed to estimate two phylogenetic analyses: one for *Diaporthe* species and one for *Diaporthe eres* complex. The first analysis was undertaken to infer the interspecific relationships in *Diaporthe*. All the *Diaporthe* isolates recovered from samples collected during this study and additional reference sequences of *Diaporthe* species were included in the dataset of combined ITS, *cal*, *his3*, *tef1*, and *tub2* regions (Table 1), with *Diaporthella corylina* (CBS 121124) as outgroup. The second analysis focused on the *Diaporthe eres* complex based on *cal*, *tef1* and *tub2* loci (Table 3) according to recent publications (Gao et al. 2014, 2015, 2016, Udayanga et al. 2014b, Tanney et al. 2016, Fan et al. 2018), with *Diaporthe citri* (AR3405) as outgroup. Maximum Parsimony analysis was performed by a heuristic search option of 1000 random-addition sequences with a tree bisection and reconnection (TBR) algorithm. Maxtrees were set to 5000, branches of zero length were collapsed and all equally parsimonious trees were saved. Other calculated parsimony scores were tree length (TL), consistency index (CI), retention index (RI) and rescaled consistency (RC). Maximum Likelihood analysis was performed with a GTR site substitution model (Guindon et al. 2010). Branch support was evaluated with a bootstrapping (BS) method of 1000 replicates (Hillis and Bull 1993).

Bayesian inference (BI) analysis, employing a Markov chain Monte Carlo (MCMC) algorithm, was performed (Rannala and Yang 1996). MrModeltest v. 2.3 was used to estimate the best-fit model of nucleotide substitution model settings for each gene (Posada and Crandall 1998). Two MCMC chains started from random trees for 1,000,000 generations and trees were sampled every 100th generation, resulting in

Table 3. Isolates and GenBank accession numbers used in the phylogenetic analyses of *Diaporthe eres* complex.

Species	Isolate/culture collection	Host	Location	GenBank accession numbers		
				CAL	TEF1-α	TUB
D. alleghaniensis	CBS 495.72	*Betula alleghaniensis*	Canada	KC343249	GQ250298	KC843228
D. alnea	CBS 146.46	*Alnus* sp.	Netherlands	KC343250	KC343734	KC343976
	CBS 159.47	*Alnus* sp.	Netherlands	KC343251	KC343735	KC343977
	LCM22b.02a	*Alnus* sp.	USA	KJ435020	KJ210557	KJ420825
	LCM22b.02b	*Alnus* sp.	USA	KJ435021	KJ210558	KJ420826
D. betulina	**CFCC 52560**	***Betula albo-sinensis***	**China**	**MH121419**	**MH121537**	**MH121577**
	CFCC 52561	***Betula costata***	**China**	**MH121420**	**MH121538**	**MH121578**
	CFCC 52562	***Betula platyphylla***	**China**	**MH121421**	**MH121539**	**MH121579**
D. bicincta	CBS 121004	*Juglans* sp.	USA	KC343376	KC343860	KC344102
D. biguttusis	CGMCC 3.17081	*Lithocarpus glabra*	China	N/A[a]	KF576257	KF576306
D. camptothecicola	CFCC 51632	*Camptotheca acuminata*	China	KY228881	KY228887	KY228893
D. celastrina	CBS 139.27	*Celastrus* sp.	USA	KC343289	KC343773	KC344015
D. chensiensis	**CFCC 52567**	***Abies chensiensis***	**China**	**MH121426**	**MH121544**	**MH121584**
	CFCC 52568	***Abies chensiensis***	**China**	**MH121427**	**MH121545**	**MH121585**
D. citri	AR3405	*Citrus* sp.	USA	KC843157	KC843071	KC843187
D. citrichinensis	ZJUD034	*Citrus* sp.	China	KC843234	KC843071	KC843187
	ZJUD034B	*Citrus* sp.	China	KJ435042	KJ210562	KJ420829
D. ellipicola	CGMCC 3.17084	*Lithocarpus glabra*	China	N/A[a]	KF576245	KF576291
D. eres	AR5193	*Ulmus laevis*	Germany	KJ434999	KJ210550	KJ420799
D. eres	AR5196	*Ulmus laevis*	Germany	KJ435006	KJ210554	KJ420817
	DP0438	*Ulmus minor*	Austria	KJ435016	KJ210553	KJ420816
	LCM114.01a	*Ulmus* sp.	USA	KJ435027	KJ210545	KJ420787
	LCM114.01b	*Ulmus* sp.	USA	KJ435026	KJ210544	KJ420786
	FAU483	*Malus* sp.	Netherlands	KJ435022	JQ807422	KJ420827
	DAN001A	*Daphne laureola*	France	KJ434994	KJ210540	KJ420781
	DAN001B	*Daphne laureola*	France	KJ434995	KJ210541	KJ420782
	AR5197	*Rhododendron* sp.	Germany	KJ435014	KJ210552	KJ420812
	CBS 439.82	*Cotoneaster* sp.	UK	JX197429	GQ250341	JX275437
	AR3519	*Corylus avellana*	Austria	KJ435008	KJ210547	KJ420789
	FAU506	*Cornus florida*	USA	KJ435012	JQ807403	KJ420792
	FAU570	*Oxydendrum arboreum*	USA	KJ435025	JQ807410	KJ420794
	AR3723	*Rubus fruticosus*	Austria	KJ435024	JQ807354	KJ420793
	FAU522	*Sassafras albida*	USA	KJ435010	JQ807406	KJ420791
	DP0666	*Juglans cinerea*	USA	KJ435007	KJ210546	KJ420788
	DP0667	*Juglans cinerea*	USA	KC843155	KC843121	KC843229
	AR3560	*Viburnum* sp.	Austria	KJ435011	JQ807351	KJ420795
	AR5224	*Hedera helix*	Germany	KJ435036	KJ210551	KJ420802
	AR5231	*Hedera helix*	Germany	KJ435038	KJ210555	KJ420818
	AR5223	*Acer nugundo*	Germany	KJ435000	KJ210549	KJ420830
	CBS 109767	*Acer* sp.	Austria	KC343317	KC343801	KC344043
	DLR12a	*Vitis vinifera*	France	KJ434996	KJ210542	KJ420783
	DLR12b	*Vitis vinifera*	France	KJ434997	KJ210543	KJ420784
	AR4347	*Vitis vinifera*	Korea	KJ435030	JQ807356	KJ420805
	AR4355	*Prunus* sp.	Korea	KJ435035	JQ807359	KJ420797
	AR4367	*Prunus* sp.	Korea	KJ435019	JQ807364	KJ420824
	AR4346	*Prunus mume*	Korea	KJ435003	JQ807355	KJ420823
	AR4348	*Prunus persici*	Korea	KJ435004	JQ807357	JQ807357
	AR3669	*Pyrus pyrifolia*	Japan	KJ435002	JQ807415	KJ420808
	AR3670	*Pyrus pyrifolia*	Japan	KJ435001	JQ807416	KJ420807
	AR3671	*Pyrus pyrifolia*	Japan	KJ435017	JQ807417	KJ420814

Species	Isolate/culture collection	Host	Location	GenBank accession numbers		
				CAL	TEF1-α	TUB
	AR3672	*Pyrus pyrifolia*	Japan	KJ435023	JQ807418	KJ420819
	DP0591	*Pyrus pyrifolia*	New Zealand	KJ435018	JQ807395	KJ420821
	AR4369	*Pyrus pyrifolia*	Korea	KJ435005	JQ807366	KJ420813
	DP0180	*Pyrus pyrifolia*	New Zealand	KJ435029	JQ807384	KJ420804
	DP0179	*Pyrus pyrifolia*	New Zealand	KJ435028	JQ807383	KJ420803
	DP0590	*Pyrus pyrifolia*	New Zealand	KJ435037	JQ807394	KJ420810
	AR4373	*Ziziphus jujuba*	Korea	KJ435013	JQ807368	KJ420798
	AR4374	*Ziziphus jujuba*	Korea	KJ434998	JQ807369	KJ420785
	AR4357	*Ziziphus jujuba*	Korea	KJ435031	JQ807360	KJ420806
	AR4371	*Malus pumila*	Korea	KJ435034	JQ807367	KJ420796
	FAU532	*Chamaecyparis thyoides*	USA	KJ435015	JQ807408	KJ435015
	CBS 113470	*Castanea sativa*	Australia	KC343388	KC343872	KC344114
	AR4349	*Vitis vinifera*	Korea	KJ435032	JQ807358	KJ420822
	AR4363	*Malus* sp.	Korea	KJ435033	JQ807362	KJ420809
	CFCC 52575	***Castanea mollissima***	**China**	**N/A[a]**	**MH121552**	**MH121592**
	CFCC 52576	***Castanea mollissima***	**China**	**MH121432**	**MH121553**	**MH121593**
	CFCC 52577	***Acanthopanax senticosus***	**China**	**MH121433**	**MH121554**	**MH121594**
	CFCC 52578	***Sorbus* sp.**	**China**	**MH121434**	**MH121555**	**MH121595**
	CFCC 52579	***Juglans regia***	**China**	**N/A[a]**	**MH121556**	**N/A[a]**
	CFCC 52580	***Melia azedarace***	**China**	**N/A[a]**	**MH121557**	**MH121596**
	CFCC 52581	***Rhododendron simsii***	**China**	**N/A[a]**	**MH121558**	**MH121597**
D. helicis	AR5211	*Hedera helix*	France	KJ435043	KJ210559	KJ420828
D. longicicola	CGMCC 3.17089	*Lithocarpus glabra*	China	N/A[a]	KF576242	KF576291
D. mahothocarpus	CGMCC 3.15181	*Lithocarpus glabra*	China	N/A[a]	KC153087	KF576312
D. maritima	DAOMC 250563	*Picea rubens*	Canada	N/A[a]	N/A[a]	KU574616
D. momicola	MFLUCC 16-0113	*Prunus persica*	China	N/A[a]	KU557631	KU55758
D. neilliae	CBS 144. 27	*Spiraea* sp.	USA	KC343386	KC343870	KC344112
D. padina	**CFCC 52590**	***Padus racemosa***	**China**	**MH121443**	**MH121567**	**MH121604**
	CFCC 52591	***Padus racemosa***	**China**	**MH121444**	**MH121568**	**MH121605**
D. phragmitis	CBS 138897	*Phragmites australis*	China	N/A[a]	N/A[a]	KP004507
D. pulla	CBS 338.89	*Hedera helix*	Yugoslavia	KC343394	KC343878	KC344120
D. vaccinii	DF5032	*Vaccinium corymbosum*	USA	KC849457	JQ807380	KC843225
	FAU633	*Vaccinium macrocarpon*	USA	KC849456	JQ807413	KC843226
	FAU446	*Vaccinium macrocarpon*	USA	KC849455	JQ807398	KC843224
	CBS 160.32	*Vaccinium macrocarpon*	USA	KC343470	GQ250326	JX270436
	FAU 468	*Vaccinium macrocarpon*	USA	KC849458	JQ807399	KC843227

Newly sequenced material is indicated in bold type.

a total of 10,000 trees. The first 25% of trees were discarded as the burn-in phase of each analysis. Branches with significant Bayesian posterior probabilities (BPP) were estimated in the remaining 7500 trees.

Sequences data were deposited in GenBank (Table 1). The multilocus sequence alignments were deposited in TreeBASE (www.treebase.org) as accession S22702 and S22703. The taxonomic novelties were deposited in MycoBank (Crous et al. 2004b).

Results

Collection of *Diaporthe* strains

Forty-two representative *Diaporthe* strains were isolated from 16 different host genera (Table 1) collected from six Provinces (Beijing, Heilongjiang, Jiangsu, Jiangxi, Shaanxi and Zhejiang) in China. All of these strains were isolated from symptomatic or non-symptomatic branches or twigs and preserved in the China Forestry Culture Collection Centre (CFCC).

Phylogenetic analyses

The first sequences dataset for the ITS, *cal*, *his3*, *tef1*, and *tub2* was analysed in combination to infer the interspecific relationships within *Diaporthe.* The combined species phylogeny of the *Diaporthe* isolates consisted of 236 sequences, including the outgroup sequences of *Diaporthella corylina* (culture CBS 121124). A total of 2948 characters including gaps (516 for ITS, 568 for *cal*, 520 for *his3*, 486 for *tef1* and 858 for *tub2*) were included in the phylogenetic analysis. The maximum likelihood tree, conducted by the GTR model, confirmed the tree topology and posterior probabilities of the Bayesian consensus tree. For the Bayesian analyses, MrModeltest suggested that all partitions should be analysed with dirichlet state frequency distributions. The following models were recommended by MrModeltest and used: GTR+I+G for ITS, *cal* and *his3*, HKY+I+G for *tef1* and *tub2*. The topology and branching order of ML were similar to BI analyses (Fig. 1). Based on the multi-locus phylogeny and morphology, 42 strains were assigned to 15 species, including 12 taxa which we describe here as new (Fig. 1).

The second dataset with *cal*, *tef1* and *tub2* sequences were analysed to focus on the *Diaporthe eres* complex. The alignment included 86 taxa, including the outgroup sequences of *Diaporthe citri* (Table 3). The aligned three-locus datasets included 1148 characters. Of these, 881 characters were constant, 105 variable characters were parsimony-uninformative and 162 characters were parsimony informative. The heuristic search using maximum parsimony (MP) generated 105 parsimonious trees (TL = 438, CI = 0.669, RI = 0.883, RC = 0.591), from which one was selected (Fig. 2). Based on the multi-locus phylogeny and morphology, seven strains were identified as *D. eres*, seven strains formed three distinct clades embedded in the *D. eres* complex, i.e. *D. betulina*, *D. chensiensis* and *D. padina*. MP and ML bootstrap support values above 50% are shown as first and second position, respectively. The branches with significant Bayesian posterior probability (≥ 0.70) in Bayesian analyses were thickened in the phylogenetic tree. The current results, based on the three genes (*cal*, *tef1* and *tub2*), suggest that *D. eres* clade could be separated from other species in this complex (Fig. 2). However, *D. biguttusis* (CGMCC 3.17081), *D. camptothecicola* (CFCC 51632), *D. ellipicola* (CGMCC 3.17084), *D. longicicola* (CGMCC 3.17089), *D. mahothocarpus* (CGMCC 3.15181) and *D. momicola* (MFLUCC 16-0113) were clustered in *D. eres* clade and thus treated as the synonyms of *D. eres* in the current study.

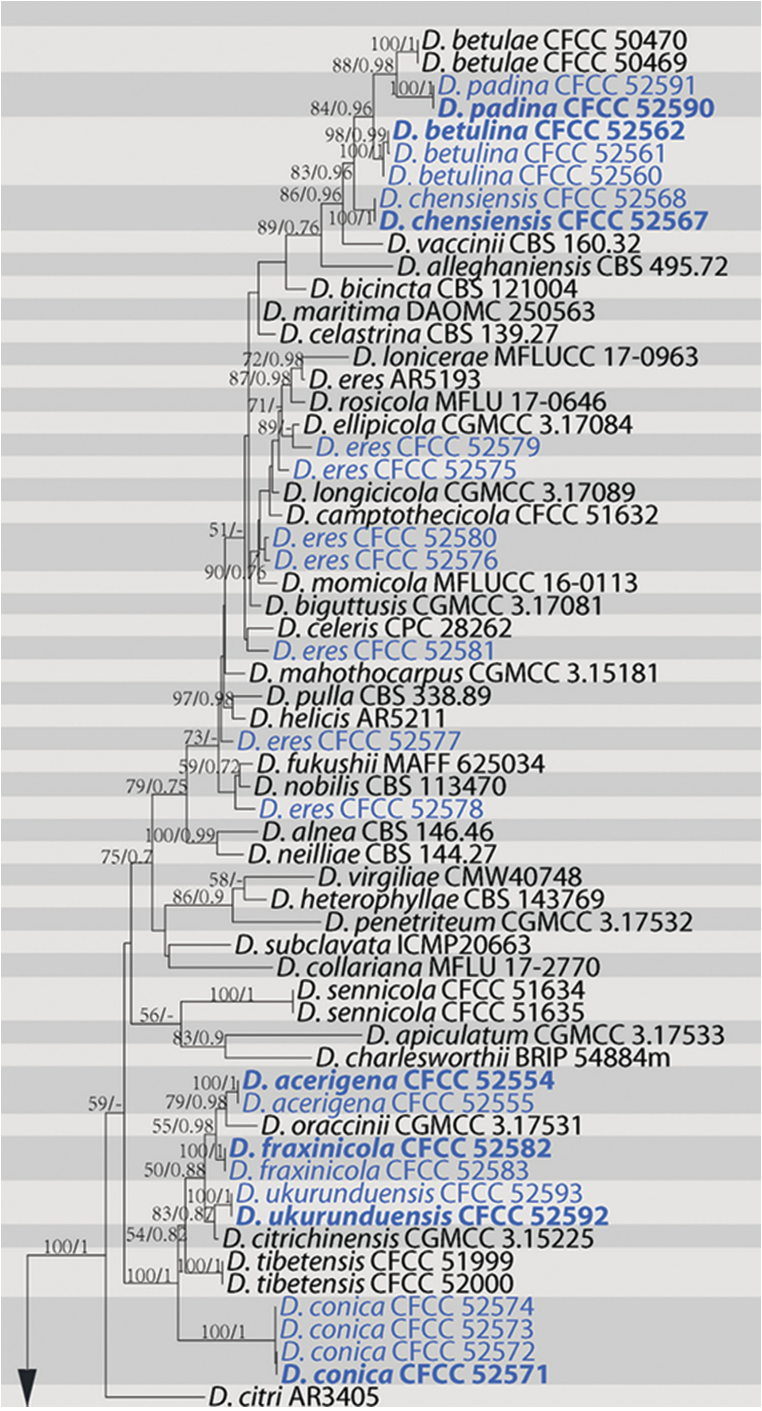

Figure 1. Phylogram of *Diaporthe* from a maximum likelihood analysis based on combined ITS, *cal*, *his3*, *tef1* and *tub2*. Values above the branches indicate maximum likelihood bootstrap (left, ML BP ≥ 50%) and bayesian probabilities (right, BI PP ≥ 0.70). The tree is rooted with *Diaporthella corylina*. Strains in the current study are in blue.

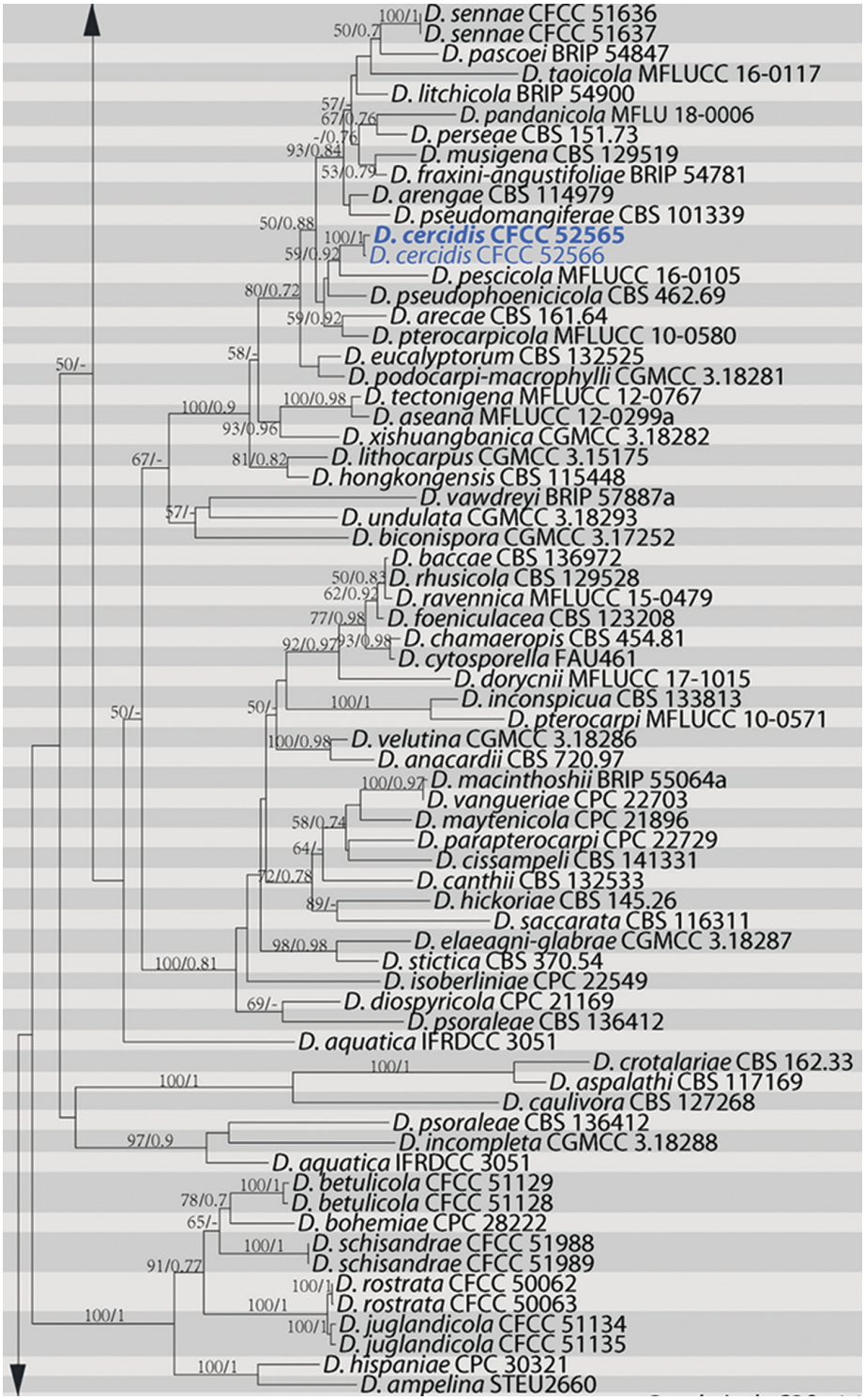

Figure 1. Continued.

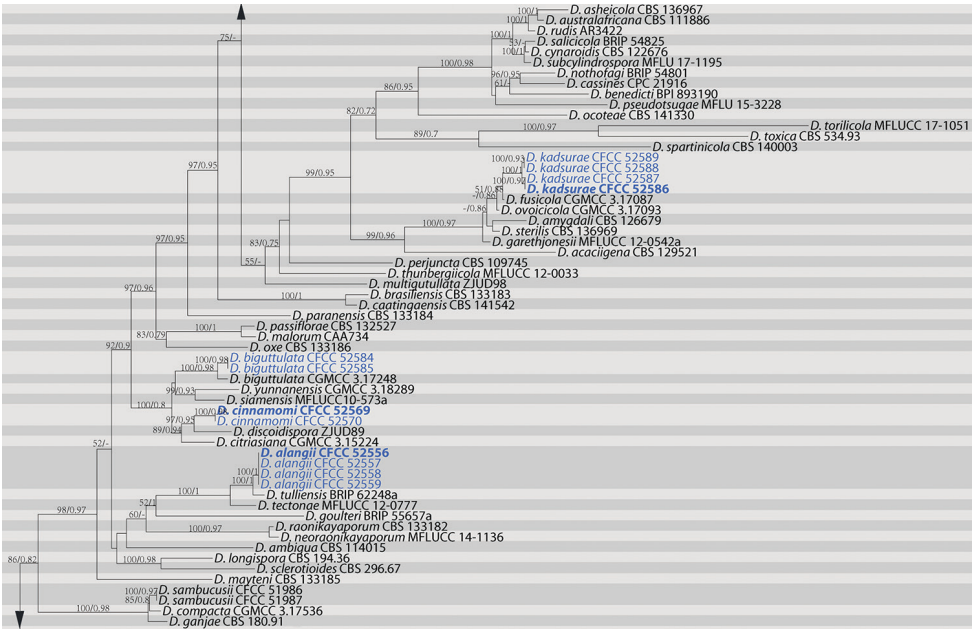

Figure 1. Continued.

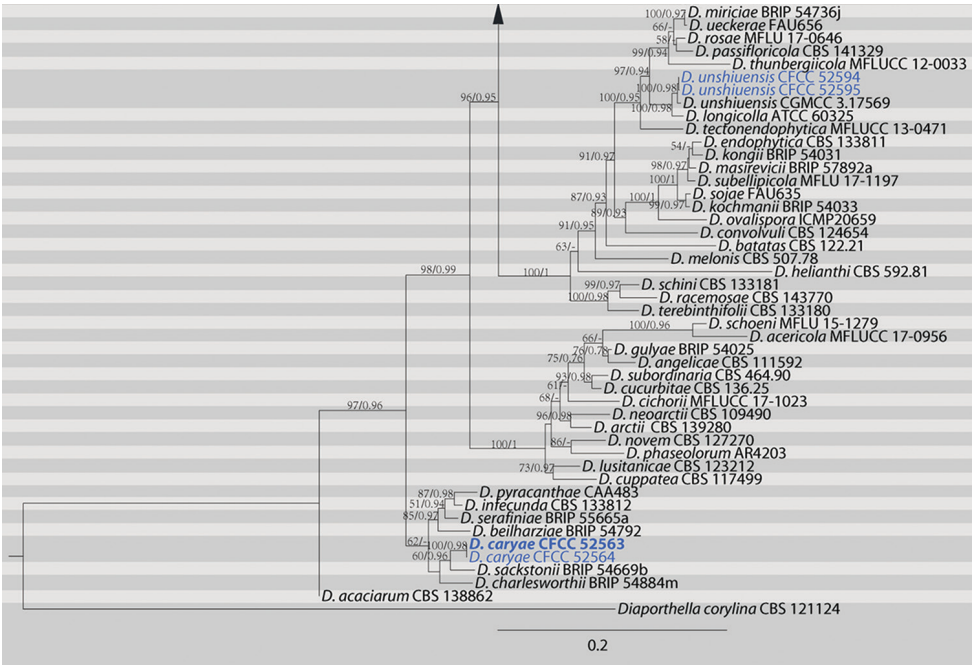

Figure 1. Continued.

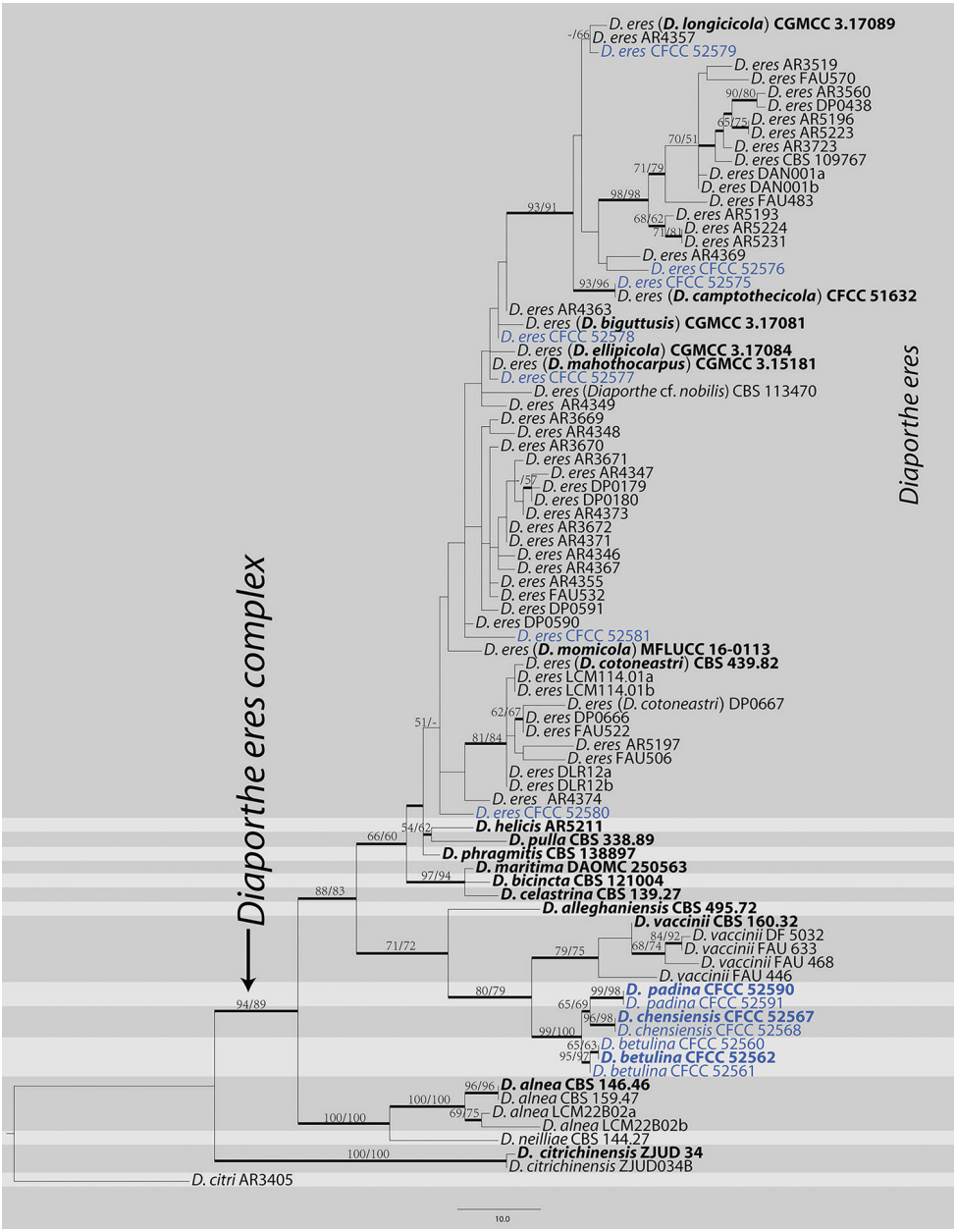

Figure 2. Phylogram of *Diaporthe eres* complex based on combined *cal*, *tef1* and *tub2*. Values above the branches indicate maximum parsimony bootstrap (left, MP BP ≥ 50%) and maximum likelihood bootstrap (right, ML BP ≥ 50%). Values below branches represent posterior probabilities (BI PP ≥ 0.70) from Bayesian inference. The tree is rooted with *Diaporthe citri*. Strains in the current study are in blue. The ex-type/ex-epitype culture is in bold.

Taxonomy

Diaporthe acerigena **C.M. Tian & Q. Yang, sp. nov.**
MycoBank: MB824703
Figure 3

Diagnosis. *Diaporthe acerigena* can be distinguished from the phylogenetically closely related species *D. oraccinii* in larger alpha conidia.

Holotype. CHINA. Shaanxi Province: Qinling Mountain, on symptomatic twigs of *Acer tataricum*, 27 June 2017, N. Jiang (holotype: BJFC-S1466; ex-type culture: CFCC 52554).

Etymology. Named after the host genus on which it was collected, *Acer*.

Description. On PDA: Conidiomata pycnidial, globose, solitary or aggregated, deeply embedded in the medium, erumpent, dark brown to black, 185–270 µm diam, whitish translucent to cream conidial drops exuding from the ostioles. Conidiophores 14.5–17 × 1.4–2.9 µm, cylindrical, hyaline, phiailidic, branched, straight to sinuous. Alpha conidia 7–10 × 2.1–2.9 µm (av. = 8.6 × 2.5 µm, n = 30), aseptate, hyaline, ellipsoidal, rounded at one end, slightly apex at the other end, usually with two-guttulate. Beta conidia not observed.

Culture characters. Cultures incubated on PDA at 25 °C in darkness. Colony at first white, becoming dark brown in the centre with age. Aerial mycelium white, dense, fluffy, with cream conidial drops exuding from the ostioles.

Additional specimens examined. CHINA. Shaanxi Province: Qinling Mountain, on symptomatic twigs of *Acer tataricum*, 27 June 2017, N. Jiang, living culture CFCC 52555 (BJFC-S1467).

Notes. Two strains representing *D. acerigena* cluster in a well-supported clade and appear most closely related to *D. oraccinii*. *Diaporthe acerigena* can be distinguished from *D. oraccinii* based on ITS, *his3*, *tef1* and *tub2* loci (5/469 in ITS, 8/429 in *his3*, 8/326 in *tef1* and 5/358 in *tub2*). Morphologically, *D. acerigena* differs from *D. oraccinii* in the longer and larger alpha conidia (8.6 × 2.5 vs. 6.6 × 1.9 µm) (Gao et al. 2016).

Diaporthe alangii **C.M. Tian & Q. Yang, sp. nov.**
MycoBank: MB824704
Figure 4

Diagnosis. *Diaporthe alangii* can be distinguished from the phylogenetically closely related species *D. tectonae* and *D. tulliensis* by the size of conidiophores and alpha conidia.

Holotype. CHINA. Zhejiang Province: Tianmu Mountain, on symptomatic branches of *Alangium kurzii*, 19 Apr. 2017, Q. Yang (holotype: BJFC-S1468; ex-type culture: CFCC 52556).

Etymology. Named after the host genus on which it was collected, *Alangium*.

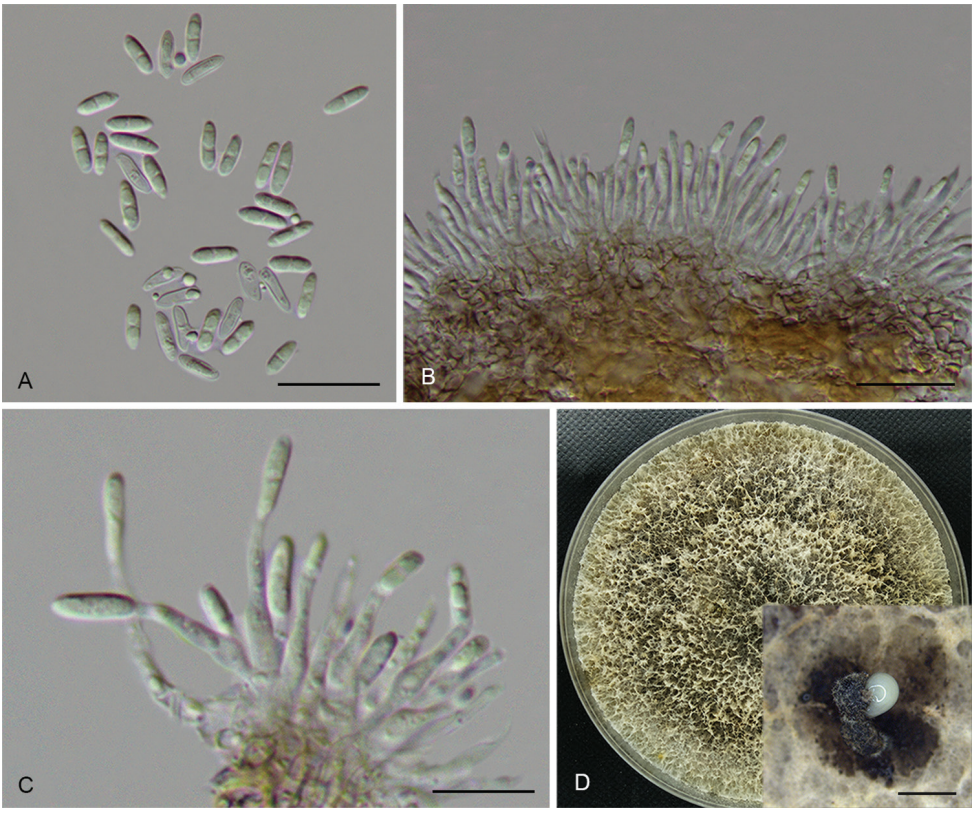

Figure 3. *Diaporthe acerigena* (CFCC 52554) **A** Alpha conidia **B–C** Conidiophores **D** Culture on PDA and conidiomata. Scale bars: 20 µm (**A–C**), 200 µm (**D**).

Description. Conidiomata pycnidial, immersed in bark, scattered, erumpent through the bark surface, discoid, with a solitary undivided locule. Ectostromatic disc black, one ostiole per disc, 135–330 µm diam. Locule circular, undivided, 290–445 µm diam. Conidiophores 6–12 × 1.4–2 µm, cylindrical, hyaline, phiailidic, unbranched, straight. Alpha conidia 6.5–8 × 2 µm (av. = 7 × 2 µm, n = 30), aseptate, hyaline, ellipsoidal, biguttulate, mostly with one end obtuse and the other acute, occasionally submedian constriction. Beta conidia not observed.

Culture characters. Cultures incubated on PDA at 25 °C in darkness. Colony initially white, producing beige pigment after 7–10 d. The colony is flat, felty with a thick texture at the centre and marginal area, with thin texture in the middle, lacking aerial mycelium, conidiomata absent.

Additional specimens examined. CHINA. Zhejiang Province: Tianmu Mountain, on symptomatic branches of *Alangium kurzii*, 19 Apr. 2017, Q. Yang, living culture CFCC 52557 (BJFC-S1469); ibid. living culture CFCC 52558 (BJFC-S1470); ibid. living culture CFCC 52559 (BJFC-S1471).

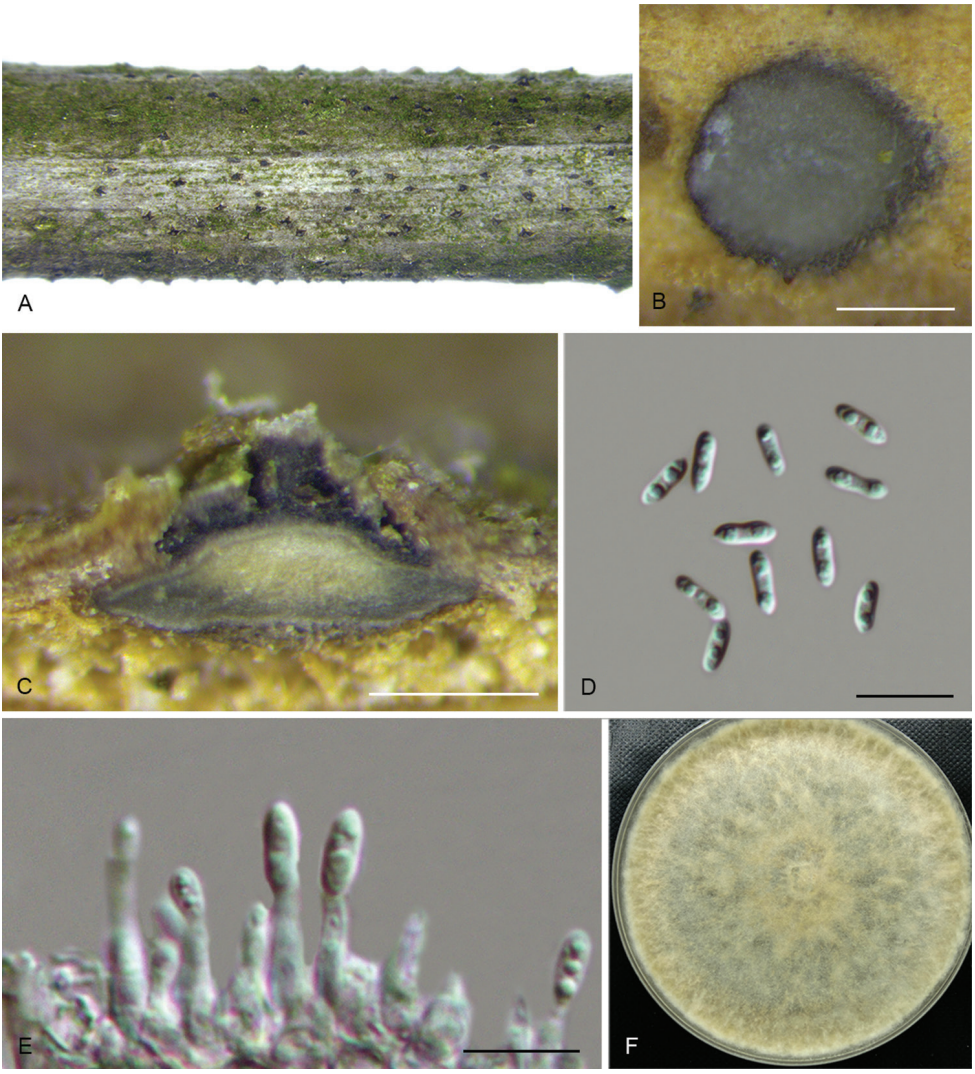

Figure 4. *Diaporthe alangii* (CFCC 52556) **A** Habit of conidiomata on branches **B** Transverse section of conidioma **C** Longitudinal section of conidioma **D** Alpha conidia **E** Conidiophores **F** Culture on PDA. Scale bars: 200 μm (**B–C**), 10 μm (**D–E**).

Notes. Four isolates clustered in a clade distinct from its closest phylogenetic neighbour, *D. tectonae* and *D. tulliensis. Diaporthe alangii* can be distinguished from *D. tectonae* in *cal*, *tef1* and *tub2* loci (6/458 in *cal*, 4/308 in *tef1* and 11/407 in *tub2*); from *D. tulliensis* in ITS, tef1 and tub2 loci (6/462 in ITS, 8/308 in *tef1* and 10/701 in *tub2*). Morphologically, *D. alangii* differs from *D. tectonae* in shorter conidiophores (6–12 vs. 11–18 μm) and longer alpha conidia (6.5–8 vs. 5.5–6 μm); from *D. tulliensis* in shorter conidiophores (6–12 vs. 15–20 μm) (Crous et al. 2015, Doilom et al. 2017).

Diaporthe betulina **C.M. Tian & Q. Yang, sp. nov.**
MycoBank: MB824705
Figure 5

Diagnosis. *Diaporthe betulina* can be distinguished from the phylogenetically closely related species *D. betulae* in smaller locule and wider alpha conidia.

Holotype. CHINA. Heilongjiang Province: Yichun city, on symptomatic branches of *Betula platyphylla*, 27 July 2016, Q. Yang (holotype: BJFC-S1472; ex-type culture: CFCC 52562).

Etymology. Named after the host genus on which it was collected, *Betula*.

Description. Conidiomata pycnidial, conical, immersed in bark, scattered, erumpent through the bark surface, with a solitary undivided locule. Ectostromatic disc brown to black, one ostiole per disc, 290–645 µm diam. Ostiole medium black, up to the level of disc. Locule undivided, 670–905 µm diam. Conidiophores 12.5–17.5 × 1.5–2 µm, cylindrical, hyaline, phiailidic, branched, straight or slightly curved. Alpha conidia hyaline, aseptate, ellipsoidal to fusiform, 0–2-guttulate, sometimes acute at both ends, 8–10 × 2.5–3 µm (av. = 9 × 2.6 µm, n = 30). Beta conidia hyaline, aseptate, filiform, straight or hamate, eguttulate, base subtruncate, tapering towards one apex, 26–32.5 × 1 µm (av. = 30 × 1 µm, n = 30).

Culture characters. Cultures incubated on PDA at 25 °C in darkness. Colony flat with white felty aerial mycelium, turning white to dark brown aerial mycelium, conidiomata irregularly distributed on the agar surface.

Additional specimens examined. CHINA. Heilongjiang Province: Yichun city, on symptomatic branches of *Betula albo-sinensis*, 27 July 2016, Q. Yang, living culture CFCC 52560 (BJFC-S1473); on symptomatic branches of *Betula costata*, 27 July 2016, Q. Yang, living culture CFCC 52561 (BJFC-S1474).

Notes. *Diaporthe betulina* was isolated from *Betula* spp. cankers in Heilongjiang Province. Three strains representing *D. betulina* cluster in a well-supported clade and appear most closely related to *D. betulae,* which was also isolated from *Betula platyphylla* in Sichuang Province (Du et al. 2016). *Diaporthe betulina* can be distinguished based o*n* ITS, *his3*, *tef1* and *tub2* loci from *D. betulae* (11/461 in ITS, 9/453 in *his3*, 12/336 in *tef1* and 7/695 in *tub2*). Morphologically, *D. betulina* differs from *D. betulae* in smaller locule (470–945 vs. 600–1250 µm) and wider alpha conidia (3–4 vs. 2.5–3 µm) (Du et al. 2016).

Diaporthe biguttulata **F. Huang, K.D. Hyde & H.Y. Li, 2015**
Figure 6

Description. Conidiomata pycnidial, immersed in bark, scattered, erumpent through the bark surface, discoid, with a single locule. Ectostromatic disc dark brown, one ostiole per disc, 160–320 µm diam. Locule undivided, 235–350 µm diam. Conidiophores 8.5–11 × 1.5 µm, cylindrical, hyaline, branched, straight or slightly curved, tapering

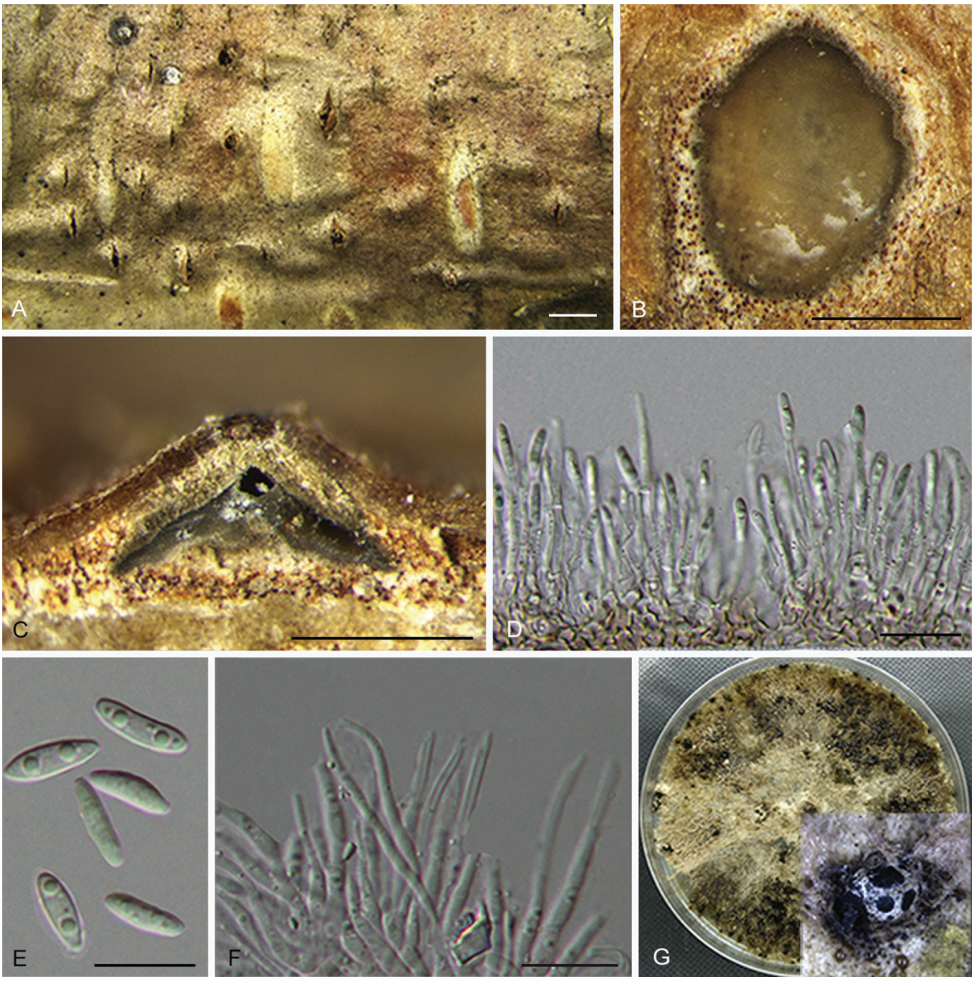

Figure 5. *Diaporthe betulina* (CFCC 52562) **A** Habit of conidiomata on branches **B** Transverse section of conidioma **C** Longitudinal section of conidioma **D** Conidiophores **E** Alpha conidia **F** Beta conidia **G** Culture on PDA and conidiomata. Scale bars: 500 µm (**A–C**), 10 µm (**D–F**).

towards the apex. Alpha conidia hyaline, aseptate, ellipsoidal to oval, 2-guttulate, usually rounded at both ends, occasionally with one end acute, 7–8.5 × 1.5–2 µm (av. = 6.5 × 2.6 µm, n = 30). Beta conidia not observed.

Culture characters. Cultures incubated on PDA at 25 °C in darkness. Colony originally flat with white aerial mycelium, becoming pale grey, with dense aerial mycelium in the centre and sparse aerial mycelium at the marginal area, conidiomata absent.

Specimens examined. CHINA. Zhejiang Province: Tianmu Mountain, on symptomatic branches of *Juglans regia*, 20 Apr. 2017, Q. Yang, living culture CFCC 52584 and CFCC 52585 (BJFC-S1504).

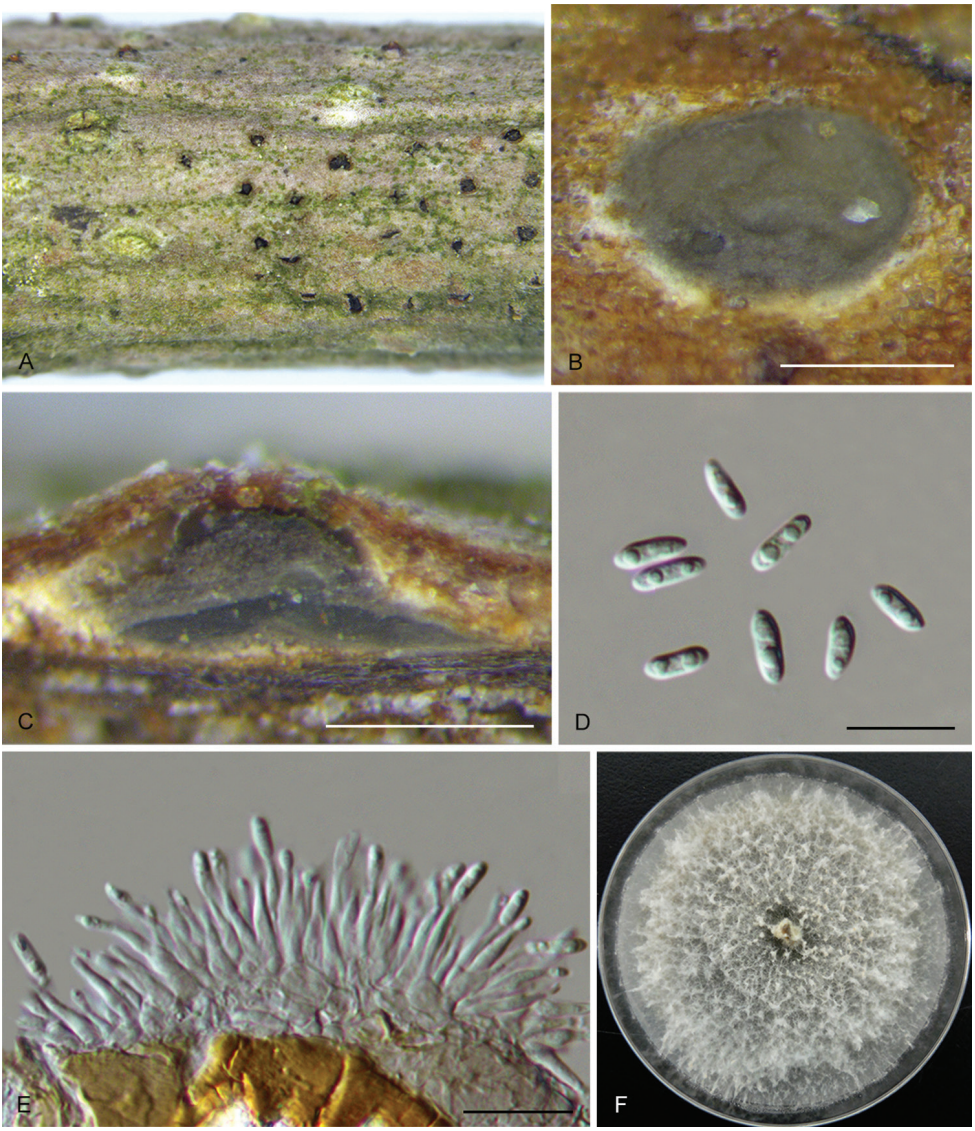

Figure 6. *Diaporthe biguttulata* (CFCC 52584) **A** Habit of conidiomata on branches **B** Transverse section of conidioma **C** Longitudinal section of conidioma **D** Alpha conidia **E** Conidiophores **F** Culture on PDA. Scale bars: 200 μm (**B–C**), 10 μm (**D–E**).

Notes. *Diaporthe biguttulata* was originally described from a healthy branch of *Citrus limon* in Yunnan Province, China (Huang et al. 2015). In the present study, two isolates (CFCC 52584 and CFCC 52585) from symptomatic branches of *Juglans regia* were congruent with *D. biguttulata* based on morphology and DNA sequences data (Fig. 1). We therefore describe *D. biguttulata* as a known species for this clade.

Diaporthe caryae **C.M. Tian & Q. Yang, sp. nov.**
MycoBank: MB824706
Figure 7

Diagnosis. *Diaporthe caryae* differs from its closest phylogenetic neighbour, *D. charlesworthii* and *D. sackstonii*, in ITS, *tef1* and *tub2* loci based on the alignments deposited in TreeBASE.

Holotype. CHINA. Jiangsu Province: Nanjing city, on symptomatic twigs of *Carya illinoensis*, 10 Nov. 2015, Q. Yang (holotype: BJFC-S1476; ex-type culture: CFCC 52563).

Etymology. Named after the host genus on which it was collected, *Carya*.

Description. Conidiomata pycnidial, immersed in bark, scattered, slightly erumpent through the bark surface, nearly flat, discoid, with a solitary undivided locule. Ectostromatic disc brown to black, one ostiole per disc. Locule undivided, 310–325 µm diam. Conidiophores 7–11 × 1.4–2.2 µm, cylindrical, phialidic, unbranched, sometimes inflated. Alpha conidia hyaline, aseptate, ellipsoidal or fusiform, eguttulate, obtuse at both ends, 7–8.5 × 2.1–2.5 µm (av. = 8 × 2.3 µm, n = 30). Beta conidia hyaline, aseptate, filiform, straight or hamate, eguttulate, base subtruncate, tapering towards one apex, 15.5–34 × 1.1–1.4 µm (av. = 27.5 × 1.2 µm, n = 30).

Culture characters. Cultures incubated on PDA at 25 °C in darkness. Colony at first flat with white felty mycelium, becoming black in the centre and black at the marginal area with age, conidiomata not observed.

Additional specimens examined. CHINA. Jiangsu Province: Nanjing city, on symptomatic twigs of *Carya illinoensis*, 10 Nov. 2015, Q. Yang, living culture CFCC 52564 (BJFC-S1477).

Notes. Two strains representing *D. caryae* cluster in a well-supported clade and appear closely related to *D. charlesworthii* and *D. sackstonii. Diaporthe caryae* can be distinguished based o*n* ITS, *tef1* and *tub2* loci from *D. charlesworthii* (50/468 in ITS, 107/338 in *tef1* and 90/707 in *tub2*); from *D. sackstonii* (4/440 in ITS, 13/340 in *tef1* and 23/701 in *tub2*). Morphologically, *D. caryae* can be distinguished from *D. charlesworthii* by its shorter conidiophores (7–11 vs. 15–35 µm); from *D. sackstonii* by its longer alpha conidia (7–8.5 vs. 6–7 µm) (Thompson et al. 2015).

Diaporthe cercidis **C.M. Tian & Q. Yang, sp. nov.**
MycoBank: MB824707
Figure 8

Diagnosis. *Diaporthe cercidis* can be distinguished from the phylogenetically closely related species *D. pescicola* in larger alpha conidia.

Holotype. CHINA. Jiangsu Province: Nanjing city, on twigs and branches of *Cercis chinensis*, 11 Nov. 2015, Q. Yang (holotype: BJFC-S1478; ex-type culture: CFCC 52565).

Etymology. Named after the host genus on which it was collected, *Cercis*.

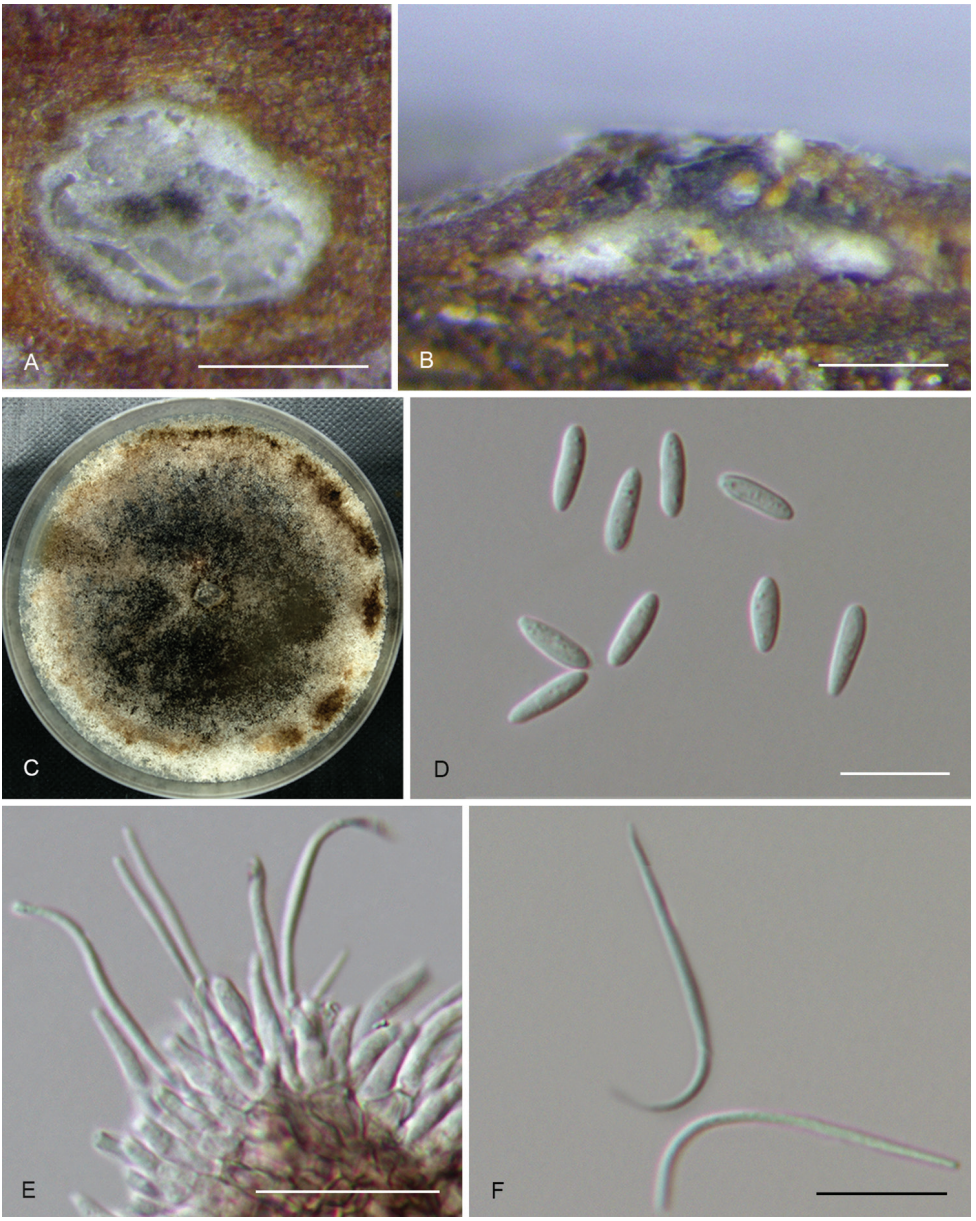

Figure 7. *Diaporthe caryae* (CFCC 52563) **A** Transverse section of conidioma **B** Longitudinal section of conidioma **C** Culture on PDA **D** Alpha conidia **E** Conidiophores **F** Beta conidia. Scale bars: 200 µm (**A**), 100 µm (**B**), 10 µm (**D, F**), 20 µm (**E**).

Description. Conidiomata pycnidial, immersed in bark, scattered, slightly erumpent through the bark surface, nearly flat, discoid, with a solitary undivided locule. Ectostromatic disc grey to brown, one ostiole per disc. Locule circular, undivided, 135–200 µm diam. Conidiophores 7–17 × 1.4–2.1 µm, phialidic, unbranched, straight or slightly curved, tapering towards the apex. Alpha conidia hyaline, aseptate, fusiform to oval, bi-

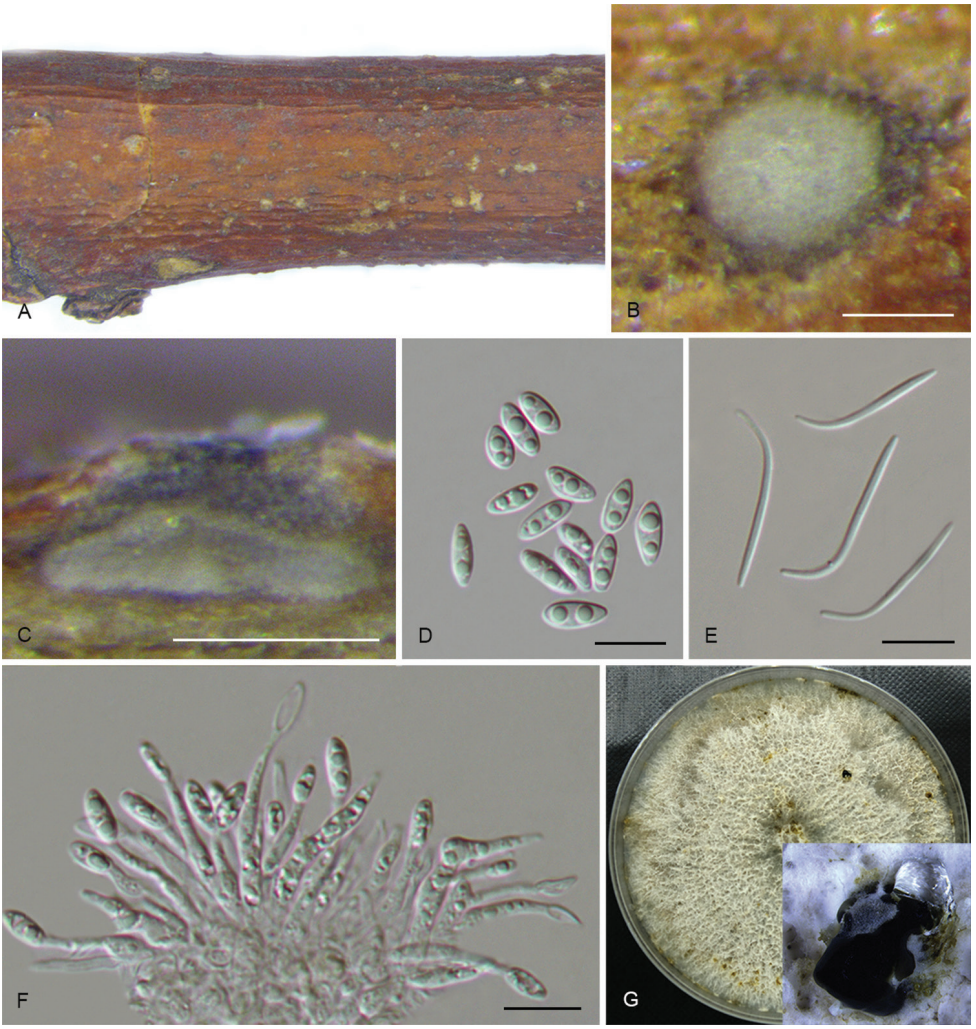

Figure 8. *Diaporthe cercidis* (CFCC 52565) **A** Habit of conidiomata on branches **B** Transverse section of conidioma **C** Longitudinal section of conidioma **D** Alpha conidia **E** Beta conidia **F** Conidiophores **G** Culture on PDA and conidiomata. Scale bars: 100 µm (**B–C**), 10 µm (**D–F**).

guttulate, 6.5–10 × 3–3.5 µm (av. = 8.6 × 3.3 µm, n = 30). Beta conidia hyaline, aseptate, filiform, straight or hamate, eguttulate, 20–28.5 × 1–1.3 µm (av. = 25.5 × 1.2 µm, n = 30).

Culture characters. Cultures incubated on PDA at 25 °C in darkness showed colony at first white, becoming pale brown with yellowish dots with age, flat, with dense and felted mycelium, with visible solitary or aggregated conidiomata at maturity.

Additional specimens examined. CHINA. Jiangsu Province: Yangzhou city, on twigs and branches of *Ginkgo biloba*, 11 Nov. 2015, N. Jiang, living culture CFCC 52566 (BJFC-S1479).

Notes. *Diaporthe cercidis* is distinguished from *D. pescicola* in the ITS, *cal* and *tef1* loci (13/458 in ITS, 47/442 in *cal* and 6/328 in *tef1*). Morphologically, *D. cercidis* dif-

fers from *D. pescicola* in shorter conidiophores (7–17 vs. 21–35 µm) and larger alpha conidia (6.5–10 × 3–3.5 vs. 6–8.5 × 2–3 µm) (Dissanayake et al. 2017a).

***Diaporthe chensiensis* C.M. Tian & Q. Yang, sp. nov.**
MycoBank: MB824708
Figure 9

Diagnosis. *Diaporthe chensiensis* differs from its closest phylogenetic neighbour, *D. vaccinii*, in ITS, *cal*, *his3* and *tef1* loci based on the alignments deposited in TreeBASE.

Holotype. CHINA. Shaanxi Province: Ningshan County, Huoditang forest farm, on symptomatic twigs of *Abies chensiensis*, 5 July 2017, Q. Yang (holotype: BJFC-S1480; ex-type culture: CFCC 52567).

Etymology. Named after the host species on which it was collected, *chensiensis*.

Description. Conidiomata pycnidial, immersed in bark, scattered, slightly erumpent through the bark surface, discoid, with a single locule. Ectostromatic disc white to brown, one ostiole per disc, 200–325 µm diam. Locule undivided, 385–540 µm diam. Conidiophores 8.5–13 × 2–3 µm, cylindrical, hyaline, phiailidic, unbranched, straight or slightly curved, tapering towards the apex. Alpha conidia hyaline, aseptate, smooth, ellipsoidal, biguttulate, rounded at both ends, 6.5–11 × 2–2.2 µm (av. = 8.5 × 2.1 µm, n = 30). Beta conidia present on the host, hyaline, eguttulate, smooth, filiform, hamate, 21–28.5 × 0.8–1.1 µm (av. = 25 × 1 µm, n = 30).

Culture characters. Cultures incubated on PDA at 25 °C in darkness. Colony originally flat with white felted aerial mycelium, becoming light brown mycelium due to pigment formation, conidiomata irregularly distributed over agar surface, with yellowish conidial drops exuding from the ostioles.

Additional specimens examined. CHINA. Shaanxi Province: Ningshan County, Huoditang forest farm, on symptomatic twigs of *Abies chensiensis*, 5 July 2017, Q. Yang, living culture CFCC 52568 (BJFC-S1481).

Notes. *Diaporthe chensiensis* occurs in an independent clade (Fig. 1) and is phylogenetically distinct from *D. vaccinii*. *Diaporhe chensiensis* can be distinguished from *D. vaccinii* by 57 nucleotides in concatenated alignment, in which 14 were distinct in the ITS region, 13 in the *cal* region, 10 in the *his3* region, 15 in the *tef1* region and 15 in the *tub2* region. Although this species belongs to the *D. eres* complex, it is, however, distinct from the known species within the complex (Fig. 2).

***Diaporthe cinnamomi* C.M. Tian & Q. Yang, sp. nov.**
MycoBank: MB824709
Figure 10

Diagnosis. *Diaporthe cinnamomi* differs from its closest phylogenetic species *D. discoidispora* in ITS, *his3* and *tef1* loci based on the alignments deposited in TreeBASE.

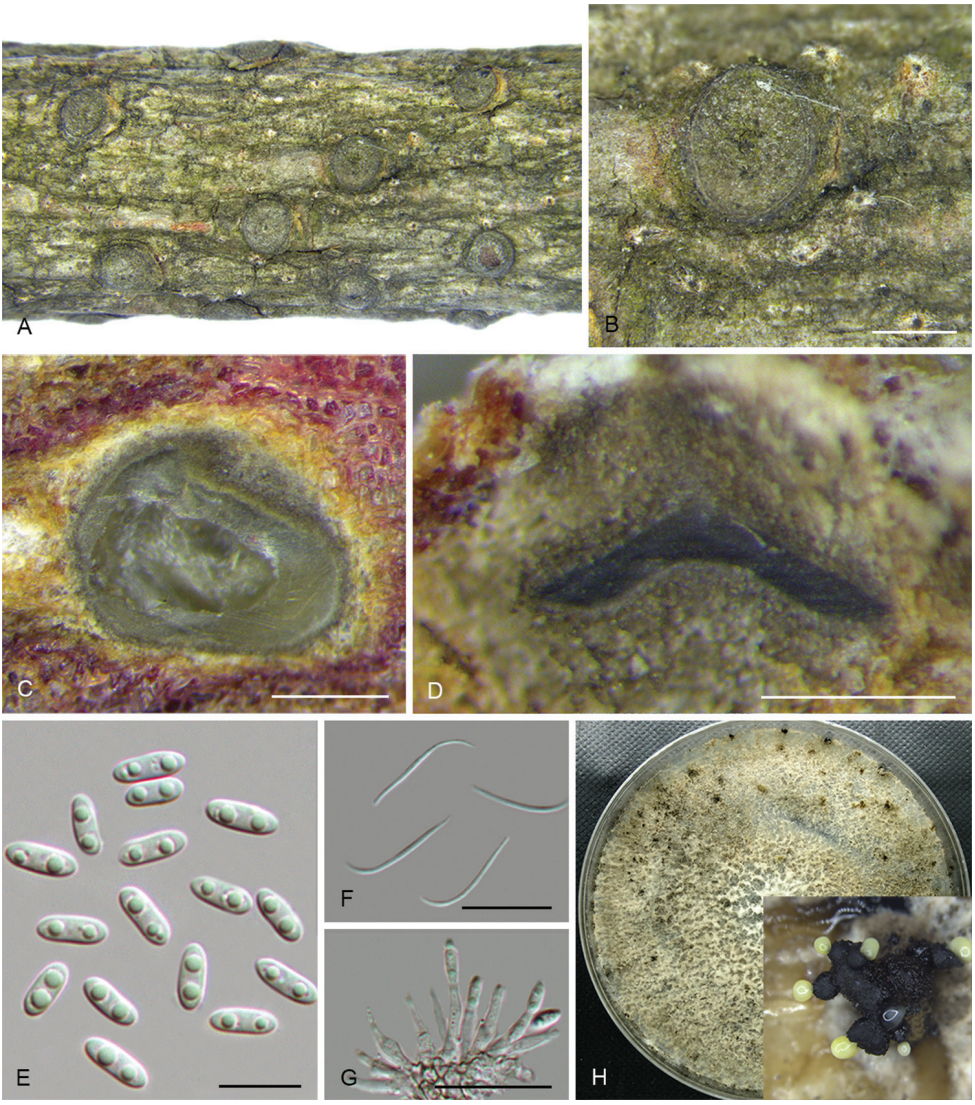

Figure 9. *Diaporthe chensiensis* (CFCC 52567) **A–B** Habit of conidiomata on branches **C** Transverse section of conidioma **D** Longitudinal section of conidioma **E** Alpha conidia **F** Beta conidia **G** Conidiophores **H** Culture on PDA and conidiomata. Scale bars: 500 μm (**B**), 200 μm (**C–D**), 10 μm (**E**), 20 μm (**F**).

Holotype. CHINA. Zhejiang Province: Linan city, on symptomatic twigs of *Cinnamomum* sp., 22 Apr. 2017, Q. Yang (holotype: BJFC-S1482; ex-type culture: CFCC 52569).

Etymology. Named after the host genus on which it was collected, *Cinnamomum*.

Description. On PDA: Conidiomata pycnidial, globose, solitary or aggregated, deeply embedded in the substrate, erumpent, dark brown to black, 170–235 μm diam., whitish translucent to cream conidial drops exuding from the ostioles. Conidiophores

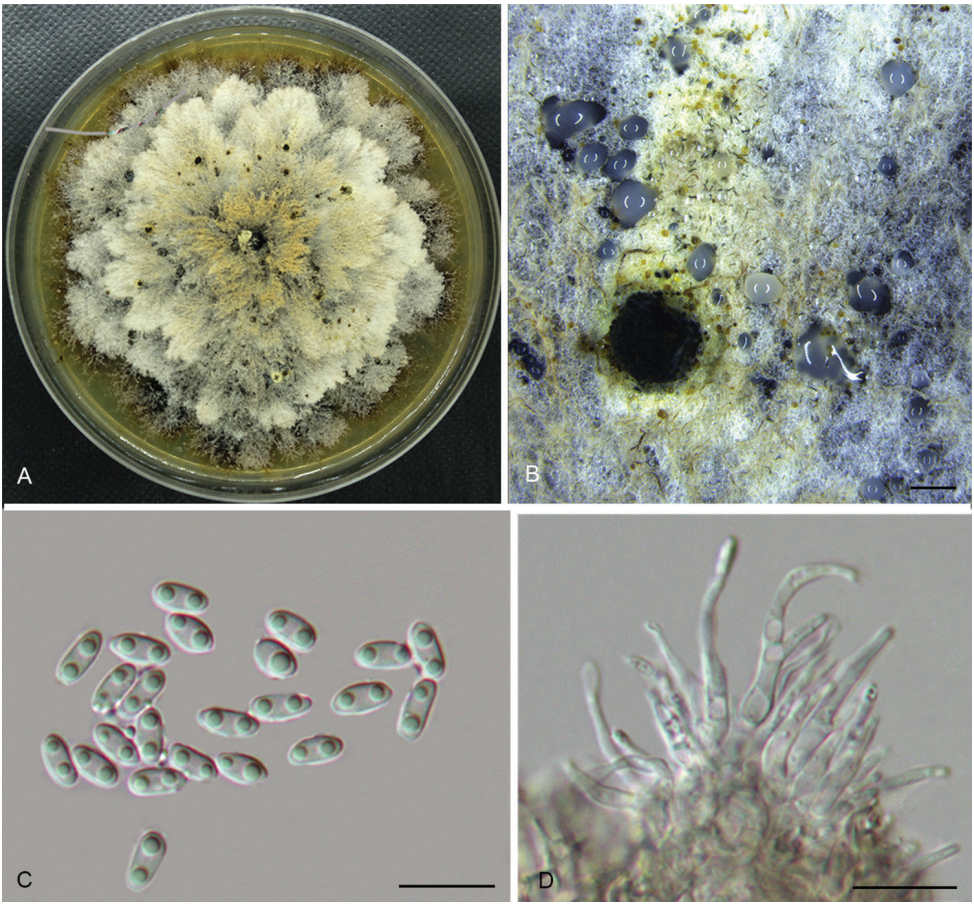

Figure 10. *Diaporthe cinnamomi* (CFCC 52569) **A** Culture on PDA **B** Conidiomata **C** Alpha conidia **D** Conidiophores. Scale bars: 200 µm (**B**), 10 µm (**C–D**).

11–25 × 1.5–2 µm, cylindrical, hyaline, branched, straight or curved, tapering towards the apex. Alpha conidia hyaline, aseptate, ellipsoidal to oval, biguttulate, rounded at both ends, 5–7 × 2.5–3 µm (av. = 6 × 2.9 µm, n = 30). Beta conidia not observed.

Culture characters. Cultures incubated on PDA at 25 °C in darkness showed colony originally flat with white felty mycelium, developing petaloid mycelium after 7–10 d and turning yellowish at the centre and brownish at the marginal area after 15 d. Conidiomata erumpent at maturity.

Additional material examined. CHINA. Zhejiang Province: Linan city, on symptomatic twigs of *Cinnamomum* sp., 22 Apr. 2017, Q. Yang, living culture CFCC 52570 (BJFC-S1483).

Notes. *Diaporthe cinnamomi* comprises strains CFCC 52569 and CFCC 52570 closely related to *D. discoidispora* in the combined phylogenetic tree (Fig. 1). *Diaporthe cinnamomi* can be distinguished based on ITS, *his3* and *tef1* loci from *D. discoidispora* (4/460 in ITS, 17/448 in *his3* and 38/339 in *tef1*).

Diaporthe conica **C.M. Tian & Q. Yang, sp. nov.**
MycoBank: MB824710
Figure 11

Diagnosis. *Diaporthe conica* is phylogenetically and morphologically distinct from *D. rostrata*, in smaller locule and alpha conidia.

Holotype. CHINA. Zhejiang Province: Tianmu Mountain, on symptomatic branches of *Alangium chinense*, 20 Apr. 2017, Q. Yang (holotype: BJFC-S1484; ex-type culture: CFCC 52571).

Etymology. Named after the conical conidiomata.

Description. Conidiomata pycnidial, 420–580 µm diam., solitary and with single necks erumpent through the host bark. Tissue around the neck is conical. Locule oval, undivided, 385–435 µm diam. Conidiophores reduced to conidiogenous cells. Conidiogenous cells unbranched, straight or sinuous, apical or base sometimes swelling, 19–23.5 × 2.8 µm. Alpha conidia hyaline, aseptate, ellipsoidal, biguttulate, 5.5–7 × 2.3–3 µm (av. = 6.5 × 2.6 µm, n = 30). Beta conidia not observed.

Culture characters. Cultures incubated on PDA at 25 °C in darkness. Colony white to yellowish, with dense and felted mycelium, lacking aerial mycelium, with maize-coloured conidial drops exuding from the ostioles.

Additional material examined. CHINA. Zhejiang Province: Tianmu Mountain, on symptomatic branches of *Alangium chinense*, 20 Apr. 2017, Q. Yang, living culture CFCC 52572 (BJFC-S1485); ibid. living culture CFCC 52573 (BJFC-S1486); ibid. living culture CFCC 52574 (BJFC-S1487).

Notes. Four isolates clustered in a clade distinct from further *Diaporthe* species based on DNA sequence data. Morphologically, this species is characterised by conical conidiomata, which is similar with *D. rostrata* from *Juglans mandshurica*. However, *D. conica* differs from *D. rostrata* by having smaller locule and alpha conidia (310–385 vs. 620–1100 µm in locule; 5.5–7 × 2.3–3 vs. 8.5–11.5 × 4–5 µm in alpha conidia) (Fan et al. 2015).

Diaporthe eres **Nitschke, 1870**
Figure 12

= *Diaporthe biguttusis* Y.H. Gao & L. Cai, 2015.
= *Diaporthe camptothecicola* C.M. Tian & Qin Yang, 2017.
= *Diaporthe ellipicola* Y.H. Gao & L. Cai, 2015.
= *Diaporthe longicicola* Y.H. Gao & L. Cai, 2015
= *Diaporthe mahothocarpus* (Y.H. Gao, W. Sun & L. Cai) Y.H. Gao & L. Cai, 2015.
= *Diaporthe momicola* Dissan., J.Y. Yan, Xing H. Li & K.D. Hyde, 2017.

Description. Conidiomata pycnidial, immersed in bark, erumpent through the bark surface, serried, with a single locule. Ectostromatic disc obviously, brown to black,

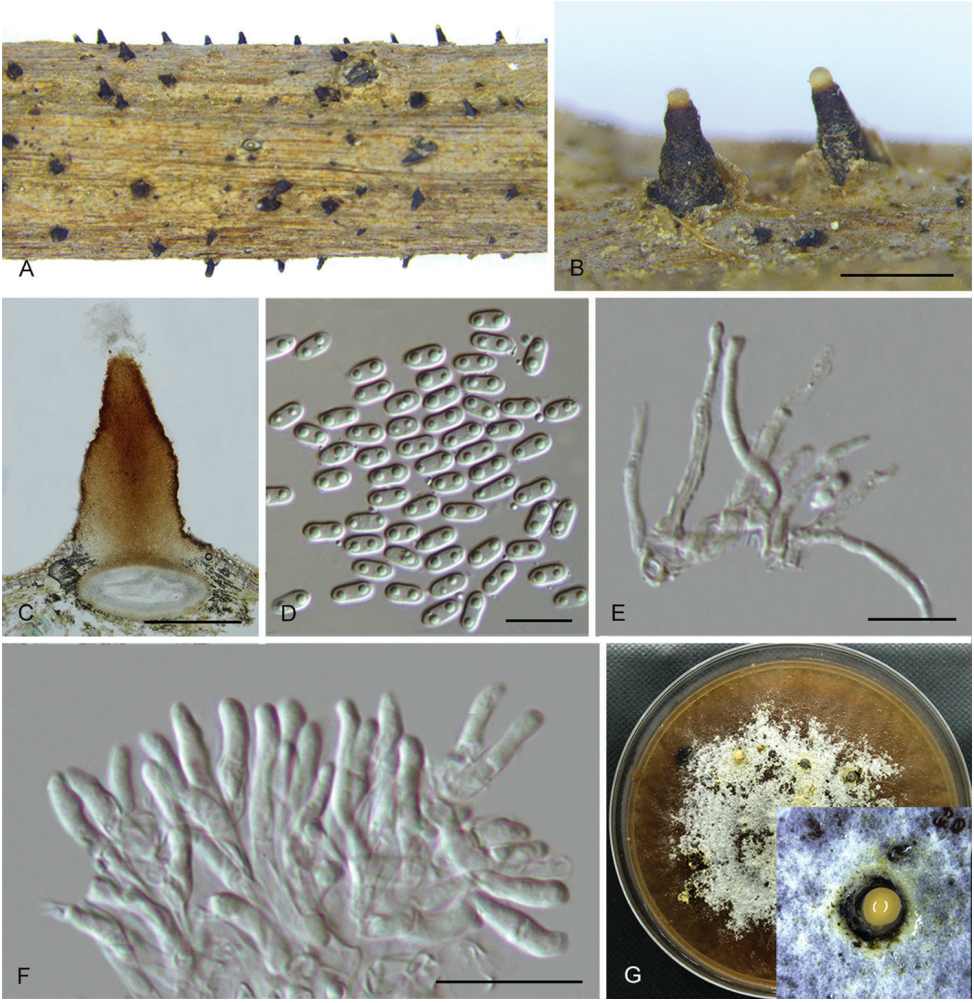

Figure 11. *Diaporthe conica* (CFCC 52571) **A–B** Habit of conidiomata on branches **C** Longitudinal section of conidioma **D** Alpha conidia **E–F** Conidiophores **G** Culture on PDA and conidiomata. Scale bars: 300 µm (**B–C**), 10 µm (**D–F**).

with one ostiole per disc, 245–572 µm diam. Ostiole medium black, up to the level of disc. Locule circular, undivided, 335–450 µm diam. Conidiophores 10.5–19 × 1–1.5 µm, cylindrical, hyaline, unbranched, straight or slightly sinuous. Conidiogenous cells phialidic, cylindrical, terminal. Alpha conidia hyaline, aseptate, ellipsoidal to lanceolate, one guttulate at each end, 6–7.5 × 1.5–2.5 µm (av. = 6.5 × 2 µm, n = 30). Beta conidia not observed.

Culture characters. Cultures on PDA incubated at 25 °C in darkness. Colony with white felty aerial mycelium, becoming white felted aerial mycelium in the centre and grey-brown mycelium at the marginal area, conidiomata irregularly distributed over agar surface.

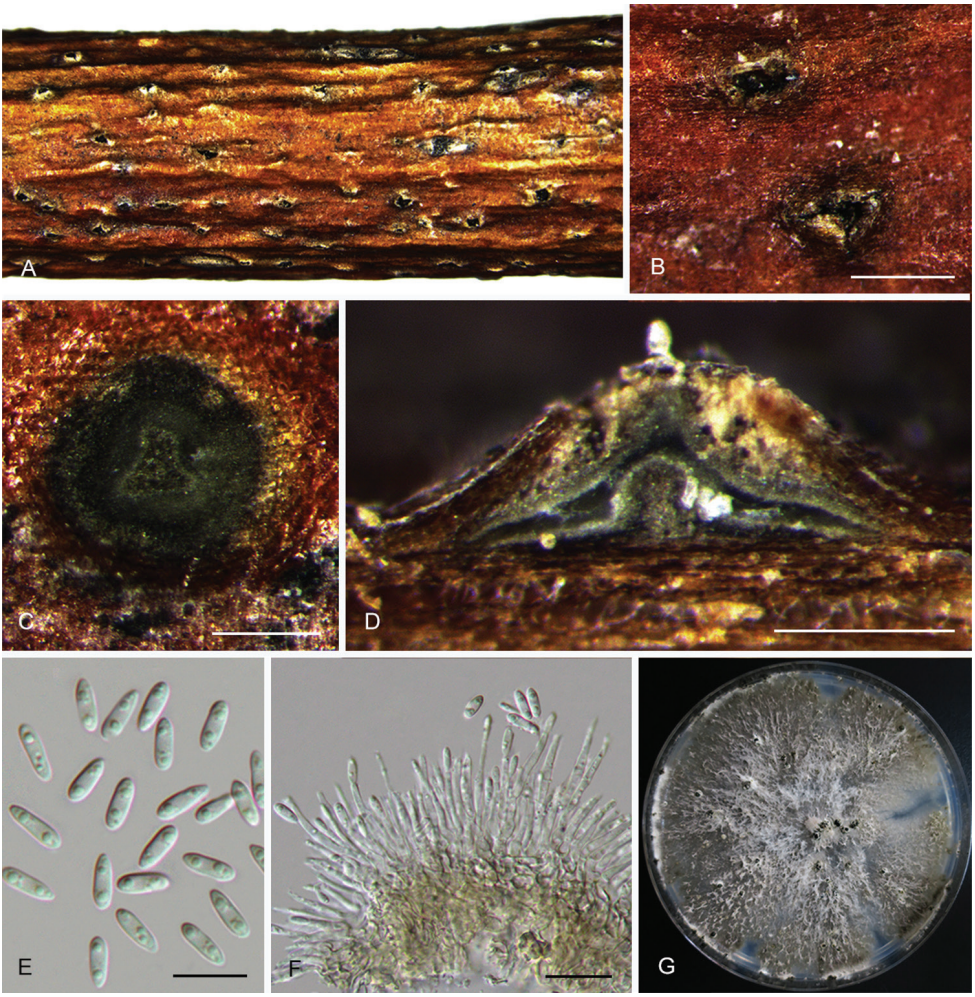

Figure 12. *Diaporthe eres* (CFCC 52575) **A–B** Habit of conidiomata on branches **C** Transverse section of conidioma **D** Longitudinal section of conidioma **E** Alpha conidia **F** Conidiophores **G** Culture on PDA and conidiomata. Scale bars: 500 µm (**B**), 200 µm (**C–D**), 10 µm (**E–F**).

Specimens examined. CHINA. Beijing: Pinggu district, on symptomatic branches of *Castanea mollissima*, 1 Nov. 2016, N. Jiang, living culture CFCC 52576 (BJFC-S1489); ibid. living culture CFCC 52577 (BJFC-S1490). Heilongjiang Province: Liangshui Nature Reserve, on symptomatic twigs of *Acanthopanax senticosus*, 29 July 2016, Q. Yang, living culture CFCC 52580 (BJFC-S1493). Heilongjiang Province: Harbin city, Botanical garden, on symptomatic twigs of *Sorbus* sp., 2 Aug. 2016, Q. Yang, living culture CFCC 52575 (BJFC-S1488). Shaanxi Province: Zhashui County, on symptomatic branches of *Juglans regia*, 29 July 2016, Q. Yang, living culture CFCC 52579 (BJFC-S1492). Zhejiang Province: Yangzhou city, on symptomatic twigs of

Melia azedarace, 8 July 2017, N. Jiang, living culture CFCC 52578 (BJFC-S1491). Zhejiang Province: Tianmu Mountain, on symptomatic twigs of *Rhododendron simsii*, 20 Apr. 2017, Q. Yang, living culture CFCC 52581 (BJFC-S1494).

Notes. *Diaporthe eres*, the type species of the genus, was described by Nitschke (1870) on *Ulmus* sp. collected in Germany, which has a widespread distribution and a broad host range as a pathogen, endophyte or saprobe causing leaf spots, stem cankers and diseases of woody plants (Udayanga et al. 2014b). Fan et al. (2018) indicated that *D. biguttusis*, *D. ellipicola*, *D. longicicola* and *D. mahothocarpus* should be treated as synonyms of *D. eres* using *cal*, *tef1* and *tub2* gene regions. In this study, we extended the work presented in Fan et al. (2018) and found seven additional strains belonging to *D. eres*. Additionally, the phylogenetic tree demonstrated that *D. camptothecicola* and *D. momicola* should also be treated as synonyms of *D. eres* (Fig. 2). *Diaporthe camptothecicola* from *Camptotheca acuminate* and *D. momicola* from *Prunus persica* are described and illustrated based on the combined ITS, *cal*, *his3*, *tef1* and *tub2* regions (Dissanayake et al. 2017a, Yang et al. 2017c). Both of the two species are embedded in the *D. eres* complex. However, ITS analysis resulted in an unresolved phylogenetic tree without definitive bootstrap at the internodes, highly discordant to the trees resulting from the other four genes (Udayanga et al. 2014b). Therefore, the ITS region was not used in the combined analysis in the current study. To further investigate this complex, a second set of four (*cal*, *his3*, *tef1* and *tub2*), three (*cal*, *tef1* and *tub2*), two (*tef1* and *tub2*) and one (*tef1*) data matrices were performed following Santos et al. (2017) and Fan et al. (2018). The results showed that the three genes analyses (*cal*, *tef1* and *tub2*) appeared to be a better species recognition (Fig. 2). When it comes to this species complex, sequences supported by Udayanga et al. (2014b) are necessary to perform a more robust phylogenetic tree, clarifying the real species boundaries in this group in the future work.

Diaporthe fraxinicola **C.M. Tian & Q. Yang, sp. nov.**
MycoBank: MB824711
Figure 13

Diagnosis. *Diaporthe fraxinicola* can be distinguished from the closely related species *D. oraccinii* and *D. acerigena* (described above) based on ITS, *tef1* and *tub2* loci. *Diaporthe fraxinicola* differs from *D. oraccinii* in larger alpha conidia and from *D. acerigena* in wider alpha conidia.

Holotype. CHINA. Shaanxi Province: Zhashui city, Niubeiliang Reserve, on symptomatic twigs of *Fraxinus chinensis*, 7 July 2017, Q. Yang (holotype: BJFC-S1495; ex-type culture: CFCC 52582).

Etymology. Named after the host genus on which it was collected, *Fraxinus*.

Description. Conidiomata pycnidial, immersed in bark, scattered, slightly erumpent through the bark surface, nearly flat, discoid, with a single locule. Ectostromatic disc grey to dark brown, circular to ovoid, one ostiole per disc, 150–325

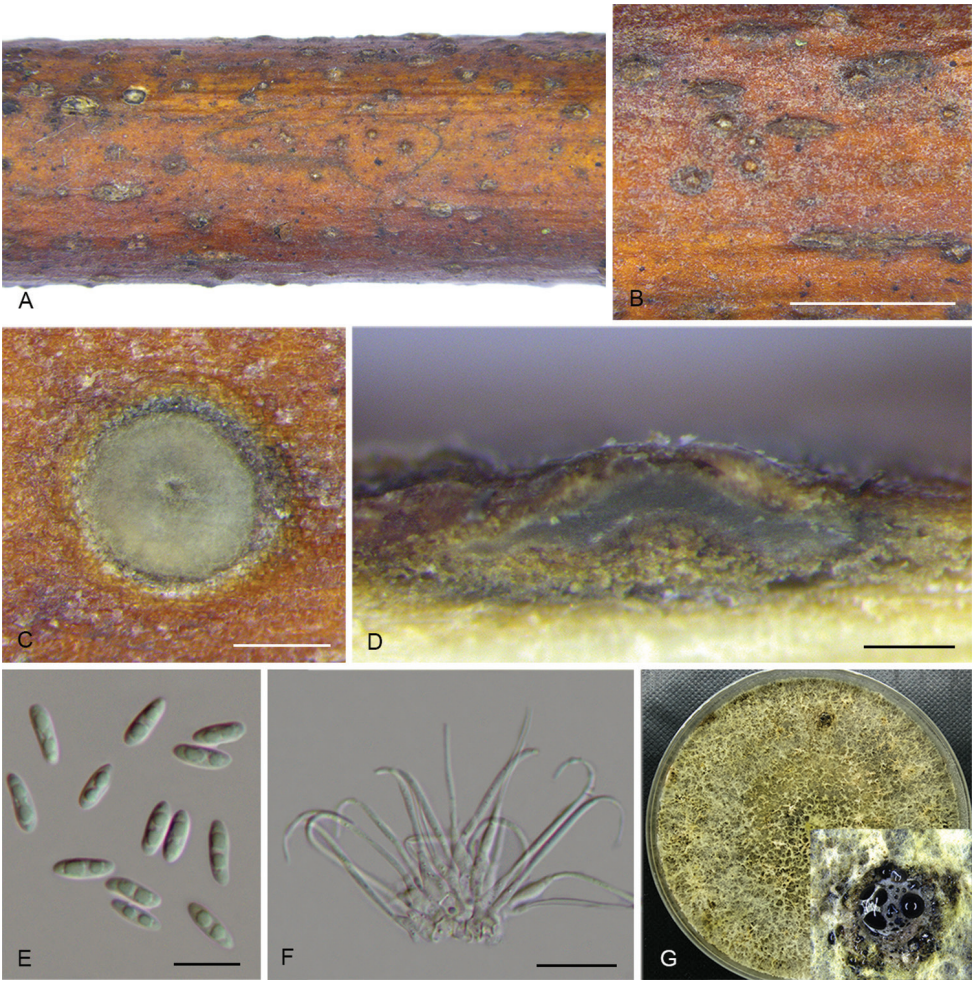

Figure 13. *Diaporthe fraxinicola* (CFCC 52582) **A–B** Habit of conidiomata on branches **C** Transverse section of conidioma **D** Longitudinal section of conidioma **E** Alpha conidia **F** Beta conidia **G** Culture on PDA and conidiomata. Scale bars: 500 µm (**B**), 200 µm (**C**), 100 µm (**D**), 10 µm (**E–F**).

µm diam. Locule circular, undivided, 275–480 µm diam. Conidiophores 10.5–17.5 × 2.1–3.2 µm, hyaline, branched, cylindrical to clavate, straight, tapering towards the apex. Alpha conidia hyaline, aseptate, ellipsoidal to oval, 2–3-guttulate, rounded at both ends, 7–10 × 2.9–3.2 µm (av. = 8.5 × 3 µm, n = 30). Beta conidia hyaline, filiform, straight or hamate, eguttulate, aseptate, base subtruncate, tapering towards one apex, 19–29.5 × 1.4 µm (av. = 24.5 × 1.4 µm, n = 30).

Culture characters. Cultures incubated on PDA at 25 °C in darkness. Colony originally flat with white aerial mycelium, becoming yellowish, dense and felted aerial mycelium with age, with visible solitary or aggregated conidiomata at maturity.

Additional material examined. CHINA. Shaanxi Province: Zhashui city, Niubeiliang Reserve, on symptomatic twigs of *Fraxinus chinensis*, 7 July 2017, Q. Yang, living culture CFCC 52583 (BJFC-S1496).

Notes. This new species is introduced as molecular data, shows it to be a distinct clade with high support (ML/BI=100/1) and it appears most closely related to *D. oraccinii* and *D. acerigena*. *Diaporthe fraxinicola* can be distinguished from *D. oraccinii* by 22 nucleotides in concatenated alignment, in which 6 were distinct in the ITS region, 8 in the *tef1* region and 8 in the *tub2* region; from *D. acerigena* by 27 nucleotides in concatenated alignment, in which 11 were distinct in the ITS region, 3 in the *tef1* region and 13 in the *tub2* region. Morphologically, *D. fraxinicola* differs from *D. oraccinii* in longer and larger alpha conidia (7–10 × 2.9–3.2 vs. 5.5–7.5 × 0.5–2 µm); differs from *D. acerigena* in larger alpha conidia (2.9–3.2 vs. 2.1–2.9 µm) (Gao et al. 2016).

***Diaporthe kadsurae* C.M. Tian & Q. Yang, sp. nov.**
MycoBank: MB824713
Figure 14

Diagnosis. *Diaporthe kadsurae* differs from its closest phylogenetic species *D. fusicola* and *D. ovoicicola* in ITS, *cal* and *tef1* loci based on the alignments deposited in TreeBASE.

Holotype. CHINA. Jiangxi Province: Shangrao city, Sanqing Mountain, on symptomatic branches of *Kadsura longipedunculata*, 1 Apr. 2017, B. Cao, Y.M. Liang & C.M. Tian (holotype: BJFC-S1497; ex-type culture: CFCC 52586).

Etymology. Named after the host genus on which it was collected, *Kadsura*.

Description. Conidiomata pycnidial, immersed in bark, scattered, slightly erumpent through the bark surface, nearly flat, discoid, with a single locule. Ectostromatic disc obviously, brown to black, one ostiole per disc. Locule undivided, 475–525 µm diam. Conidiophores 7–11 × 1.8–2.9 µm, cylindrical, hyaline, unbranched, straight or slightly curved, tapering towards the apex. Alpha conidia hyaline, aseptate, oval or fusoid, biguttulate, 5.5–7.5 × 2.1–2.9 µm (av. = 6.5 × 2.5 µm, n = 30). Beta conidia not observed.

Culture characters. Cultures incubated on PDA at 25 °C in darkness. Colony originally flat with white aerial mycelium, becoming dense and felted aerial mycelium in the centre and grey to black mycelium at the marginal area with solitary conidiomata at maturity.

Additional specimens examined. CHINA. Jiangxi Province: Shangrao city, Sanqing Mountain, on symptomatic branches of *Kadsura longipedunculata*, 1 Apr. 2017, B. Cao, Y.M. Liang & C.M. Tian, living culture CFCC 52587 (BJFC-S1498); Yunbifeng National Forest Park, on symptomatic twigs of *Acer* sp., 31 Mar. 2017, B. Cao, Y.M. Liang & C.M. Tian, living culture CFCC 52588 (BJFC-S1499); ibid. living culture CFCC 52589 (BJFC-S1500).

Notes. This new species is introduced as molecular data show it to be a distinct clade with high support (ML/BI=100/1) and it appears most closely related to *D. fusi-*

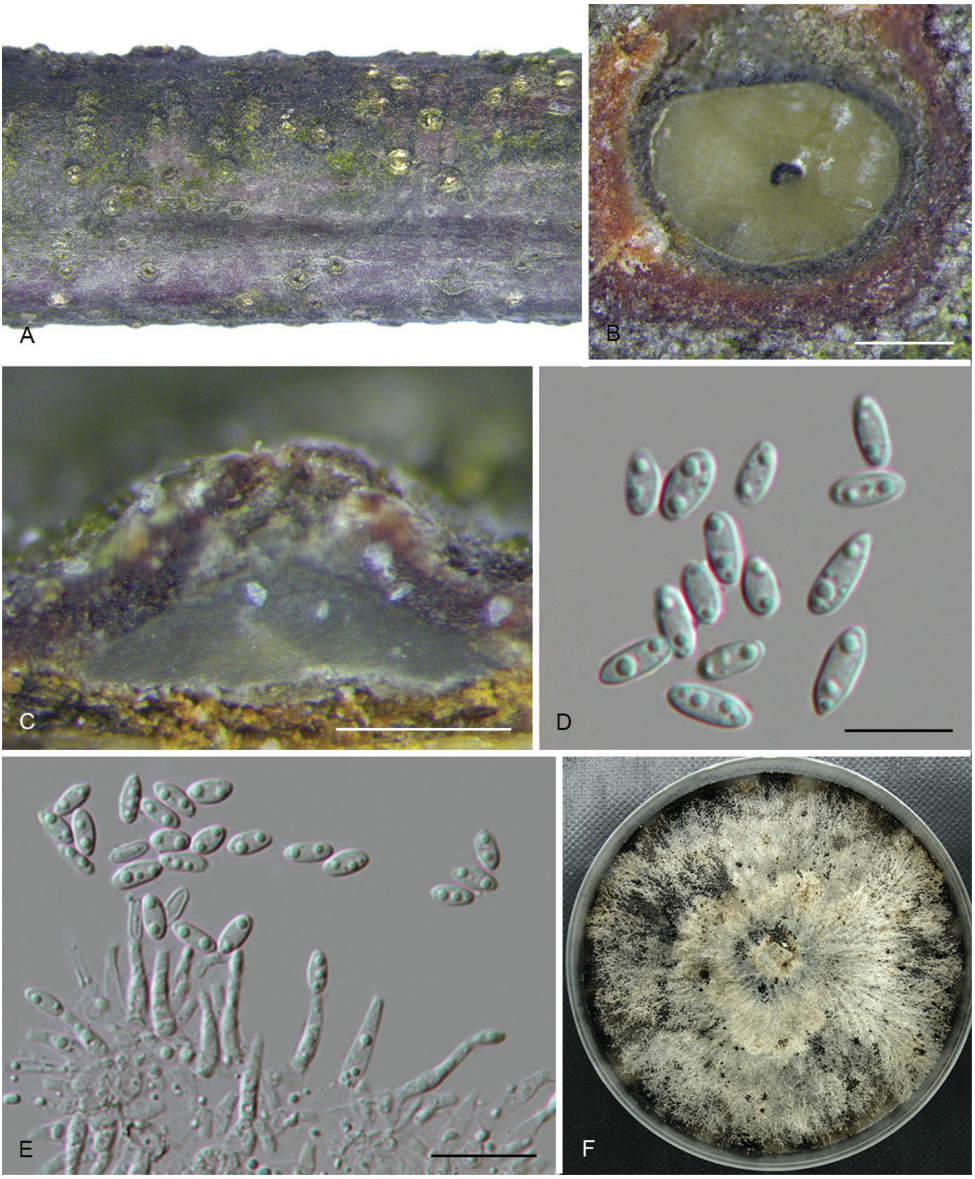

Figure 14. *Diaporthe kadsurae* (CFCC 52586) **A** Habit of conidiomata on branches **B** Transverse section of conidioma **C** Longitudinal section of conidioma **D** Alpha conidia **E** Conidiophores **F** Culture on PDA. Scale bars: 200 μm (**B–C**), 10 μm (**D–E**).

cola and *D. ovoicicola*. *Diaporthe kadsurae* can be distinguished from *D. fusicola* by 11 nucleotides in concatenated alignment, in which 4 were distinct in the ITS region and 7 in the *cal* region; from *D. ovoicicola* by 25 nucleotides in concatenated alignment, in which 12 were distinct in the ITS region, 6 in the *cal* region and 7 in the *tef1* region. Morphologically, *D. kadsurae* differs from *D. fusicola* and *D. ovoicicola* in shorter co-

nidiophores (7–11 µm in *D. kadsurae* vs. 11–24.1 µm in *D. fusicola*; 7–11 µm in *D. kadsurae* vs. 14.2–23.6 µm in *D. ovoicicola*) (Gao et al. 2014).

Diaporthe padina **C.M. Tian & Q. Yang, sp. nov.**
MycoBank: MB824714
Figure 15

Diagnosis. *Diaporthe padina* can be distinguished from the phylogenetically closely related species *D. betulae* in smaller conidiomata and alpha conidia.

Holotype. CHINA. Heilongjiang Province: Liangshui Nature Reserve, on symptomatic twigs of *Padus racemosa*, 31 July 2016, Q. Yang (holotype: BJFC-S1501; ex-type culture: CFCC 52590).

Etymology. Named after the host genus on which it was collected, *Padus*.

Description. Conidiomata pycnidial, immersed in bark, scattered, slightly erumpent through the bark surface, discoid, with a single locule. Ectostromatic disc light brown, one ostiole per disc, 330–520 µm diam. Locule circular, undivided, 250–550 µm diam. Conidiophores 5.5–12.5 × 1–1.5 µm, hyaline, unbranched, cylindrical, straight or slightly curved. Alpha conidia hyaline, aseptate, ellipsoidal to fusiform, eguttulate, 7–8 × 1.5–2 µm (av. = 7.5 × 1.8 µm, n = 30). Beta conidia hyaline, filiform, straight or hamate, eguttulate, aseptate, base truncate, 21–24 × 1 µm (av. = 22 × 1 µm, n = 30).

Culture characters. Cultures incubated on PDA at 25 °C in darkness. Colony originally flat with white aerial mycelium, becoming grey to brown in the centre, with pale grey, felted, valviform mycelium at the marginal area and aggregated conidiomata at maturity.

Additional material examined. CHINA. Heilongjiang Province: Liangshui Nature Reserve, on symptomatic twigs of *Padus racemosa*, 31 July 2016, Q. Yang, living culture CFCC 52591 (BJFC-S1502).

Notes. Four strains representing *D. padina* cluster in a well-supported clade and appear closely related to *D. betulae*. This species is phylogenetically closely related to, but clearly differentiated from, *D. betulae* by 40 different unique fixed alleles in ITS, *cal*, *his3*, *tef1* and *tub2* loci (4, 7, 10, 13 and 6 respectively) based on the alignments deposited in TreeBASE. Morphologically, *D. padina* differs from *D. betulae* in smaller conidiomata and alpha conidia (250–550 vs. 600–1250 µm in conidiomata; 7–8 × 1.5–2 vs. 8.5–11 × 3–4 µm in alpha conidia) (Du et al. 2016).

Diaporthe ukurunduensis **C.M. Tian & Q. Yang, sp. nov.**
MycoBank: MB824715
Figure 16

Diagnosis. *Diaporthe ukurunduensis* can be distinguished from the phylogenetically closely related species *D. citrichinensis* in longer conidiophores and shorter alpha conidia.

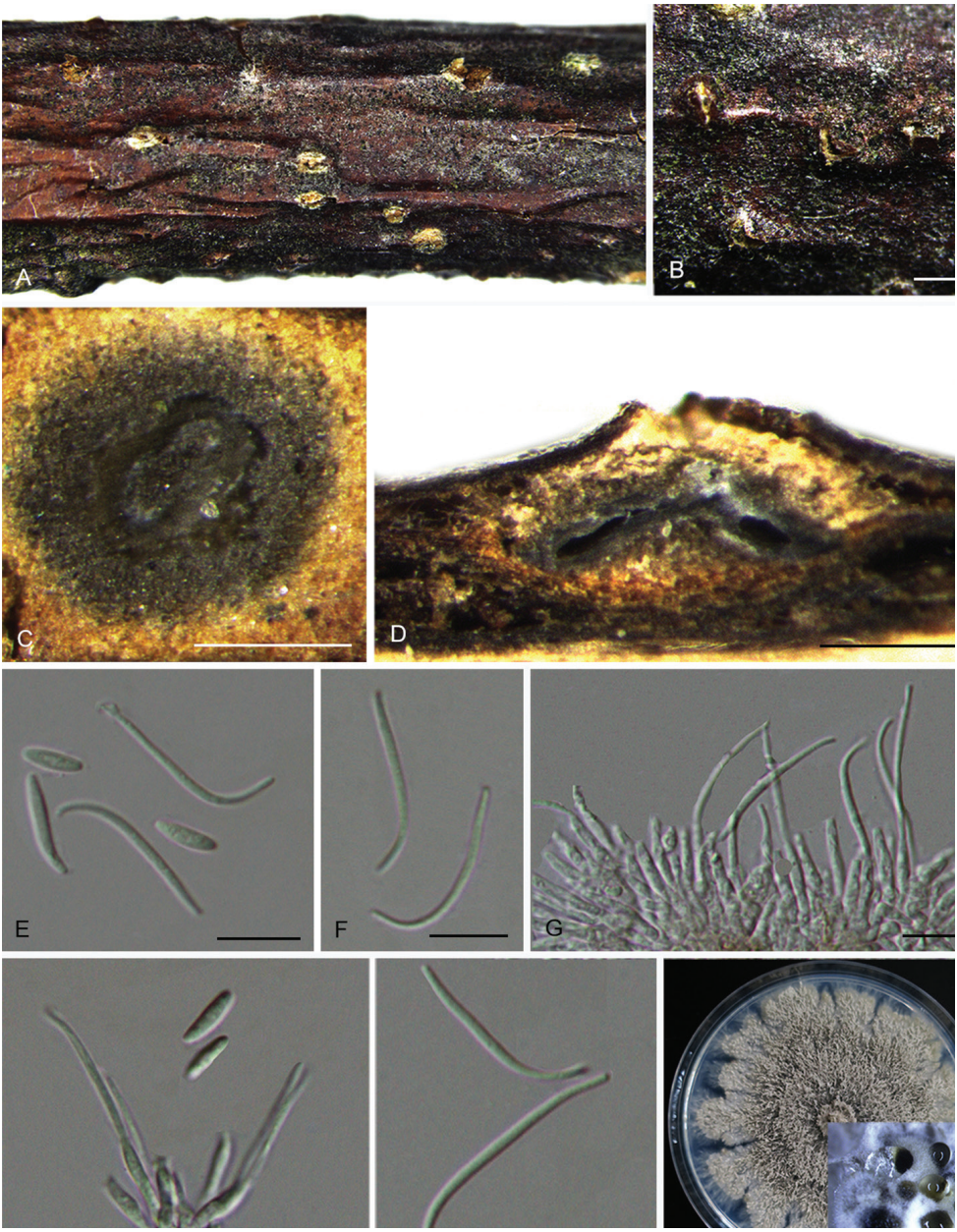

Figure 15. *Diaporthe padina* (CFCC 52590) **A–B** Habit of conidiomata on branches **C** Transverse section of conidioma **D** Longitudinal section of conidioma **E** Alpha and beta conidia **F, I** Beta conidia **G–H** Conidiophores **J** Culture on PDA and conidiomata. Scale bars: 500 µm (**B**), 200 µm (**C–D**), 10 µm (**E–I**).

Holotype. CHINA. Shaanxi Province: Qinling Mountain, on symptomatic twigs of *Acer ukurunduense*, 27 June 2017, Q. Yang (holotype: BJFC-S1503; ex-type culture: CFCC 52592).

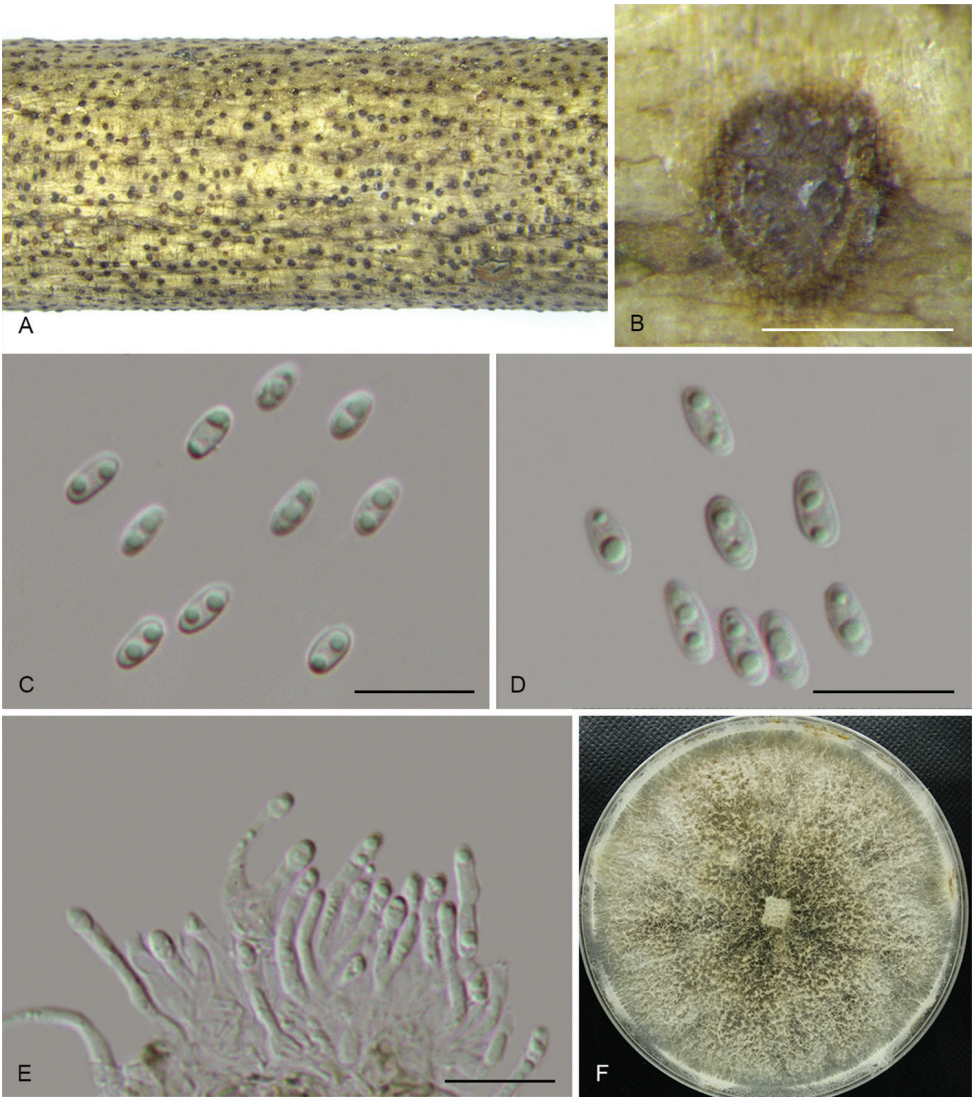

Figure 16. *Diaporthe ukurunduensis* (CFCC 52592) **A** Habit of conidiomata on branches **B** Transverse section of conidioma **C–D** Alpha conidia **E** Conidiophores **F** Culture on PDA. Scale bars: 200 μm (**B**), 10 μm (**C–E**).

Etymology. Named after the host species on which it was collected, *Acer ukurunduense*.

Description. Conidiomata pycnidial, immersed in bark, serried, slightly erumpent through the bark surface, nearly flat, discoid, with a single locule. Ectostromatic disc dark brown to black, one ostiole per disc. Locule circular, undivided, 165–215 μm diam. Conidiophores 11.5–18 × 1.5 μm, hyaline, branched, cylindrical, straight or curved. Alpha conidia hyaline, aseptate, ellipsoidal to oval, biguttulate, 5–6 × 2.1–2.9 μm (av. = 5.5 × 2.5 μm, n = 30). Beta conidia not observed.

Culture characters. Cultures incubated on PDA at 25 °C in darkness. Colony originally flat with white aerial mycelium, becoming brown to pale black in the centre, dense, felted, conidiomata not observed.

Additional specimens examined. CHINA. Shaanxi Province: Qinling Mountain, on symptomatic twigs of *Acer ukurunduense*, 27 June 2017, Q. Yang, living culture CFCC 52593 (BJFC-S1503).

Notes. *Diaporthe ukurunduensis* comprises strains CFCC 52592 and CFCC 52593 closely related to *D. citrichinensis* in the combined phylogenetic tree (Fig. 1). *Diaporthe ukurunduensis* can be distinguished from *D. citrichinensis* based on ITS and *tef1* loci (10/470 in ITS and 4/336 in *tef1*).

Diaporthe unshiuensis F. Huang, K.D. Hyde & H.Y. Li, 2015

Figure 17

Description. On PNA: Conidiomata pycnidial, globose or rostrated, black, erumpent in tissue, erumpent at maturity, 260–500 µm diam, often with translucent conidial drops exuding from the ostioles. Conidiophores 18–28.5 × 1.4–2.1 µm, cylindrical, hyaline, branched, septate, straight or curved, tapering towards the apex. Alpha conidia abundant in culture, hyaline, aseptate, ellipsoidal to fusiform, biguttulate, sometimes with one end obtuse and the other acute, 6.5–8.5 × 2.1–2.5 µm (av. = 7.8 × 2.3 µm, n = 30). Beta conidia not observed.

Culture characters. Cultures incubated on PNA at 25 °C in darkness. Colony entirely white at surface, reverse with pale brown pigmentation, white, fluffy aerial mycelium.

Specimens examined. CHINA. Jiangsu Province: Nanjing city, on non-symptomatic twigs of *Carya illinoensis*, 10 Nov. 2015, Q. Yang, living culture CFCC 52594 and CFCC 52595 (BJFC-S1476).

Notes. *Diaporthe unshiuensis* was originally described from twigs of non-symptomatic *Fortunella margarita* in Zhejiang Province, China (Huang et al. 2015). In the present study, two isolates from twigs of asymptomatic *Carya illinoensis* were congruent with *D. unshiuensis* based on morphology and DNA sequences data (Fig. 1). We therefore describe *D. unshiuensis* as a known species for this clade.

Discussion

The current study described 15 *Diaporthe* species from 42 strains based on a large set of freshly collected specimens. It includes 12 new species and 3 known species, which were sampled from 16 host genera distributed over six Provinces of China (Table 1). In this study, 194 reference sequences (including outgroup) were selected based on BLAST searches of NCBIs GenBank nucleotide database and included in the phylogenetic analyses (Table 1). Phylogenetic analyses based on five combined loci (ITS, *cal*, *his3*, *tef1*

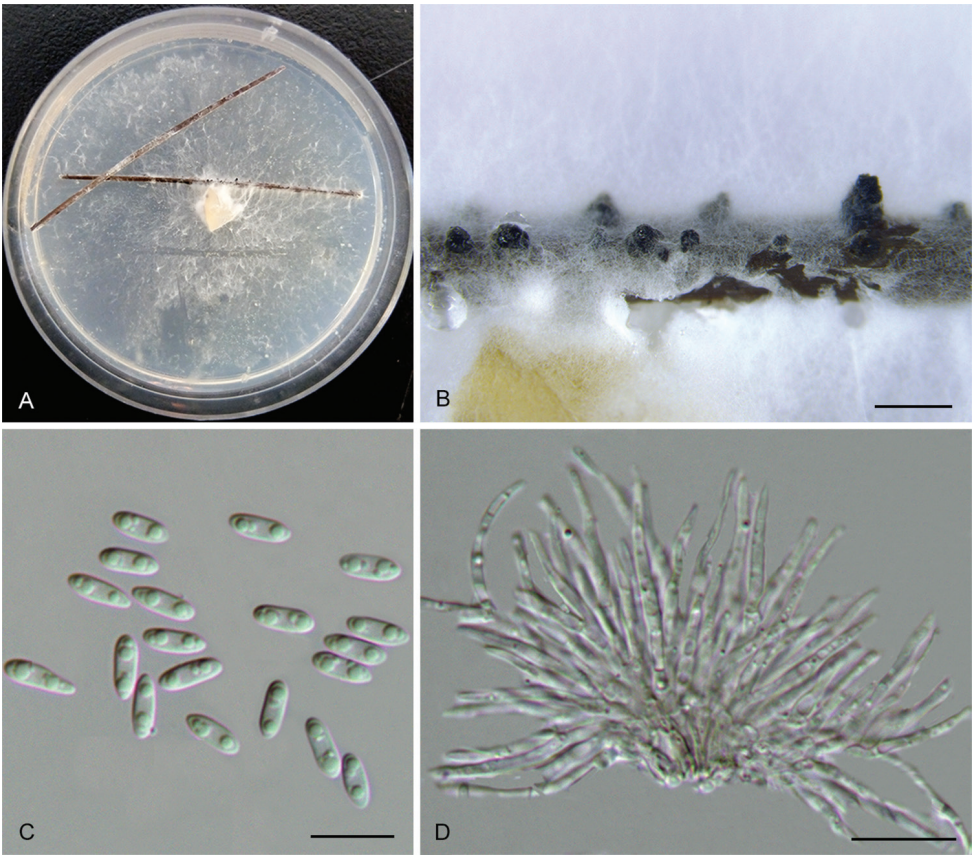

Figure 17. *Diaporthe unshiuensis* (CFCC 52594) **A** Culture on PNA **B** Conidiomata **C** Alpha conidia **D** Conidiophores. Scale bars: 500 µm (**B**), 10 µm (**C–D**).

and *tub2*), as well as morphological characters, revealed the diversity of *Diaporthe* species in China, mainly focusing on diebacks from major ecological or economic forest trees.

Several studies have been conducted associated with various hosts in China. For instance, the research conducted by Huang et al. (2015) revealed seven apparently undescribed endophytic *Diaporthe* species on *Citrus*. Gao et al. (2016) demonstrated that *Diaporthe* isolates, associated with *Camellia* spp., could be assigned to seven species and two species complexes. Recently, *Diaporth*e has been revealed as paraphyletic by Gao et al. (2017), showing that *Ophiodiaporthe*, *Pustulomyces*, *Phaeocytostroma* and *Stenocarpella* embed in *Diaporthe s. lat*. and eight new species of *Diaporthe* were introduced from leaves of several hosts. However, the identification of *Diaporthe* species associated with dieback of forest trees has rarely been studied, thus a large-scale investigation of *Diaporthe* spp. was conducted from 2015 to 2017. This study provides the first molecular phylogenetic frame of *Diaporthe* diversity associated with dieback in China, combined with morphological descriptions.

Diaporthe eres, the type species of the genus, was initially described by Nitschke (1870), from *Ulmus* sp. collected in Germany. The major problem with this generic type was the lack of an ex-type culture or ex-epitype culture, although a broad species concept has historically been associated with *D. eres* (Udayanga et al. 2014b). Udayanga et al. (2014b) designed strain AR5193 as the epitype of *D. eres* and provided the phylogram of this complex using seven loci (ITS, *act*, Apn2, *cal*, *his3*, FG1093, *tef1* and *tub2*), amongst which the *tef1*, Apn2 and *his3* genes were recognised as the best markers for defining species in the *D. eres* complex. Moreover, they showed that poorly supported non-monophyletic grouping was observed when ITS sequences were included in the combined analysis. In this study, although we conducted phylogenetic analysis as performed in previous studies on *Diaporthe* species (Santos et al. 2017), much confusion has, however, occurred in species separation of *the D. eres* complex (Fig. 1). Especially, the ITS region could lead to a confused taxonomic situation within this species complex. We found the three-gene analysis, excluding the ITS and *his3* regions, resulted in a more robust tree congruent with Udayanga et al. (2014b) and resolved the species boundaries within the *D. eres* species complex. The isolates, clustering with *D. eres* in this study, occur on multiple hosts from many different geographic locations. This study revealed three new species belonging to the *D. eres* complex, i.e. *D. betulina*, *D. chensiensis* and *D. padina*. It also shows *D. biguttusis*, *D. camptothecicola*, *D. ellipicola*, *D. longicicola*, *D. mahothocarpus* and *D. momicola* were clustered in *D. eres* and should be treated as synonyms of *D. eres*, which is in conformity with Fan et al. (2018).

The initial species concept of *Diaporthe*, based on the assumption of host-specificity, resulted in the introduction of more than 1000 taxa (http://www.indexfungorum.org/). Thus, during the past decade, a polyphasic approach, employing multi-locus DNA data together with morphology and ecology, has been employed for species boundaries in the genus (Crous et al. 2012, Udayanga et al. 2014a, b, Huang et al. 2015, Gao et al. 2016, 2017, Guarnaccia and Crous 2017, 2018, Hyde et al. 2017, 2018, Yang et al. 2017a, b, 2018, Guarnaccia et al. 2018, Jayawardena et al. 2018, Perera et al. 2018a, b, Tibpromma et al. 2018, Wanasinghe et al. 2018).

Further studies are required in order to conduct an extensive collection of *Diaporthe* isolates, to resolve taxonomic questions and to redefine species boundaries. Multiple strains from different locations should also be subjected to multi-gene phylogenetic analysis to determine intraspecific variation. The descriptions and molecular data of *Diaporthe* species provided in this study represent a resource for plant pathologists, plant quarantine officials and taxonomists for identification of *Diaporthe*.

Acknowledgements

This study is financed by National Natural Science Foundation of China (Project No.: 31670647). We are grateful to Chungen Piao, Minwei Guo (China Forestry Culture Collection Center (CFCC), Chinese Academy of Forestry, Beijing.

References

Carbone I, Kohn LM (1999) A method for designing primer sets for speciation studies in filamentous ascomycetes. Mycologia 3: 553–556. https://doi.org/10.2307/3761358

Chi PK, Jiang ZD, Xiang MM (2007) Flora Fungorum Sinicorum. Vol.34. *Phomopsis*. Science Press, Beijing.

Crous PW, Gams W, Stalpers JA, Robert V, Stegehuis G (2004a) MycoBank: an online initiative to launch mycology into the 21st century. Studies in Mycology 50: 19–22.

Crous PW, Groenewald JZ, Risède JM, Simoneau P, Hywel-Jones NL (2004b) *Calonectria* species and their *Cylindrocladium* anamorphs: species with sphaeropedunculate vesicles. Studies in Mycology 50: 415–430.

Crous PW, Summerell BW, Shivas RG, Burgess TI, Decock CA, Dreyer LL, Granke LL, Guest DI, Hardy GEStJ, Hausbeck MK, Hüberli D, Jung T, Koukol O, Lennox CL, Liew ECY, Lombard L, McTaggart AR, Pryke JS, Roets F, Saude C, Shuttleworth LA, Stukely MJC, Vánky K, Webster BJ, Windstam ST, Groenewald JZ (2012) Fungal Planet description sheets: 107–127. Persoonia: Molecular Phylogeny and Evolution of Fungi 28: 138–182. https://doi.org/10.3767/003158512X652633

Crous PW, Wingfield MJ, Le Roux JJ, Richardson DM, Strasberg D, Shivas RG, Alvarado P, Edwards J, Moreno G, Sharma R, Sonawane MS, Tan YP, Altés A, Barasubiye T, Barnes CM, Blanchette RA, Boertmann D, Bogo A, Carlavilla JR, Cheewangkoon R, Daniel R, de Beer ZW, de Jesús Yáñez-Morales M, Duong TA, Fernández-Vicente J, Geering ADW, Guest DI, Held BW, Heykoop M, Hubka V, Ismail AM, Kajale SC, Khemmuk W, Kolařík M, Kurli R, Lebeuf R, Lévesque CA, Lombard L, Magista D, Manjón JL, Marincowitz S, Mohedano JM, Nováková A, Oberlies NH, Otto EC, Paguigan ND, Pascoe IG, Pérez-Butrón JL, Perrone G, Rahi P, Raja HA, Rintoul T, Sanhueza RMV, Scarlett K, Shouche YS, Shuttleworth LA, Taylor PWJ, Thorn RG, Vawdrey LL, Solano-Vidal R, Voitk A, Wong PTW, Wood AR, Zamora JC, Groenewald JZ (2015) Fungal Planet description sheets: 371–399. Persoonia: Molecular Phylogeny and Evolution of Fungi 35: 264. https://doi.org/10.3767/003158515X690269

Desjardins P, Hansen JB, Allen M (2009) Microvolume protein concentration determination using the NanoDrop 2000c spectrophotometer. Journal of visualized experiments: JoVE 33: 1–3. https://doi.org/10.3791/1610

Diogo E, Santos JM, Phillips AJ (2010) Phylogeny, morphology and pathogenicity of *Diaporthe* and *Phomopsis* species on almond in Portugal. Fungal Diversity 44: 107–115. https://doi.org/10.1007/s13225-010-0057-x

Dissanayake AJ, Phillips AJL, Hyde KD, Yan JY, Li XH (2017b) The current status of species in *Diaporthe*. Mycosphere 8(5): 1106–1156. https://doi.org/10.5943/mycosphere/8/5/5

Dissanayake AJ, Zhang W, Liu M, Hyde KD, Zhao WS, Li XH, Yan JY (2017a) *Diaporthe* species associated with peach tree dieback in Hubei, China. Mycosphere 8: 533–549. https://doi.org/10.5943/mycosphere/8/5/3

Doilom M, Dissanayake AJ, Wanasinghe DN, Wanasinghe DN, Boonmee S, Liu JK, Bhat DJ, Taylor JE, Bahkali AH, McKenzie EHC, Hyde KD (2017) Microfungi on *Tectona gran-*

dis (teak) in Northern Thailand. Fungal Diversity 82: 107–182. https://doi.org/10.1007/s13225-016-0368-7

Doyle JJ, Doyle JL (1990) Isolation of plant DNA from fresh tissue. Focus 12: 13–15.

Du Z, Fan XL, Hyde KD, Yang Q, Liang YM, Tian CM (2016) Phylogeny and morphology reveal two new species of *Diaporthe* from *Betula* spp. in China. Phytotaxa 269: 90–102. https://doi.org/10.11646/phytotaxa.269.2.2

Erincik O, Madden L, Ferree D, Ellis M (2001) Effect of growth stage on susceptibility of grape berry and rachis tissues to infection by *Phomopsis viticola*. Plant Disease 85: 517–520. https://doi.org/10.1094/PDIS.2001.85.5.517

Fan XL, Hyde KD, Udayanga D, Wu XY, Tian CM (2015) *Diaporthe rostrata*, a novel ascomycete from *Juglans mandshurica* associated with walnut dieback. Mycological Progress 14: 1–8. https://doi.org/10.1007/s11557-015-1104-5

Fan XL, Yang Q, Bezerra JDP, Alvarez LV, Tian CM (2018) *Diaporthe* from walnut tree (*Juglans regia*) in China, with insight of *Diaporthe eres* complex. Mycological Progress: 1–13. https://doi.org/10.1007/s11557-018-1395-4

Gao YH, Liu F, Cai L (2016) Unravelling *Diaporthe* species associated with *Camellia*. Systematics and Biodiversity 14: 102–117. https://doi.org/10.1080/14772000.2015.1101027

Gao YH, Liu F, Duan W, Crous PW, Cai L (2017) *Diaporthe* is paraphyletic. IMA fungus 8: 153–187. https://doi.org/10.5598/imafungus.2017.08.01.11

Gao YH, Su YY, Sun W, Cai L (2015) *Diaporthe* species occurring on *Lithocarpus glabra* in China, with descriptions of five new species. Fungal Biology 115: 295–309. https://doi.org/10.1016/j.funbio.2014.06.006

Gao YH, Sun W, Su YY, Cai L (2014) Three new species of *Phomopsis* in Gutianshan Nature Reserve in China. Mycological Progress 13: 111–121. https://doi.org/10.1007/s11557-013-0898-2

Garcia-Reyne A, López-Medrano F, Morales JM, Esteban CG, Martín I, Eraña I, Meije Y, Lalueza A, Alastruey-Izquierdo A, Rodríguez-Tudela JL, Aguado JM (2011) Cutaneous infection by *Phomopsis longicolla* in a renal transplant recipient from Guinea: first report of human infection by this fungus. Transplant Infectious Disease 13: 204–207. https://doi.org/10.1111/j.1399-3062.2010.00570.x

Glass NL, Donaldson GC (1995) Development of primer sets designed for use with the PCR to amplify conserved genes from filamentous ascomycetes. Applied and Environmental Microbiology 61: 1323–1330.

Gomes RR, Glienke C, Videira SIR, Lombard L, Groenewald JZ, Crous PW (2013) *Diaporthe*: a genus of endophytic, saprobic and plant pathogenic fungi. Persoonia: Molecular Phylogeny and Evolution of Fungi 31: 1. https://doi.org/10.3767/003158513X666844

Guarnaccia V, Crous PW (2017) Emerging citrus diseases in Europe caused by species of *Diaporthe*. IMA Fungus 8: 317–334. https://doi.org/10.5598/imafungus.2017.08.02.07

Guarnaccia V, Crous PW (2018) Species of *Diaporthe* on *Camellia* and *Citrus* in the Azores Islands. Phytopathologia Mediterranea. https://doi.org/10.14601/Phytopathol_Mediterr-23254

Guarnaccia V, Groenewald JZ, Woodhall J, Armengol J, Cinelli T, Eichmeier A, Ezra D, Fontaine F, Gramaje D, Gutierrez-Aguirregabiria A, Kaliterna J, Kiss L, Larignon P, Luque J, Mugnai L, Naor V, Raposo R, Sándor E, Váczy KZ, Crous PW (2018) *Diaporthe* diversity

and pathogenicity revealed from a broad survey of grapevine diseases in Europe. Persoonia: Molecular Phylogeny and Evolution of Fungi 40: 135–153. https://doi.org/10.3767/persoonia.2018.40.06

Guarnaccia V, Vitale A, Cirvilleri G, Aiello D, Susca A, Epifani F, Perrone G, Polizzi G (2016) Characterisation and pathogenicity of fungal species associated with branch cankers and stem-end rot of avocado in Italy. European Journal of Plant Pathology 146: 963–976. https://doi.org/10.1007/s10658-016-0973-z

Guindon S, Dufayard JF, Lefort V, Anisimova M, Hordijk W, Gascuel O (2010) New algorithms and methods to estimate maximum-likelihood phylogenies: assessing the performance of PhyML 3.0. Systematic Biology 59: 307–321. https://doi.org/10.1093/sysbio/syq010

Hewitt W, Pearson R (1988) *Phomopsis* cane and leaf spot. Compendium of grape diseases: 17–18. APS Press, St Paul, Minnesota.

Hillis DM, Bull JJ (1993) An empirical test of bootstrapping as a method for assessing confidence in phylogenetic analysis. Systematic Biology 42: 182–192. https://doi.org/10.1093/sysbio/42.2.182

Huang F, Hou X, Dewdney MM, Fu Y, Chen G, Hyde KD, Li HY (2013) *Diaporthe* species occurring on *citrus* in China. Fungal Diversity 61: 237–250. https://doi.org/10.1007/s13225-013-0245-6

Huang F, Udayanga D, Wang X, Hou X, Mei X, Fu Y, Hyde KD, Li HY (2015) Endophytic *Diaporthe* associated with *Citrus*: A phylogenetic reassessment with seven new species from China. Fungal Biology 119: 331–347. https://doi.org/10.1016/j.funbio.2015.02.006

Hyde KD, Chaiwan N, Norphanphoun C, Boonmee S, Camporesi E, Chethana KWT, Dayarathne MC, de Silva NI, Dissanayake AJ, Ekanayaka AH, Hongsanan S, Huang SK, Jayasiri SC, Jayawardena RS, Jiang HB, Karunarathna A, Lin CG, Liu JK, Liu NG, Lu YZ, Luo ZL, Maharachchimbura SSN, Manawasinghe IS, Pem D, Perera RH, Phukhamsakda C, Samarakoon MC, Senwanna C, Shang QJ, Tennakoon DS, Thambugala KM, Tibpromma S, Wanasinghe DN, Xiao YP, Yang J, Zeng XY, Zhang JF, Zhang SN, Bulgakov TS, Bhat DJ, Cheewangkoon R, Goh TK, Jones EBG, Kang JC, Jeewon R, Liu ZY, Lumyong S, Kuo CH, McKenzie EHC, Wen TC, Yan JY, Zhao Q (2018) Mycosphere notes 169–224. Mycosphere 9(2): 271–430. https://doi.org/10.5943/mycosphere/9/2/8

Hyde KD, Norphanphoun C, Abreu VP, Bazzicalupo A, Chethana KT, Clericuzio M, Dayarathne MC, Dissanayake AJ, Ekanayaka AH, He MQ, Hongsanan S, Huang SK, Jayasiri SC, Jayawardena RS, Karunarathna A, Konta S, Kušan I, Lee H, Li J, Lin CG, Liu NG, Lu YZ, Luo ZL, Manawasinghe IS, Mapook A, Perera RH, Phookamsak R, Phukhamsakda C, Siedlecki I, Soares AM, Tennakoon DS, Tian Q, Tibpromma S, Wanasinghe DN, Xiao YP, Yang J, Zeng XY, Abdel-Aziz FA, Li WJ, Senanayake IC, Shang QJ, Daranagama DA, de Silva NI, Thambugala KM, Abdel-Wahab MA, Bahkali AH, Berbee ML, Boonmee S, Bhat DJ, Bulgakov TS, Buyck B, Camporesi E, Castañeda-Ruiz RF, Chomnunti P, Doilom M, Dovana F, Gibertoni TB, Jadan M, Jeewon R, Jones EBG, Kang JC, Karunarathna SC, Lim YW, Liu JK, Liu ZY, Plautz Jr. HL, Lumyong S, Maharachchikumbura SSN, Matočec N, McKenzie EHC, Mešić A, Miller D, Pawłowska J, Pereira OL, Promputtha I, Romero AI, Ryvarden L, Su HY, Suetrong S, Tkalčec Z, Vizzini A, Wen TC, Wisitrassameewong K, Wrzosek M, Xu JC, Zhao Q, Zhao RL, Mortimer PE (2017) Fungal diversity

notes 603–708: taxonomic and phylogenetic notes on genera and species. Fungal Diversity 87(1): 1–235. https://doi.org/10.1007/s13225-017-0391-3

Jayawardena RS, Hyde KD, Chethana KWT, Daranagama DA, Dissanayake AJ, Goonasekara ID, Manawasinghe IS, Mapook A, Jayasiri SC, Karunarathna A, Li CG, Phukhamsakda C, Senanayake IC, Wanasinghe DN, Camporesi E, Bulgakov TS, Li XH, Liu M, Zhang W, Yan JY (2018) Mycosphere Notes 102–168: Saprotrophic fungi on Vitis in China, Italy, Russia and Thailand. Mycosphere 9(1): 1–114. https://doi.org/10.5943/mycosphere/9/1/1

Katoh K, Toh H (2010) Parallelization of the MAFFT multiple sequence alignment program. Bioinformatics 26: 1899–1900. https://doi.org/10.1093/bioinformatics/btq224

Lombard L, Van Leeuwen GCM, Guarnaccia V, Polizzi G, Van Rijswick PC, Karin Rosendahl KC, Gabler J, Crous PW (2014) *Diaporthe* species associated with *Vaccinium*, with specific reference to Europe. Phytopathologia Mediterranea 53: 287–299. https://doi.org/10.14601/Phytopathol_Mediterr-14034

Marin-Felix Y, Hernández-Restrepo M, Wingfield MJ, Akulov A, Carnegie AJ, Cheewangkoon R, Gramaje D, Groenewald JZ, Guarnaccia V, Halleen F, Lombard L, Luangsa-ard J, Marincowitz S, Moslemi A, Mostert L, Quaedvlieg W, Schumacher RK, Spies CFJ, Thangavel R, Taylor PWJ, Wilson AM, Wingfield BD, Wood AR, Crous PW (2018) Genera of phytopathogenic fungi: GOPHY2. Studies in Mycology. https://doi.org/10.1016/j.simyco.2018.04.002.

Mostert L, Crous PW, Kang JC, Phillips AJ (2001) Species of *Phomopsis* and a *Libertella* sp. occurring on grapevines with specific reference to South Africa: morphological, cultural, molecular and pathological characterization. Mycologia 93: 146–167. https://doi.org/10.2307/3761612

Mondal SN, Vincent A, Reis RF, Timmer LW (2007) Saprophytic colonization of citrus twigs by *Diaporthe citri* and factors affecting pycnidial production and conidial survival. Plant Disease 91: 387–392. https://doi.org/10.1094/PDIS-91-4-0387

Muntañola-Cvetković M, Mihaljčević M, Petrov M (1981) On the identity of the causative agent of a serious *Phomopsis-Diaporthe* disease in sunflower plants. Nova Hedwigia 34: 417–435.

Muralli TS, Suryanarayanan TS, Geeta R (2006) Endophytic *Phomopsis* species: host range and implications for diversity estimates. Canadian Journal of Microbiology 52: 673–680. https://doi.org/10.1139/w06-020

Nitschke T (1870) Pyrenomycetes Germanici 2. Eduard Trewendt, Breslau, 245.

O'Donnell K, Cigelnik E (1997) Two divergent intragenomic rDNA ITS2 types within a monophyletic lineage of the fungus *Fusarium* are nonorthologous. Molecular Phylogenetics and Evolution 7: 103–116. https://doi.org/10.1006/mpev.1996.0376

Perera RH, Hyde KD, Dissanayake AJ, Jones EB, Liu JK, Wei D, Liu ZY (2018b) *Diaporthe collariana* sp. nov., with prominent collarettes associated with *Magnolia champaca* fruits in Thailand. Studies in Fungi 3(1): 141–151. https://doi.org/10.5943/sif/3/1/16

Perera RH, Hyde KD, Peršoh D, Jones EBG, Liu JK, Liu ZY (2018a) Additions to wild seed and fruit fungi 1: The sexual morph of *Diaporthe rosae* on *Magnolia champaca* and *Senna siamea* fruits in Thailand. Mycosphere 9(2): 256–270. https://doi.org/10.5943/mycosphere/9/2/7

Posada D, Crandall KA (1998) Modeltest: testing the model of DNA substitution. Bioinformatics 14: 817–818. https://doi.org/10.1093/bioinformatics/14.9.817

Rannala B, Yang Z (1996) Probability distribution of molecular evolutionary trees: a new method of phylogenetic inference. Journal of Molecular Evolution 43: 304–311. https://doi.org/10.1007/BF02338839

Rayner RW (1970) A mycological colour chart. Commonwealth Mycological Institute, Kew.

Rehner SA, Uecker FA (1994) Nuclear ribosomal internal transcribed spacer phylogeny and host diversity in the coelomycete *Phomopsis*. Canadian Journal of Botany 72: 1666–1674. https://doi.org/10.1139/b94-204

Rossman AY, Adams GC, Cannon PF, Castlebury LA, Crous PW, Gryzenhout M, Jaklitsch WM, Mejia LC, Stoykov D, Udayanga D, Voglmayr H, Walker DM (2015) Recommendations of generic names in *Diaporthales* competing for protection or use. IMA Fungus 6: 145–154. https://doi.org/10.5598/imafungus.2015.06.01.09

Rossman AY, Farr DF, Castlebury LA (2007) A review of the phylogeny and biology of the Diaporthales. Mycoscience 48: 135–144. https://doi.org/10.1007/s10267-007-0347-7

Saccardo PA, Roumeguère C (1884) Reliquiae mycologicae Libertianae. IV. Revue Mycologique, Toulouse 6: 26–39.

Santos JM, Correia VG, Phillips AJL (2010) Primers for mating-type diagnosis in *Diaporthe* and *Phomopsis*, their use in teleomorph induction in vitro and biological species definition. Fungal Biology 114: 255–270. https://doi.org/10.1016/j.funbio.2010.01.007

Santos JM, Phillips AJL (2009) Resolving the complex of *Diaporthe* (*Phomopsis*) species occurring on *Foeniculum vulgare* in Portugal. Fungal Diversity 34: 111–125.

Santos JM, Vrandečić K, Ćosić J, Duvnjak T, Phillips AJL (2011) Resolving the *Diaporthe* species occurring on soybean in Croatia. Persoonia: Molecular Phylogeny and Evolution of Fungi 27: 9–19. https://doi.org/10.3767/003158511X603719

Santos L, Alves A, Alves R (2017) Evaluating multi-locus phylogenies for species boundaries determination in the genus *Diaporthe*. PeerJ 5: e3120. https://doi.org/10.7717/peerj.3120

Smith H, Wingfeld MJ, Coutinho TA, Crous PW (1996) *Sphaeropsis sapinea* and *Botryosphaeria dothidea* endophytic in *Pinus* spp. and *Eucalyptus* spp. in South Africa. South African Journal of Botany 62: 86–88. https://doi.org/10.1016/S0254-6299(15)30596-2

Tai FL (1979) Sylloge fungorum sinicorum. Science press, 1527 pp.

Tamura K, Stecher G, Peterson D, Filipski A, Kumar S (2013) MEGA6: molecular evolutionary genetics analysis version 6.0. Molecular Biology and Evolution 30: 2725–2729. https://doi.org/10.1093/molbev/mst197

Tanney JB, Mcmullin DR, Green BD, Miller JD, Seifert KA (2016) Production of antifungal and antiinsectan metabolites by the *Picea* endophyte *Diaporthe maritima* sp. nov. Fungal Biology 120: 1448–1457. https://doi.org/10.1016/j.funbio.2016.05.007

Teng SC (1963) Fungi of China. Science press, 808 pp.

Thompson SM, Tan YP, Shivas RG, Neate SM, Morin L, Bissett A, Aitken EAB (2015) Green and brown bridges between weeds and crops reveal novel *Diaporthe* species in Australia. Persoonia: Molecular Phylogeny and Evolution of Fungi 35: 39. https://doi.org/10.3767/003158515X687506

Thompson SM, Tan YP, Young AJ, Neate SM, Aitken EAB, Shivas RG (2011) Stem cankers on sunflower (*Helianthus annuus*) in Australia reveal a complex of pathogenic *Diaporthe* (*Phomopsis*) species. Persoonia: Molecular Phylogeny and Evolution of Fungi 27: 80. https://doi.org/10.3767/003158511X617110

Tibpromma S, Hyde KD, Bhat JD, Mortimer PE, Xu J, Promputtha I, Mingkwan D, Yang JB, Tang AMC, Karunarathna SC (2018) Identification of endophytic fungi from leaves of Pandanaceae based on their morphotypes and DNA sequence data from southern Thailand. MycoKeys 33: 25. https://doi.org/10.3897/mycokeys.33.23670

Udayanga D, Castlebury LA, Rossman AY, Chukeatirote E, Hyde KD (2014b) Insights into the genus *Diaporthe*: phylogenetic species delimitation in the *D. eres* species complex. Fungal Diversity 67: 203–229. https://doi.org/10.1007/s13225-014-0297-2

Udayanga D, Castlebury LA, Rossman AY, Chukeatirote E, Hyde KD (2015) The *Diaporthe sojae* species complex: Phylogenetic re-assessment of pathogens associated with soybean, cucurbits and other field crops. Fungal Biology 119: 383–407. https://doi.org/10.1016/j.funbio.2014.10.009

Udayanga D, Castlebury LA, Rossman AY, Hyde KD (2014a) Species limits in *Diaporthe*: molecular re-assessment of *D. citri*, *D. cytosporella*, *D. foeniculina* and *D. rudis*. Persoonia: Molecular Phylogeny and Evolution of Fungi 32: 83–101. https://doi.org/10.3767/003158514X679984

Udayanga D, Liu X, Crous PW, McKenzie EH, Chukeatirote E, Chukeatirote E, Hyde KD (2012a) A multi-locus phylogenetic evaluation of *Diaporthe* (*Phomopsis*). Fungal Diversity 56: 157–171. https://doi.org/10.1007/s13225-012-0190-9

Udayanga D, Liu X, McKenzie EH, Chukeatirote E, Bahkali AH, Hyde KD (2011) The genus *Phomopsis*: biology, applications, species concepts and names of common phytopathogens. Fungal Diversity 50: 189–225. https://doi.org/10.1007/s13225-011-0126-9

Udayanga D, Liu X, McKenzie EH, Chukeatirote E, Hyde KD (2012b) Multi-locus phylogeny reveals three new species of *Diaporthe* from Thailand. Cryptogamie, Mycologie 33: 295–309. https://doi.org/10.7872/crym.v33.iss3.2012.295

Uecker FA (1988) A world list of *Phomopsis* names with notes on nomenclature, morphology and biology. Mycological Memoirs 13: 1–231.

Wanasinghe DN, Phukhamsakda C, Hyde KD, Jeewon R, Lee HB, Jones EG, Tibpromma S, Tennakoon DS, Dissanayake AJ, Jayasiri SC, Gafforov Y, Camporesi E, Bulgakov TS, Ekanayake AH, Perera RH, Samarakoon MC, Goonasekara ID, Mapook A, Li WJ, Senanayake IC, Li J, Norphanphoun C, Doilom M, Bahkali AH, Xu JC, Mortimer PE, Tibell L, Tibell S, Karunarathna SC (2018) Fungal diversity notes 709–839: taxonomic and phylogenetic contributions to fungal taxa with an emphasis on fungi on Rosaceae. Fungal Diversity 89(1): 1–236. https://doi.org/10.1007/s13225-018-0395-7

Wei JC (1979) Identification of Fungus Handbook. Science press, 780 pp.

White TJ, Bruns T, Lee S, Taylor J (1990) Amplification and direct sequencing of fungal ribosomal RNA genes for phylogenetics. PCR Protocols: A Guide to Methods and Applications 18: 315–322.

Yang Q, Du Z, Tian CM (2018) Phylogeny and morphology reveal two new species of *Diaporthe* from Traditional Chinese Medicine in Northeast China. Phytotaxa 336: 159–170. https://doi.org/10.11646/phytotaxa.336.2.3

Yang Q, Fan XL, Du Z, Liang YM, Tian CM (2017c). *Diaporthe camptothecicola* sp. nov. on *Camptotheca acuminata* in China. Mycotaxon 132: 591–601. https://doi.org/10.5248/132.591

Yang Q, Fan XL, Du Z, Tian CM (2017a) *Diaporthe* species occurring on *Senna bicapsularis* in southern China, with descriptions of two new species. Phytotaxa 302: 145–155. https://doi.org/10.11646/phytotaxa.302.2.4

Yang Q, Fan XL, Du Z, Tian CM (2017b) *Diaporthe juglandicola* sp. nov. (Diaporthales, Ascomycetes), evidenced by morphological characters and phylogenetic analysis. Mycosphere 8: 817–826. https://doi.org/10.5943/mycosphere/8/5/3